

THE OMNIDIRECTIONAL SCATTERING OF ACOUSTIC WAVES
FROM ROUGH SURFACES
WITH APPLICATION TO ELECTROMAGNETIC SCATTERING

by

Bowen E. Parkins

CRES Report #48-4

Supported by:

NASA Grant NsG-298

NASA Contract NSR 17-004-003

NSF Grant GP 2259

TABLE OF CONTENTS

<u>CHAPTER</u>	<u>PAGE</u>
ACKNOWLEDGEMENT	i
ABSTRACT	ii
I. Introduction	1
A. The Nature of Scattering Problems	1
B. The Description of the Completed Research	3
II. The Reflection and Scattering of Acoustic Waves from Rough Surfaces	6
A. The Re-radiation from a Rough Surface; the Several Methods of Calculation	6
B. The Method of Physical Optics and the Consideration of Imperfect Reflectivity	14
C. The Average Power and its Separation into Scatter and Specular Components	20
D. The Average Differential Scattering Cross Section and its Calculation	27
III. The Measurement of the Scattering Cross Section and Comparison with Theory	38
A. Historical Development of Measurement Techniques	38
B. The Technique of Measurement	41
C. The Description of the Experimental Facility and Conduct of the Experiment	45
D. Description of Rough Surfaces	57
E. The Experimental Results and Comparison with Theory	70
IV. Application of the Acoustic Results to Electromagnetic Scattering	103
V. Summary and Conclusions	125
VI. Recommendations for Further Work	127

APPENDIX I	Definition of Constants	128
APPENDIX II	Calculation of the Means of Terms Contributing to the Average of the Re-radiated Power	129
APPENDIX III	Calculation of the Order of Magnitude of the Partially Integrated Terms Occurring in the Expression for Re-radiated Power	134
APPENDIX IV	Calculation of the Aperture Effect	136
APPENDIX V	Derivation of a Vector Form of the Helmholtz Integral .	139
BIBLIOGRAPHY		143

ACKNOWLEDGEMENT

I am very grateful for the advice and direction of my advisor, Professor R. K. Moore, who suggested the topic.

I wish to express my appreciation to Dr. J. Vanden Boom and the Continental Oil Company of Ponca City, Oklahoma for the assistance in performing certain of the numerical calculations.

The financial support of the National Science Foundation under grant GP 2259 and the National Aeronautics and Space Administration under grant NsG-298 and contract NSR 17-004-003 is gratefully acknowledged.

Also, I wish to thank Mrs. D. D. Sommerfeld for her secretarial assistance.

ABSTRACT

In recent years there has been much work in rough surface scattering. The greatest part of this has been done in the area of electromagnetics because of the greater possible rewards from radar. However, there has been much progress in acoustic wave scattering and both areas have benefited from the similarity of the phenomena. This work is a study of the scattering of acoustic waves from randomly rough surfaces and the extent of the similarity to the analogous electromagnetics problem.

A theory is developed using the method of physical optics for the scattering of acoustic waves from randomly rough surfaces which are imperfectly reflecting yet homogeneous with respect to material parameters. This development is made for a surface which is given by a stationary, ergodic process with a Gaussian distribution of surface heights. The expression for the far zone acoustic power density is derived and the separation into scattered and reflected power components is made. For a surface sufficiently rough, the reflected component becomes negligibly small and there is near-total conversion to scattered power. For this case the average differential scattering cross section is computed from the scattered power density for the cases of exponential and Gaussian dependence of the autocorrelation coefficient of surface heights.

The theory is compared with the results of omnidirectional measurements using surfaces constructed to satisfy the assumptions of the physical optics method. The statistical parameters of the surfaces were determined from sampled data measurements and were used in the calculation of the

theoretical values. The comparison of theory with experiment is favorable and the theory is concluded to be a valid one.

The similarity between acoustic and electromagnetic re-radiation from surfaces is investigated by comparing analogous expressions for the re-radiated fields. The expressions for the electromagnetic field are derived using the method of physical optics as are the acoustic expressions, and the determination is valid only for surfaces to which this method applies. Similarities are found to exist and there are cases where an exact acoustic simulation can be made. In other situations the vector effects of the electromagnetic re-radiation dominate but some aspects of the re-radiation can be modeled acoustically.

I.A The Nature of Scattering Problems

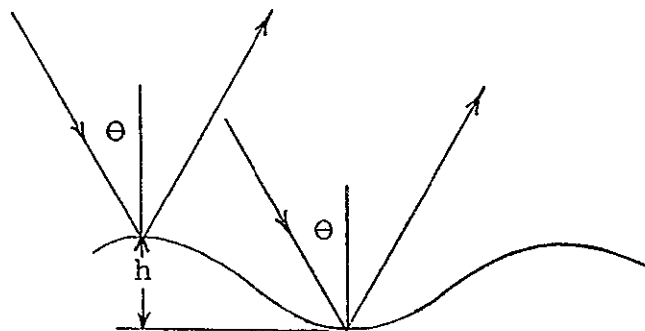
The analysis of the re-radiation of acoustic and electromagnetic waves from surfaces is a very broad problem with many different phenomena to be studied. The simplest form of re-radiation from a surface is reflection from an infinite plane. One of the distinguishing features of this reflection is that the re-radiated energy flows in a single direction which can be determined from the well known laws. Similar to reflection is the re-radiation from other geometric shapes such as spheres, cones, paraboloids, etc. The re-radiation from these surfaces differs, however, from the reflection from a plane in that the energy flow is not in a single direction but is scattered in many. When the incident wave is re-radiated from a regularly rough surface such as a corrugated plane (for instance in the shape of a sinusoid), the same scattering of energy occurs but in general it is expected to be more diffuse (on an intuitive basis) than that for a smooth but non-planar body. This, however, depends on the size of the structure of the regular roughness relative to the wavelength of the incident radiation.

Lord Rayleigh [1896], an early investigator of scattering phenomena, developed a criterion for surface smoothness, now known as the "Rayleigh criterion," which provides an approximate measure of the degree to which energy is scattered. For a plane wave of wavelength λ incident upon the corrugated surface shown in figure I.1, there is a phase difference

$$\Delta\beta = \frac{4\pi h \cos \theta}{\lambda}$$

for the two rays shown. When $\Delta\beta = \pi$, there is cancellation in the direction of mirror reflection (specular reflection) and energy is consequently flowing in other directions. Raleigh made the arbitrary choice of $\Delta\beta = \pi/2$ to establish his criterion for delineation of rough surfaces from smooth ones ($\Delta\beta = 0$); consequently, the Rayleigh criterion for a surface to be smooth is

$$h < \frac{\lambda}{8 \cos \theta}$$



Formulation of the Rayleigh Criterion

Figure I. 1

Surfaces which form a class for which the re-radiation process is different from that of the regular surfaces are those generated by random processes. The difference lies in the way in which the phase elements from all parts of the surface combine to produce the re-radiated power. For a randomly generated surface which is sufficiently rough, a linear superposition of the powers from the elemental surface areas is possible while for the regular surface a phasor addition taking into account the phase differences between the elements of the re-radiated field is necessary. For a random surface not rough enough to produce diffuse scattering, a division can be made between scattered power and reflected power, i. e., power for which the elemental phases are important. This difference in the re-radiation processes for these two classes of surfaces necessitates the use of different techniques for the description, both theoretical and experimental, of the radiation phenomena associated with each class.

For a wave incident upon a general surface the field re-radiated in all directions from the surface must be given as a function of the parameters defining the media involved. For randomly rough surfaces this implies a statistical description of the field and also of the media. The problem of re-radiation from regularly rough surfaces and geometric shapes is a "deterministic" one and a statistical description is not required.

I. B The Description of the Completed Research

The goal of this study was the description, both theoretical and experimental, of the re-radiation in all directions (omnidirectional re-radiation) of acoustic waves from randomly rough surfaces and the determination of the applicability of the results of the acoustic study to the similar problem of electromagnetics. There have been many investigations into this general area of study (see Section III A) but all with the exception of a few have been restricted to the case of backscattering. However, to make a complete investigation it is necessary to determine the characteristics of the re-radiation from rough surfaces omnidirectionally; by doing this, all phenomena are observed and an opportunity is afforded to test theoretical work over a wider range of angles.

There are many types of randomly rough surfaces for which the re-radiation characteristics can be investigated. These can roughly be categorized in one way by relating the size of the surface irregularity to the wavelength of the radiation. The investigation was restricted to surfaces with structures large with respect to wavelength and that are described as "gently undulating." For surfaces of this type, the re-radiation can be investigated using the method of physical optics or the Kirchhoff method as discussed in Section II B. This approach has been used before and successfully. However, there have been questions raised recently about the use of the method [Hagfors, 1964] and one of the purposes of this work is to determine the validity of this approach.

The re-radiation of acoustic waves from randomly rough surfaces is investigated by determining the re-radiated pressure in the far zone through the use of the Kirchhoff method. This is done for a surface which is generated by a random process which is taken to be stationary and ergodic with a Gaussian distribution of heights, as discussed in Section II C and Appendix II. The surface is not restricted to be perfectly reflecting, as is usually done, but is allowed to be an imperfect reflector; however, it is assumed to be of homogeneous material (see Sections II B and III D). From the re-radiated pressure field the power density is calculated and the separation between reflected and scattered power mentioned earlier is made (see Section III C). The reflected power is shown to decrease

to a negligibly low value for a surface sufficiently rough (as [Davies , 1954] and other workers have shown). Making a restriction to such surfaces, the scattered power is then used to calculate the average differential scattering cross section, which is a particularly convenient and meaningful quantity for the description of scattering (see Section III D). This quantity depends upon the form of the autocorrelation function of surface heights and is calculated for the cases of exponential and Gaussian dependences, i. e., for autocorrelation functions that take the forms

$$r = \exp\left\{-\frac{x}{L}\right\} \quad r = \exp\left\{-\left(\frac{x}{L}\right)^2\right\}$$

To determine the validity of the theory as developed using the method of physical optics, the average differential scattering cross section was experimentally determined for surfaces specially constructed to be gently undulating. Measurements were made omnidirectionally for two surfaces of different roughnesses and different materials; these results are shown graphically in Section III E, and the technique of measurement and the equipment used are described in Sections II B and III C. To make the experiments especially useful in determining the validity of the theory, the statistical parameters of the surfaces were measured and the sample probability distributions of surface heights were computed. It was found that the processes were close to being Gaussian and stationary with the sample correlation coefficients having a functional dependence lying between Gaussian and exponential behavior, the actual variation being closer to Gaussian (see Section III D). The measured values of the statistical parameters were used in the theoretical expression for average differential scattering cross section and values of this quantity were computed for comparison with experiment. This comparison, which is made in Section III E, is a favorable one and the conclusion is reached that the Kirchhoff method is valid as it is used in this work.

The characteristics of the re-radiation of acoustic waves from surfaces are known to be similar in some respects to analogous electromagnetic re-radiation. These similarities have been utilized in acoustic simulations of electromagnetic problems such as scattering in turbulent media and radar backscattering. To determine how closely the scalar

acoustic waves simulate the re-radiation of the vector electromagnetic waves, comparison was made between analogous expressions for the two cases. The electromagnetic expressions used in the comparison were derived through use of the Kirchhoff method and the comparison made is valid only for surfaces which are gently undulating. In making the comparison it was found that under certain conditions an exact simulation of the re-radiation of electromagnetic waves is possible. In other situations, simulations can be made with varying degrees of approximation. These results are contained in Chapter IV.

CHAPTER II THE REFLECTION AND SCATTERING
OF ACOUSTIC WAVES FROM ROUGH SURFACES

II. A The Re-radiation from a Rough Surface; the Several Methods of Calculation

A calculation of the re-radiation of acoustic (and electromagnetic) waves from surfaces which are randomly rough must give the quantities which describe the process and relate these to the parameters which define it. These quantities are the probability distributions of the amplitude and phase of the re-radiated field, the mean and variance of the field and the mean of its intensity. This does not provide a complete description in a statistical sense but from the viewpoint of application it is sufficient. The parameters defining the process are those describing the medium in which the source and the observation point are located and those describing the randomly rough surface. The medium is taken to be an ideal fluid defined by its density ρ and compressibility K . The set of parameters defining the surface is composed of two sub-sets which are taken to be independent. The roughness of the surface is given by the statistical parameters which describe the random height process. The material parameters are the other set which complete the description of the surface. These parameters can also have a random variation; however, the material is taken to be homogeneous and is defined by specifying the Lamé constants λ' and μ . For the ideal fluid, the rigidity, μ , is zero and $\lambda' = K$.

The acoustic field in an ideal fluid is scalar and is defined completely by giving the pressure ϕ . This is seen from Constant [1954] who gives the following equations which describe the acoustic field

$$\rho \frac{\partial \vec{v}}{\partial t} = -\nabla \phi \quad \nabla \cdot \vec{v} = -K \frac{\partial \phi}{\partial t}$$

where \vec{v} is the velocity vector which has its time derivative given by the gradient of the scalar pressure. From these equations, the wave equation for ϕ is obtained; this is

$$\nabla^2 \phi = \rho k \frac{\partial^2 \phi}{\partial t^2}$$

Therefore, the solution to the re-radiation problem is a scalar quantity which must satisfy the wave equation; at the bounding surface of the fluid the situation is more complicated. A scalar wave propagating in an ideal fluid and incident upon the boundary of a solid excites both scalar and vector (shear) waves which propagate in the solid, which is taken to be infinite.

The boundary conditions that the solution must satisfy are that the normal stresses and the normal velocity are continuous across the interface and the tangential stress goes to zero [Ewing, Jardetsky, and Press, 1957]. Since the tangential stresses are zero at the surface, "slippage" occurs.

The acoustic wave incident upon the rough, planar surface, $z = \xi(x, y)$, (see figure I.1) is taken to be a plane wave

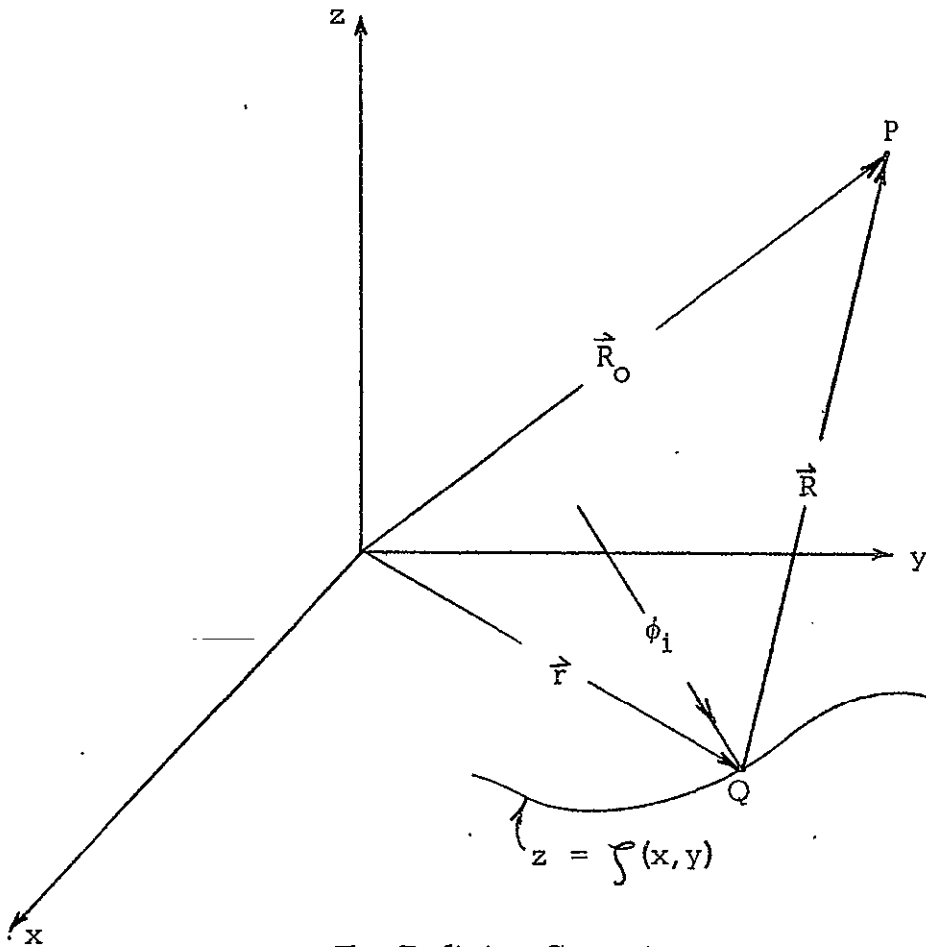
$$\phi_i = \phi_+ e^{-i \vec{k}_i \cdot \vec{r}}$$

where $\vec{k}_i = k (\hat{i} \cos \theta_{ix} + \hat{j} \cos \theta_{iy} + \hat{k} \cos \theta_{iz})$ is the incident wave vector, k is the wave number and $\vec{r} = \hat{i}x + \hat{j}y + \hat{k}z$ is the radius vector of the coordinate system. Harmonic time variation of the form $e^{i\omega t}$ is assumed. The total field at the observation point P is

$$\phi = \phi_i + \phi_r$$

where ϕ_r is the field re-radiated from the surface and is the quantity to be determined.

The calculation of the re-radiated field is one which has been done many times in many different ways, both for the acoustic case and for the more complicated electromagnetic case as well. In general, techniques



The Defining Geometry

Figure II. 1

used for the one case are applicable for the other. These techniques can be roughly classed into two areas with, of course, some important exceptions. These two classifications are: the Rayleigh method, named after Lord Rayleigh, and the physical optics or Kirchhoff method. The

several methods of calculations falling into these two broad classifications, as well as others, are discussed and compared in a review paper by Lysanov [1958] and in a book by Beckmann [1963]. The methods which are Rayleigh methods and several others are discussed here to show the relation between these methods and the method of physical optics which is discussed extensively and used in the next section. The methods chosen for discussion and comparison were selected to be illustrative and not because of any special relative importance. There are several other methods not presented such as those of Twersky [1951a] and Ament [1956] which are important but are sufficiently different in approach so as not to contribute materially to this discussion.

The Rayleigh Method

The Rayleigh method utilizes a superposition of plane waves to express the field re-radiated from an uneven (not necessarily randomly rough) surface. The technique was introduced by Rayleigh [1896] who was concerned with the reflection and scattering of normally incident acoustic waves from periodically uneven surfaces. This method was extended to angles of incidence other than normal and used by La Casce and Tamarkin [1956] for the prediction of results of an experiment in which sinusoids were used as the reflecting surface for acoustic waves. Meecham [1956a] used a variational technique to improve the accuracy of the solutions and Parker [1956] has generalized the method for the acoustic case by introducing integral transform techniques. Rice [1951], working with electromagnetic waves, extended the method to randomly rough surfaces and Lapin [1964] has done a similar thing for the acoustic case.

The rough surface is expressed in a Fourier series

$$\zeta(x,y) = \sum_{m,n=-\infty}^{\infty} P(m,n) \exp\{-i\alpha(m x + n y)\}$$

where $\alpha = 2\pi/\Lambda$ and Λ is the wavelength of the fundamental component which is considered arbitrarily large. The field re-radiated from $\zeta(x,y)$ is

$$\phi_r = \sum_{m,n=-\infty}^{\infty} A_{mn} \exp\{-ia(mx+ny) - ib(m,n)z\}$$

where

$$b(m,n) = \begin{cases} [k^2 - a^2 m^2 - a^2 n^2]^{1/2} & m^2 + n^2 < (k/a)^2 \\ -i[a^2 m^2 + a^2 n^2 - k^2]^{1/2} & m^2 + n^2 > (k/a)^2 \end{cases}$$

For each set of integers (m,n) , there is a plane wave of amplitude A_{mn} traveling in the direction given by the direction cosines

$$\cos \theta_{0x} = \frac{am}{k} \quad \cos \theta_{0y} = \frac{an}{k} \quad \cos \theta_{0z} = \frac{\text{Re } b(m,n)}{k}$$

For a randomly rough surface, $P(m,n)$ and the A_{mn} become statistical quantities. At the boundary, $\zeta(x,y)$, the boundary conditions on the total field are applied; from this a set of linear equations in the unknowns A_{mn} is obtained. In general, this set is not solvable and approximations must be made. To obtain an approximate solution, it is necessary to require that

$$|\zeta(x,y)k| \ll 1 \quad \left| \frac{\partial \zeta(x,y)}{\partial x} \right| \ll 1 \quad \left| \frac{\partial \zeta(x,y)}{\partial y} \right| \ll 1$$

For the randomly rough surfaces, the approximate solution for ϕ_r is used to compute the statistical quantities which complete the description of the re-radiation. This is done by making use of the statistical properties of the $P(m,n)$.

The Rayleigh method, as far as the formal technique is concerned, is an "exact" one; i. e. it does not require the use of approximate boundary conditions (as the physical optics method does). However, the method is restricted in its application to surfaces which are gently sloping and have deviations small relative to a wavelength.

The Integral Equation Method

The integral equation method makes use of Green's theorem to obtain an integral equation for the field on the irradiated surface. The kernel of this equation, upon solution, is integrated over the surface to obtain the re-radiated field. Lyzanov [1956] and Meecham [1956], working independently, developed this method for the acoustic case and the electromagnetic case when the incident wave is horizontally polarized and applied it to surfaces which are periodically uneven in one dimension and perfectly reflecting.

The re-radiated field at the observation point P is written as an integral using Green's theorem [Stratton, 1941]; this is often called the Helmholtz integral and takes the form

$$\phi_i(P) = \frac{1}{4\pi} \iint_S [G(P|Q) \nabla_Q \phi(Q) - \phi(Q) \nabla_Q G(P|Q)] \cdot \vec{n} \, dS \quad \text{II.1}$$

where Q is the source point on the surface of integration S , $G(P|Q)$ is the Green's function for free space, $\phi(Q)$ is the total field on the surface, ∇_Q is the gradient operator which operates on points at the surface and \vec{n} is the unit normal of the surface. For three dimensional problems the Green's function takes the form

$$G(P|Q) = \frac{e^{-ik|\vec{R}_0 - \vec{r}|}}{|\vec{R}_0 - \vec{r}|} = \frac{e^{-ikR}}{R} \quad \text{II.2}$$

where \vec{R} is the vector from Q to P . The total field at P is the sum of the incident and re-radiated fields; this is

$$\begin{aligned} \phi(P) &= \phi_i(P) + \phi_r(P) \\ &= \phi^+ e^{-ik_1 \cdot \vec{r}} + \frac{1}{4\pi} \iint_S [G(P|Q) \nabla_Q \phi(Q) \\ &\quad - \phi(Q) \nabla_Q G(P|Q)] \cdot \vec{n} \, dS \end{aligned} \quad \text{II.3}$$

When the observation point becomes a surface point, eq. (II. 3) becomes an integral equation with the unknown being the field on S . When the field and its normal derivative on S are known, $\phi_r(P)$ is found using eq. (II. 1).

The integral equation is greatly simplified if the surface is one for which $\phi(Q) = 0$, or a free surface. For this case, eq. (II. 3) becomes

$$-\phi^+ e^{-i\vec{k}_1 \cdot \vec{r}_s} = \frac{1}{4\pi} \iint_S G(P|Q) \nabla_Q \phi(Q) \cdot \vec{n} dS$$

where \vec{r}_s denotes evaluation on S . The unknown for this equation is $\nabla_Q \phi(Q)$ and solution for this quantity completes the problem, for again $\phi_r(P)$ can be found using eq. (II. 1). The solution for $\nabla_Q \phi(Q)$ can be accomplished using a Wiener-Hopf technique [Morse and Feshbach, 1953], but it is first necessary to approximate the kernel. The approximation, as in the case of the Rayleigh method, leads to a restriction in the application of the method to moderately smooth surfaces. Meecham shows for the two dimensional case that the surface must be one for which

$$|k \zeta(x,y)| < 1 \quad \left[\frac{\partial \zeta(x,y)}{\partial x} \right]^2 \ll 1$$

Lysanov, quoting work not available, obtains a different condition for the same problem; he requires

$$\frac{1}{2} \left[\frac{\partial \zeta(x,y)}{\partial x} \right]^2 \ll 1 \quad \left| k \zeta(x,y) \frac{\partial \zeta(x,y)}{\partial x} \right| \ll 1$$

Also, from the above, the method is not applicable to surfaces that are not free.

The Method of Small Perturbations

The method of small perturbations is a technique by which an approximation to the field on the mean surface is found and used in the Helmholtz integral which now is an integration over this mean surface. Miles [1954] has used this method in studying acoustic re-radiation and Bass and Bocharov [1957] and Feinberg [1951] have applied it to the electromagnetic case.

The approximate field on the mean surface is found by making a transfer of the boundary conditions to the mean surface from the perturbed surface and then performing an iteration of solutions. The transfer of the boundary conditions is accomplished by expanding the total field, ϕ , in a power series about the mean surface $z = M = 0$ with respect to $z = \zeta(x, y)$ and then substituting this series into the boundary conditions on $z = \zeta(x, y)$. The series for ϕ is

$$\phi = \phi(z=0) + \left(\frac{\partial\phi}{\partial z}\right)_{z=0} \zeta + \frac{1}{2} \left(\frac{\partial^2\phi}{\partial z^2}\right)_{z=0} \zeta^2 + \dots$$

The solution for the total field is taken to be

$$\phi = \phi^{(0)} + \phi^{(1)} + \phi^{(2)} + \dots$$

where $\phi^{(0)}$ is $O(\zeta^0)$ (this is the sum of ϕ_1 and its specular reflection from the mean surface), $\phi^{(1)}$ is $O(\zeta^1)$, etc. In the iteration of solutions in the transferred boundary conditions $\phi^{(1)}$ is found in terms of $\phi^{(0)}$, $\phi^{(2)}$ in terms of $\phi^{(1)}$, etc.

The success of this method depends upon the deviations from the mean surface being small; Miles found that it was necessary to require

$$|k\zeta(x, y)| \ll 1 \quad \left| \frac{\partial\zeta(x, y)}{\partial x} \right| \ll 1 \quad \left| \frac{\partial\zeta(x, y)}{\partial y} \right| \ll 1$$

Therefore, this method is restricted to the same class of surfaces as the Rayleigh method and the integral equation method (Lysanov's class of surfaces is different, however) and there is, perhaps, nothing to recommend one of these methods over the other. The essential difference between the methods lies in the treatment of the boundary conditions. The Rayleigh method uses the exact boundary conditions and an approximation is required to obtain a solution. The integral equation method and the method of small perturbations are techniques in which approximate fields on the boundary are determined and then used in the Helmholtz integral.

II. B The Method of Physical Optics and the Consideration of Imperfect Reflectivity

The re-radiation of waves incident upon a rough surface cannot be determined by the Rayleigh method or by any of the other methods described above when the surface irregularities are not small relative to a wavelength (Lysanov's method is an exception). This restriction limited greatly the scattering and reflection phenomena that could be described and predicted until the development of a method by Brekhovskikh [1951] that allows the treatment of large-scale roughness. This is the method of physical optics, often called the Kirchhoff method because of the similarity to Kirchhoff's postulate in diffraction theory.

Because of its applicability to large-scale roughness, the Kirchhoff method has been used often in the solution of practical problems, mostly in the area of electromagnetic scattering with many applications to scattering from the moon. An early application was that of Isakovich [1952] who was the first to apply the method to the scattering of acoustic and electromagnetic waves from randomly rough surfaces, Brekhovskikh's treatment being restricted to regularly rough surfaces. Working in the area of acoustics, Eckart [1953] used the method to describe scattering from the surface of the sea. Davies [1954], in the first use of the method to predict radar return from natural surfaces, obtained a rough description of his own data on sea clutter [Davies and McFarlane, 1946]. Several important developments in the method were made by Hoffman [1955] whose results are used later in this chapter. Use of the method in predicting radar return from the earth was made by Hayre and Moore [1961]. Applications to lunar scattering have been made by Hughes [1961], Hayre [1961], Hagfors [1961, 1964], Daniels [1961, 1963], Fung [1964], Fung and Moore [1964] and Beckmann [1964].

The method of physical optics is based on the assumption that the incident field is "locally" reflected at a point on the irregular surface as if an infinite plane were tangent to the surface at that point; this is known as the "Kirchhoff Approximation." Clearly, this fundamental assumption does not restrict the method to roughness of any particular size relative to

a wavelength; it does, however, restrict its use to surfaces which are "locally flat" with respect to a wavelength. Brekhovskikh's criterion for applicability is

$$4\pi R_c \cos \theta \gg \lambda$$

where R_c is the radius of curvature of the surface at the point, θ is the local angle of incidence that $(-\vec{k}_i)$ makes with the unit normal \vec{n} , and λ is the wavelength. If the material parameters are allowed to vary, a restriction as to their variation must also be made.

There are several complications of a fundamental nature that arise in the use of the Kirchhoff method. One of these is the occurrence of multiple scattering, or secondary reflection. The method does not deny the presence of multiple scattering but, at present, there is no way to take it into account. All earlier applications have neglected it and this is done here. The other methods described above allow multiple scattering and tacitly account for it. The second complication is that of the over-shadowing of one part of the surface by another and the consequent reduction of the irradiated area, particularly at low grazing angles. Beckmann [1964] and Bass and Fuks [1964] have recently investigated this. In the work here, restriction is made to surfaces smooth enough to allow overshadowing to be neglected.

The total field at a point on the irradiated surface is written as the sum of the incident field evaluated at this point and the "local" reflection of the incident field. This is

$$\phi(Q) = \phi_i + \phi_i \Gamma = \phi_i e^{-i\vec{k}_i \cdot \vec{r}} (1 + \Gamma) \quad \text{II. 4}$$

where Γ is the "infinite plane" or Fresnel reflection coefficient [Stratton, 1941]. In general, for a wave incident in an ideal fluid upon a semi-infinite solid surface, the reflection coefficient is [Ewing, Jardetsky, and Press, 1957]

$$\Gamma = \frac{-\rho d c^4 / (\beta')^2 + \mu' a \left\{ \left[\frac{c^2}{(\beta')^2} - 2 \right]^2 + 4 d e \right\}}{\rho d c^4 / (\beta')^2 + \mu' a \left\{ \left[\frac{c^2}{(\beta')^2} - 2 \right]^2 + 4 d e \right\}} \quad \text{II. 5}$$

$$\text{where } c = \frac{\sqrt{k/\mu}}{\sin \theta}$$

$$d = \sqrt{\left\{ \frac{k\rho'}{\rho[(\lambda')' + \mu'] \sin^2 \theta} \right\} - 1}$$

$$e = \sqrt{\frac{k\rho}{\rho\mu' \sin^2 \theta} - 1}$$

$$a = \cot \theta$$

where the primes refer to the parameters of the solid and θ is the local angle of incidence defined above. The unit normal is

$$\vec{n} = \frac{-\hat{x} Z_x - \hat{y} Z_y + \hat{k}}{\sqrt{1 + Z_x^2 + Z_y^2}}$$

where Z_x and Z_y are the partial derivatives of z with respect to x and y , respectively, and $z = \zeta(x, y)$. Since $\zeta(x, y)$ is a function of position on the surface, \vec{n} is also and, consequently, θ and Γ . Therefore, the reflection coefficient is a random function of the random variable and, through this functional relationship and that of eq. (II.4), the total field on the surface becomes a random variable. This was first pointed out by Brekhovskikh and later by Aksenov [1958] and Kovalev and Pozdnyak [1961].

When the total field on the surface is known, the re-radiated field at P is given by the Helmholtz integral; using the three dimensional Green's function given earlier, this gives

$$\phi_i(P) = \frac{1}{4\pi} \iint_S \left[\frac{e^{-ikR}}{R} \nabla_Q \phi(Q) - \phi(Q) \nabla_Q \frac{e^{-ikR}}{R} \right] \cdot \vec{n} ds \quad \text{II.6}$$

where $\phi(Q)$ is given by eq. (II.4). At this point, the analysis is usually specialized to a perfectly reflecting surface; i. e., one for which $|\Gamma| = 1$. However, this specialization can be avoided if the dependence of Γ upon Z_x and Z_y is brought out and made use of by expanding Γ in a Taylor series

in Z_x and Z_y about the mean angle of incidence, α . For most surfaces of interest, this is the angle between $(-\vec{k}_1)$ and \vec{k} . A similar thing has been done for the electromagnetic case by Kovalev and Pozdinyak [1961] and Fung, Moore, and Parkins, [1965]. The expansion is

$$\Gamma(\theta) = \Gamma(\alpha) + B_{1x}Z_x + B_{1y}Z_y + B_{2x}Z_x^2 + B_{2xy}Z_xZ_y + B_{2y}Z_y^2 + \dots \quad \text{II.7}$$

where

$$B_{1x} = \left(\frac{\partial \Gamma}{\partial Z_x} \right)_{Z_x=0, Z_y=0}, \quad B_{1y} = \left(\frac{\partial \Gamma}{\partial Z_y} \right)_{Z_x=0, Z_y=0}, \quad B_{2x} = \frac{1}{2} \left(\frac{\partial^2 \Gamma}{\partial Z_x^2} \right)_{Z_x=0, Z_y=0} \text{ etc.}$$

The coefficients in the expression are not necessarily small. This is probably best seen by considering a surface rough in only one dimension. In this case the B's are approximately the slope and higher derivatives of the curve of reflection coefficient against angle of incidence, which is, in general, complicated [Ergin, 1952]. Using eq. 's (II.4) and (II.7) in eq. (II.6) and specializing to the far field where $k \gg \frac{1}{R}$ gives

$$\begin{aligned} \phi_r(P) = & \frac{1}{4\pi} \iint_S \frac{e^{-ikR}}{R} \left\{ -i\vec{n} \cdot \vec{k}_1 e^{-i\vec{k}_1 \cdot \vec{r}} \phi^+ \left[1 - \Gamma(\alpha) - B_{1x}Z_x - B_{1y}Z_y - \dots \right] \right. \\ & + \phi^+ e^{-i\vec{k}_1 \cdot \vec{r}} \vec{n} \cdot \left[\vec{i} (B_{1x}Z_{xx} + B_{1y}Z_{xy} + \dots) + \vec{j} (B_{1y}Z_{yy} + B_{1x}Z_{xy} + \dots) \right] \\ & \left. - \phi^+ e^{-i\vec{k}_1 \cdot \vec{r}} \left[1 + \Gamma(\alpha) + B_{1x}Z_x + B_{1y}Z_y + \dots \right] (i\vec{k}_0 \cdot \vec{n}) \right\} dS \end{aligned}$$

II.8

where $\vec{k}_0 = \vec{i}_R k$. The surface is now restricted to be an aperture of a size small enough to permit the approximation

$$\vec{r}_R \approx \vec{r}_{R_0} \quad R \approx R_0 - \vec{r} \cdot \vec{r}_{R_0}$$

yet large enough to have sufficient variation to define the random process of the surface. Substitution of this approximation into eq. (II.8) gives the result

$$\begin{aligned} \phi_r(P) = & \frac{\phi^+ e^{-ikR_0}}{4\pi R_0} \iint_S \left\{ (-i\vec{n} \cdot \vec{k}_1) \left[1 - \Gamma(\alpha) - B_{1x}Z_x - B_{1y}Z_y - \dots \right] \right. \\ & + \vec{n} \cdot \left[\vec{k} (B_{1x}Z_{xx} + B_{1y}Z_{xy} + \dots) + \vec{j} (B_{1y}Z_{yy} + B_{1x}Z_{xy} + \dots) \right] \\ & \left. - \left[1 + \Gamma(\alpha) + B_{1x}Z_x + B_{1y}Z_y + \dots \right] (i\vec{k}_0 \cdot \vec{n}) \right\} e^{i\vec{K} \cdot \vec{r}} dS \end{aligned}$$

II.9

where $\vec{K} = \vec{k}_0 - \vec{k}_1$, and the variation of R is considered to be important only in the exponential. Eq. (II.9) is the far field expression for the re-radiated field which results from the use of the method of physical optics.

The transition from physical optics to geometric optics, and to some techniques of calculation [Muhleman, 1964], is made by applying the method of stationary phase [Wilf, 1962] to eq. (II.9). The integral for $\phi_r(P)$ has a stationary point whenever the exponent

$$\vec{K} \cdot \vec{r} = K_x x + K_y y + K_z z = (k_{0x} - k_{1x})x + (k_{0y} - k_{1y})y + (k_{0z} - k_{1z})z$$

is such that

$$\frac{\partial \vec{K} \cdot \vec{r}}{\partial x} = \frac{\partial \vec{K} \cdot \vec{r}}{\partial y} = 0$$

The condition for stationarity at a point is then

$$\frac{\partial \mathcal{F}(x,y)}{\partial x} (k_{0z} - k_{1z}) + (k_{0x} - k_{1x}) = \frac{\partial \mathcal{F}(x,y)}{\partial y} (k_{0z} - k_{1z}) + (k_{0y} - k_{1y}) = 0$$

or the two conditions

$$\frac{\partial \mathcal{F}(x,y)}{\partial x} = - \frac{(k_{0x} - k_{1x})}{(k_{0z} - k_{1z})} \quad \frac{\partial \mathcal{F}(x,y)}{\partial y} = - \frac{(k_{0y} - k_{1y})}{(k_{0z} - k_{1z})}$$

must be satisfied simultaneously at a point (x, y) . Applying these conditions to the expressions for \vec{n} , eq. (II. 6), it is easily shown that the stationary points are those points that have a normal with the property that

$$\vec{n} \cdot \vec{k}_1 = -\vec{n} \cdot \vec{k}_0$$

These are the points at which the fundamental laws of reflection are satisfied relative to the observation point P . For example, in the specular direction ($k_{0x} = k_{1x}$, $k_{0y} = k_{1y}$, $k_{0z} + k_{1z} = 0$) the conditions for a stationary point lead to

$$\frac{\partial \mathcal{F}(x,y)}{\partial x} = \frac{\partial \mathcal{F}(x,y)}{\partial y} = 0$$

or only those parts of the surface which have tangents parallel to the mean surface (taken to be $z = 0$) contribute and the reflection coefficient is that for the mean plane taken at the angle α . For the backscatter case ($\vec{k}_0 = -\vec{k}_1$), the reflection coefficient is that for normal incidence and only those regions which have normals oriented back towards the source make a contribution to the return.

The method of stationary phase is not an exact one and the results obtained are only approximate. Wilf shows that the correction term to the first approximation is $O(k^{-3/5})$ while the approximation itself is $O(k^{-1/2})$; therefore, a large value of k is needed for a good approximation. To apply the method of physical optics it is only required that

$$4\pi R_c \cos \theta \gg \lambda$$

or

$$2\pi R_c \cos \theta \gg \frac{1}{k}$$

which can be satisfied for small k as long as the radius of curvature is large enough [Fung, Moore, and Parkins, 1965]. Therefore, physical optics cannot be supplanted by geometric optics except under certain circumstances, and methods which do so must be carefully applied.

II. C The Average Power and its Separation into Scatter and Specular Components

The field re-radiated from the rough surface, ϕ_r , is a complex random variable which depends upon the random process $z = \zeta(x, y)$. The statistical description of the re-radiation is facilitated by a resolution of ϕ_r into two component fields: the specular, or coherent, field and the scatter, or incoherent, field [Twersky, 1963], [Moore, 1957], [Hayre, 1962]. The specular field is defined as

$$\langle \phi_r \rangle = B e^{i b} \quad \text{II.10}$$

where the brackets denote the configuration average which is taken over an ensemble of surfaces. The term coherent is appropriate since B and b are determined experimentally in the same manner as for steady, coherent fields. Using this definition of the specular field as a basis, the scatter field ϕ_s is defined as

$$\phi_r = \langle \phi_r \rangle + \phi_s \quad ; \quad \phi_s = D e^{i d} \quad \text{II.11}$$

where $\langle \phi_s \rangle = 0$. The intensities of the two component fields can be shown to obey the relation

$$\langle \phi_r \phi_r^* \rangle = B^2 + D^2$$

where the asterisk denotes the complex conjugate. The average far field power density of the re-radiated field is given by

$$\vec{\lambda}_{R_0} \langle P \rangle = \frac{1}{2} \text{Re} \langle \phi_r \phi_r^* \rangle Z_0 \vec{\lambda}_{R_0} \quad \text{II.12a}$$

$$\vec{\lambda}_{R_0} \langle P \rangle = \langle \phi_r \phi_r^* \rangle Z_0 \vec{\lambda}_{R_0} \quad \text{II.12b}$$

where $Z_0 = \sqrt{K/\rho}$ which is real for the ideal fluid assumed here. In terms of the specular and scatter intensities, this is

$$\langle P \rangle = \frac{1}{2} (B^2 + D^2) Z_0 \quad \text{II.13}$$

The expression for the far field power density is obtained by using eq. (II.9) in eq. (II.12b). This calculation is done under the restriction that the surface is smooth enough to neglect the second degree terms of the surface in the expression for ϕ_r . Using the expression for the differential area

$$dS = dx dy = \sqrt{1 + Z_x^2 + Z_y^2}$$

and the expression for \vec{n} given earlier, the power density is, under this restriction

$$\begin{aligned} \rho = \frac{Z_0}{2} \left(\frac{\phi^+}{4\pi R_0} \right)^2 \iiint_S \iiint_{S'} e^{i\vec{k} \cdot (\vec{r} - \vec{r}')} & \left\{ \left[(k_{1z} + k_{0z}) + \Gamma(\alpha)(k_{0z} - k_{1z}) \right] \right. \\ & + Z_x \left[B_{1x}(k_{0z} - k_{1z}) + \Gamma(\alpha)(k_{1x} - k_{0x}) - (k_{1x} + k_{0x}) \right] \\ & \left. + Z_y \left[B_{1y}(k_{0z} - k_{1z}) + \Gamma(\alpha)(k_{1y} - k_{0y}) - (k_{1y} + k_{0y}) \right] \right\} \\ & \left\{ \left[(k_{0z} + k_{1z}) + \Gamma^*(\alpha)(k_{0z} - k_{1z}) \right] \right. \\ & + Z_{x'} \left[B_{1x}^*(k_{0z} - k_{1z}) + \Gamma^*(\alpha)(k_{1x} - k_{0x}) - (k_{1x} + k_{0x}) \right] \\ & \left. + Z_{y'} \left[B_{1y}^*(k_{0z} - k_{1z}) + \Gamma^*(\alpha)(k_{1y} - k_{0y}) - (k_{1y} + k_{0y}) \right] \right\} dx dy dx' dy' \end{aligned}$$

Using the coefficients defined in Appendix I, this is rewritten as

$$\begin{aligned}
 p = \frac{Z_0}{2} \left(\frac{\phi^+}{4\pi R_0} \right)^2 \iiint_S \iiint_{S'} e^{i \vec{k} \cdot (\vec{r} - \vec{r}')} & \left\{ a_1^2 + a_1 a_2^* Z_{x'} \right. \\
 & + a_1^* a_2 Z_x + a_1 a_3^* Z_{y'} + a_1^* a_3 Z_y + a_2 a_2^* Z_x Z_{x'} \\
 & \left. + a_2 a_3^* Z_x Z_{y'} + a_2^* a_3 Z_{x'} Z_y + a_3 a_3^* Z_y Z_{y'} \right\} dx dy dx' dy'
 \end{aligned}
 \tag{II.14}$$

The average of p is a configuration average, to be done over an ensemble of surfaces. The random height process, is assumed to be ergodic and the mean is taken by averaging "along" the process. The process is assumed to be a "single" one as opposed to a composite surface made up of a sum of sub-processes as discussed by Isakovitch [1952] and Beckmann [1964]. The problem of averaging is further simplified here by making the additional assumptions that the random height process is stationary and Gaussian with the parameters being the standard deviation of heights, σ , the mean, and the autocorrelation coefficient, r . The mean is taken to be zero with no loss in generality. The assumption of a Gaussian height distribution is justified by the results of measurements made on the experimental surfaces, as described in Chapter III. The assumption of stationarity for $\zeta(x, y)$ is, perhaps, not wholly warranted in almost any practical situation but it is necessary to make it here to obtain tractable expressions for $\langle p \rangle$.

The average of p is carried out using the work of Hoffman [1955b], the pertinent parts of which are detailed in Appendix II. Making use of the assumptions of ergodicity and stationarity and the expressions in Appendix II, the average of the power density given by eq. (II.14) is

$$\langle P \rangle = \frac{Z_0}{2} \left(\frac{\phi^+}{4\pi R_0} \right)^2 \int_{-l}^l \int_{-l}^l \int_{x-l}^{x+l} \int_{y-l}^{y+l} \left\{ a_1^2 + i k_2 \sigma^2 \frac{\partial \Gamma}{\partial \mu} (a_1 a_2^* + a_1^* a_2) \right.$$

$$\begin{aligned}
& +ik_2\sigma^2\frac{\partial\Gamma}{\partial v}(a_1a_3^*+a_1^*a_3) - a_2a_2^* \left[\sigma^2\frac{\partial^2\Gamma}{\partial\mu^2} + K_2^2\sigma^4\left(\frac{\partial\Gamma}{\partial\mu}\right)^2 \right] \\
& - a_3a_3^* \left[\sigma^2\frac{\partial^2\Gamma}{\partial v^2} + K_2^2\sigma^4\left(\frac{\partial\Gamma}{\partial v}\right)^2 \right] \\
& - (a_2a_3^*+a_2^*a_3) \left[\sigma^2\frac{\partial^2\Gamma}{\partial\mu\partial v} + K_2^2\sigma^4\frac{\partial\Gamma}{\partial\mu}\frac{\partial\Gamma}{\partial v} \right] \Bigg\} \\
& \exp\left\{-\left[K_2^2\sigma^2(1-r)+i(K_x\mu+K_yv)\right]\right\}d\mu dv dx dy
\end{aligned}$$

II. 15

where the change of variables

$$\mu = x' - x \quad v = y' - y'$$

has been made and the aperture has been taken to be square with dimension 2.1. This expression is still general in so far as no explicit assumption has been made regarding the autocorrelation coefficient r , except that it must fall off quite rapidly relative to the dimensions of the aperture in order that the random process, $\zeta(x, y)$, be defined and the average determined with high confidence. It must also, because of the stationarity assumption, be a function only of u and v not of x and y ; i. e., the correlation of the heights does not depend upon absolute position within the aperture.

The resolution of the average power density into scatter and specular components is completed by determining the specular power density and then using eq. (II. 15) to find the scatter power density. From eq's. (II. 10) and (II. 13), the specular power density, $\langle p \rangle_{sp}$, is

$$\langle P \rangle_{sp} = \frac{1}{2} |\langle \phi_r \rangle|^2 Z_0 \quad \text{II. 16}$$

Making the same approximations on eq. (II. 9) that were used in obtaining eq. (II. 14) and using the results of Appendix II, the average field is

$$\langle \phi_r \rangle = \frac{-i\phi^+}{4\pi R_0} e^{-\frac{(k_z\sigma)^2}{2}} \iint_S a_i e^{i(k_x x + k_y y)} dx dy$$

Therefore, the specular power density is

$$\langle P \rangle_{sp} = \frac{1}{2} \left(\frac{\phi^+}{4\pi R_0} \right)^2 16 a_i^2 e^{-\frac{(k_z\sigma)^2}{2}} \frac{\sin^2 k_x l \sin^2 k_y l}{k_x^2 k_y^2} \quad \text{II.17}$$

for a square aperture of dimension $2l$. Davies [1954] has obtained a similar expression.

The effect of the roughness, as described by the parameters σ and r , upon the relative magnitudes of the specular and scatter power densities is determined using eq. (II.17). The power re-radiated from a smooth aperture is

$$P = \iint_{\sigma=0} \langle P \rangle_{sp} \left| \vec{\lambda}_{R_0} \cdot \vec{n}' \right| dS$$

where the integration takes place over the halfspace above the aperture (in the far field). The specular power re-radiated when the surface is rough is given by this same integral with $\sigma \neq 0$. The ratio of the latter to the former is not greater than

$$\exp \left\{ - \left(\frac{2\pi\sigma}{\lambda} \omega_s \theta_{12} \right)^2 \right\}$$

Therefore, as σ increases and the surface becomes rougher, a smaller fraction of the incident power is specularly reflected and an increasingly larger amount is scattered. When $\left(\frac{2\pi\sigma}{\lambda} \omega_s \theta_{12} \right)^2$ is about five or greater, for most practical purposes, there is total conversion to scatter power. It is important to note that this conversion depends only upon σ and not r .

Clearly, the occurrence of

$$\langle \phi_r \rangle = \text{Re } i^b \approx 0$$

as the roughness increases denotes the total conversion to scatter power. At this point, the field is given by

$$\phi_r = \langle \phi_r \rangle + D e^{i d}$$

$\approx D e^{i d}$

as described above. Beckmann [1963] has shown that the amplitude D of the scatter field is Rayleigh distributed; i. e.

$$\Phi(D) = \begin{cases} \frac{D}{M^2} e^{-D/2M^2} & D \geq 0 \\ 0 & D \leq 0 \end{cases}$$

where Φ denotes the probability density function, and the phase, d , is uniformly distributed from zero to 2π . The uniformity of the phase distribution indicates that the scatter field (now the total field) is given completely by its intensity which can be found from eq. (II.15).

The resolution of the total power density into components is accomplished in a more straight-forward manner by operating directly on eq. (II.15), although it is necessary to make use of eq. (II.17). The exponential in the integrand of eq. (II.15) is written using a power series as

$$e^{-k_z^2 \sigma^2 (1-r)} = e^{-k_z^2 \sigma^2} \sum_{n=0}^{\infty} \frac{(k_z^2 \sigma^2 r)^n}{n!} \quad \text{II.18}$$

Similar expansions have been made but in a more specialized way by Clarke [1963a] and [Fung 1964]. Using this expansion in eq. (II.15), the first term of the integral becomes

$$\frac{Z_0}{2} \left(\frac{\phi^+}{4\pi R_0} \right)^2 \int_{-l}^l \int_{-l}^l \int_{x-l}^{x+l} \int_{y-l}^{y+l} \frac{1}{q_1^2} \sum_{n=0}^{\infty} \frac{(k_z^2 \sigma^2 r)^n}{n!} e^{-i(k_x u + k_y v)} du dv dx dy$$

II.19

The zeroth term in this infinite series of integrals (after interchanging summation and integration) is recognized from eq. (II.17) to be the specular power density. The other terms in this summation beginning with $n = 1$ and the remaining terms in the integral are scatter power-density terms. The terms in eq. (II.19) starting with $n = 1$ comprise what is often called the "quasi-specular" term primarily, it seems, because it does not involve the partial derivatives of the surface.

The expression for specular power density obtained from eq. (II.18) does not contain the autocorrelation coefficient (because it is the $n = 0$ term); however, all other terms, the quasi-specular and the partial derivative terms, do. Because of this, the integrand of the integral for the scatter power density falls off as the distance from a point on the u, v surface increases as long as the partial derivatives of the autocorrelation coefficient and their products are approximately of the same order as the autocorrelation coefficient itself. Assuming this is so, the integration over u and v is therefore a summation of the contributions made by the elements of the surface over which there is correlation of surface heights. Because r is a function of u and v only, the integration over u and v is a function of x and y only through the limits. This function, again because of the assumption of stationarity, is a constant function of x and y with variation only near the edge of the aperture. This variation constitutes only a small fraction of the total because the aperture is assumed to be large relative to the decay of the autocorrelation coefficient. Therefore, the integration over x and y is a linear superposition of the contributions from all parts of the surface with the portions from the edges being small providing the aperture is large relative to the variations of the surface. This is in contrast to the integration for the specular power density from which it is seen that the re-radiation from the different regions of the surface must add in phase to constitute a return. Also, it is this linear superposition of powers from regions of the surface that marks the difference between scattering from surfaces that are randomly rough and those which are regularly rough.

II. D The Average Differential Scattering Cross Section and its Calculation

When the conversion to scatter power is complete, the specular field being essentially zero, the re-radiation is described completely by giving the variation of its intensity or scatter power density as a function of the angle of incidence and angles of observation. This variation is given in a very meaningful way by introducing the average differential scattering cross section [Kerr, 1951]. This quantity is defined as the average power scattered per unit solid angle, per unit incident power density, per unit area of the mean scattering surface, and is usually denoted by σ_0 . This definition is motivated by the fact that power is scattered on a per unit area basis for a sufficiently rough surface, as described above. Clearly, the differential scattering cross section cannot describe the re-radiation when both specular and scatter components are present; however, the definition can be applied to the scatter component only and a reflection coefficient introduced for the specular component.

Assuming the specular component is negligible, the expression for σ_0 is obtained by applying the definition to eq. (II.15). In making this application it is necessary to make several approximations. These are best made after eq. (II.15) is simplified through a series of partial integrations. The first and second derivatives of the surface with respect to u and v are written as

$$\frac{\partial^2 \Gamma}{\partial u^2} e^{k_z^2 \sigma^2 r - i(k_x u + k_y v)} = \frac{\partial}{\partial u} \left[\frac{\partial \Gamma}{\partial u} e^{k_z^2 \sigma^2 r - i(k_x u + k_y v)} \right]$$

$$- \left[\left(\frac{\partial \Gamma}{\partial u} \right)^2 k_z^2 \sigma^2 - i k_x \frac{\partial \Gamma}{\partial u} \right] e^{k_z^2 \sigma^2 r - i(k_x u + k_y v)}$$

$$\frac{\partial^2 \Gamma}{\partial \nu^2} e^{k_2^2 \sigma^2 r - i(K_x \mu + K_y \nu)} = \frac{\partial}{\partial \nu} \left[\frac{\partial \Gamma}{\partial \nu} e^{k_2^2 \sigma^2 r - i(K_x \mu + K_y \nu)} \right]$$

$$- \left[\left(\frac{\partial \Gamma}{\partial \nu} \right)^2 k_2^2 \sigma^2 - i K_y \frac{\partial \Gamma}{\partial \nu} \right] e^{k_2^2 \sigma^2 r - i(K_x \mu + K_y \nu)}$$

II. 20b

$$\frac{\partial^2 \Gamma}{\partial \mu \partial \nu} e^{k_2^2 \sigma^2 r - i(K_x \mu + K_y \nu)} = \frac{\partial}{\partial \mu} \left[\frac{\partial \Gamma}{\partial \nu} e^{k_2^2 \sigma^2 r - i(K_x \mu + K_y \nu)} \right]$$

$$- \left[\left(\frac{\partial \Gamma}{\partial \mu} \right) \left(\frac{\partial \Gamma}{\partial \nu} \right) k_2^2 \sigma^2 - i K_x \frac{\partial \Gamma}{\partial \nu} \right] e^{k_2^2 \sigma^2 r - i(K_x \mu + K_y \nu)}$$

II. 20c

$$\frac{\partial \Gamma}{\partial \mu} e^{k_2^2 \sigma^2 r - i(K_x \mu + K_y \nu)} = \frac{1}{k_2^2 \sigma^2} \frac{\partial e}{\partial \mu} e^{k_2^2 \sigma^2 r - i(K_x \mu + K_y \nu)}$$

$$+ \frac{i K_x}{k_2^2 \sigma^2} e^{k_2^2 \sigma^2 r - i(K_x \mu + K_y \nu)}$$

II. 20d

$$\frac{\partial r e}{\partial u} k_z^2 \sigma^2 r - i(k_x u + k_y v) = \frac{1}{k_z^2 \sigma^2} \frac{\partial e}{\partial v} k_z^2 \sigma^2 r - i(k_x u + k_y v)$$

$$+ \frac{i k_y}{k_z^2 \sigma^2} e^{k_z^2 \sigma^2 r - i(k_x u + k_y v)}$$

II. 20e

Substituting eq. 's (II. 20) into eq. (II. 15) and performing the partial integrations gives

$$\begin{aligned} \langle P \rangle = & \frac{Z_0}{2} \left(\frac{\phi^+}{4\pi R_0} \right)^2 \left[\int_{-l}^l \int_{-l}^l \int_{x-l}^{x+l} \int_{y-l}^{y+l} \left\{ a_1^2 + \frac{i k_x}{k_z^2} \left[i k_z (a_1^* a_2 + a_1 a_2^*) \right. \right. \right. \\ & \left. \left. \left. - i k_x a_2 a_2^* \right] + \frac{i k_y}{k_z^2} \left[i k_z (a_1^* a_3 + a_1 a_3^*) - i k_y a_3 a_3^* - i k_x (a_2 a_3^* + a_2^* a_3) \right] \right\} \right. \\ & \left. e^{-[k_z^2 \sigma^2 (1-r) + i(k_x u + k_y v)]} du dv dx dy \right. \\ & - a_2 a_2^* \sigma^2 \int_{-l}^l \int_{-l}^l \int_{y-l}^{y+l} \left. \frac{\partial r e}{\partial u} e^{-[k_z^2 \sigma^2 (1-r) + i(k_x u + k_y v)]} \right|_{x-l}^{x+l} du dx dy \\ & - a_3 a_3^* \sigma^2 \int_{-l}^l \int_{-l}^l \int_{x-l}^{x+l} \left. \frac{\partial r e}{\partial v} e^{-[k_z^2 \sigma^2 (1-r) + i(k_x u + k_y v)]} \right|_{y-l}^{y+l} du dx dy \\ & - (a_2^* a_3 + a_2 a_3^*) \int_{-l}^l \int_{-l}^l \int_{y-l}^{y+l} \left. \frac{\partial r e}{\partial v} e^{-[k_z^2 \sigma^2 (1-r) + i(k_x u + k_y v)]} \right|_{x-l}^{x+l} du dx dy \end{aligned}$$

$$\begin{aligned}
& + \left[\frac{i k_z (a_1 a_2^* + a_1^* a_2) - i k_x a_2 a_2^*}{k_z^2} \right] \\
& \quad \int_{-l}^l \int_{-l}^l \int_{y-l}^{y+l} e^{-[k_z^2 \sigma^2 (1-r) + i(k_x u + k_y v)]} \Big|_{x-l}^{x+l} du dx dy \\
& + \left[\frac{i k_z (a_1^* a_3 + a_1 a_3^*) - i k_y a_3 a_3^* - i k_x (a_2^* a_3 + a_2 a_3^*)}{k_z^2} \right] \\
& \quad \int_{-l}^l \int_{-l}^l \int_{x-l}^{x+l} e^{-[k_z^2 \sigma^2 (1-r) + i(k_x u + k_y v)]} \Big|_{y-l}^{y+l} du dx dy
\end{aligned}$$

II. 21

In Appendix III it is shown that because of the assumption regarding the decay of the autocorrelation coefficient and its derivatives made earlier, the "integrated out" terms are of the order of the specular term or lower and hence negligible. The definition for σ_0 is now applied to eq. (II. 21) by dividing by the incident power density, $(\phi^+)^2 Z_0 / 2$, multiplying by R_0^2 , and taking the integrand of the integral over x and y ; this gives

$$\sigma_0 = \left(\frac{1}{4\pi} \right)^2 \int_{-l}^l \int_{-l}^l \left\{ a_1^2 + \frac{i k_x}{k_z^2} \left[i k_z (a_1^* a_2 + a_1 a_2^*) - i k_x a_2 a_2^* \right] \right.$$

$$+ \frac{i K_y}{k_z^2} \left[i k_z (a_1 a_3^* + a_1^* a_3) - i k_y a_3 a_3^* - i k_x (a_2 a_3^* + a_2^* a_3) \right] \left. \right\} \\ e^{- \left[k_z^2 \sigma^2 (1-r) + i (k_x u + k_y v) \right]} du dv$$

II. 22

where the variation of the integral with x and y is neglected and the integration takes place over the aperture.

This expression for σ_0 is put in a more tractable form if the region of integration can be made infinite. The difficulty in doing this is that the specular component, while small and negligible, is not zero and will contribute. The $n = 0$ term of eq. (II.19) (the specular term) upon integration over infinite limits will, in fact, yield a Dirac delta function which is a misleading result. The problem can be resolved in two ways. One of these is to use the expansion given by eq. (II.18) and then simply neglect the $n = 0$ term when the region of integration is made infinite. The other solution is to approximate the autocorrelation coefficient in the exponent by the first several terms of a power series about $u = v = 0$; a similar thing has been done by Daniels [1961], Hughes [1962] and Fung [1964]. The approximation is

$$r \approx 1 - A_1 (u^2 + v^2)^{1/2} - A_2 (u^2 + v^2) \quad \text{II. 23}$$

where A_1 and A_2 are greater than or equal to zero in order that $|r| \leq 1$ near the origin. Of the two possible courses, the latter is chosen to avoid a series solution for σ_0 . Substitution of eq. (II.23) into eq. (II.22) gives

$$\sigma_0 = \left(\frac{1}{4\pi} \right)^2 \int_{-\infty}^{\infty} \int_{-\infty}^{\infty} \left\{ a_1^2 + \frac{i k_x}{k_z^2} \left[i k_z (a_1^* a_2 + a_1 a_2^*) - i k_x a_2 a_2^* \right] \right.$$

$$+ \frac{iK_y}{K_z^2} \left[iK_z (a_1^* a_3 + a_1 a_3^*) - iK_y a_3 a_3^* - iK_x (a_2^* a_3 + a_2 a_3^*) \right] \Bigg\}$$

$$\exp \left\{ -K_z^2 \sigma^2 \left[A_1 (u^2 + v^2)^{1/2} + A_2 (u^2 + v^2) \right] - i(K_x u + K_y v) \right\} du dv$$

II. 24

This approximation for σ_0 is recognized to be the Fourier transform (within a constant, depending upon definition) of the integrand with respect to K_x and K_y .

The solution for σ_0 is completed when a choice is made for the autocorrelation coefficient, the A's evaluated, and the integration of eq. (II. 24) carried out. There are a rather large number of possible autocorrelation coefficients from which to choose that have been successful in describing stationary rough surfaces [Hayre, 1962]. The choice is limited, however, to functions which can be closely fit at the origin, $u = v = 0$, by a small number of terms and that are of such a nature that the resulting approximation can be integrated analytically. The integration of eq. (II. 29) can be done analytically only when A_1 or A_2 is zero. The functions which give this tractability and at the same time are successful in the description of rough surfaces are the Gaussian function

$$r = \exp \left\{ -\frac{u^2 + v^2}{L^2} \right\} \quad \text{II. 25}$$

where $A_1 = 0$ and $A_2 = 1/L^2$ and the exponential function

$$r = \exp \left\{ -\left(\frac{u^2 + v^2}{L^2} \right)^{1/2} \right\} \quad \text{II. 26}$$

where $A_2 = 0$ and $A_1 = 1/L$. The quantity L is commonly called the "correlation distance." Clearly, any other function which has a linear or a parabolic behavior near the origin yields a result under the

approximation given by eq. (II. 23) which cannot be distinguished from that obtained using the exponential or the Gaussian functions, respectively.

The calculation of σ_0 for the approximation to the Gaussian function is made by substituting $A_1 = 0$ and $A_2 = 1/L^2$ into eq. (II. 24) and then integrating using the tables of Bierens de Haan [1939]. The result is

$$\sigma_0 = \left\{ \frac{a_1^2}{K_z^2 \sigma^2 / L^2} - \frac{K_x (a_1^* a_2 + a_1 a_2^*)}{K_z^3 \sigma^2 / L^2} - \frac{K_y (a_1^* a_3 + a_1 a_3^*)}{K_z^3 \sigma^2 / L^2} \right. \\ \left. + \frac{K_x^2 a_2 a_2^*}{K_z^4 \sigma^2 / L^2} + \frac{K_y^2 a_3 a_3^*}{K_z^4 \sigma^2 / L^2} + \frac{K_x K_y (a_2^* a_3 + a_2 a_3^*)}{K_z^4 \sigma^2 / L^2} \right\} \\ \frac{\exp \left\{ - \frac{K_x^2 + K_y^2}{(2 K_z \sigma / L)^2} \right\}}$$

II. 28

The terms are arranged in the following order: the quasi-specular or zero degree term is first, the second and third terms are of the first degree arising from the first derivatives of the autocorrelation coefficient, and the remaining terms are of the second degree.

The relative importance of the terms of eq. (II. 28) and the behavior of the important exponential factor are determined primarily by the magnitude of the quantity $2(\sigma/L)^2$ and the manner in which K_x , K_y , and K_z appear, as well as their variation. The quantity $2(\sigma/L)^2$ is the variance of surface slopes as they would be measured on a profile made along any cut

of the surface as discussed in Section III D. As the surface becomes smoother and the slopes smaller the variance of the slopes decreases. This results in the exponential factor decreasing more rapidly as the angle of observation is changed from the specular direction, where $K_x = K_y = 0$ and the exponential is unity. Since all terms except the quasi-specular term have either K_x or K_y or both as a factor and are therefore zero in the specular direction, the quasi-specular term is the dominant one and it takes on the maximum value for σ_0 because of the behavior of the exponential. As the angle of observation moves away from the specular direction, the other terms increase in size and diminish the quasi-specular term in importance. This is so because, roughly, the numerators of these terms are increasing and the denominators decreasing as the angle moves from the specular direction and decreases from the vertical. Finally, as the grazing angle is approached away from the specular direction, it is the second degree terms which dominate. This is so to the extent that K_z does not decrease to the point that $K_z^2 \sigma^2$ is so small that the approximation upon which the result is based is invalidated.

The effect of the reflectivity of the surface at any observation point is determined by the relative size of the terms of eq. (II.28). The constant a_1^2 of the quasi-specular term involves only the value of the reflection coefficient evaluated at the angle of incidence measured with respect to the mean normal \vec{K} . The constants of all other terms are determined in part by the rate of variation of the reflection coefficient with angle of incidence. This means that the power scattered in the specular direction is diminished by a factor determined only by the reflection coefficient, and the magnitude of the reflection coefficient can be measured in a quite straight-forward manner. As the observation point moves away from the specular direction, the other terms increase in importance and the reflection coefficient, of itself, is no longer the determining factor.

It is interesting as well as important to compare the result for the Gaussian correlation function obtained through partial integration to that result obtained through a direct integration of eq. (II.20) after the approximation of eq. (II.23) is made. Making this approximation, and

then substituting $A_1 = 0$, $A_2 = 1/L^2$, and eq. (II.25) into the approximated integral and performing the integration gives the result (a straight-forward but tedious process)

$$\begin{aligned} \sigma_0 = & \frac{a_1^2 \exp\left\{-\frac{K_x^2 + K_y^2}{2(K_2^2 \sigma^2/L)^2}\right\}}{16\pi(K_2^2 \sigma^2/L)^2} - \frac{K_2 K_x (a_1^* a_2 + a_1 a_2^*) \sigma^2 L^2}{(K_2^2 \sigma^2 + 1)^2 16\pi} \\ & \exp\left\{-\frac{K_x^2 + K_y^2}{4(K_2^2 \sigma^2 + 1)/L^2}\right\} - \frac{K_2 K_y (a_1^* a_3 + a_1 a_3^*) \sigma^2 L^2}{(K_2^2 \sigma^2 + 1)^2 16\pi} \exp\left\{-\frac{K_x^2 + K_y^2}{4(K_2^2 \sigma^2 + 1)/L^2}\right\} \\ & + \frac{a_2 a_2^* \sigma^2}{(K_2^2 \sigma^2 + 1)^2 16\pi} \left[\frac{K_x^2}{(K_2^2 \sigma^2 + 1)/L^2} - 2 \right] \exp\left\{-\frac{K_x^2 + K_y^2}{4(K_2^2 \sigma^2 + 1)/L^2}\right\} \\ & + \frac{a_2 a_2^* K_2^2 \sigma^4}{(K_2^2 \sigma^2 + 2)^2 16\pi} \left[\frac{K_x^2}{(K_2^2 \sigma^2 + 2)/L^2} - 2 \right] \exp\left\{-\frac{K_x^2 + K_y^2}{4(K_2^2 \sigma^2 + 2)/L^2}\right\} \\ & + \frac{a_3 a_3^* \sigma^2}{(K_2^2 \sigma^2 + 1)^2 16\pi} \left[\frac{K_y^2}{(K_2^2 \sigma^2 + 1)/L^2} - 2 \right] \exp\left\{-\frac{K_x^2 + K_y^2}{4(K_2^2 \sigma^2 + 1)/L^2}\right\} \\ & + \frac{a_3 a_3^* \sigma^2}{(K_2^2 \sigma^2 + 2)^2 16\pi} \left[\frac{K_y^2}{(K_2^2 \sigma^2 + 2)/L^2} - 2 \right] \exp\left\{-\frac{K_x^2 + K_y^2}{4(K_2^2 \sigma^2 + 2)/L^2}\right\} \end{aligned}$$

$$\begin{aligned}
& + \frac{(a_2 a_2^* + a_3 a_3^*) 2 \sigma^2}{(K_z^2 \sigma^2 + 1) 16 \pi} \exp \left\{ - \frac{K_x^2 + K_y^2}{4(K_z^2 \sigma^2 + 1)/L^2} \right\} \\
& + \frac{(a_2 a_3 + a_2 a_3^*) \sigma^2 L^2 K_x K_y}{(K_z^2 \sigma^2 + 1)^3 16 \pi} \exp \left\{ - \frac{K_x^2 + K_y^2}{4(K_z^2 \sigma^2 + 1)/L^2} \right\} \\
& + \frac{(a_2 a_3 + a_2 a_3^*) \sigma^4 K_z^2 K_x K_y L^2}{(K_z^2 \sigma^2 + 2)^3 16 \pi} \exp \left\{ - \frac{K_x^2 + K_y^2}{4(K_z^2 \sigma^2 + 2)/L^2} \right\} \quad \text{II. 29}
\end{aligned}$$

Examination of eq. (II. 29) shows that as the phase modulation, $K_z \sigma$, increases and becomes large with respect to unity this result tends toward eq. (II. 28). This is as expected because for the "integrated out" term to be negligible it was necessary to require $\exp(-K_z^2 \sigma^2)$ to become small. It is recalled that this is also a necessary condition for the calculation of the scattering cross section.

The calculation of σ_0 for the approximation to the exponential correlation function proceeds similarly to that for the Gaussian function. Substitution of $A_2 = 0$ and $A_1 = 1/L$ into eq. (II. 24) and the integrating using the tables of Bierens de Haan [1939] gives

$$\begin{aligned}
\sigma_0 = & \left\{ a_1^2 - \frac{K_x}{K_z} (a_1^* a_2 + a_1 a_2^*) - \frac{K_y}{K_z} (a_1^* a_3 + a_1 a_3^*) \right. \\
& \left. + \frac{K_x^2}{K_z^2} a_2 a_2^* + \frac{K_y^2}{K_z^2} a_3 a_3^* + \frac{K_x K_y}{K_z^2} (a_2^* a_3 + a_2 a_3^*) \right\} \\
& \frac{K_z^2 \sigma^2 / L}{8 \pi \left[\left(\frac{K_z^2 \sigma^2}{L} \right)^2 + K_x^2 + K_y^2 \right]^{3/2}}
\end{aligned} \quad \text{II. 30}$$

where the arrangement of the terms is like that of eq. (II. 28).

The behavior here is similar to that obtained using the Gaussian function in that the quasi-specular term dominates in the specular direction and then diminishes in importance at side and backscatter with the attendant effects due to the reflectivity of the surface. The quantity which determines the rapidity with which σ_0 falls off as the angle of observation changes from the specular direction is not the variance of slopes but is instead.

$$K_z^2 \sigma^2 / L$$

This, perhaps, can be considered to be indicative of the roughness in two ways: one of these is through the "slope" σ/L , and the other is through the phase modulation $K_z \sigma$.

A very tangible difference between the two results, eq. 's (II. 28) and (II. 30), is in the behavior in the specular direction. The Gaussian result has no variation other than that due to the change in reflection coefficient with angle of incidence and for a perfectly reflecting surface would be a constant. This contrasts sharply with the result obtained using the approximation to the exponential function which has the variation of the reflection coefficient superposed on the σ_0 for a perfectly reflecting surfaces which increases with decreasing grazing angle.

CHAPTER III

THE MEASUREMENT OF THE SCATTERING
CROSS SECTION AND COMPARISON WITH THEORYIII. A Historical Development of Measurement Techniques

The re-radiation of waves incident upon statistically rough surfaces is a problem that can be treated analytically in only a few cases. This is true principally for two reasons: Firstly, the present methods of analysis are applicable generally only when the wavelength is very large or very small relative to the size of the irregularities, as discussed earlier. Secondly, most of the naturally occurring surfaces are so complex that for many applications they defy analytical description, as discussed in Section III D. Because of these theoretical difficulties and the urgent need for answers to pressing practical problems, many past and present experimental programs have been undertaken. The vast majority of these programs, past and present, are to determine the characteristics of backscattered radar signals from a variety of rough surfaces. Despite this preponderance of radar backscattering experiments, there are few if any forms of scattering that have not received some strong experimental effort.

A period of much progress, both in terms of results and measurements techniques developed, began during World War II with a series of experiments performed to determine the radar backscattering characteristics of the sea. The initial experiments of this series were done by the Radiation Laboratory of the Massachusetts Institute of Technology [Kerr, 1951] [Clapp, 1946] [Cowan, 1946] and the Telecommunications Establishment of the United Kingdom [MacLusky and Davies, 1945] [Davies and McFarlane, 1946]. Later measurements over the sea were made by Wiltse, Shlesinger, and Johnson [1957], Macdonald [1956] and Campbell [1958, 1959]. Grant and Yaplee [1957] have investigated backscattering from the surface of a river. Experimental programs now in progress are being conducted jointly by the Naval Research Laboratory and the Applied Physics Laboratory of the Johns Hopkins University.

Following closely after the initial sea clutter experiments were the beginnings of large scale experiments to investigate the radar back-scattering from the generally more complicated terrestrial, lunar, and planetary surfaces. The terrestrial measurement programs have been largely devoted to obtaining data from a wide variety of naturally occurring surfaces. Programs were established early by the Radiation Laboratory [Clapp, 1946] , the Sandia Corporation [Edison, Moore, and Warner, 1960] , the Goodyear Aircraft Corporation [Reitz, 1958] , the Ohio State University [Cosgriff, Peake, and Taylor, 1957] , the General Precision Laboratory [Campbell, 1958, 1959] and the Philco Corporation (no reference available). Later programs were established by the Ryan Aircraft Company, the U. S. Army, and more recently by the University of Kansas. Radar investigations of the moon have been made with high frequency since the end of World War II. The earliest lunar explorations were made by an organization in Hungary [Bay, 1946] and the U. S. Army [Moffensen, 1946] [Dewitt and Stodola, 1949] . Since these, investigations have been made by groups in Australia [Kerr, Shain, and Higgins, 1949] [Kerr and Shain, 1951] , the United Kingdom [Browne et al., 1956] [Evans, 1957] [Evans et al., 1959] [Hey and Hughes, 1959] [Hughes, 1960] , and in this country at the Lincoln Laboratory of the Massachusetts Institute of Technology [Pettengill, 1960] [Evans and Pettengill, 1963] , the U. S. Naval Research Laboratory [Trexler, 1958] [Yaplee et al., 1958, 1959] , University of Texas in conjunction with the Royal Radar Establishment [Straiton and Tolbert, 1960] , and the Jet Propulsion Laboratory. Radar contact with Venus has been made by the Lincoln Laboratory [Price et al., 1959] and the beginnings of an exploration program carried out by the Jet Propulsion Laboratory [Victor et al., 1961] .

Although most radar experiments have been restricted to the back-scattering mode for reasons of practical application or because of necessity (lunar and planetary experiments), a number of investigations of the forward re-radiation mode (reflection and scatter) have been directed toward the solution of radio communication problems. A much smaller number have attacked the general problem of obtaining a complete description of the re-radiation from rough surfaces by making omnidirectional measurements of reflection and scatter. The problem of radio communication over a rough earth is an old one that has received much attention, both theoretical

and experimental, since before World War II. A discussion of the experimental techniques and results is contained in the book by Beckmann and Spizzichino [1963]. The general problem of radar scatter and reflection in all directions is one that has been dealt with experimentally only recently. Early experiments were done in the United Kingdom by Manton [1958] who made measurements of radar signals re-radiated from rippled water in a laboratory tank. Experiments carried out over a variety of surfaces have been made and are continuing to be made in a program at the Ohio State University [Taylor, 1964].

Paralleling somewhat the progress made in radar measurement programs has been the progress made in various programs undertaken, mostly by the U. S. Navy, to investigate by acoustical means the natural surfaces which are the boundaries of the ocean. These programs have not been nearly as numerous nor as ambitious as the analogous radar programs, although often the needs of the two sets of programs have been similar as are the measurement techniques themselves. Much of the work done has been directed toward determining the characteristics of the backscatter, or reverberation, from the ocean bottom at sonar frequencies (100 to 40,000 cps). Early work which took the form of backscattering from harbor bottoms was done by the Naval Research Laboratory [Urlick, 1953]. Later work has been done by Jones et al. [1963], Mackenzie [1961] and McKinney and Anderson [1963]. Of these, the latter two have obtained a catalog of returns from a variety of bottoms. Nolle et al. [1963] have performed experiments under laboratory condition with sands of known density as the re-radiating bottoms. A smaller number of experiments have been made on the surface of the ocean. Urlick and Hoover [1956] obtained backscattering data as a function of wind velocity and Mellen [1964] and Lieberman [1963] have performed measurements on doppler-shifted backscattered signals to investigate the spectral density of the wave motion. Additional data have come as a by-product of the acoustical simulation of radar return. The simulation program at the University of New Mexico [Edison, 1961] has given much information on the statistics of the signals backscattered from rough surfaces and also on the return from a variety of surfaces by way of determining materials suitable for modeling.

III. B The Technique of Measurement

An experimental investigation of the re-radiation of waves, acoustic or electromagnetic, incident upon rough surfaces requires, in general, the description of both the reflection and scatter components of the re-radiated field. This is done through a determination of the reflection coefficient and the average differential scattering cross section for all angles of incidence and observation as a function of the frequency of the incident radiation. For the case of electromagnetic waves, the polarization of the incident and re-radiated fields must also be considered, as discussed subsequently. The case considered here is that of re-radiation from a surface sufficiently rough at the frequency used that the amount of energy reflected is negligible. Therefore, it is sufficient to determine only the scattering cross section. This is done as a function of the angles of incidence and observation (see figure III. 1) through performance of experiments based upon the equation derived from the definition of the average differential scattering cross section. This equation, which is commonly called the radar equation, or, depending upon application, the sonar equation, is for the general case of bi-static scattering considered here

$$\langle P(\phi_0, \phi_1, \phi_2) \rangle = \int_S \frac{P_T G_T(\Psi_T)}{4\pi r_T^2} \sigma_0 \frac{\lambda^2 G_R(\Psi_R)}{4\pi r_R^2} dA \quad \text{III. 1}$$

where: $\langle P(\phi_0, \phi_1, \phi_2) \rangle$ is the average of the received power obtained over an ensemble of surfaces.

P_T is the transmitted power.

$G_T(\Psi_T)$ is the gain function of the transmitting antenna (or transducer) which is assumed to be circularly symmetric and a function of Ψ_T only.

$G_R(\Psi_R)$ is the gain function of the receiving antenna, also assumed to be circularly symmetric.

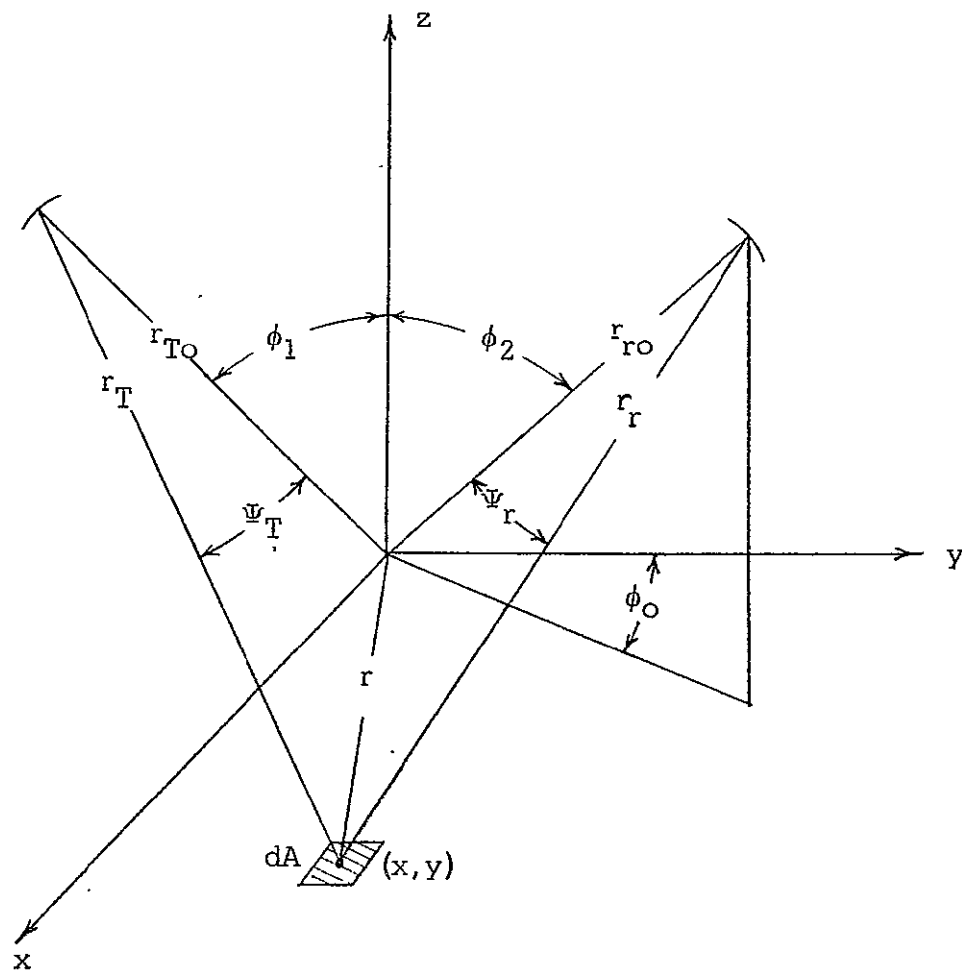
λ is the wavelength of the radiation.

S is the mean surface upon which the radiation is incident.

The integrand of eq. (III.1) is written in the following order: the first term is the incident power density, the second term is the scattering cross section, and the third term is the receiving antenna aperture divided by the square of the distance, which is the solid angle subtended by the receiving aperture. The incident power density is that of the spherical wave front at the surface as modified by the gain function of the transmitting antenna. It is recalled that the scattering cross section is defined on the basis of a plane incident wave front, primarily for mathematical simplicity. As long as the region over which there is correlation of surface heights is small enough so that the spherical wave front is approximately plane the difference is negligible.

It is perhaps a misnomer to call eq. (III.1) the radar equation because the vector nature of the electromagnetic scattering process is not evident in this equation. However, this phraseology has been used often in the past, and it has only been fairly recently that vector scattering has received much attention [The Ohio State University, 1963]. The vector nature of the scattering is brought out by introducing separate scattering cross sections for the description of the fields scattered in and normal to the plane of incidence for each of the two orthogonal polarization components. Clearly, there is no difficulty encountered in calling eq. (III.1) the sonar equation because of the scalar nature of the acoustic scattering process.

Bi-static measurements of the differential scattering cross section can be made for both acoustic and electromagnetic waves through the use of a transmitting or receiving antenna (can be both) that has a beam width (between half power points) only several degrees wide. This enables the approximation to be made that the scattering cross section is constant over the area defined by the intersection of the cones of the antenna patterns and the mean surface S , which can be called the "effective illuminated area." For the bi-static measurement considered here there is no time variation of the amplitude of the incident radiation over the effective illuminated area and the steady state is assumed to exist. This is shown in eq. (III.1) by treating P_T as a constant. This existence of the steady state in pulsed radar or sonar work is referred to as "beam width limitation." This is to be contrasted with "pulse width limitation" in which the area defined on the ground by the antenna gain functions is



Geometry of Bi-Static Scattering
Figure III. 1

not completely illuminated at any instant of time due to the shortness of the physical extent of the radar or sonar pulse [Moore and Williams, 1957].

Making the restriction of high directivity, eq. (III. 1) becomes

$$\langle P(\phi_0, \phi_1, \phi_2) \rangle = \sigma_0(\phi_0, \phi_1, \phi_2) \iint_S \frac{P_T G_T(\Psi_T) \lambda^2 G_R(\Psi_R)}{(4\pi)^2 r_r^2 r_T^2} dA$$

III.2

It is convenient to normalize the average received power with respect to the power received upon direct transmission of the power P_T . This power is

$$P_D = \frac{P_T G_T(0) G_R(0) \lambda^2}{(4\pi r_n)^2}$$

III.3

where r_n is the distance of separation between the transmitting and receiving antennas and $G_T(0)$ and $G_R(0)$ are the gains of these antennas, respectively. Dividing eq. (III. 2) by the normalizing power, P_D , gives

$$\begin{aligned} \langle P_n(\phi_0, \phi_1, \phi_2) \rangle &\stackrel{\text{def}}{=} \frac{\langle P(\phi_0, \phi_1, \phi_2) \rangle}{P_D} \\ &= \sigma_0(\phi_0, \phi_1, \phi_2) r_n^2 \iint_S \frac{g_T(\Psi_T) g_R(\Psi_R)}{r_r^2 r_T^2} dA \end{aligned}$$

III.4

where $g_T(\Psi_T)$ and $g_R(\Psi_R)$ are the normalized gain functions of the antennas and have a maximum value of unity. The integration accounts for the so-called "aperture effect" which is the processing of the scattered signals by the gain functions of the antennas.

The determination of σ_0 for a set of angles (ϕ_0, ϕ_1, ϕ_2) is then a measurement of the average, normalized power and an evaluation of the aperture effect at this set of angles. The aperture effect evaluation is a straight-forward calculation which is given in Appendix IV. The measurement of the average, normalized power is not so straight-forward and it is necessary to carefully design the experiment so that an accurate measurement results. It is critically important that the effective area illuminated be large enough to permit the surface to have a sufficient number of variations to define the random process. Clarke[1963a] has shown that the dimensions of this area should be at least ten times the correlation distance of the random process of the surface. Therefore, it is necessary as the beam width of either the transmitting or receiving antenna is decreased to improve the approximation of eq. (III. 2) to move the antenna back from the mean surface thereby increasing the area of the intersection between the mean surface and the cones defined by the half power points of the beams.

III. C The Description of the Experimental Facility and the Conduct of the Experiment

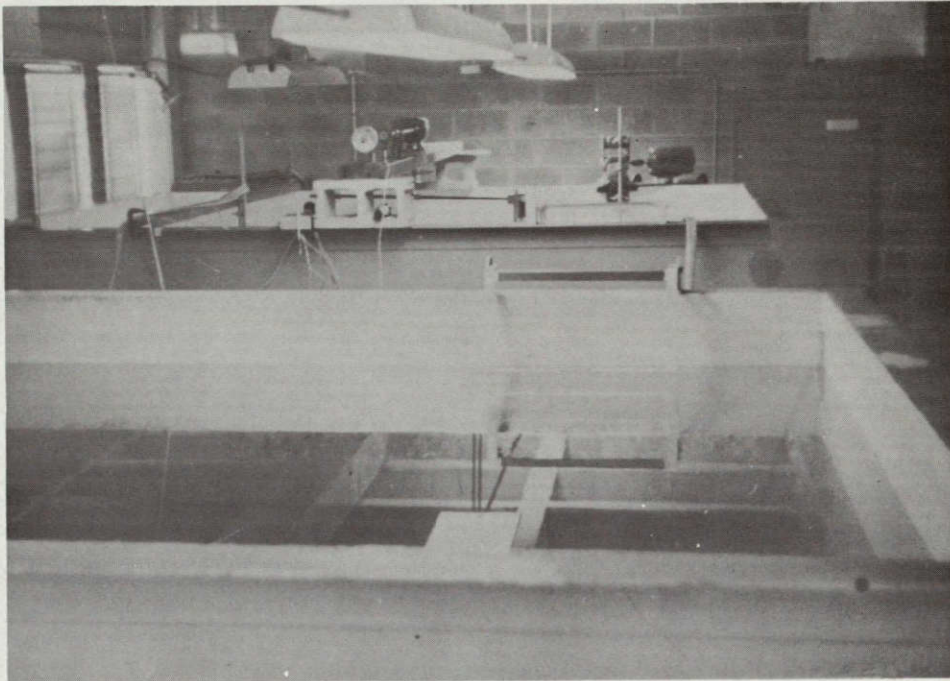
The aim of the experimental investigation is to obtain data with which the theoretical results of Chapter II can be compared. The experiments consist of the measurement of the average differential scattering cross section of surfaces with known statistical properties and surface parameters. A complete set of measurements to achieve this goal would be the determination of σ_0 for all values of the set of angles (ϕ_0, ϕ_1, ϕ_2) as a function of wavelength for a wide range of statistical parameters and surface properties. This, of course, is very ambitious and a compromise was reached which was designed to bring out features of omnidirectional scattering considered to be most important and at the same time provide experimental results that could be considered predictable from the assumptions of the theory of Chapter II. It was decided to set aside the important question of frequency dependence and measure at a single frequency the σ_0 of two surfaces that are smooth enough at this frequency to be called locally flat. The surfaces were chosen to be highly reflecting, different

in their statistical properties, and, at the frequency used, sufficiently rough so that reflection is negligible. The description of the surfaces and the measurement of their properties are given in Section III D. The series of angles at which σ_{\circ} is measured is a compromise between complete description and undue work.

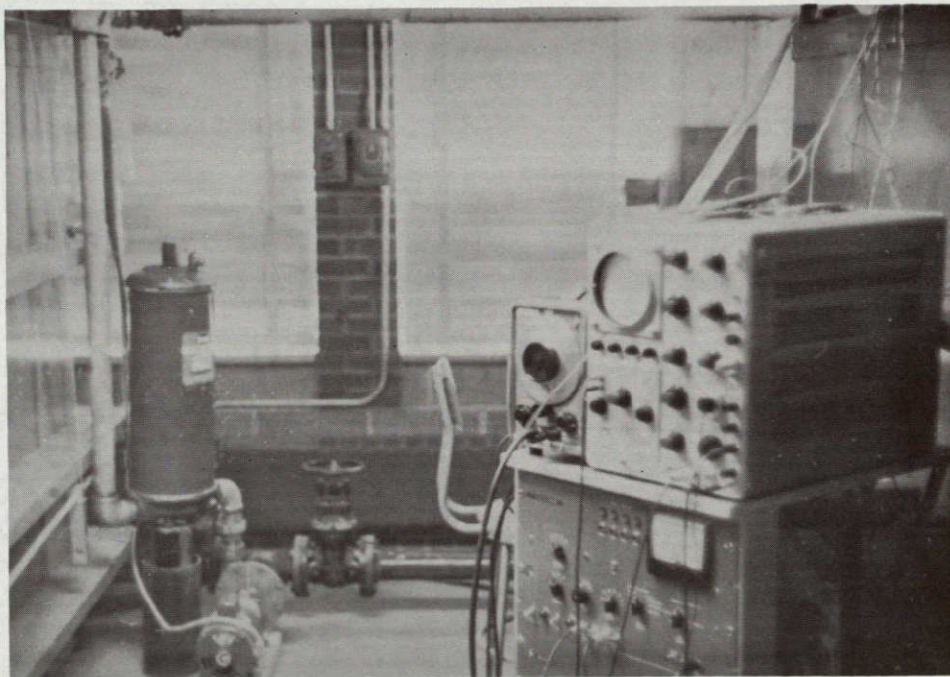
The measurement of σ_{\circ} , as discussed earlier, requires the measurement of the average of the received power over an ensemble of surfaces and the measurement of the antenna gain functions of the transducers for the evaluation of the aperture effect. These measurements were performed at the acoustic facility of the Remote Sensing Laboratory of the Center for Research, Inc. This facility consists of a system of two water tanks (one serving as a reservoir) with the associated pumping system; a mechanical system for positioning transducers and providing motion of the rough surface targets; and an electronic system for the generation, reception and processing of ultrasonic signals. The arrangement of the equipment about the tanks is shown in figure III. 3 and the tanks themselves in figure III. 2.

The mechanical system shown schematically with laboratory parameters in figure III. 4 and photographically in figures III. 5 and III. 6 is really two independent systems. One of these is the equipment used to align and position the transducers in the tank. The operation of this equipment is crucially important as the receiving and transmitting transducers must be "looking" at the same area of the mean surface of the target for all relative angular positions to make the evaluation of aperture effect practically possible. The other system is the rotary table that is used to rotate the target through the intersecting beams of the transducers thereby providing the ensemble of surfaces necessary for the calculation of the average of the received power. The axes of rotation of the transducer positioning system and the rotary table are offset as shown so that the illuminated area of the target changes as the table rotates.

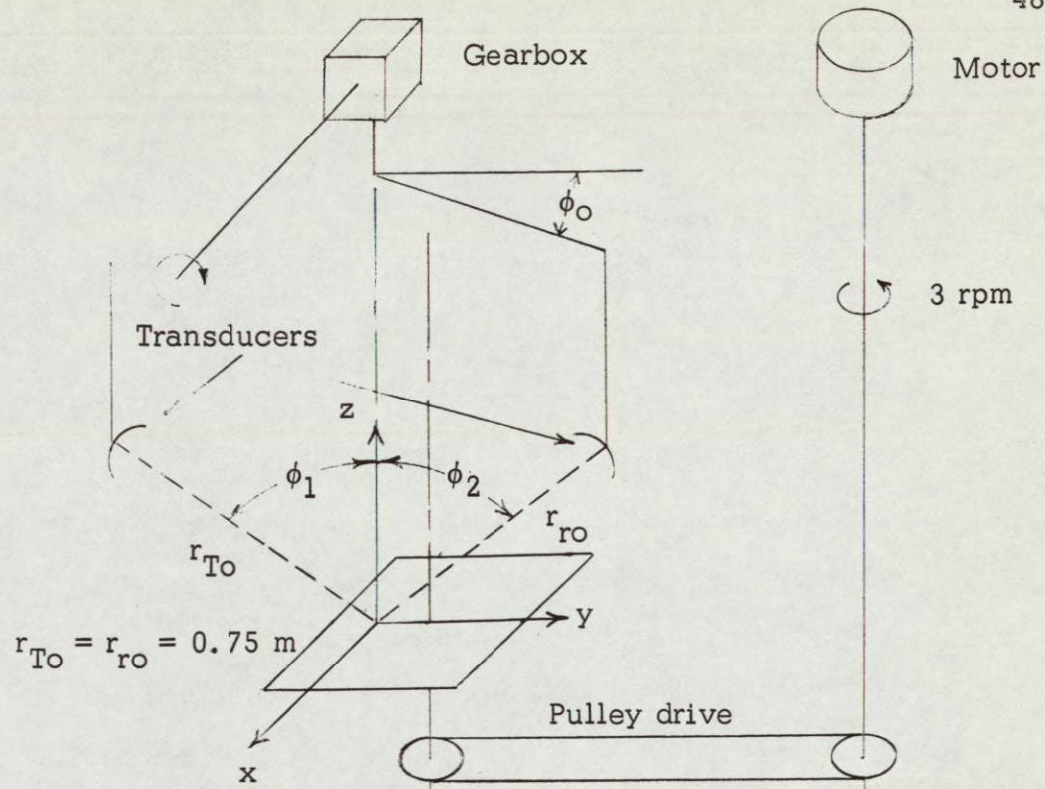
The electronic system shown in block diagram form with the laboratory parameters in figure III. 7 and photographically in figure III. 8 is composed of three sub-systems: the transmitting sub-system, the



The Acoustic Tanks of the Remote Sensing Laboratory
Figure III. 2

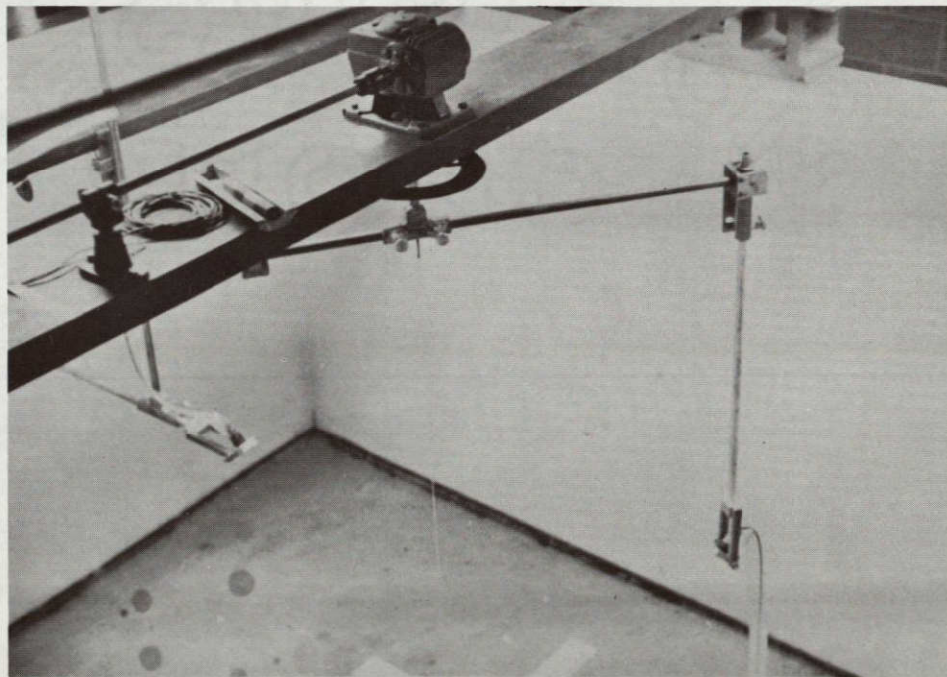


The Acoustic Tanks and Peripheral Equipment
Figure III. 3



Schematic Diagram of the Mechanical System

Figure III. 4



Transducer Positioning System

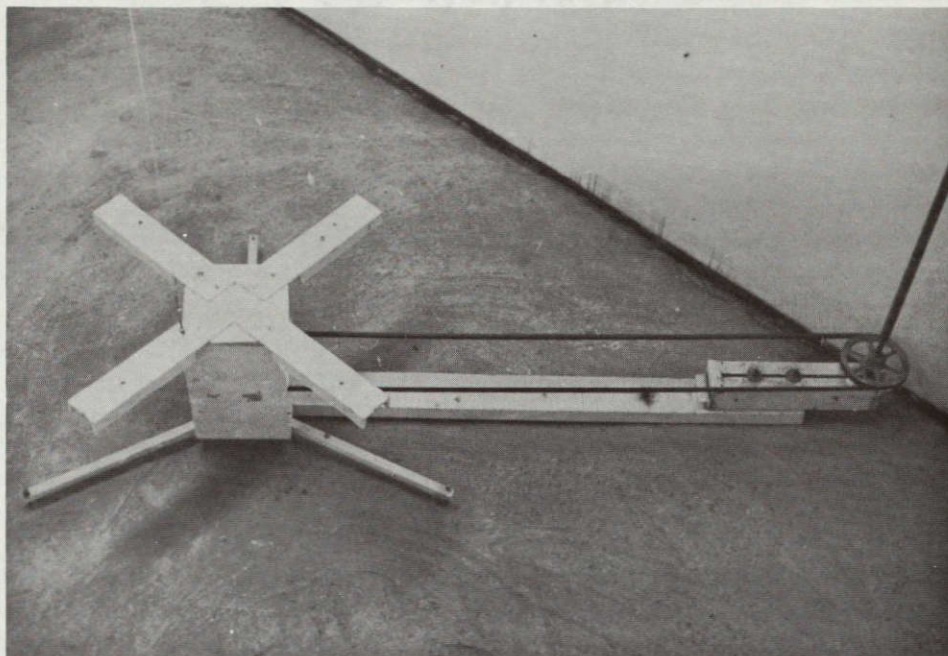
Figure III. 5

receiving sub-system, and the data processing sub-system. The operation of each of these sub-systems in conjunction with the others is discussed in turn below.

The transmitting sub-system consists of a pulse modulated sine wave power oscillator and the transducer which it drives. It is necessary to use a pulsed system instead of the simpler continuous wave system because the tank is not "dark." The unwanted reflections from the walls of the tank and the surface of the water are gated out upon reception. These reflections, or reverberations, manifest themselves as a type of noise after several bounces; however, this was not a problem here because of the high signal level. The pulse width (PW) of the modulating pulse was chosen to provide the beam width limitation necessary to the measurement technique. The width of 600 microseconds gave a discernible steady state condition for the extreme case when the depression angle was $\phi_1 = 70^\circ$. The pulse repetition frequency (PRF) of the modulating pulse was chosen to produce a time series of statistically independent received pulses. This was a choice made relative to the choice of angular velocity of the target which was the low value of 3 rpm to minimize turbulence of the water. For this value of 3 rpm the PRF of 5 cps was sufficiently low to produce independent data points for the two targets used in the experiment.

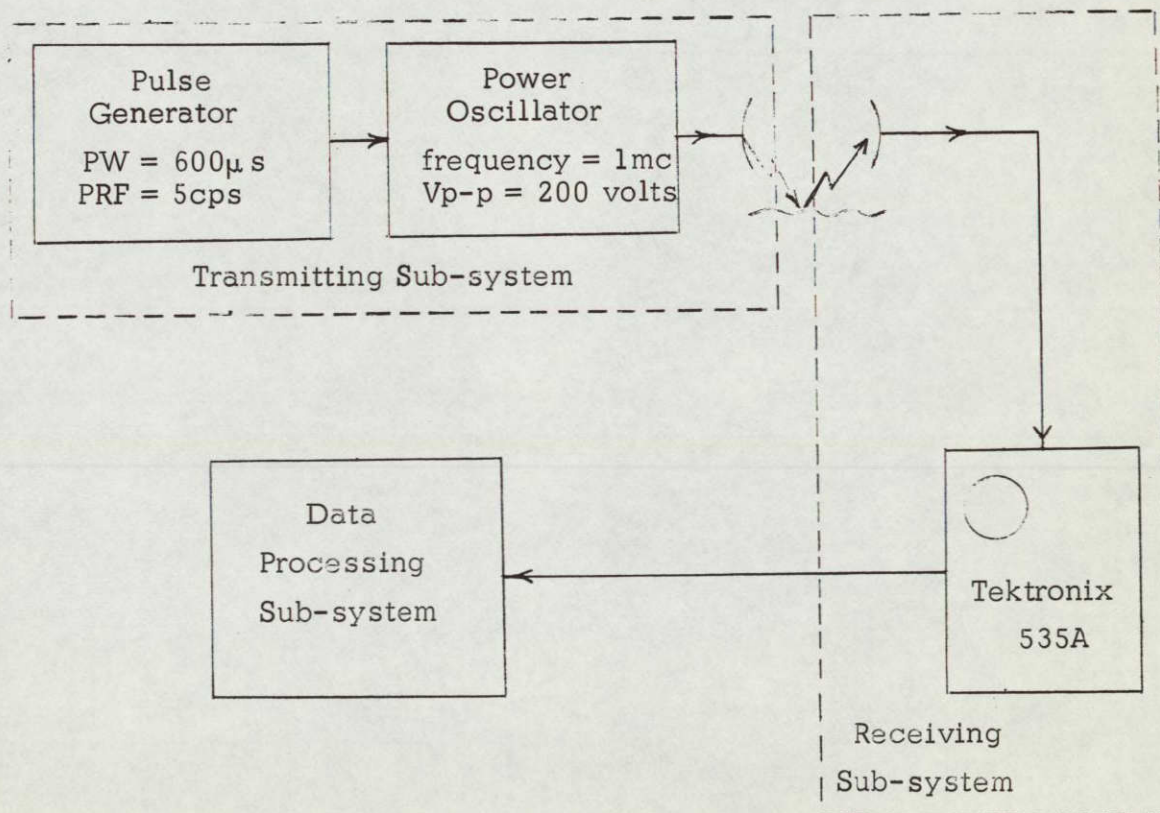
The source of acoustic energy was a piezoelectric crystal transducer of the piston type, shown in figure III.9. The transducers used were supplied by the Branson Instruments Company and have a nominal diameter of 7/8 inches. The antenna patterns of the transducers used (several transducer failures occurred) were measured and each was found to have the same pattern (shown in figure III.10) within the limits of experimental error. Also, the mechanical and acoustical axes of each transducer were the same. The antenna pattern predicted by theory for a piston transducer is [Morse, 1948]

$$\frac{2 J_1(k a \sin \theta)}{k a \sin \theta}$$



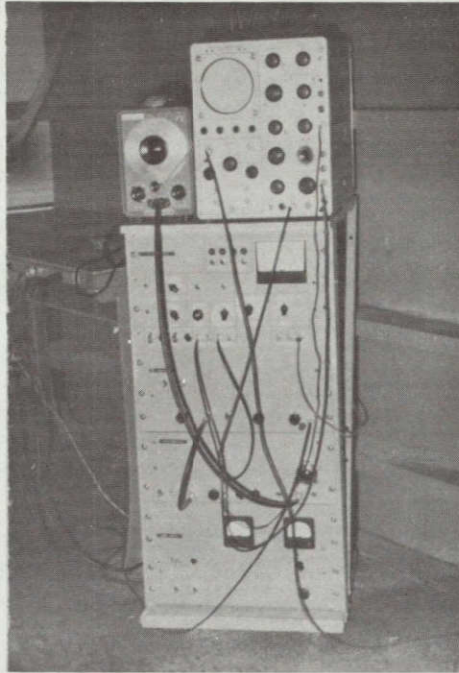
Rotary Table and Drive Mechanism

Figure III. 6



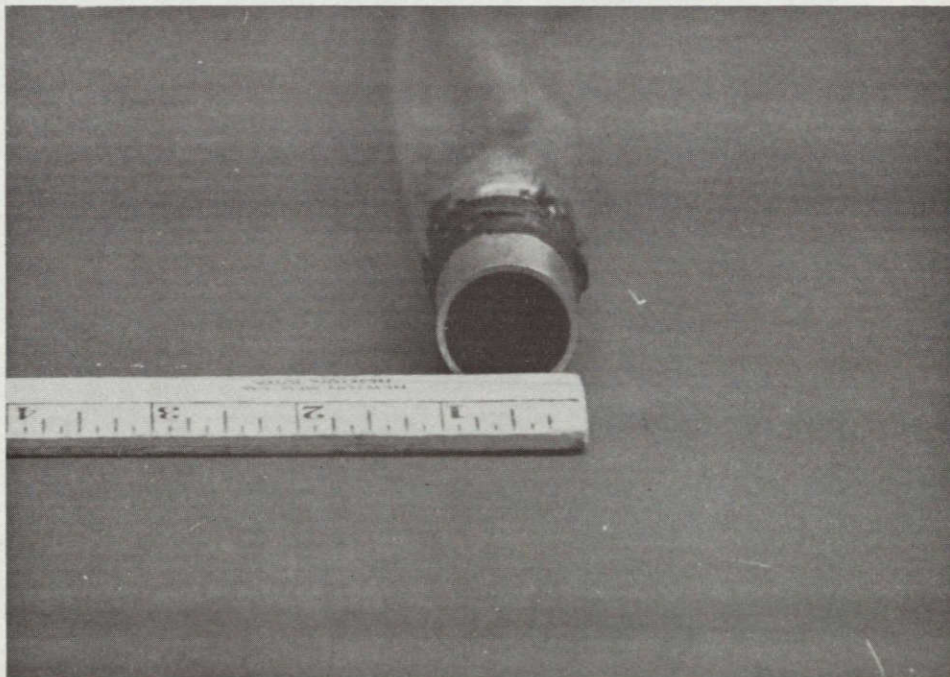
Block Diagram of the Electronic System

Figure III. 7



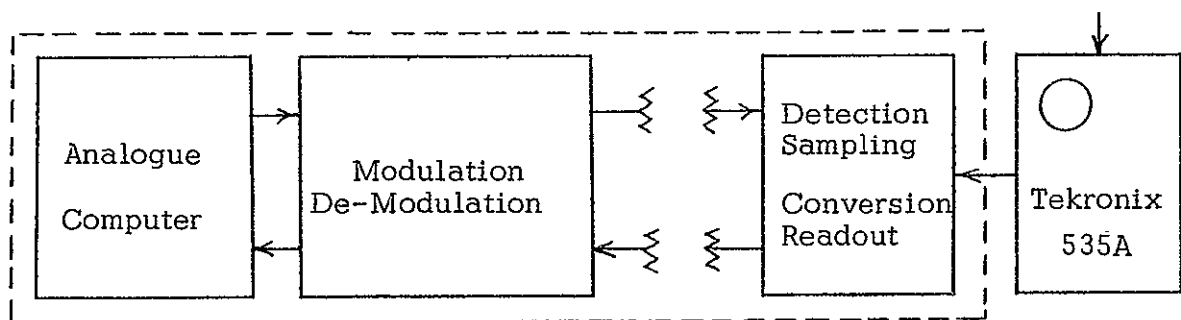
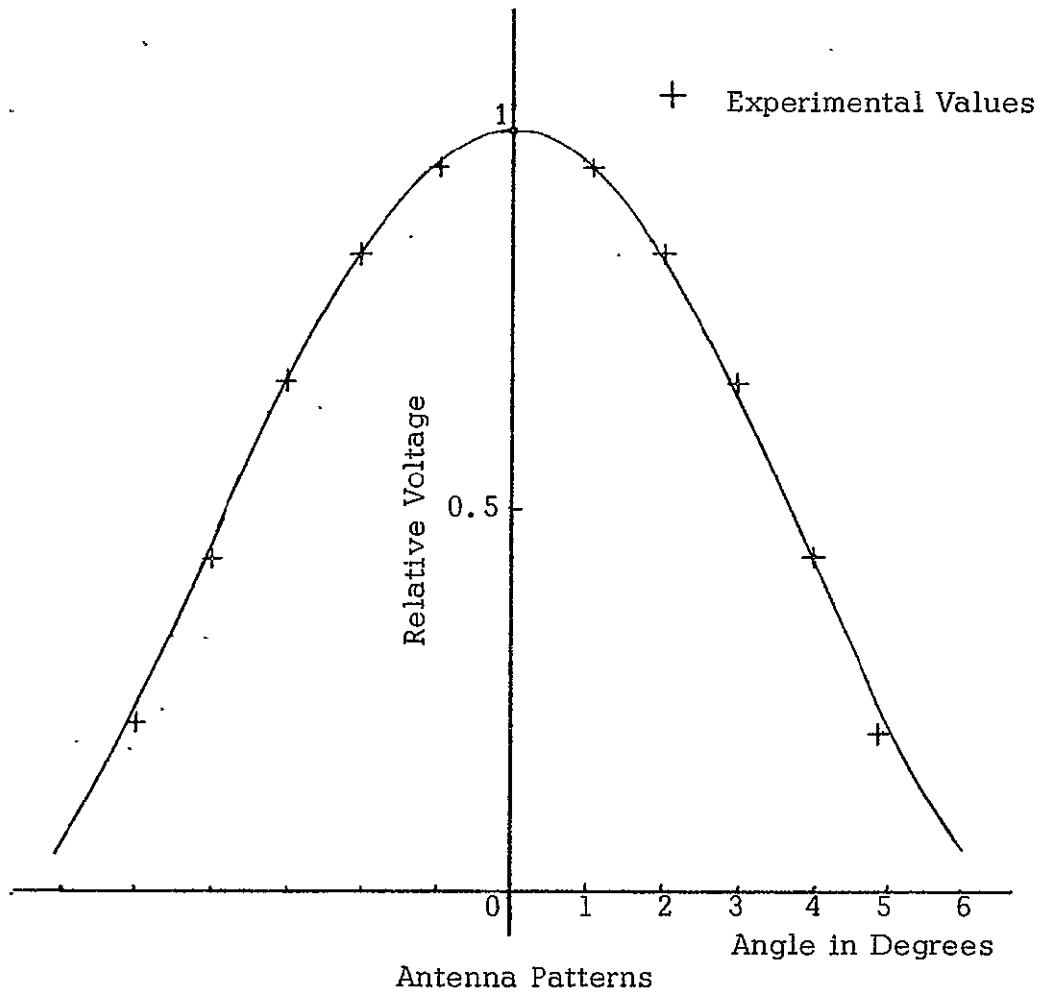
Principle Components of the Electronic System

Figure III.8



Piston Transducers

Figure III.9



power averaged over the ensemble of surfaces generated by the rotating target as each pulse in the time series is energy which has been scattered from a part of the rough surface sensibly different from the remainder.

The calculation of the average of the time series of RF signals in this way is achieved through a conversion of the series to a continuous waveform from which the time average of the power is obtained. The series of signals and the waveform to which they are converted are shown in figure III.12 (note the effect of beam width limitation).

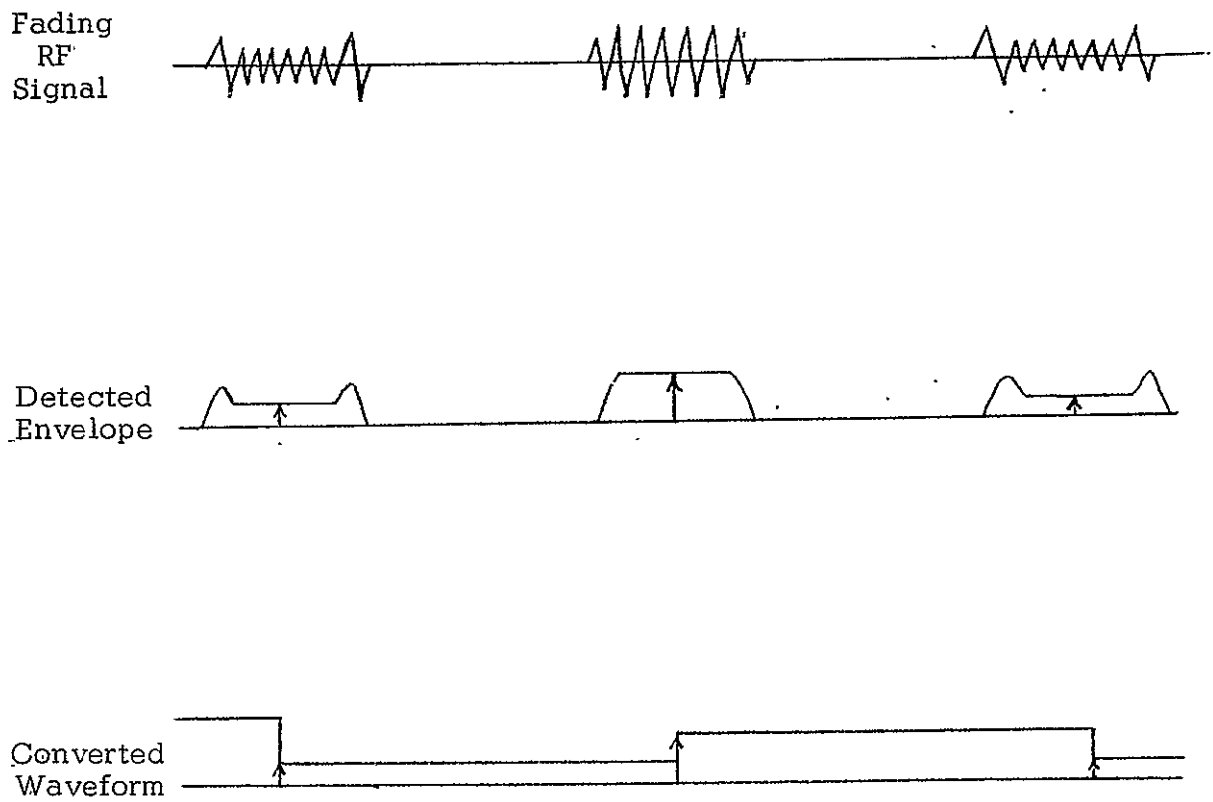
The conversion process begins by detecting the RF signal and then sampling each detected pulse during its steady state portion, thereby determining the voltage samples from which the average power is computed. The time of sampling is determined by the arrival of a gate pulse generated in the oscilloscope to intensify the screen during the chosen portion of the waveform. The portion chosen here is from that part of the signal which is in the steady state. The series of voltage samples is converted to a series of dc voltage levels with each voltage level being equal to that of the corresponding sample from which it is derived. This series of dc levels is then made the input to the analogue computer which computes the time average power of the waveform

$$\frac{1}{T} \int_0^T v^2 dt$$

which is equivalent to computing the arithmetic average of the power of each of the voltage samples of dc levels.

The practical application of this scheme of calculation was made difficult by the fact that the data was taken at a point physically removed from the analogue computer by approximately one mile. This separation made it necessary to telemeter the series of dc voltage levels to the analogue computer and then telemeter back the resulting answer. The information was sent over the telephone lines by means of a telemetry system designed for the general transmission of analogue data.

The calculation of the average power was done on a relative basis as the system was normalized with respect to a calibration power level. This calibration power was the power received by the receiving transducer upon transmission of a given power level by the transmitting transducer



Conversion of RF Waveforms for Data Processing
Figure III.12

one meter away. The procedure used in taking data was to read all calculations of average power from fading (scattered) signals relative to the average power obtained with the non-fading, calibrating received signal as the input. By following this procedure, the gains of the transducers and the transmitted power level were eliminated from the calculation of σ_o , and eq. (III. 4) was used directly with $r_n = 1$ because it is $\langle P_n(\phi_o, \phi_1, \phi_2) \rangle$ that was measured.

The measurement of the average received power is clearly a complicated process and therefore one in which the likelihood of experimental error is high. The error occurring in the measurement process can be put into two independent categories: those generated by the electronic system and those which have their origin in the mechanical system. The experimental error due to the electronic system is believed to be negligible because of the many precautionary measures that were taken. Before and after each measurement run the receiving and data processing equipment were calibrated on the power level of the power oscillator which was monitored throughout the experiment. If any change in calibration occurred, the data was discarded. The accuracy of the data processing equipment was checked several times by recording the fading signal on film and performing a manual calculation of the average power from which to make a comparison check. In each instance the agreement was good. The greatest source of experimental error is believed to be the mechanical system, and this was due to transducer pointing error. It is necessary that the transducers "look" at the same area on the mean surface (for the way aperture effect is evaluated) and this requirement is difficult to fulfill because of the small beamwidths. The transducer mounts were optically aligned, and the alignment was checked before and after each measurement run. The post-experiment alignment was frequently found to be poor with always some minor deviation which had an effect which is difficult to evaluate.

To insure the quality of the experimental data, runs were repeated until agreement within a db between two runs was obtained. It was, however, not possible to do this for the data on which the results of figures III. 23 and III. 25 of Section III E are based because the experimental surface became badly cracked and unusable. These results are, therefore, possibly in error. Other results for this surface shown in figure III. 21 are, however, based on repeated data and presumably good.

III. D Description of the Rough Surfaces

The characteristics of the re-radiation of waves from surfaces is determined, in general, by the properties of two random processes. These processes are the variation of surface heights and the variation of material parameters. For most surfaces, natural and artificial, these processes are of such complexity they can be described in only a very approximate way if at all. The problem of description is complicated by the lack of statistical independence between these two processes and their non-stationarity in space. A further complication is introduced by the possibility of a variation in time. Consider, for example, the problem of describing farmland on a large scale. Here the lack of statistical independence is shown by the fact that vegetation growing in valleys differs from that on the crowns of hills. The non-stationarity of both processes in space is evident from the variety of farm crops with different surface textures and material properties and the variation in time is caused by the changing weather conditions. Because little is known about the nature of spatial non-stationarities, the effects of the weather, and the dependence of vegetation growth upon surface structure, it would not be possible to obtain a description of the terrain even if there were a way to treat the statistical features of vegetation.

There are, however, natural surfaces that are more amenable to mathematical description. The surface of the ocean has received much attention [Pierson, 1960] and progress has been made to the point that a prediction of radar return is now possible which takes into account, to a degree, the statistical features of the ocean's surface*. This case is much less difficult because of the simpler structure of the surface and also because the material variation is caused, primarily, by foam on the surface which is probably negligible for many problems. However, the spatial non-stationarity and the variation in time exist, and these are the phenomena which are of great interest to oceanographers. Therefore, even in the simpler cases, there is great difficulty in obtaining a description of the surface which has some degree of completeness.

* Work now in progress at the Remote Sensing Laboratory of the Center for Research, Inc.

The surfaces used in the experiments were chosen not to have the general complexity of a surface generated by two random processes and the material variation was eliminated by using homogeneous materials. The goal was to construct stationary surfaces of roughnesses that could be described mathematically and also be smooth enough so that, at the frequency used, the locally flat approximation would be valid. To an acceptable degree, this was achieved.

Two surfaces of different roughnesses and different reflectivities were constructed. One of these was made by striking mild steel sheet (of the kind used to repair automobile bodies) randomly with the ball (of approximately 3/4 inches) of a ball pean hammer and then gluing this to an aluminum sheet using a dense paste to eliminate air-pockets. The other surface was made by flowing grout over a sand surface which had been smoothed by coating it heavily with fiberglass. The sand surface was made by gluing sand particles to an aluminum sheet. The presence of the sand destroys, to a degree, the homogeneity of the surface material. The reflectivities of the surfaces were not measured, and because the targets were not infinitely deep, the reflectivities near normal incidence are difficult to predict. In fact, because of the type construction used in making the targets, the problem is not unlike the layered media problem with the surface layer being rough.

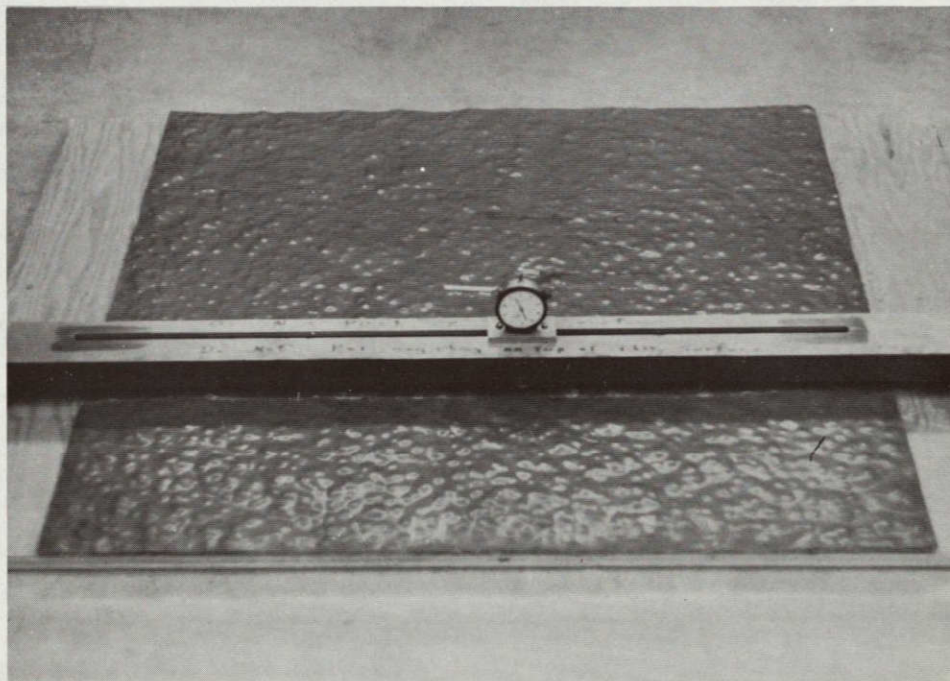
The differences in the materials used to make the targets appear as differences in the critical angles for the two surfaces. The critical angle is the angle beyond which all energy is reflected and none refracted. At this angle the quantity

$$e = \sqrt{\frac{k\rho'}{\rho\mu \sin^2\theta} - 1}$$

in eq. (II. 5) becomes zero and with a further increase in θ becomes imaginary causing $|\Gamma|$ to become unity. Estimates of the critical angles for the two surfaces were made by estimating the value of the phase velocities of the shear waves, $\sqrt{\mu'/\rho'}$, in the materials by using representative values of the phase velocities of the longitudinal waves, $\sqrt{(\lambda')^2 + 2\mu'}$, and assuming the Poisson relation, $\mu' = (\lambda')'$, to hold. ρ' The representative

values for the phase velocities of the longitudinal waves were taken from the Handbook of Physics and Chemistry [1960-1961] and are 5000 meters per second for steel and 4000 meters per second for the rock-like grout. Using a phase velocity of 1500 meters per second for water, the critical angles are $\Theta_c = 30^\circ$ (measured from the vertical) for the steel and $\Theta_c = 40^\circ$ for the grout.

The properties of the surface roughnesses of the two targets were investigated by making estimates of the probability distribution function of surface heights, the autocorrelation function of surface heights as a function of lateral distance, and the stationarity of the processes. These estimates were computed from series of sampled height measurements that were taken along profiles of each target. The measurements were made using a depth gauge mounted on a machined surface and driven by a lead screw mechanism which allowed the sampling interval to be varied. This apparatus is shown mounted over a target surface in figure III.13.



Apparatus for Making a Profile of a Rough Surface
Figure III.13

The sampled height measurements were made along several profiles of each target. The profiles were separated a distance sufficient (several correlation distances) to insure independence of the data points of separate measurement runs. The probability distribution function and autocorrelation function were computed for each of these runs as well as the mean, m , and standard derivation of heights, σ . Similarity of the computed results from different parts of the same surface then gives an indication of the stationarity of the process over the surface. A serious difficulty encountered in making an estimate of the stationarity and the other functions as well was caused by the presence of large scale irregularities created in the construction of the targets. These irregularities, which created what are called "regional slopes," were of a lateral extent large relative to the variations of the surface and had the effect of causing the deformation of the mean plane into some other unknown surface. The "regional slopes" were not great enough to cause serious error in the measurement of the scattering cross section but did prevent, for some discarded profiles, an accurate determination of the small scale structure superposed on them.

The estimate of the correlation function was calculated using the statistical estimator (the overbar indicates sample function)

$$F(l\Delta x) = \frac{\frac{1}{N-l} \sum_{i=1}^{N-l} (h_i - \bar{m})(h_{i+l} - \bar{m})}{\frac{1}{N} \sum_{i=1}^N (h_i - \bar{m})^2}$$

III. 5

where: h_i is the i^{th} height in the series of N points.

l is the lag.

Δx is the sampling interval.

$$\bar{m} = \frac{1}{N} \sum_{i=1}^N h_i \quad \text{is the sample mean.}$$

The denominator of eq. (III. 5) is the sample variance, $\overline{\sigma}^2$, or the square of the sample standard deviation. The maximum lag used in the calculation of \overline{r} , as recommended by Blackman and Tukey [1958], was $N/10$ where N was made sufficiently large for the particular sampling interval used to adequately define \overline{r} . The criterion for the selection of the sampling interval, according to the sampling theorem [Bendat, 1958], is that it must not exceed half the period of the highest frequency present in the record of the profile. For the surfaces used in the experiment, the value of $\Delta x = 0.01$ inches amply satisfied this criterion. The number of points taken in the measurement of both surfaces was 1000 which corresponds to a record length of ten inches. This provided a maximum lag of one inch which is sufficient to adequately define the falls of the sample autocorrelation coefficients. The one exception to this was a measurement made over the steel surface with a lag of 0.1 inches and a record length of 17 inches. This measurement was made to investigate the behavior of the autocorrelation coefficient at longer lag distances. The sample autocorrelation coefficients computed (by machine calculation) are shown together with the sample variances for each of the surfaces in figures III.14 and III.15.

The behaviors of the sample autocorrelation coefficients indicate by the smooth falls and following rises that the surfaces are gently undulating and, to a degree, periodic. The rises could not be thoroughly investigated in the case of the steel surface because of the regional slopes difficulty. The periodicity is evidence of the artificiality of the surfaces as the estimated period of the low frequency components was approximately the spacing between the surface variations. This estimate was very gross for the steel target but easily made for the grout surface. The presence of the periodicity indicates that the sample autocorrelation coefficients are probably not well described by any simple function [Pierson, 1960]. However, since this low frequency behavior is dominated strongly by the falls of the autocorrelation coefficients from the origin it is this region of the curves near the origin that was investigated. It was found that near the origin the sample autocorrelation coefficients are closely approximated by the function

$$r = \exp\left\{-\left(\frac{x}{L}\right)^{3/2}\right\}$$

although this is not shown in the figures. However, away from the origin,

all the curves but one fall off more rapidly than this and a better overall approximation is the Gaussian function

$$r = \exp \left\{ - \left(\frac{x}{L} \right)^2 \right\}$$

The probability distribution functions of the sampled heights were determined for each of the profiles for which a sample autocorrelation function was calculated. However, no calculation was done for the profile of the steel target made with the larger sampling interval. These results are shown in figures III.16 through III.19 together with plots of the Gaussian distribution function

$$\Psi(h \leq H) = \int_{-\infty}^H \frac{\exp \left\{ - \frac{(h-m)^2}{2\sigma^2} \right\}}{\sqrt{2\pi\sigma^2}} dh$$

obtained using for m and σ^2 values of the sample mean, \bar{m} , and the sample variance, $\bar{\sigma}^2$. Comparison of the experimental curves to those calculated shows the near-Gaussian nature of the random height process as sampled from the four profiles.

The estimates made of the autocorrelation function and probability distribution function are very similar from profile to profile for both of the experimental surfaces and the processes are considered to be, for practical purposes, stationary. Therefore, because of the Gaussian behavior of the sample distribution functions, the joint probability density function is, for both surfaces, approximately [Middleton, 1960]

$$\Phi [h_1(x_1, y_1); h_2(x_2, y_2)] = \frac{1}{2\pi \sigma_1^2 \sigma_2^2 \sqrt{1-r^2}}$$

$$\exp \left\{ - \left[\left(\frac{h_1 - m_1}{\sigma_1} \right)^2 + \left(\frac{h_2 - m_2}{\sigma_2} \right)^2 - 2r \left(\frac{h_1 - m_1}{\sigma_1} \right) \left(\frac{h_2 - m_2}{\sigma_2} \right) \right] / 2(1-r^2) \right\}$$

where, because of stationarity, $m_1 = m_2 = m$, $\sigma_1 = \sigma_2 = \sigma$ and r depends only upon the relative distance between (x_1, y_1) and (x_2, y_2) . The values of σ , m , and r used in this expression are averages of the values obtained from the measurements of each profile.

Since the random height processes for the two surfaces are, for the purposes at hand, Gaussian and stationary, the surface slopes, $\frac{\partial h}{\partial l}$ where l is the distance along a profile of the surface, are, according to Middleton [1960], normally distributed with mean zero and variance

$$-\sigma^2 \frac{d^2 r}{dl^2} \Big|_{l=0}$$

For a Gaussian autocorrelation function, the variance is

$$2 \frac{\sigma^2}{L^2}$$

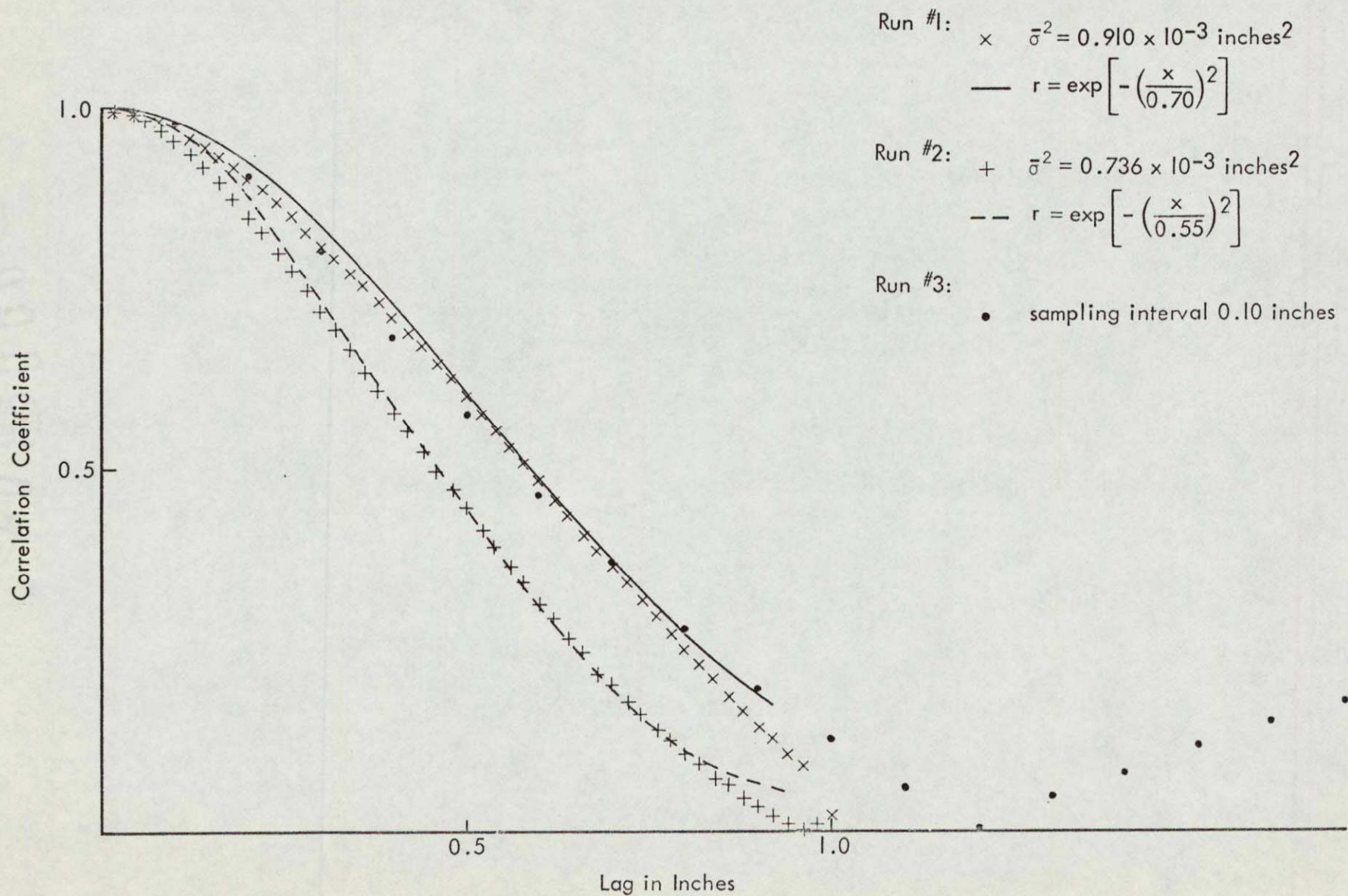
Although, the sample autocorrelation coefficients are clearly not fit well by the Gaussian function, especially near the origin, the variance of slopes can be estimated by using the values of sample variance and the calculated L 's, as given on figures III.14 and III.15. For the steel surface, the values of the variance of slopes for the two profiles made with the shorter sampling interval are estimated to be

$$4.89 \times 10^{-3} \qquad 3.72 \times 10^{-3}$$

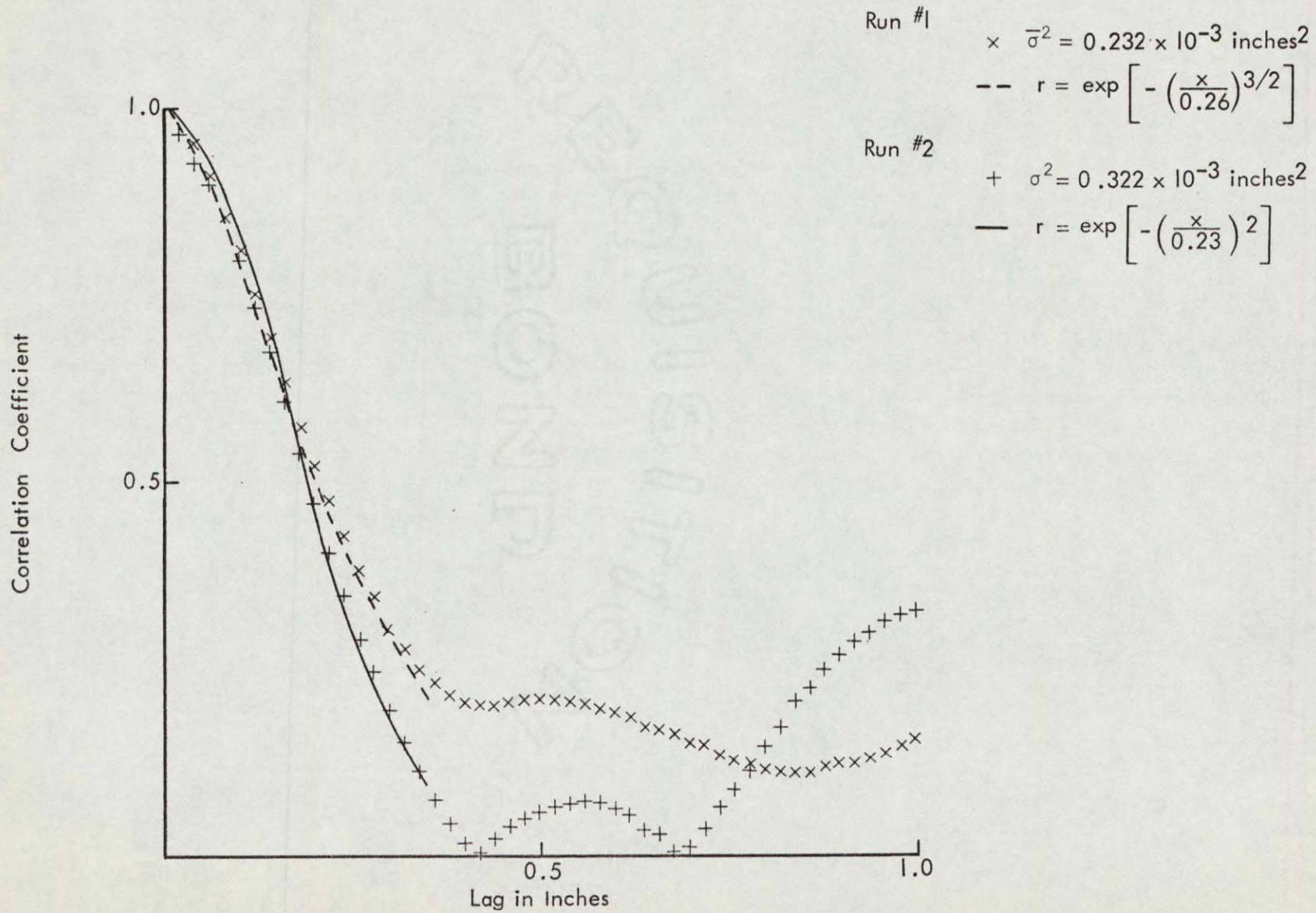
with the average of these being 4.30×10^{-3} . For the grout surface this estimate is more difficult to make because one of the curves is closely fit by the three halves power function. The problem is circumvented by sending a Gaussian function through the point $\bar{r} = 1/e$, and using the corresponding value of L (0.26 inches) in the calculation of the variance of slopes. Doing this and proceeding as above for the other experimental curve gives the results

$$12.16 \times 10^{-3} \qquad 6.84 \times 10^{-3}$$

with the average being 9.5×10^{-3} . Therefore, on the average, the grout surface is approximately twice as rough as the steel surface using the variance of slopes as a criterion.

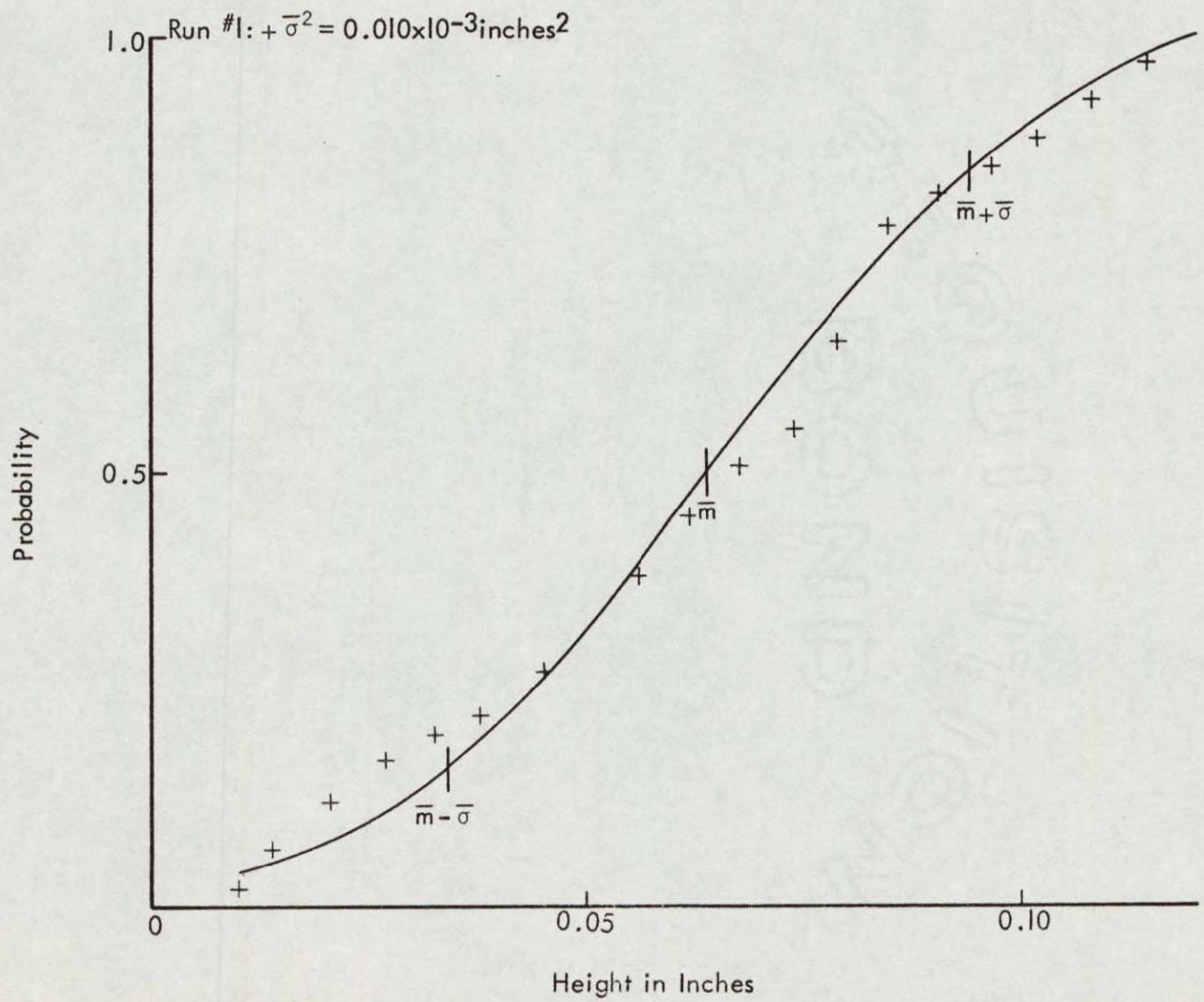


SAMPLE AUTO CORRELATION FUNCTIONS FOR THE STEEL SURFACE
 Figure III. 14

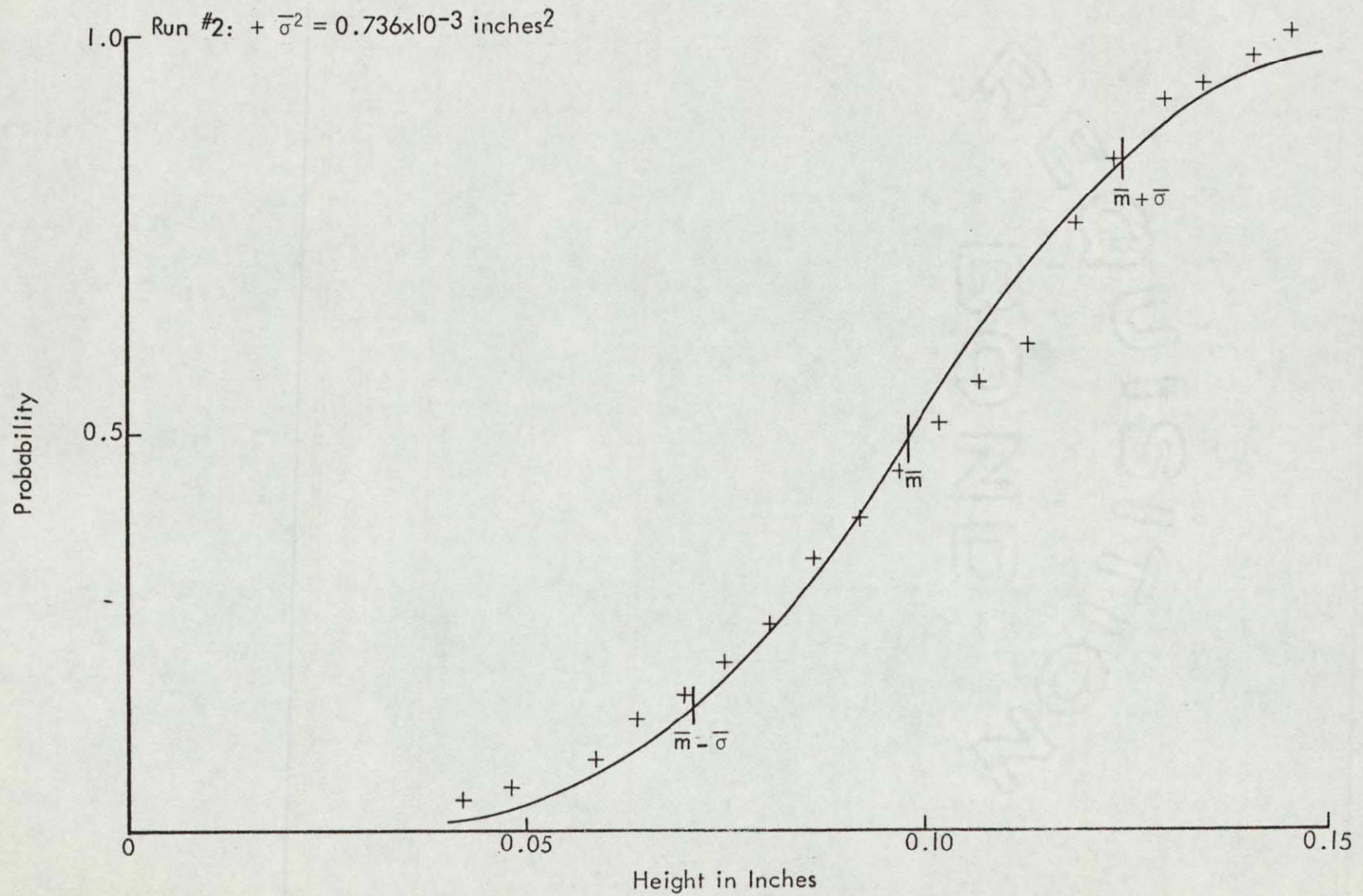


SAMPLE AUTOCORRELATION FUNCTION FOR THE GROUT SURFACE

Figure III. 15

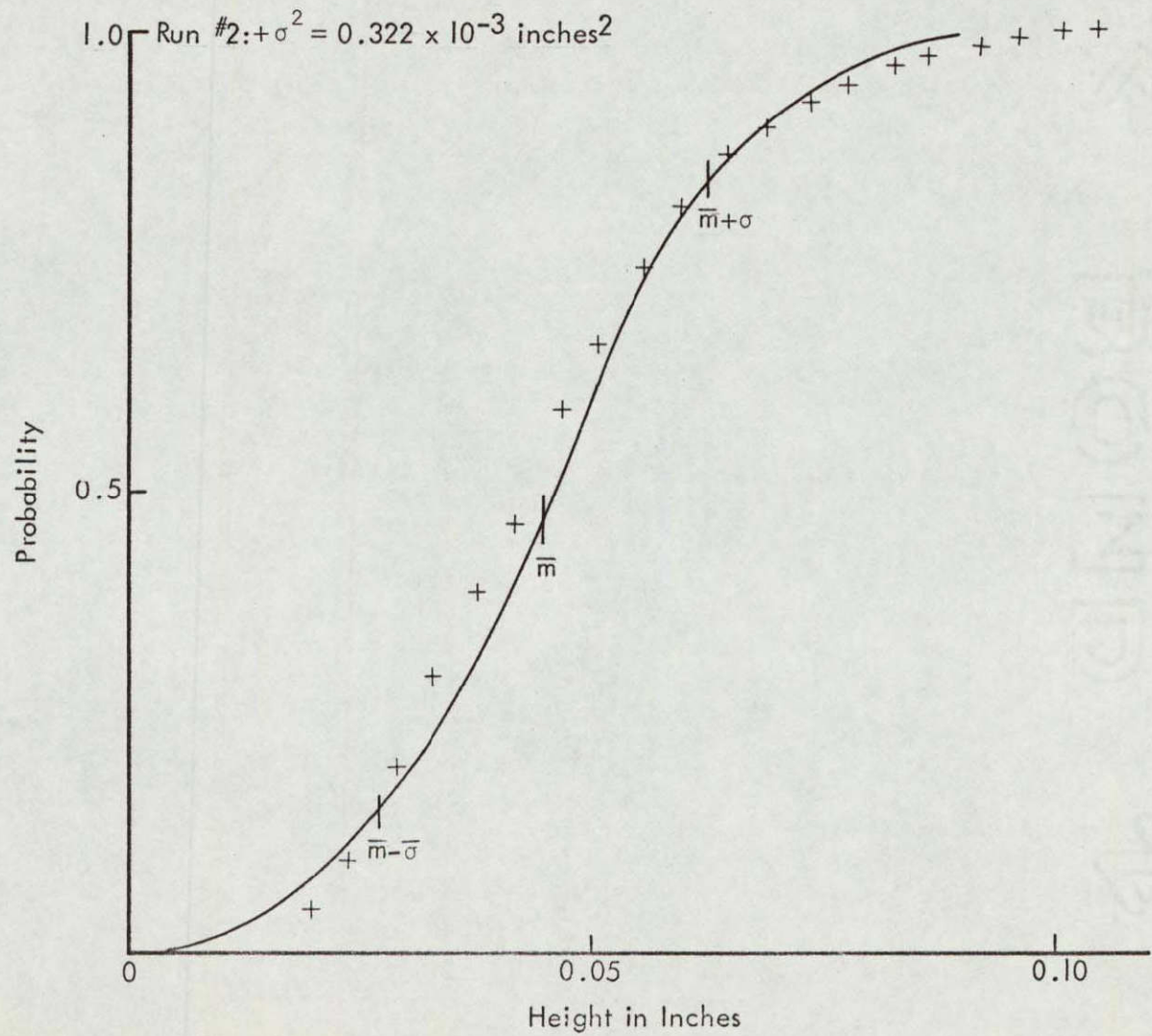


SAMPLE PROBABILITY DISTRIBUTION FUNCTION FOR STEEL SURFACE
Figure III. 16



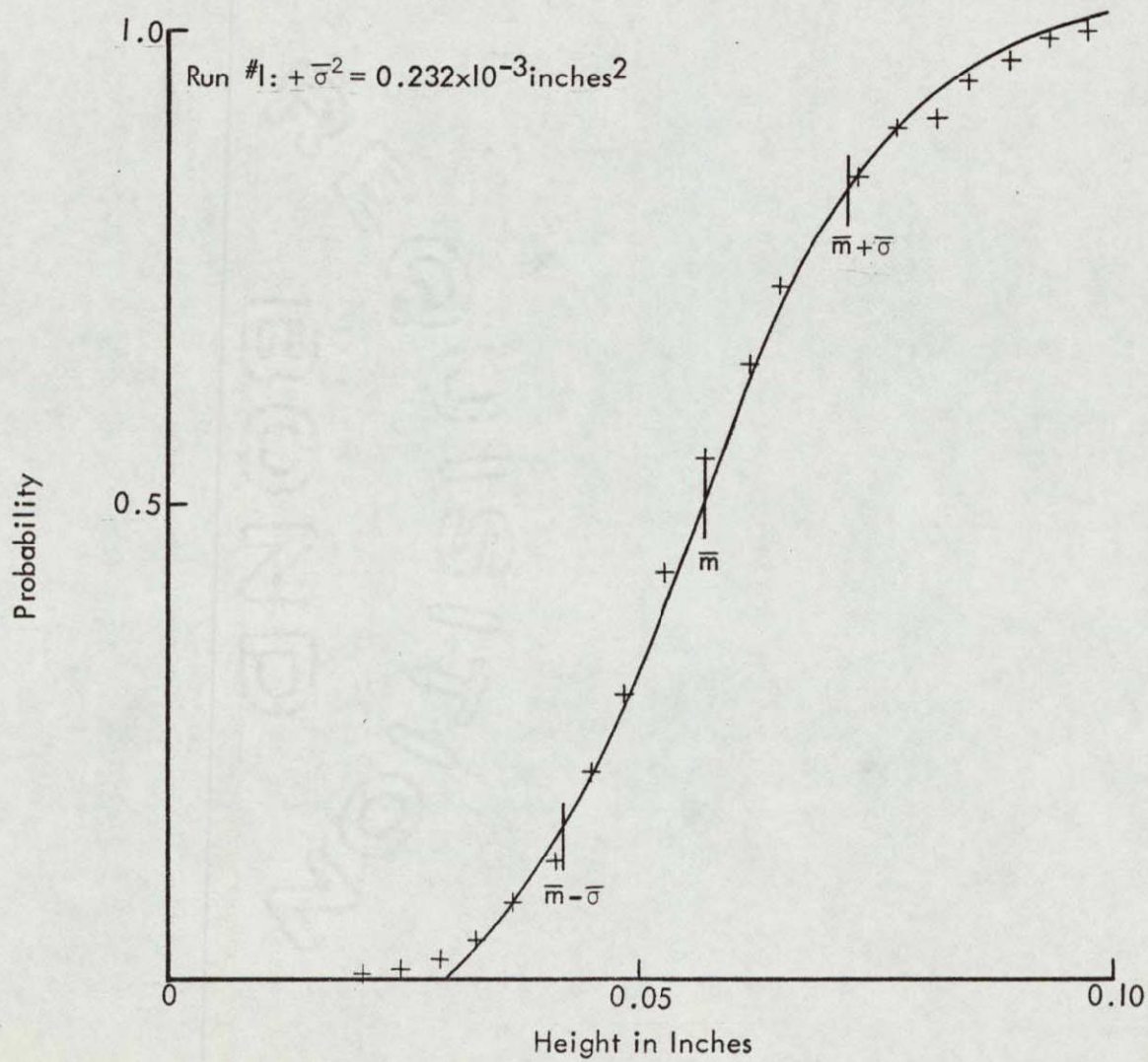
SAMPLE PROBABILITY DISTRIBUTION FUNCTION FOR THE STEEL SURFACE

Figure III. 17



SAMPLE PROBABILITY DISTRIBUTION FUNCTION FOR THE GROUT SURFACE

Figure III. 18



SAMPLE PROBABILITY DISTRIBUTION FUNCTION FOR THE GROUT SURFACE

Figure III. 19

III. E The Experimental Results and Comparison with Theory

The experiment to determine the average differential scattering cross section as a function of the angles (ϕ_0, ϕ_1, ϕ_2) was performed in a way designed to show the characteristics of two distinct features of rough surface scattering. One of these is the nature of the scattering when the transmitter and receiver depression angles are held equal throughout their variation ($\phi_1 = \phi_2$). This includes scatter in the specular direction ($\phi_0 = 0^\circ$) and also backscatter ($\phi_0 = 180^\circ$). The measurement of scatter in the specular direction as a function of depression angle is important because the differences in surface properties, both material and roughness, are so strongly evident there. Backscatter is, of course, important for practical reasons and also because of the large amount of accumulated data with which comparison can be made. The other feature of omnidirectional scattering which influenced design of the experiments is the nature of the scattering for one transducer held fixed in angular position ($\phi_1 = \text{constant}$) and the other variable. The behavior in the plane of incidence ($\phi_0 = 0^\circ$) under this condition is of interest because a comparison can be made between the results of La Casce and Tamarkin [1956] for scattering from regularly rough surfaces and those obtained here for randomly rough surfaces.

The results of the measurements made with the receiver and transmitter depression angles equal are shown in figure III. 20 for the steel surface and figure III. 21 for the grout surface. These are curves with σ_0 plotted against ϕ_0 with $\phi_1 = \phi_2$ varying parametrically. Comparison of the results for the two surfaces shows, at least on an intuitive basis, that the grout surface is rougher than the steel. This is seen from the smaller values of σ_0 measured in the specular direction and also from the slower decrease of σ_0 with depression angle for angles away from the specular direction, although this is not as evident. The values in the specular direction for both surfaces are seen to be nearly constant with no discernible pattern to the small (on the db scale) changes. The results for the steel surface have an anomaly that is not present in the grout surface results. This is the crossing of the curves for angles $\phi_1 = \phi_2 = 50^\circ, 60^\circ$ by the curves for lower depression angle $\phi_1 = \phi_2 = 30^\circ, 40^\circ$.

This is not believed to be the result of an experimental error because the experiments were repeated several times to observe this phenomenon.

The experimental results for ϕ_1 held constant at 40° and ϕ_2 variable are shown in figures III. 22 and III. 23 for the steel and grout surfaces, respectively. For these curves, σ_o is again plotted against ϕ_o with ϕ_2 as the parameter. To show some features of these results with greater clarity cuts of $\phi_o = \text{constant}$ were made in figures III. 22 and III. 23 to obtain plots in which σ_o is plotted against ϕ_2 with ϕ_o as the parameter. These curves are shown in figure III. 24 for the steel surface and figure III. 25 for the grout surface. The results given in figures III. 22 and III. 24 for the steel surface are seen in greater perspective in the three dimensional representation of these results shown photographically in figure III. 26. The three dimensional figure is formed by the radius vectors emanating from the intersection of the principal rays of the antennas, which is the origin of the coordinate system of figure III. 1. The length of a radius vector is proportional to the σ_o in db for the angles of observation (ϕ_o, ϕ_2) in which the vector is oriented. The principal ray of the transmitting antenna which defines the angle of incidence $\phi_1 = 40^\circ$ relative to the normal of the mean plane of the rough surface is depicted by the shaft piercing the figure. The view of figure III. 26a is that seen from the sidescatter position, $\phi_1 = 90^\circ$. The views of III. 26b and III. 26c are those seen from $\phi_o = 45^\circ$ and $\phi_o = 135^\circ$, respectively. The results for the grout surface are not shown three dimensionally because of their similarity in form to those for the steel surface. The principal difference between the results for the two surfaces is that the peak of σ_o in the specular direction is more pronounced for the steel surface which indicates that the grout surface is the rougher of the two. The relative roughness is shown in another way by the vertical extent of the curves of figures III. 22 through III. 25; for the steel surface the values of σ_o vary over a 35 db range while the variation for the grout is only about 20 db. A peculiar feature which distinguishes the curves of figure III. 24 from those of figure III. 25 is the behavior far away from specular ($\phi_o > 60^\circ$). For the steel surface there is an increase and then slight decrease as the depression angle increases while the grout surface has a general decrease with depression angle with a hint of an increase near $\phi_2 = 30^\circ$. It is recalled that these results for the

grout surface are suspect (see Section III C) and perhaps no great amount of credence should be placed in this peculiar difference in the curves. However, considering the anomalous behavior of the steel target results mentioned above it is not unlikely that this is a similar phenomenon.

The experimental results shown in figures III. 20 through III. 25 were computed using values of re-radiated power that were assumed to be predominantly scatter. It is recalled that this is, in fact, a condition for computing a differential scattering cross section. The degree to which the power was being reflected was not determined and a separation into scatter and specular components is not possible. However, from Section II C it is seen that the factor of the specular power density

$$\exp \left\{ -k_z^2 \sigma^2 \right\} \quad \text{III. 6}$$

can be used to indicate to what degree reflection is occurring. Using average values of the variances given for the two surfaces in figures III. 14 and III. 15, the factor III. 6 becomes

$$\exp \left\{ -9.5 (\cos \phi_1 + \cos \phi_2)^2 \right\} \quad \text{III. 7a}$$

for the steel surface and

$$\exp \left\{ -3.1 (\cos \phi_1 + \cos \phi_2)^2 \right\} \quad \text{III. 7b}$$

for the grout surface, where the conversion $\phi_2 = \theta_{oz}$, $\phi_1 = 180^\circ - \theta_{1z}$ has been made. For the depression angles $\phi_1 = \phi_2 = 0$ it is seen that the quantities III. 7 are quite small. However, for larger depression angles they increase in size and at $\phi_1 = \phi_2 = 70^\circ$ (the limit of the range of angles over which data was taken) become

$$e^{-4.23}$$

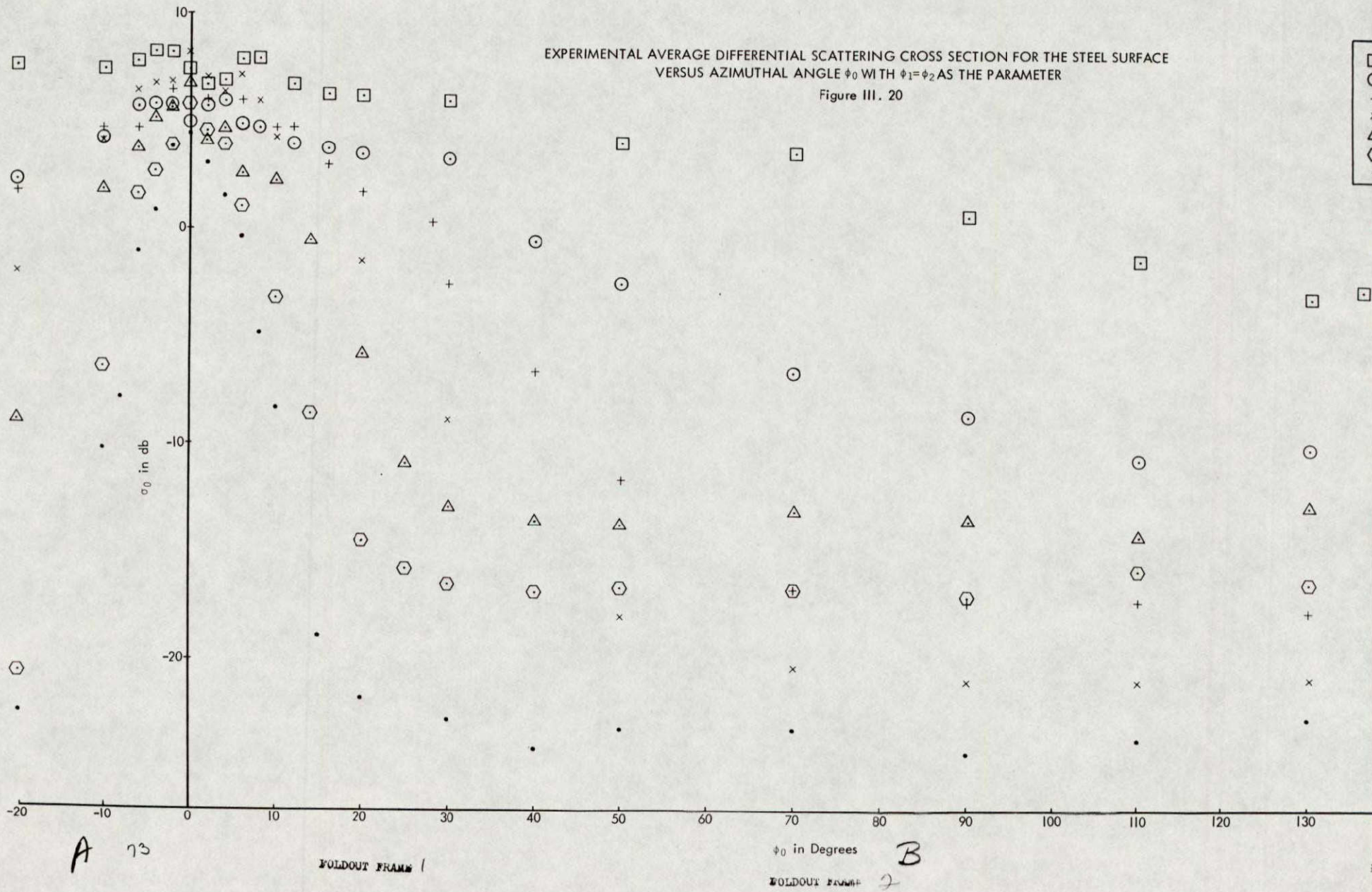
for the steel surface and

$$e^{-1.44}$$

for the grout surface. The factor for the steel surface is still quite small;

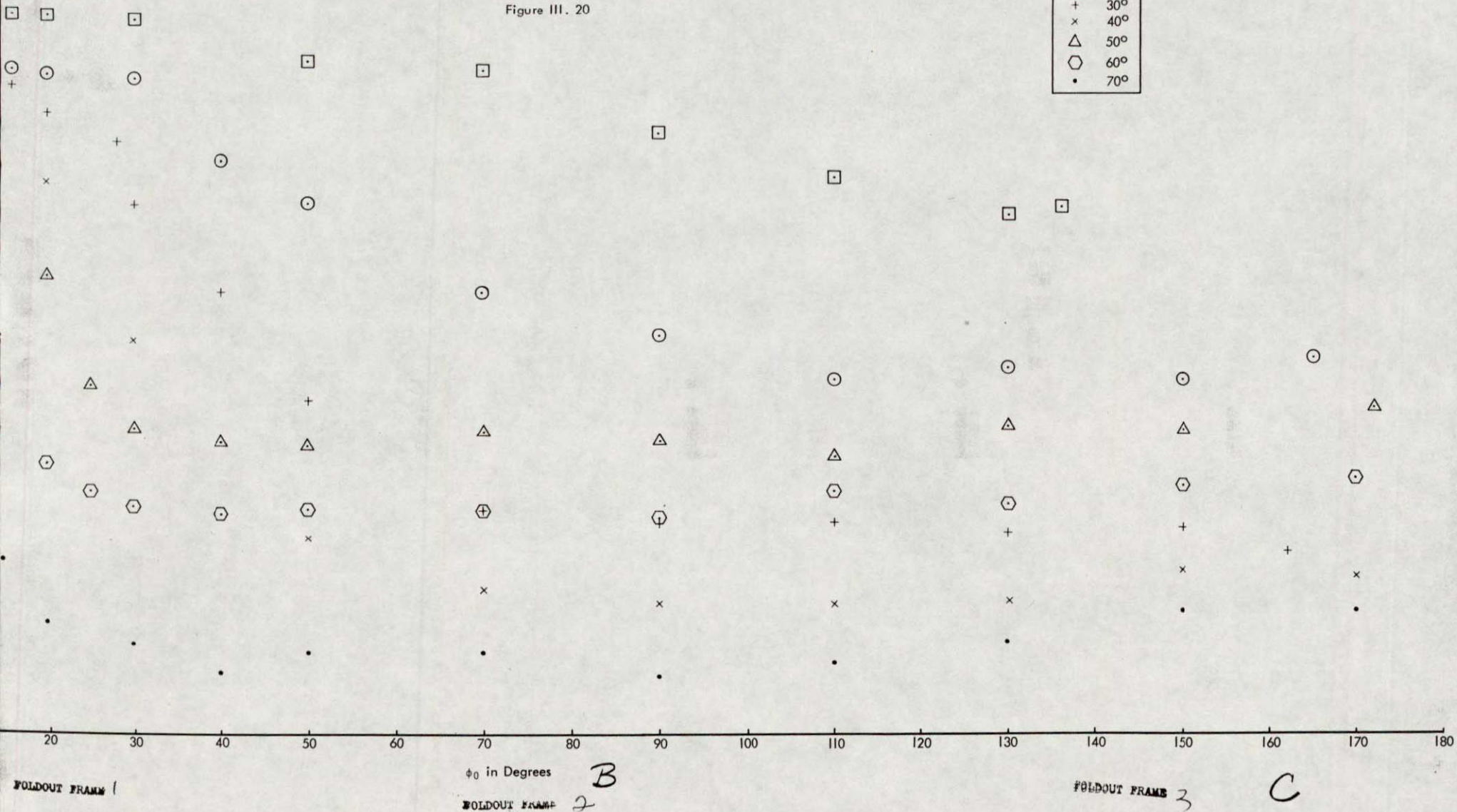
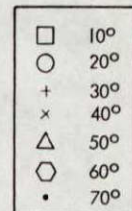
EXPERIMENTAL AVERAGE DIFFERENTIAL SCATTERING CROSS SECTION FOR THE STEEL SURFACE
VERSUS AZIMUTHAL ANGLE ϕ_0 WITH $\phi_1 = \phi_2$ AS THE PARAMETER

Figure III. 20



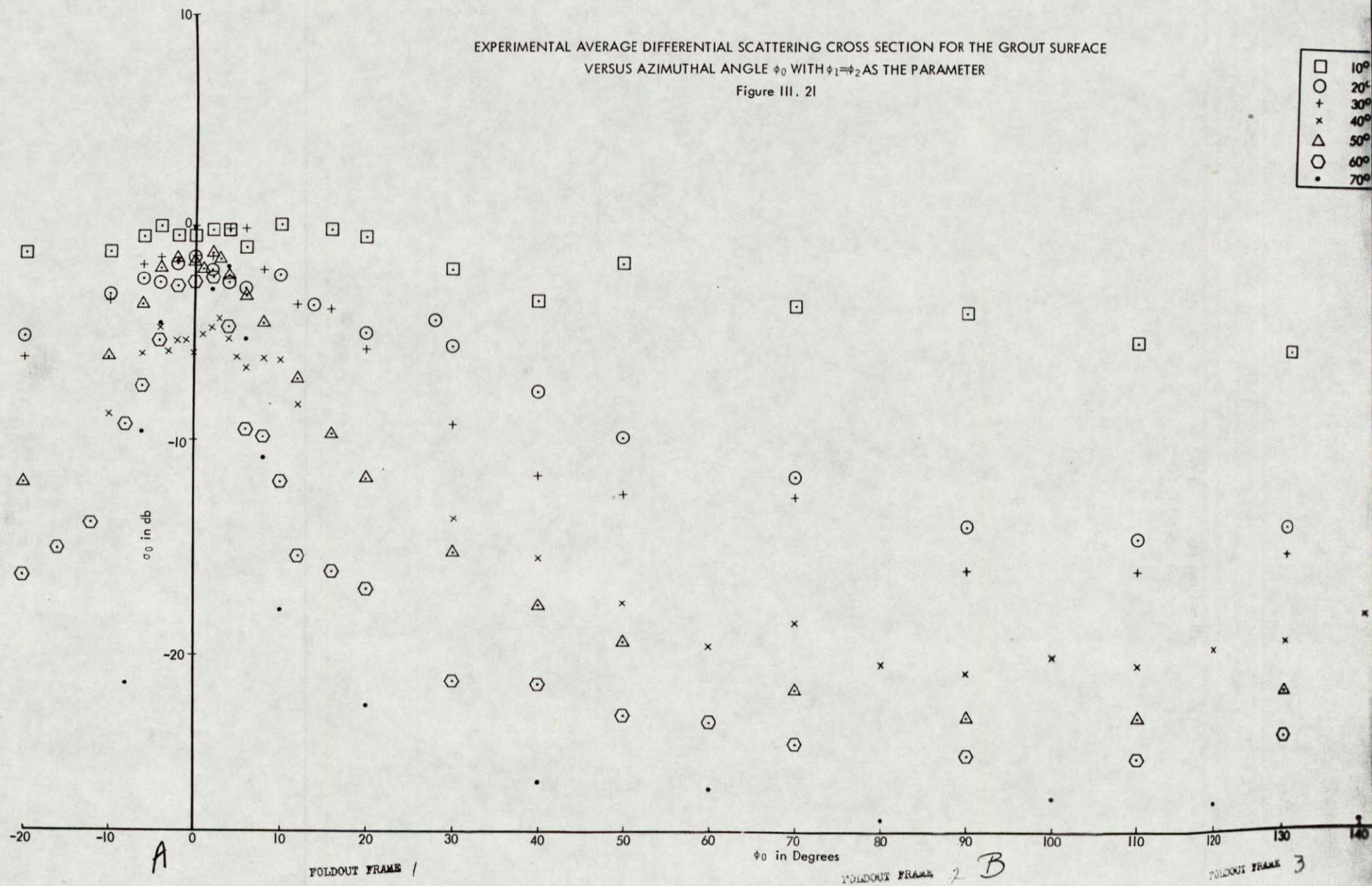
EXPERIMENTAL AVERAGE DIFFERENTIAL SCATTERING CROSS SECTION FOR THE STEEL SURFACE
 VERSUS AZIMUTHAL ANGLE ϕ_0 WITH $\phi_1 = \phi_2$ AS THE PARAMETER

Figure III. 20



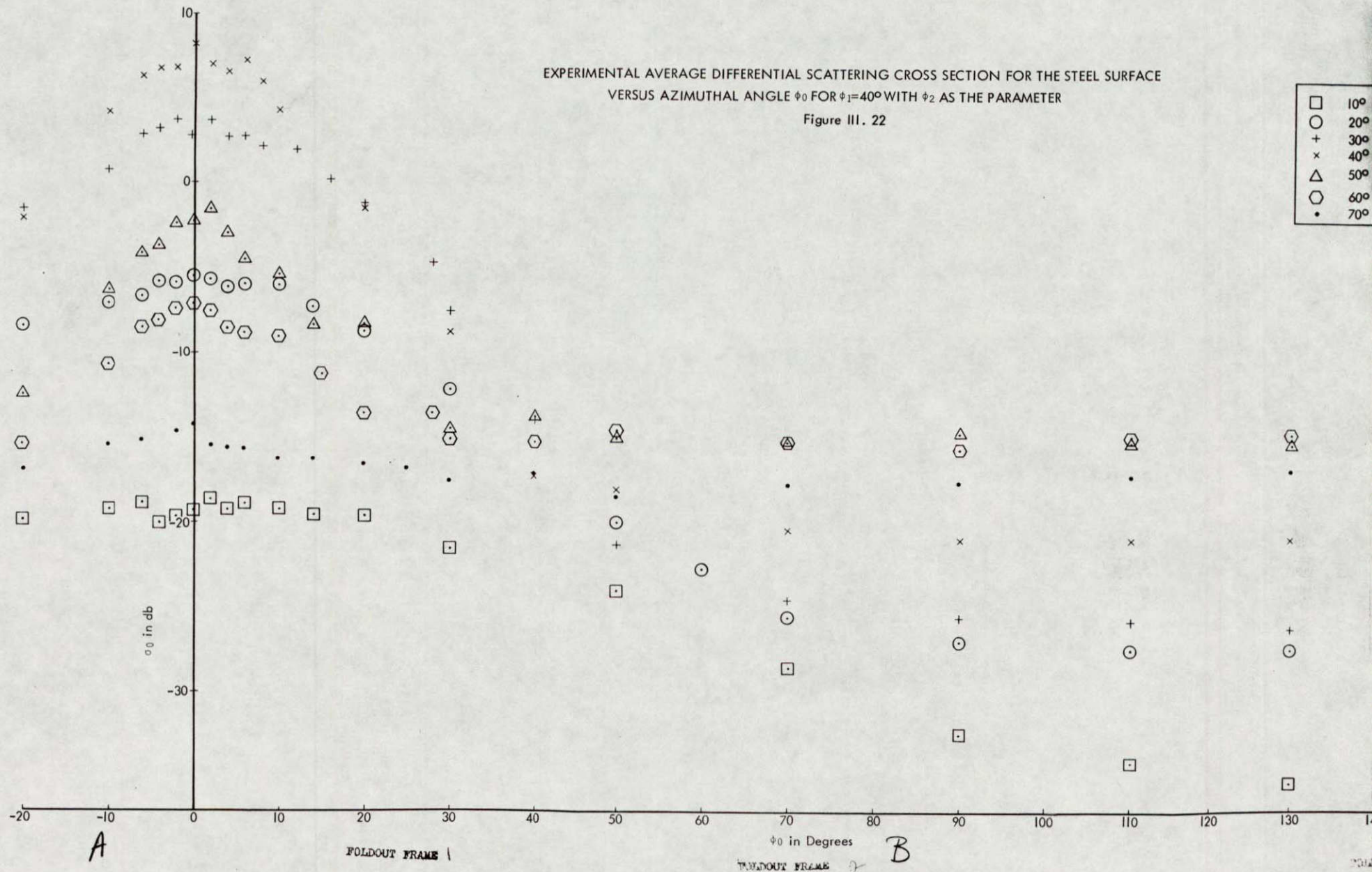
EXPERIMENTAL AVERAGE DIFFERENTIAL SCATTERING CROSS SECTION FOR THE GROUT SURFACE
 VERSUS AZIMUTHAL ANGLE ϕ_0 WITH $\phi_1=\phi_2$ AS THE PARAMETER

Figure III. 21



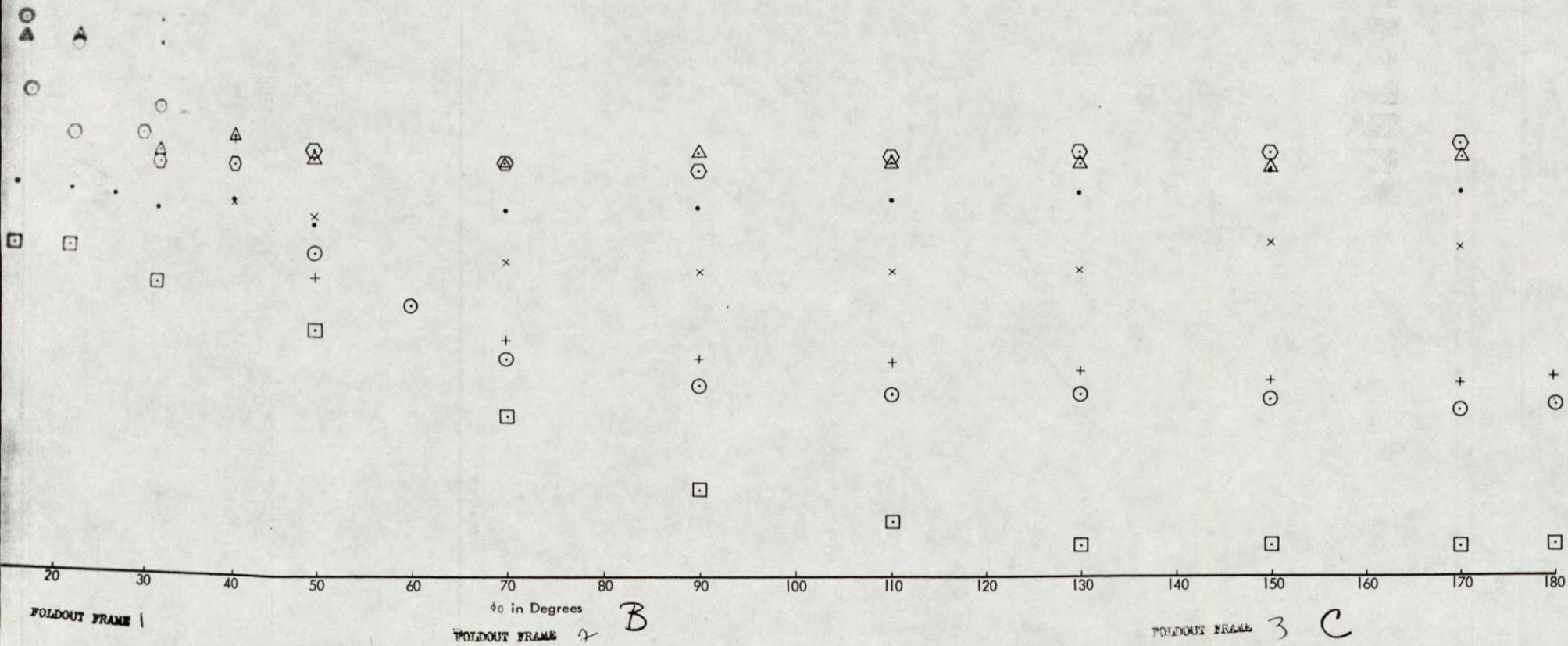
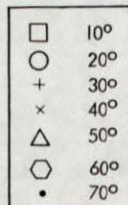
EXPERIMENTAL AVERAGE DIFFERENTIAL SCATTERING CROSS SECTION FOR THE STEEL SURFACE
 VERSUS AZIMUTHAL ANGLE ϕ_0 FOR $\phi_1=40^\circ$ WITH ϕ_2 AS THE PARAMETER

Figure III. 22



EXPERIMENTAL AVERAGE DIFFERENTIAL SCATTERING CROSS SECTION FOR THE STEEL SURFACE
 VERSUS AZIMUTHAL ANGLE ϕ_0 FOR $\phi_1=40^\circ$ WITH ϕ_2 AS THE PARAMETER

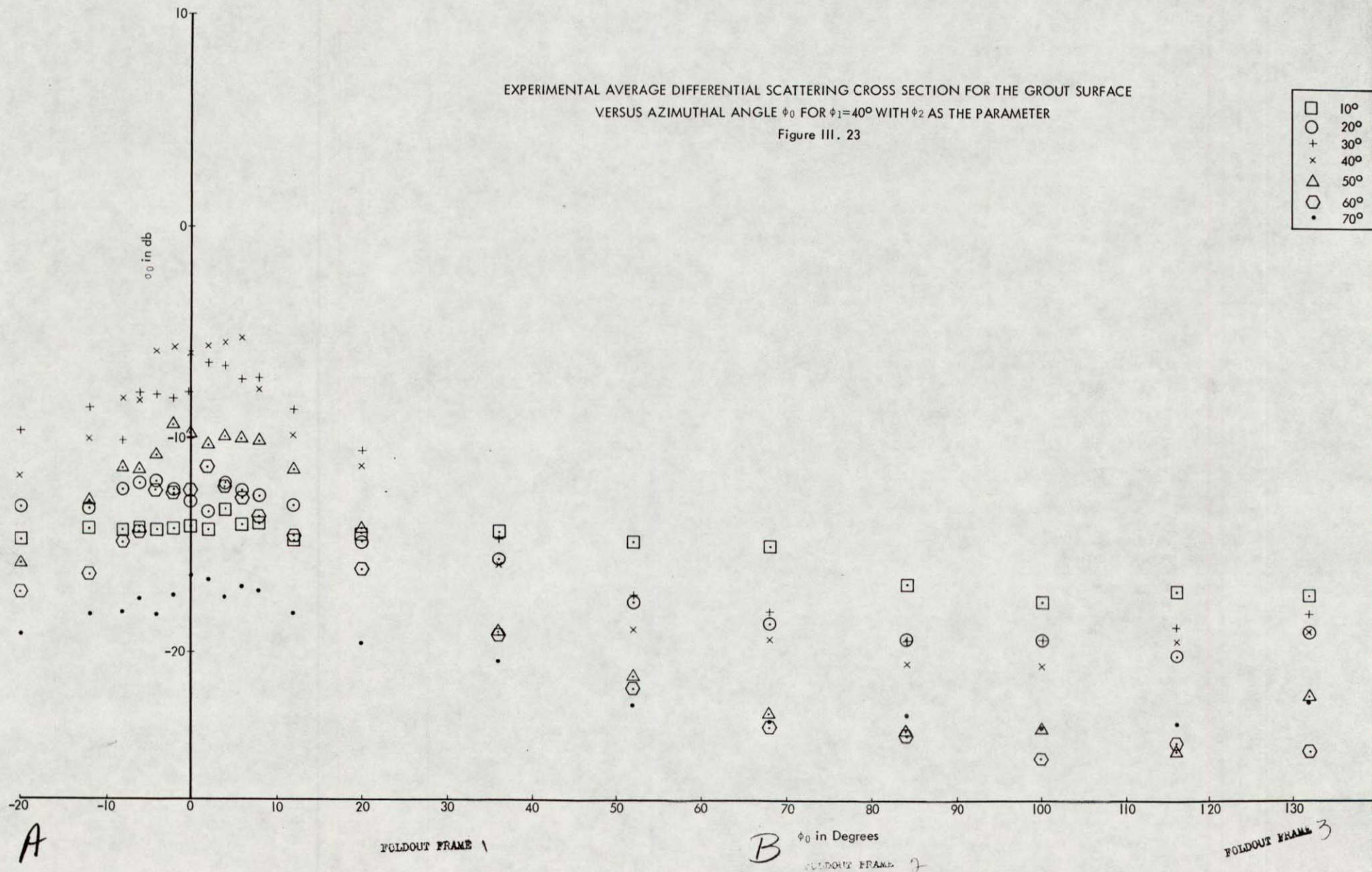
Figure III. 22



EXPERIMENTAL AVERAGE DIFFERENTIAL SCATTERING CROSS SECTION FOR THE GROUT SURFACE
 VERSUS AZIMUTHAL ANGLE ϕ_0 FOR $\phi_1=40^\circ$ WITH ϕ_2 AS THE PARAMETER

Figure III. 23

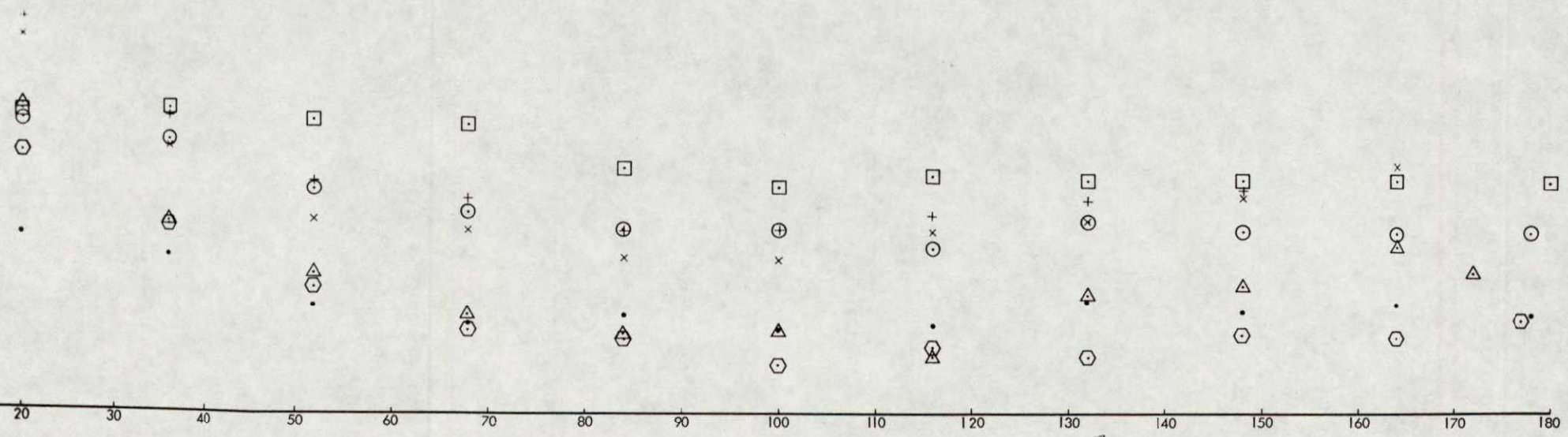
- | | |
|---|-----|
| □ | 10° |
| ○ | 20° |
| + | 30° |
| x | 40° |
| △ | 50° |
| ⊕ | 60° |
| • | 70° |



EXPERIMENTAL AVERAGE DIFFERENTIAL SCATTERING CROSS SECTION FOR THE GROUT SURFACE
 VERSUS AZIMUTHAL ANGLE ϕ_0 FOR $\phi_1=40^\circ$ WITH ϕ_2 AS THE PARAMETER

Figure III. 23

□	10°
○	20°
+	30°
×	40°
△	50°
⬡	60°
•	70°



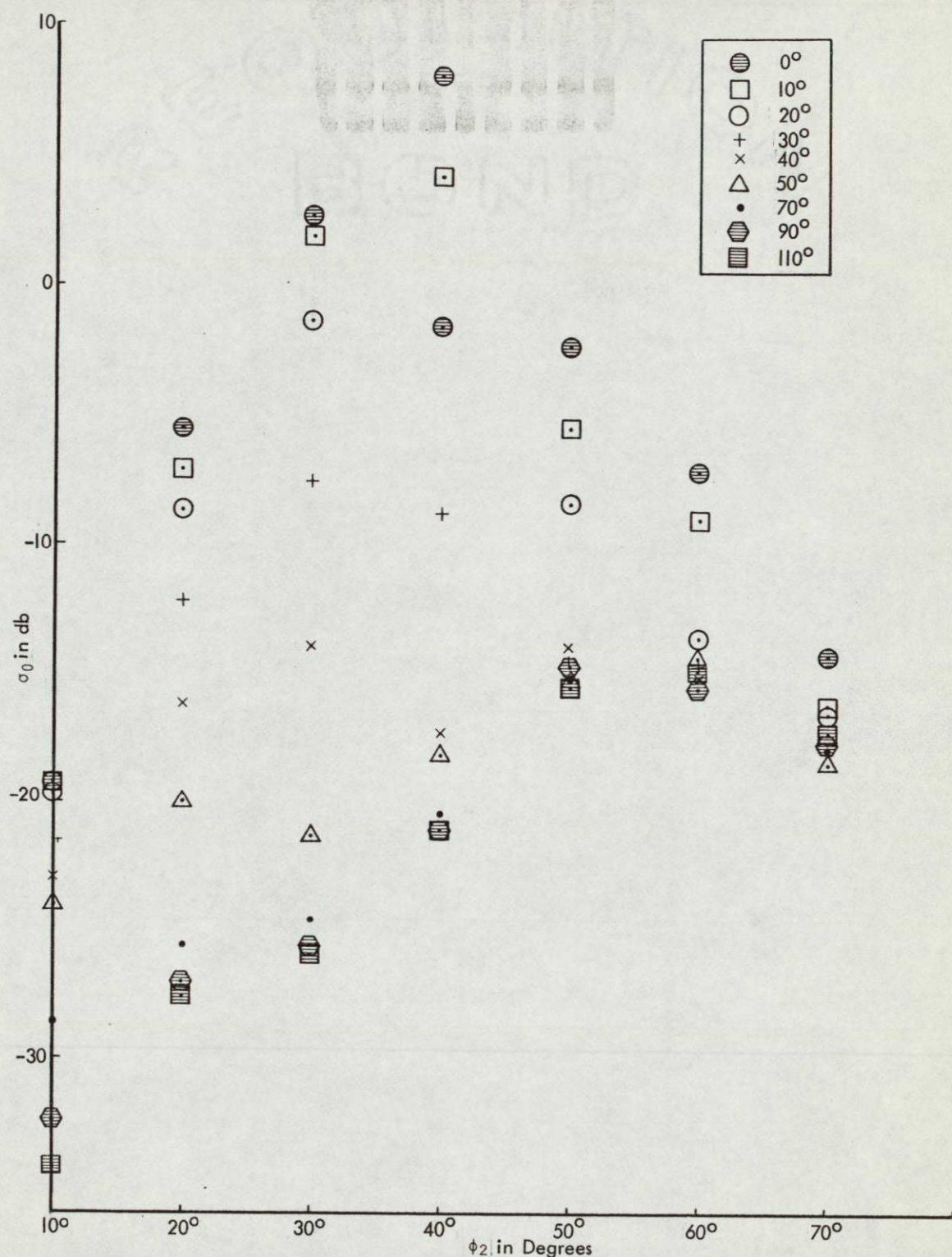
FOLDOUT FRAME 1

B ϕ_0 in Degrees
 FOLDOUT FRAME 2

FOLDOUT FRAME 3

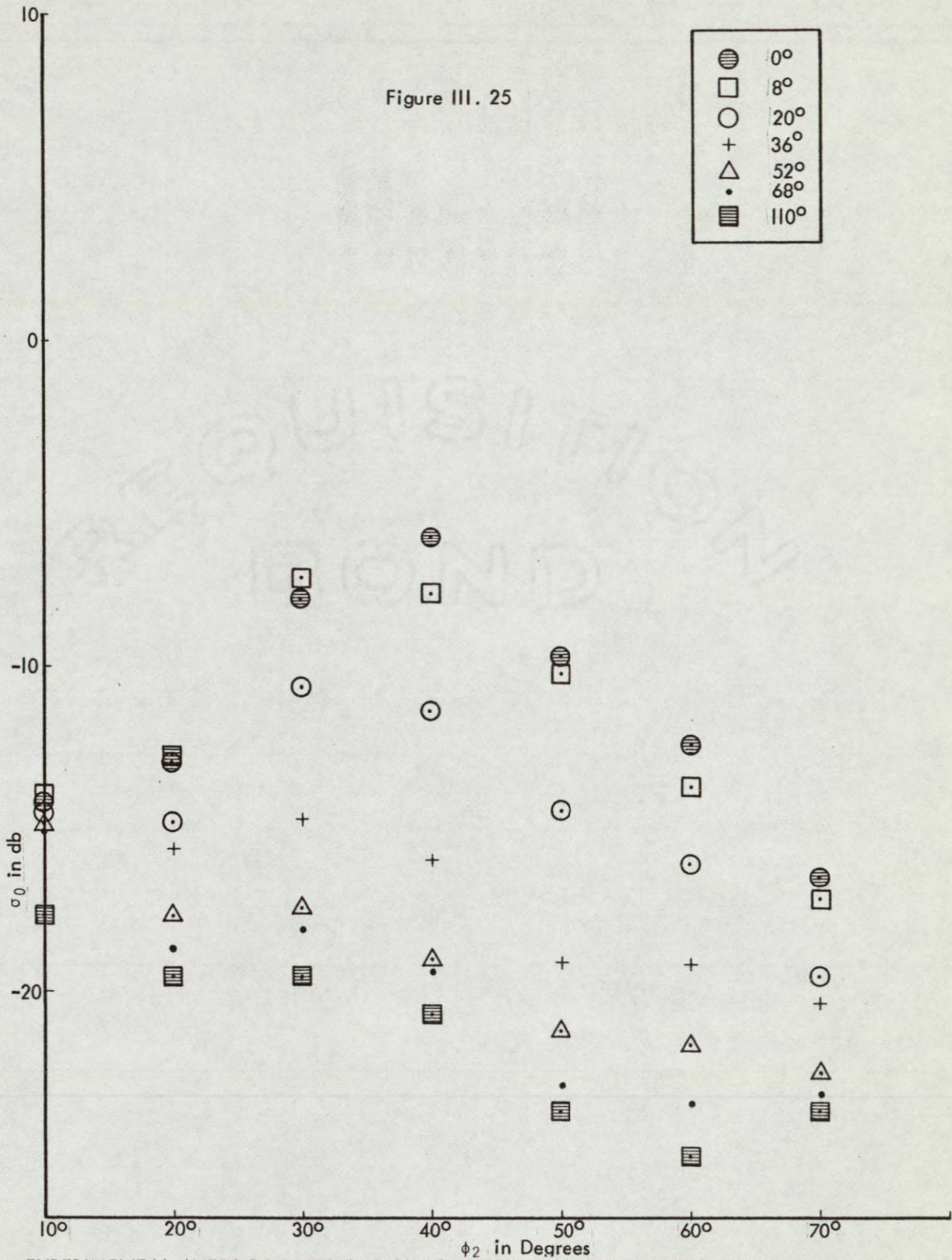
C

FOLDOUT FRAME



EXPERIMENTAL AVERAGE DIFFERENTIAL SCATTERING CROSS SECTION FOR THE STEEL SURFACE
 VERSUS POLAR ANGLE ϕ_2 FOR $\phi_1 = 40^\circ$ WITH ϕ_0 AS THE PARAMETER
 Figure III. 24

Figure III. 25



EXPERIMENTAL AVERAGE DIFFERENTIAL SCATTERING CROSS SECTION FOR THE GROUT SURFACE VERSUS POLAR ANGLE ϕ_2 , FOR $\phi_1=40^\circ$ WITH ϕ_0 AS THE PARAMETER

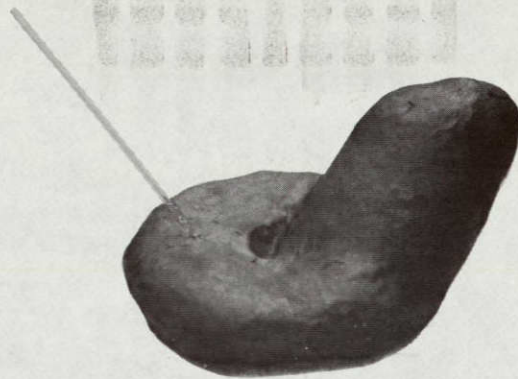


Figure III. 26a

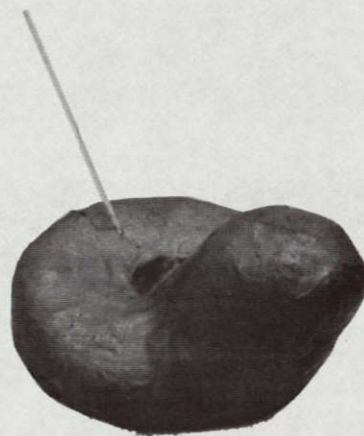


Figure III. 26b

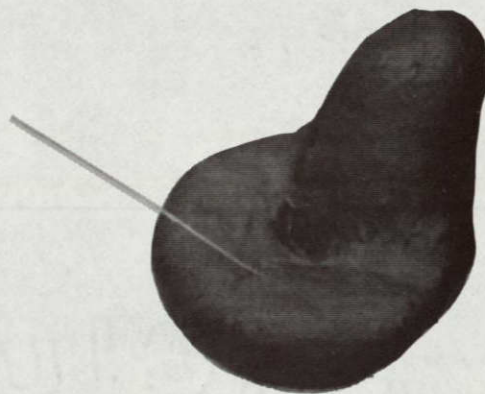


Figure III. 26c

Three Dimensional Representation of Omnidirectional Scattering

$$\begin{aligned} \exp\{-K_2^2 \sigma^2\} &= \exp\left\{-\left(\frac{2\pi\sigma}{\lambda}\right)^2 (\cos \theta_{0z} - \cos \theta_{1z})^2 (1-r)\right\} \\ &= \exp\left\{-\left(\frac{2\pi\sigma}{\lambda}\right)^2 (\cos \phi_1 + \cos \phi_2)^2 (1-r)\right\} \end{aligned}$$

III. 8

From this it is seen that the range of bracketing must extend from the origin where $r = 1$ to a point where r is small enough to make the quantity negligible. The values of σ used in III. 8 in the determination of the range of r and those calculated for III. 6. Substituting these gives

$$\exp\{-9.5(\cos \phi_1 + \cos \phi_2)^2 (1-r)\} \quad \text{III.9a}$$

for the steel surface and

$$\exp\{-3.1(\cos \phi_1 + \cos \phi_2)^2 (1-r)\} \quad \text{III.9b}$$

for the grout. It is seen that the range of bracketing depends upon the angles of incidence and observation. To insure bracketing over the range of angles for which there is experimental data, the angles for the steel surface are chosen to be $\phi_1 = \phi_2 = 70^\circ$, and III. 9a becomes

$$\exp\{-4.23(1-r)\} \quad \text{III.10a}$$

A similar choice cannot be made for the grout surface because the factor of $(1-r)$ becomes too small (from earlier, it is 1.44) for even $r = 0$ to make the exponential negligible, as required. It is this inability of the exponential to become negligible that leads to the appreciable specular component at these angles, as discussed earlier in this section and in Section II D. A marginal choice for the grout surface is $\phi_1 = \phi_2 = 60^\circ$; for this set of angles III. 9b then becomes

$$\exp\{-3.1(1-r)\} \quad \text{III.10b}$$

For the exponents of III.10, the range of bracketing is chosen to be from $r = 1$ to $r = 1/e$; this choice is motivated in part by the fact that the Gaussian functions of figures III.14 and III.15 pass through these points. Therefore, the correlation distances for both the exponential and Gaussian function are those lag distances corresponding to the points $r = 1/e$ on the curves of sample autocorrelation function; for the two profiles made for each surface, these values are

$$L = 0.26, 0.23 \text{ inches}$$

for the grout surface and

$$L = 0.55, 0.70 \text{ inches}$$

for the steel.

The other difficulty encountered in applying the theory is that the reflection coefficient is unknown near normal incidence, as mentioned above. Away from the vertical, past the critical angle, the reflection coefficient approaches unity and as it does so the surface becomes perfectly rigid. Because of this, the results of Chapter II are used under the condition that the surface is perfectly reflecting, and comparison is made between theory and experiment for angles past the critical.

The expressions used in the comparison are eq. 's (II.28) and (II.29) after specialization to the condition of a perfectly rigid surface. This specialization is made through the a 's which become for $\Gamma = 1$

$$a_1 = 2k \cos \theta_{oz}$$

$$a_2 = -2k \cos \theta_{ox}$$

$$a_3 = -2k \cos \theta_{oy}$$

Substituting these values and the expressions for the K 's which are

$$K_x = k(\cos \theta_{ox} - \cos \theta_{1x})$$

$$K_y = k(\cos \theta_{oy} - \cos \theta_{1y})$$

$$K_z = k(\cos \theta_{oz} - \cos \theta_{1z})$$

into eq. 's (II.28) and (II.29) and manipulating gives the results

$$\begin{aligned}
\sigma_0 = & \left\{ \cos^2 \theta_{0z} + 2 \frac{(\cos \theta_{0x} - \cos \theta_{1x})}{(\cos \theta_{0z} - \cos \theta_{1z})} \cos \theta_{0z} \cos \theta_{0x} \right. \\
& + 2 \frac{(\cos \theta_{0y} - \cos \theta_{1y})}{(\cos \theta_{0z} - \cos \theta_{1z})} \cos \theta_{0z} \cos \theta_{0y} \\
& + \frac{(\cos \theta_{0x} - \cos \theta_{1x})^2}{(\cos \theta_{0z} - \cos \theta_{1z})^2} \cos^2 \theta_{0x} \\
& + \frac{(\cos \theta_{0y} - \cos \theta_{1y})^2}{(\cos \theta_{0z} - \cos \theta_{1z})^2} \cos^2 \theta_{0y} \\
& \left. + 2 \frac{(\cos \theta_{0x} - \cos \theta_{1x})(\cos \theta_{0y} - \cos \theta_{1y})}{(\cos \theta_{0z} - \cos \theta_{1z})^2} \cos \theta_{0x} \cos \theta_{0y} \right\} \\
& \exp \left\{ - \frac{(\cos \theta_{0x} - \cos \theta_{1x})^2 + (\cos \theta_{0y} - \cos \theta_{1y})^2}{\frac{4\sigma^2}{L^2} (\cos \theta_{0z} - \cos \theta_{1z})^2} \right\} \\
& \frac{4\pi\sigma^2}{L^2} (\cos \theta_{0z} - \cos \theta_{1z})^2
\end{aligned}$$

III.11

for the Gaussian autocorrelation coefficient and

$$\begin{aligned}
\sigma_0 = & \left\{ \cos^2 \theta_{0z} + 2 \frac{(\cos \theta_{0x} - \cos \theta_{1x})}{(\cos \theta_{0z} - \cos \theta_{1z})} \cos \theta_{0x} \cos \theta_{0x}' \right. \\
& + 2 \frac{(\cos \theta_{0y} - \cos \theta_{1y})}{(\cos \theta_{0z} - \cos \theta_{1z})} \cos \theta_{0z} \cos \theta_{0y} \\
& + \frac{(\cos \theta_{0x} - \cos \theta_{1x})^2}{(\cos \theta_{0z} - \cos \theta_{1z})^2} \cos^2 \theta_{0x} \\
& + \frac{(\cos \theta_{0y} - \cos \theta_{1y})^2}{(\cos \theta_{0z} - \cos \theta_{1z})^2} \cos^2 \theta_{0y} \\
& \left. + 2 \frac{(\cos \theta_{0x} - \cos \theta_{1x})(\cos \theta_{0y} - \cos \theta_{1y})}{(\cos \theta_{0z} - \cos \theta_{1z})^2} \cos \theta_{0x} \cos \theta_{0y} \right\} \\
& \frac{\left[\frac{L/\lambda}{(\sigma/\lambda)^2} \right] (\cos \theta_{0z} - \cos \theta_{1z})^2}{\left\{ (2\pi)^2 (\cos \theta_{0z} - \cos \theta_{1z})^4 + \left[\frac{L/\lambda}{(\sigma/\lambda)^2} \right]^2 \left[(\cos \theta_{0x} - \cos \theta_{1x})^2 + (\cos \theta_{0y} - \cos \theta_{1y})^2 \right] \right\}^{3/2}}
\end{aligned}$$

III.12

for the exponential autocorrelation coefficient. The conversion from the direction cosines of the directional angles (θ_{0x} , θ_{0y} , θ_{0z} , θ_{1x} , θ_{1y} , θ_{1z}) to the spherical system (ϕ_0 , ϕ_1 , ϕ_2) is given by

$$\begin{aligned}
\cos \theta_{1x} &= 0 & \cos \theta_{0z} &= \cos \phi_2 \\
\cos \theta_{1y} &= \sin \phi_1 & \cos \theta_{0y} &= \cos \phi_0 \sin \phi_2 \\
\cos \theta_{1z} &= -\cos \phi_1 & \cos \theta_{0x} &= \sin \phi_0 \sin \phi_2
\end{aligned}$$

The values for the variance of slopes used in the expressions for σ_0 for the Gaussian autocorrelation function are those average values determined in Section III D for the two surfaces. The σ_0 for the exponential autocorrelation function depends upon the quantity

$$\left[\frac{L/\lambda}{(\sigma/\lambda)^2} \right]^2$$

The values of this quantity used in eq. III.12 are averages obtained using the variances for each surface given in figures III.14 and III.15 and the correlation distances given above. These average values are

$$2.54 \times 10^3$$

for the grout surface and

$$1.872 \times 10^3$$

for the steel surface.

The theoretical results for the exponential correlation function are shown, together with the experimental curves, in figure III.27 for the steel surface and figure III.28 for the grout surface for the angles $\phi_1 = \phi_2 = 10^\circ, 30^\circ, 50^\circ, 70^\circ$. For the angles $\phi_1 = \phi_2 = 20^\circ, 40^\circ, 60^\circ$ the results are shown in figures III.29 and III.30 for the steel and grout surfaces, respectively. A comparison between the experimental and predicted values for the steel surface shows that there is closer agreement for the angles $\phi_1 = \phi_2 = 50^\circ, 60^\circ, 70^\circ$ with the best agreement occurring for the two larger depression angles. For all smaller depression angles the agreement is not close especially in the neighborhood of the specular direction. As backscatter is approached, the agreement improves with the only serious difference occurring for the anomalous curves for the angles $\phi_1 = \phi_2 = 30^\circ, 40^\circ$. A comparison for the grout surface shows fair agreement between the predicted and experimental results but near specular there are wide differences especially for the larger depression angles where agreement should occur. It is clear that for both surfaces the theoretical results obtained using the exponential autocorrelation function do not generally give accurate predictions of the experimental results for angles in and near the specular direction. This is not surprising as the sample autocorrelation functions are not fit closely at all by the exponential function. What is surprising is the closeness of the agreement between theory and experiment away from the specular direction near backscatter.

The predictions of the experimental results made using the Gaussian autocorrelation function are shown in figure III. 31 for the steel surface and figure III. 32 for the grout for the angles $\phi_1 = \phi_2 = 10^\circ, 30^\circ, 50^\circ, 70^\circ$. The results for the angles $\phi_1 = \phi_2 = 20^\circ, 40^\circ, 60^\circ$ are shown in figures III. 33 and III. 34 for the steel and grout surfaces, respectively. The predictions for each of these surfaces are shifted downward; for the steel surface each curve is smaller by the factor 0.5 than that calculated and for the grout surface the factor is 0.22. It is seen that by doing this close agreement is obtained for both surfaces for angles that do not differ greatly (about 25°) from the specular. However, far away from the specular direction, the theory disagrees greatly with the experimental results and is of little value. For angles less than the critical angle it is expected that the predicted values for $\Gamma = 1$ would have to be shifted downward. However, for angles beyond the critical this should not be necessary and there should be agreement on an absolute basis. Since the agreement is only relatively close, the use of the Gaussian autocorrelation function is seen to lead to error in the specular direction as well as away from it, although to a much lesser degree. Also, the error is greater by about the factor two for the results for the grout surface than for those of the steel surface, which is expected as the steel surface is, from Section III D, described more closely by the Gaussian autocorrelation function than is the grout surface.

The theoretical results for ϕ_1 constant at 40° are shown in figures III. 35 and III. 36 for the steel and grout surfaces, respectively, for the exponential autocorrelation function. The general agreement for both surfaces is clearly not good. The results for the steel surface give rather close agreement for the angles $\phi_2 = 50^\circ, 60^\circ, 70^\circ$, but elsewhere there are wide differences. It is recalled that the agreement in figures III. 27 and III. 29 is also closer for these angles than for others. The theoretical results for the grout surface would be closer to the experimental values if they were to be shifted downward by 5 db. A shift in either direction would bring no improvement to the results for the steel surface. It is important to note that the theory predicts for the grout surface the general decrease of σ_o with increasing depression angle, ϕ_2 , for angles far away from the specular direction, as discussed earlier in connection with

figures III. 24 and III. 25. The increase of σ_o with depression angle observed for the steel surface is not accounted for by the theory.

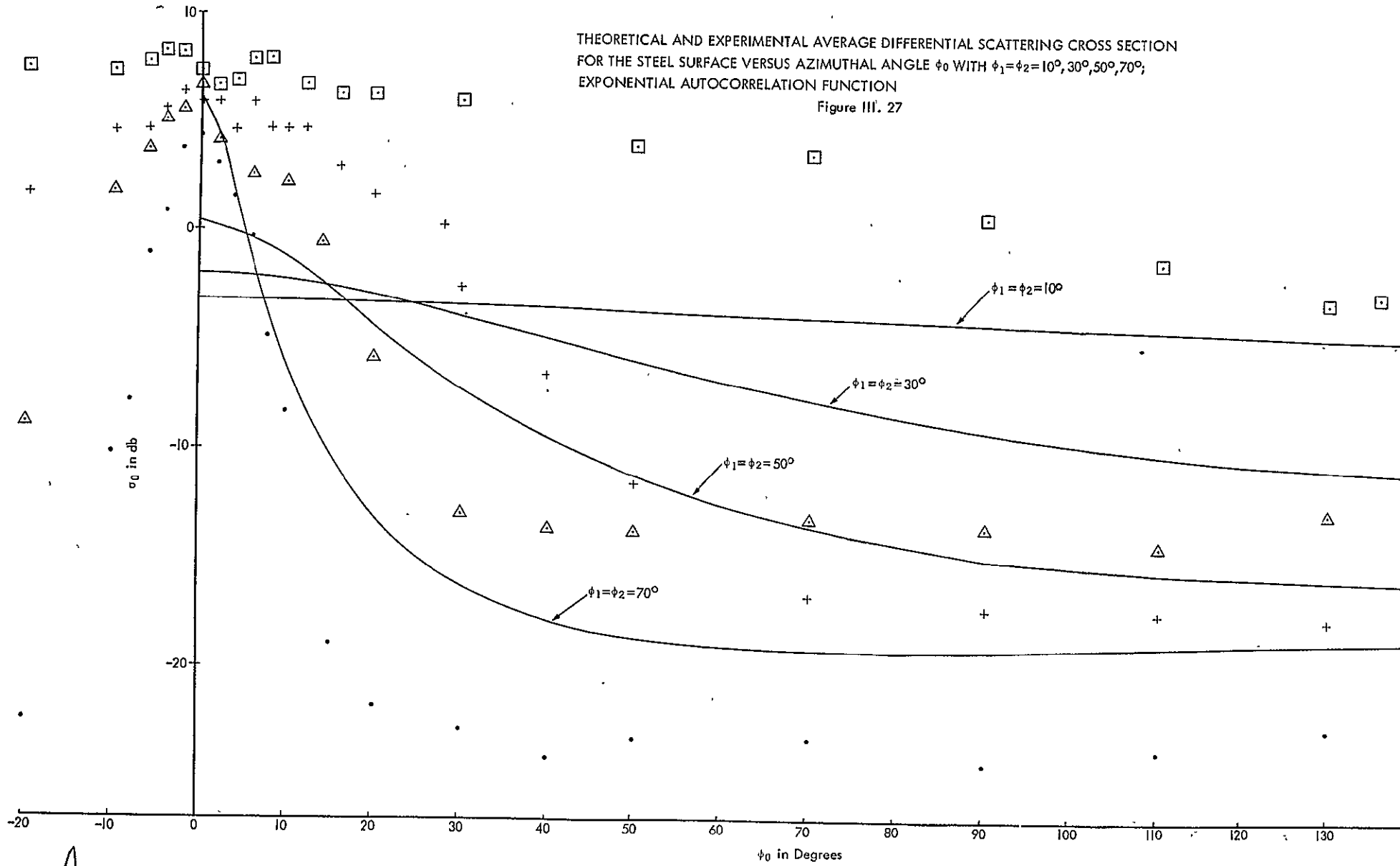
The predictions made using the Gaussian autocorrelation coefficient are shown in figures III. 37 and III. 38 for the steel and grout surfaces, respectively, for ϕ_1 a constant of 40° . The values for both surfaces are shifted downward by the same factors used for the results shown in figures III. 31 through III. 35. By doing this, fairly close agreement is found for angles that are near the specular but elsewhere there are great differences; this is the same result as found earlier for the Gaussian function. The values for the steel surface compare more favorably with experiment than those for the grout. The predictions for the grout surface would be in closer agreement if all values were shifted downward an additional 3 db; that this is so indicates the possibility of experimental error, which is suspected for these results.

In the comparison of the experimental results shown in figures III. 20 through III. 25 to the predicted values for both the exponential and Gaussian functions, several important features of the agreement between theory and experiment become apparent. The results based on the exponential autocorrelation function are seen to agree with experiment over a wider range than do those for the Gaussian function. It is surprising that this is so considering how well the curves of sample autocorrelation coefficient are fit by the Gaussian function. It is true, however, that the Gaussian-based predictions give a better description of the experimental results in and near the specular direction, especially for the steel surface which has a sample autocorrelation coefficient more closely fit by the Gaussian function than the grout. It is this goodness of fit in and near the specular direction which is the principal success in the use of this function; its most disappointing failure is its inability to predict the experimental results at other angles of observation. It is in these directions, those away from the specular, that the results for the exponential autocorrelation function are most successful. These agreements (and disagreements) of theory with experiment are seen more clearly in figures III. 39 and III. 40 in which the theoretical curves for both autocorrelation functions are plotted against the experimental results

for both surfaces for $\phi_1 = \phi_2 = 40^\circ$; the results for the Gaussian function are shifted downward as before. Comparison is made for the steel surface in figure III. 39 and the results for the grout surface are compared in figure III. 40. The results for the two autocorrelation functions are seen to bracket the experimental values for the full range of azimuthal angles with the exception of the results for the grout surface in and near the specular direction for which the experimental values fall below the theoretical ones. This bracketing, which occurs for other polar angles, gives strong evidence from the viewpoint of comparing theory with experiment that the true autocorrelation coefficient lies between the exponential and Gaussian functions. Since this is the case, it is concluded that the theory as based upon the Kirchhoff approximation is a valid one.

THEORETICAL AND EXPERIMENTAL AVERAGE DIFFERENTIAL SCATTERING CROSS SECTION FOR THE STEEL SURFACE VERSUS AZIMUTHAL ANGLE ϕ_0 WITH $\phi_1 = \phi_2 = 10^\circ, 30^\circ, 50^\circ, 70^\circ$; EXPONENTIAL AUTOCORRELATION FUNCTION

Figure III. 27



A

FOLDOUT FRAME \

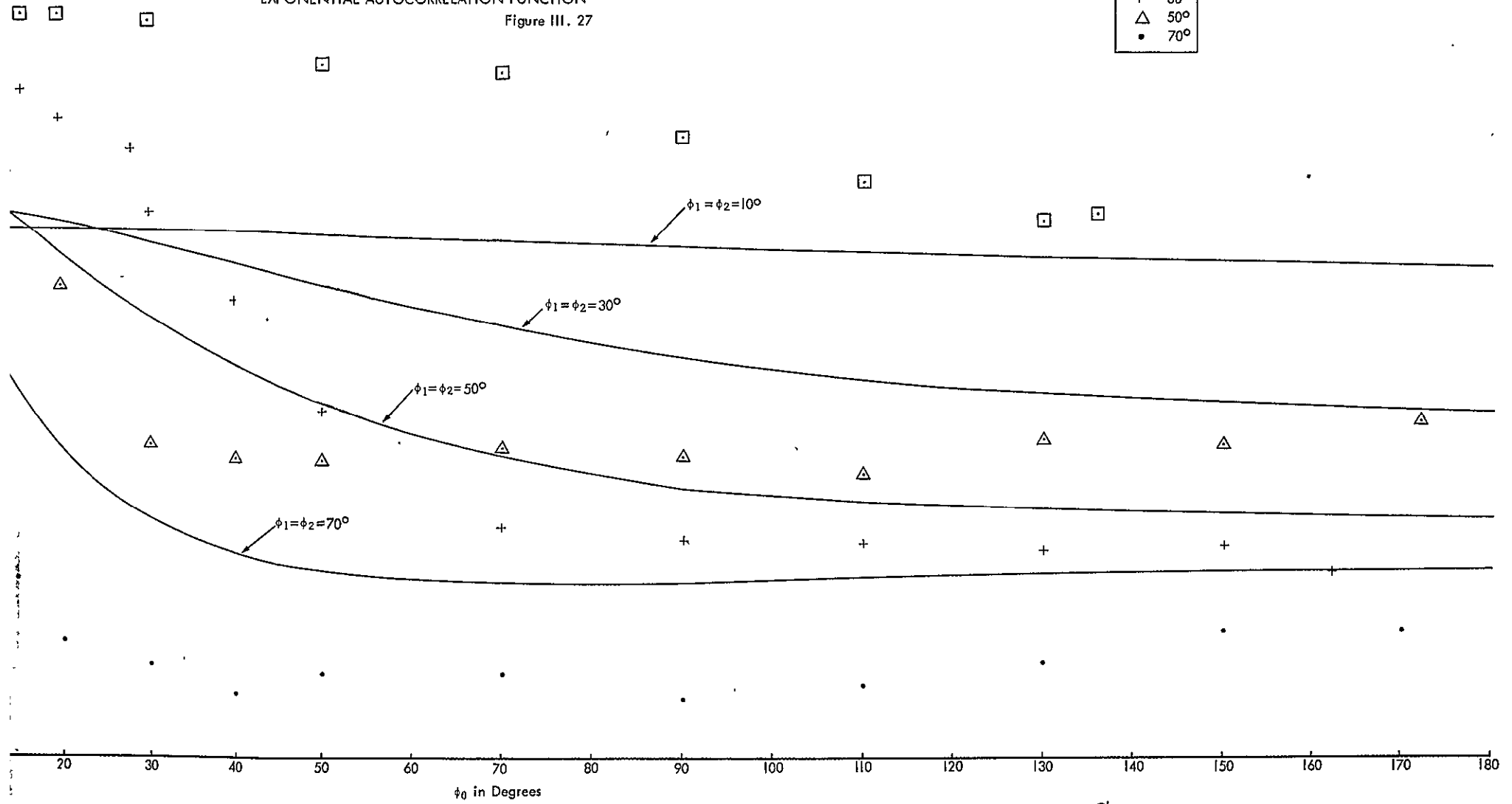
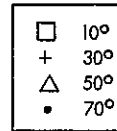
B

FOLDOUT FRAME

C

THEORETICAL AND EXPERIMENTAL AVERAGE DIFFERENTIAL SCATTERING CROSS SECTION FOR THE STEEL SURFACE VERSUS AZIMUTHAL ANGLE ϕ_0 WITH $\phi_1 = \phi_2 = 10^\circ, 30^\circ, 50^\circ, 70^\circ$; EXPONENTIAL AUTOCORRELATION FUNCTION

Figure III. 27



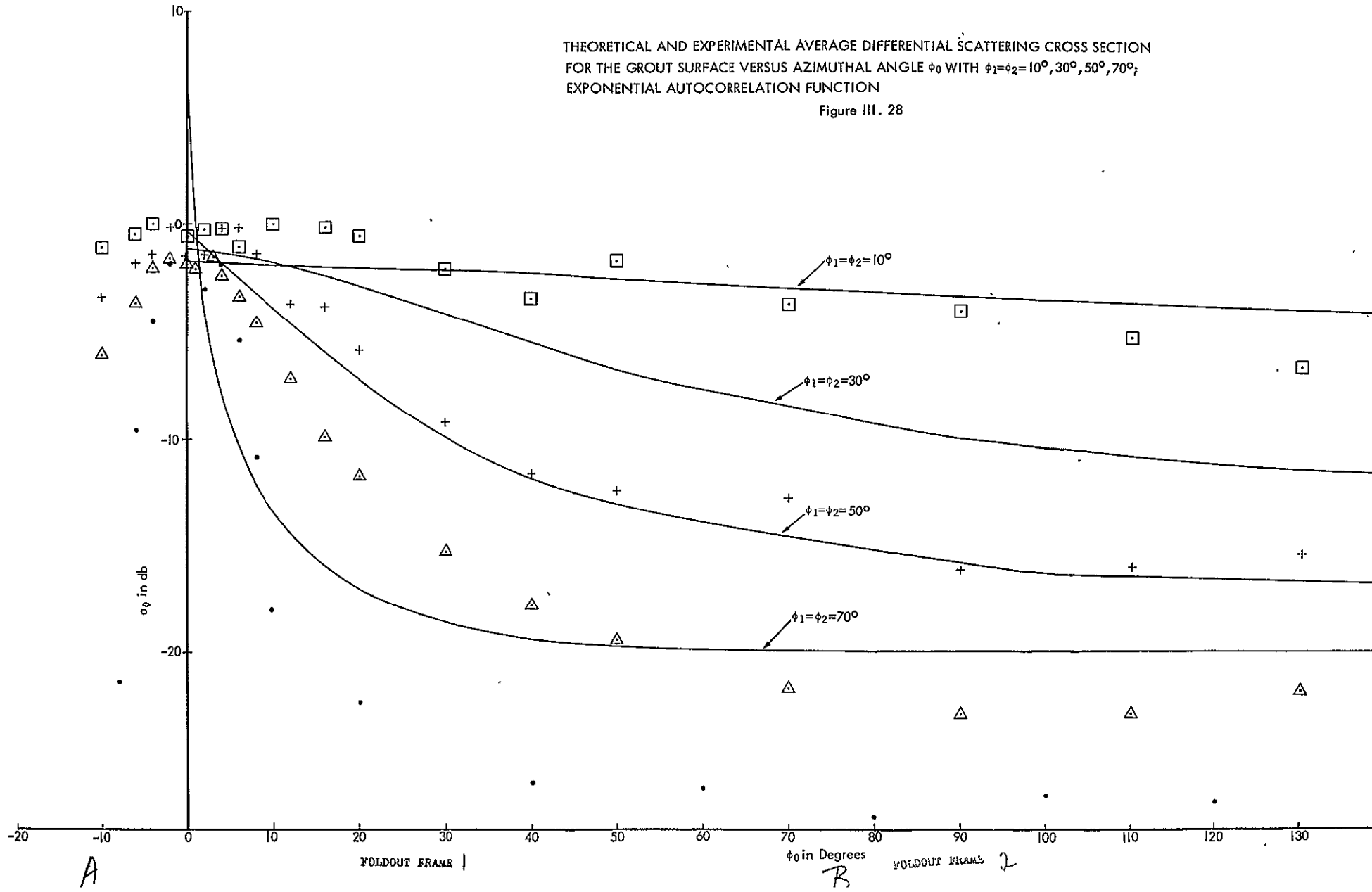
FOLDOUT FRAME \

R

C FOLDOUT FRAME 3

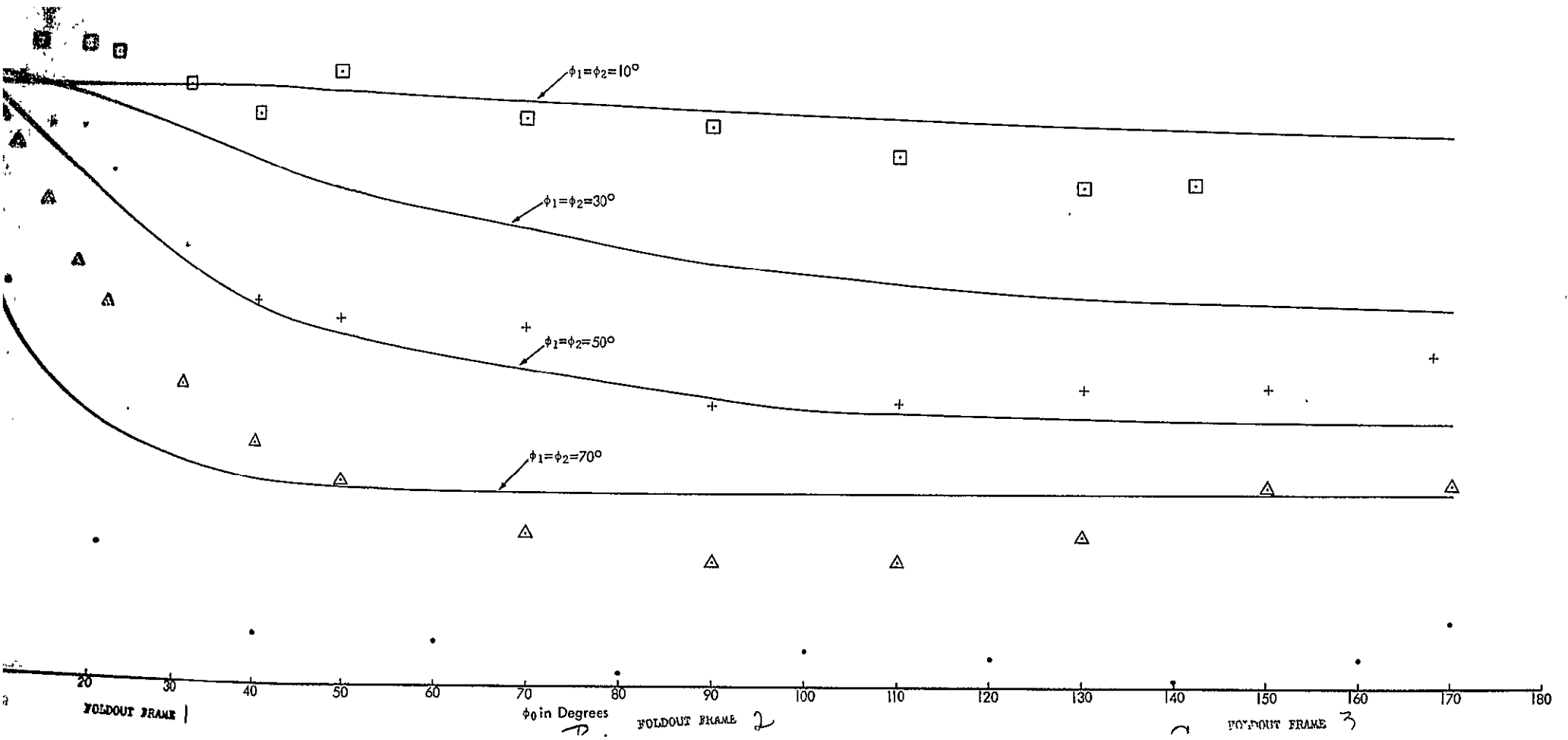
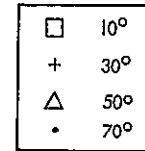
THEORETICAL AND EXPERIMENTAL AVERAGE DIFFERENTIAL SCATTERING CROSS SECTION
 FOR THE GROUT SURFACE VERSUS AZIMUTHAL ANGLE ϕ_0 WITH $\phi_1=\phi_2=10^\circ, 30^\circ, 50^\circ, 70^\circ$;
 EXPONENTIAL AUTOCORRELATION FUNCTION

Figure III. 28



THEORETICAL AND EXPERIMENTAL AVERAGE DIFFERENTIAL SCATTERING CROSS SECTION
 FOR THE GROUT SURFACE VERSUS AZIMUTHAL ANGLE ϕ_0 WITH $\phi_1=\phi_2=10^\circ, 30^\circ, 50^\circ, 70^\circ$;
 EXPONENTIAL AUTOCORRELATION FUNCTION

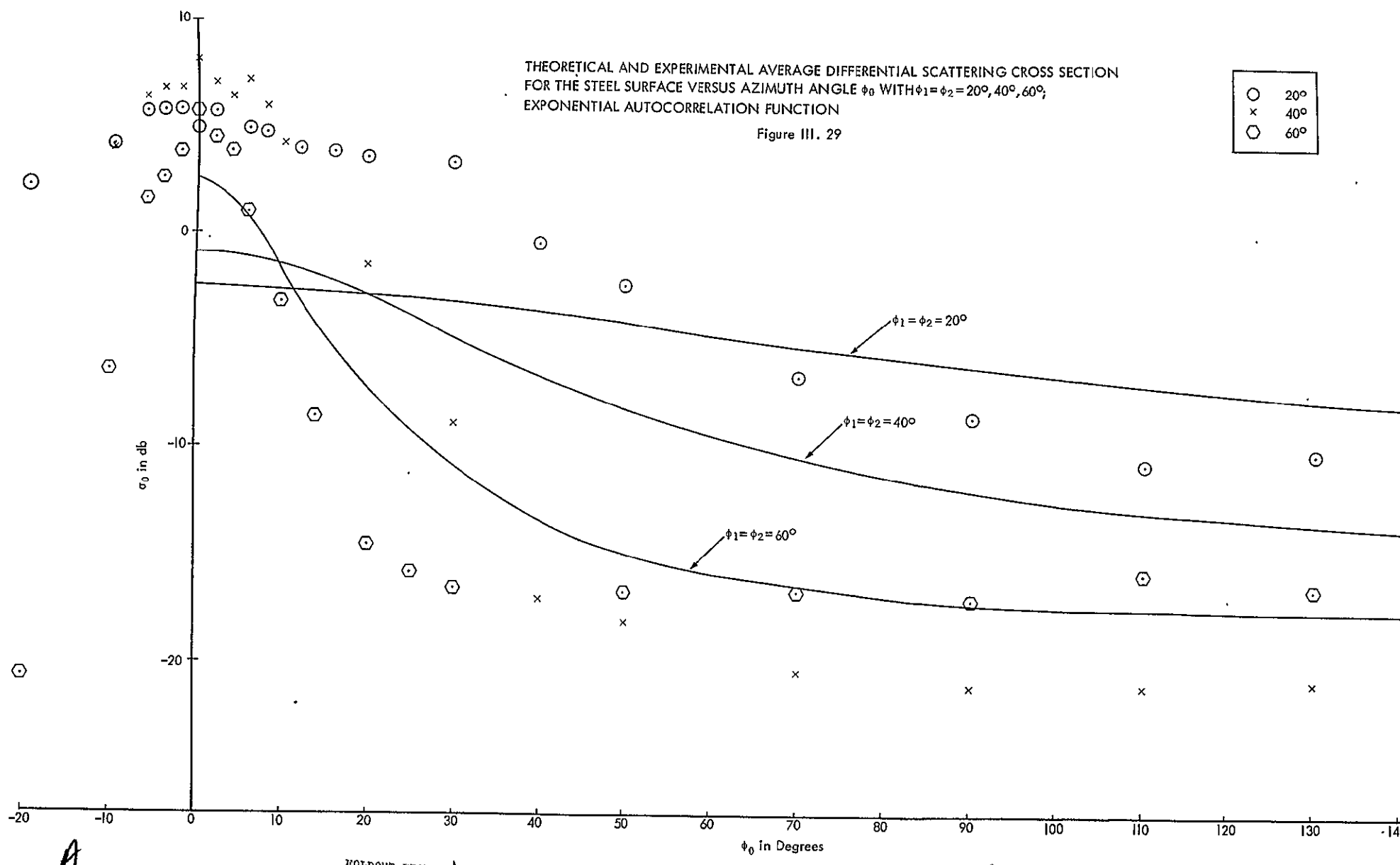
Figure III. 28



THEORETICAL AND EXPERIMENTAL AVERAGE DIFFERENTIAL SCATTERING CROSS SECTION
 FOR THE STEEL SURFACE VERSUS AZIMUTH ANGLE ϕ_0 WITH $\phi_1 = \phi_2 = 20^\circ, 40^\circ, 60^\circ$;
 EXPONENTIAL AUTOCORRELATION FUNCTION

Figure III. 29

○	20°
x	40°
⊕	60°

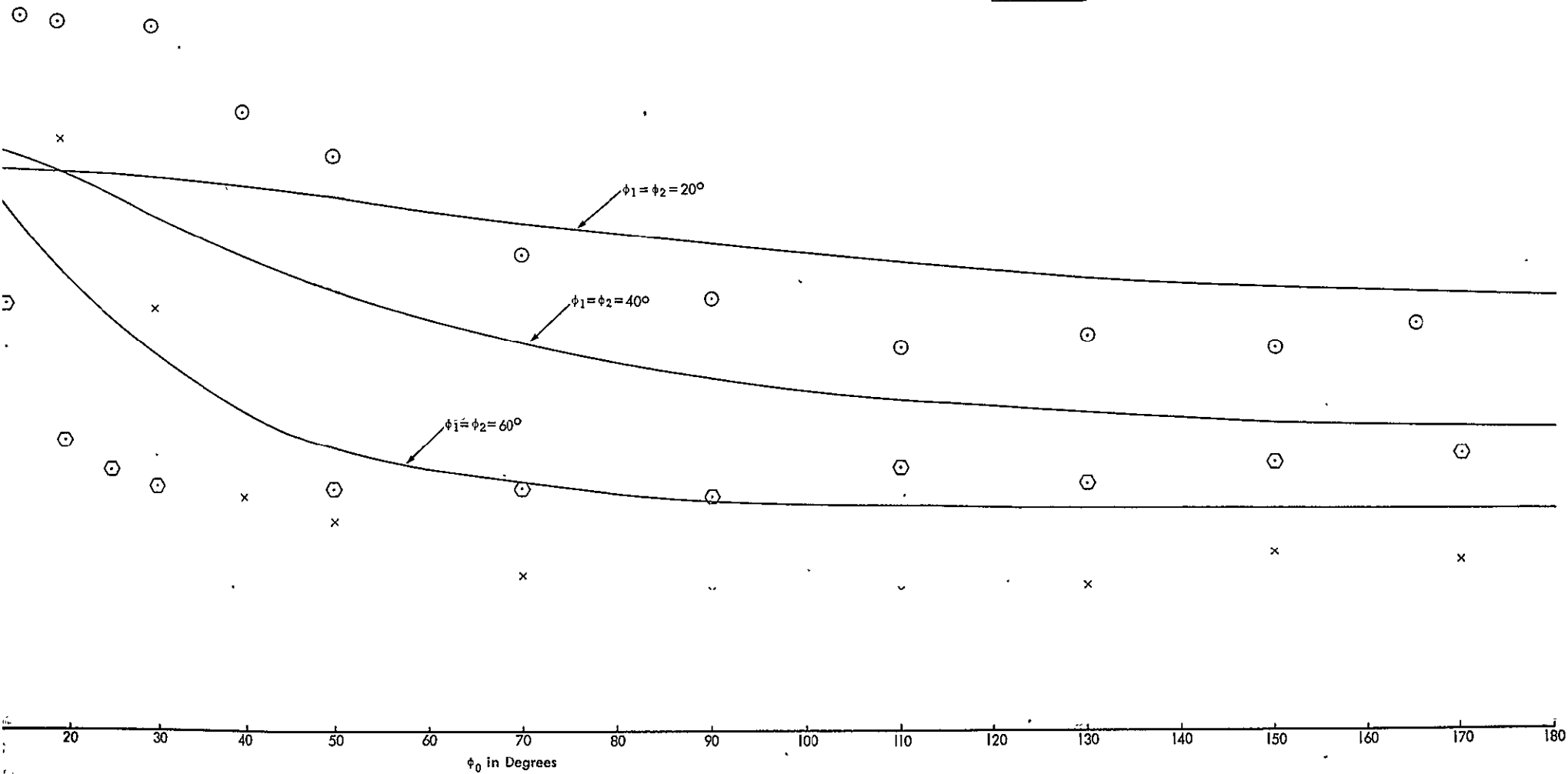
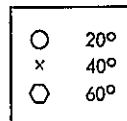


WOLDOUT FRAME 1

WOLDOUT FRAME 2

THEORETICAL AND EXPERIMENTAL AVERAGE DIFFERENTIAL SCATTERING CROSS SECTION
 FOR THE STEEL SURFACE VERSUS AZIMUTH ANGLE ϕ_0 WITH $\phi_1 = \phi_2 = 20^\circ, 40^\circ, 60^\circ$;
 EXPONENTIAL AUTOCORRELATION FUNCTION

Figure III. 29



FOLDOUT FRAME 1

R

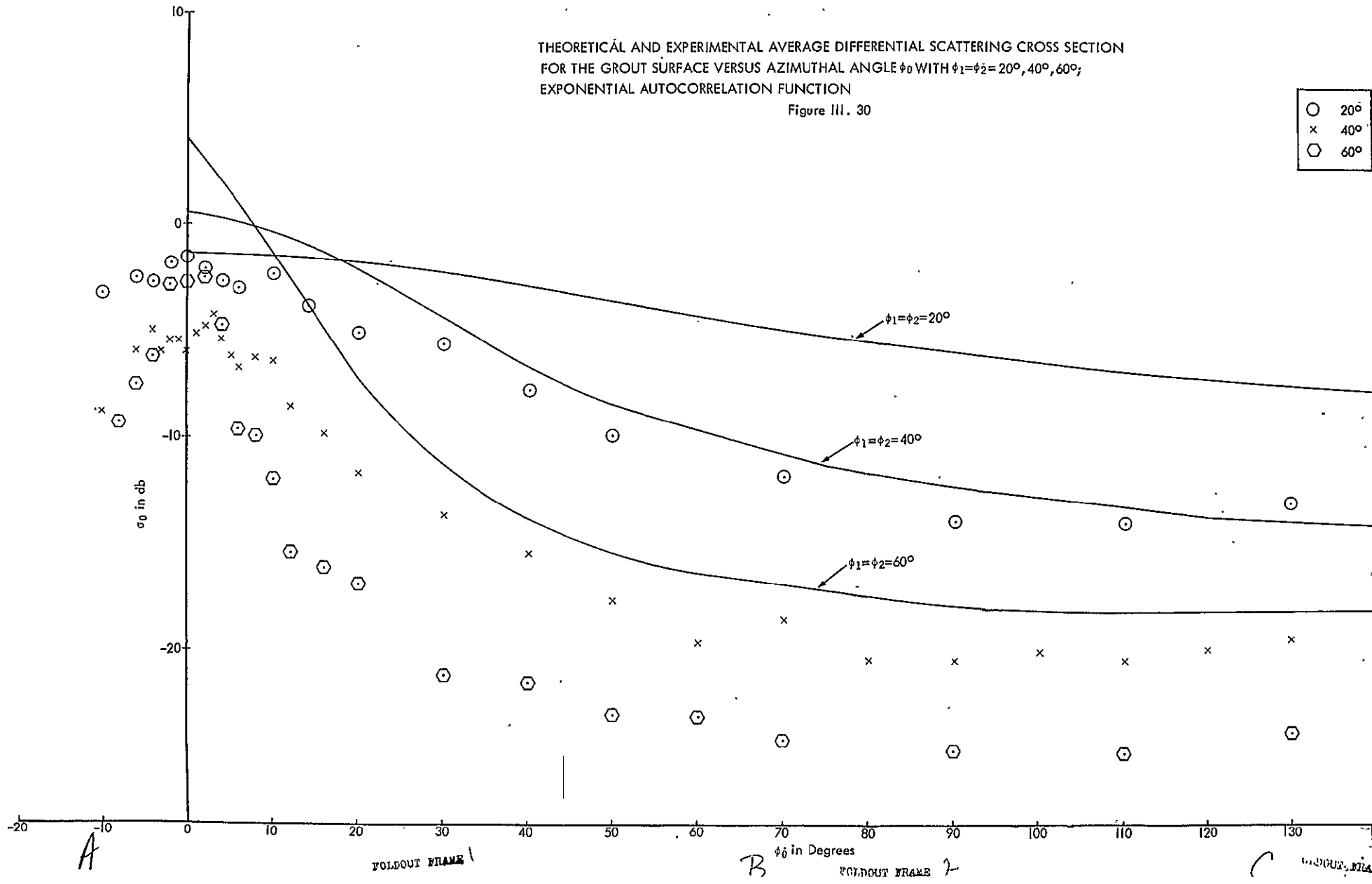
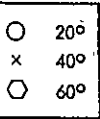
FOLDOUT FRAME 2

C

FOLDOUT FRAME 3

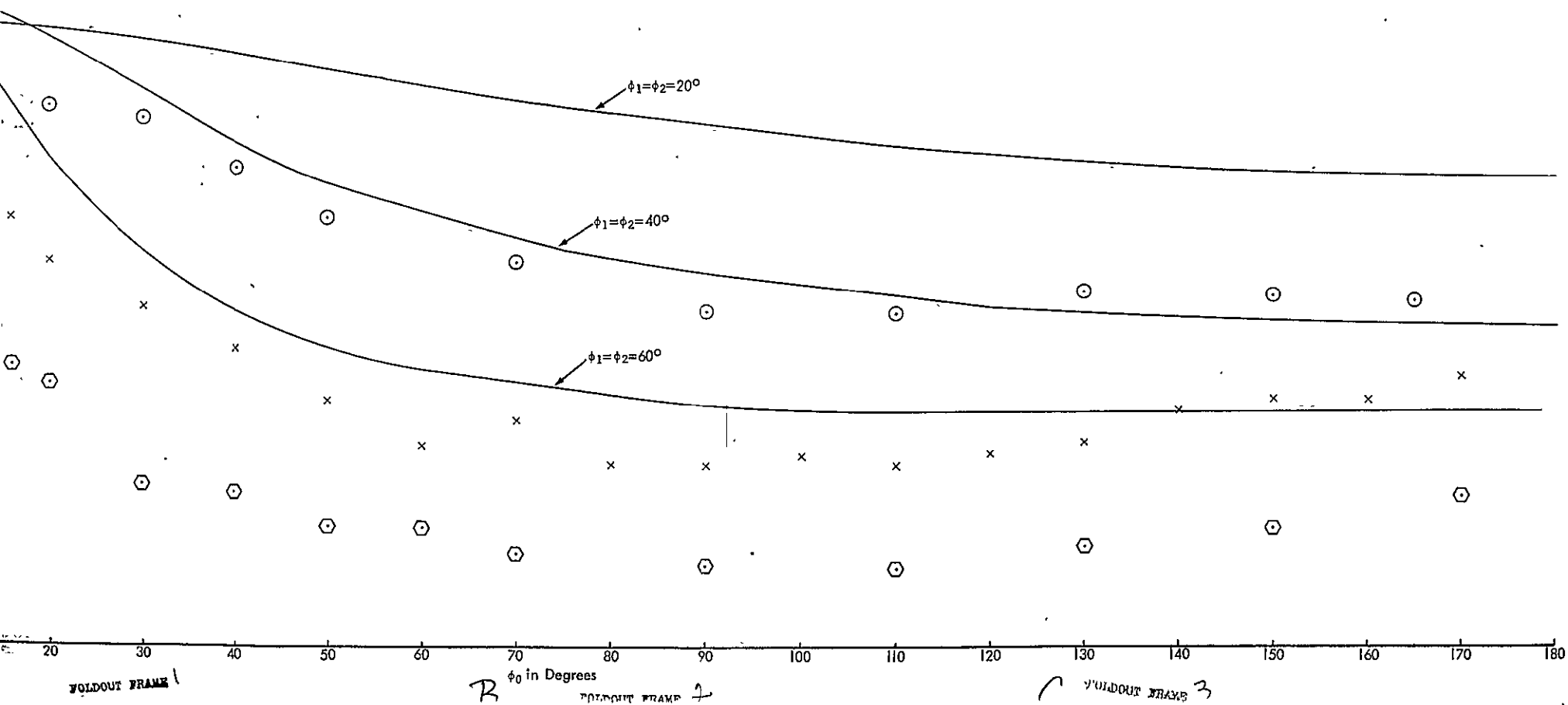
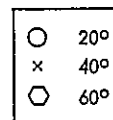
THEORETICAL AND EXPERIMENTAL AVERAGE DIFFERENTIAL SCATTERING CROSS SECTION
 FOR THE GROUT SURFACE VERSUS AZIMUTHAL ANGLE ϕ_0 WITH $\phi_1=\phi_2=20^\circ, 40^\circ, 60^\circ$;
 EXPONENTIAL AUTOCORRELATION FUNCTION

Figure III. 30



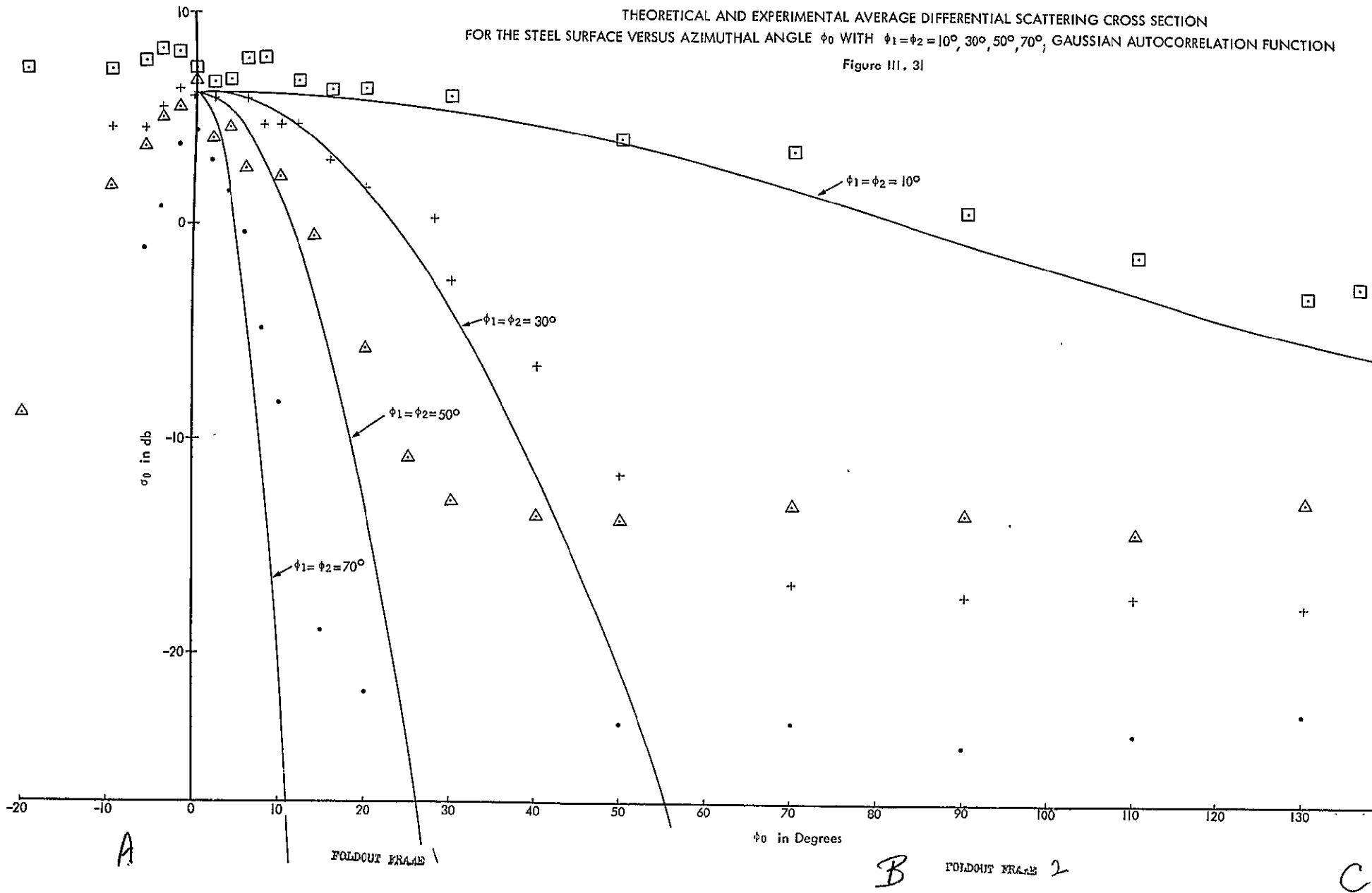
THEORETICAL AND EXPERIMENTAL AVERAGE DIFFERENTIAL SCATTERING CROSS SECTION
 FOR THE GROUT SURFACE VERSUS AZIMUTHAL ANGLE ϕ_0 WITH $\phi_1 = \phi_2 = 20^\circ, 40^\circ, 60^\circ$;
 EXPONENTIAL AUTOCORRELATION FUNCTION

Figure III. 30



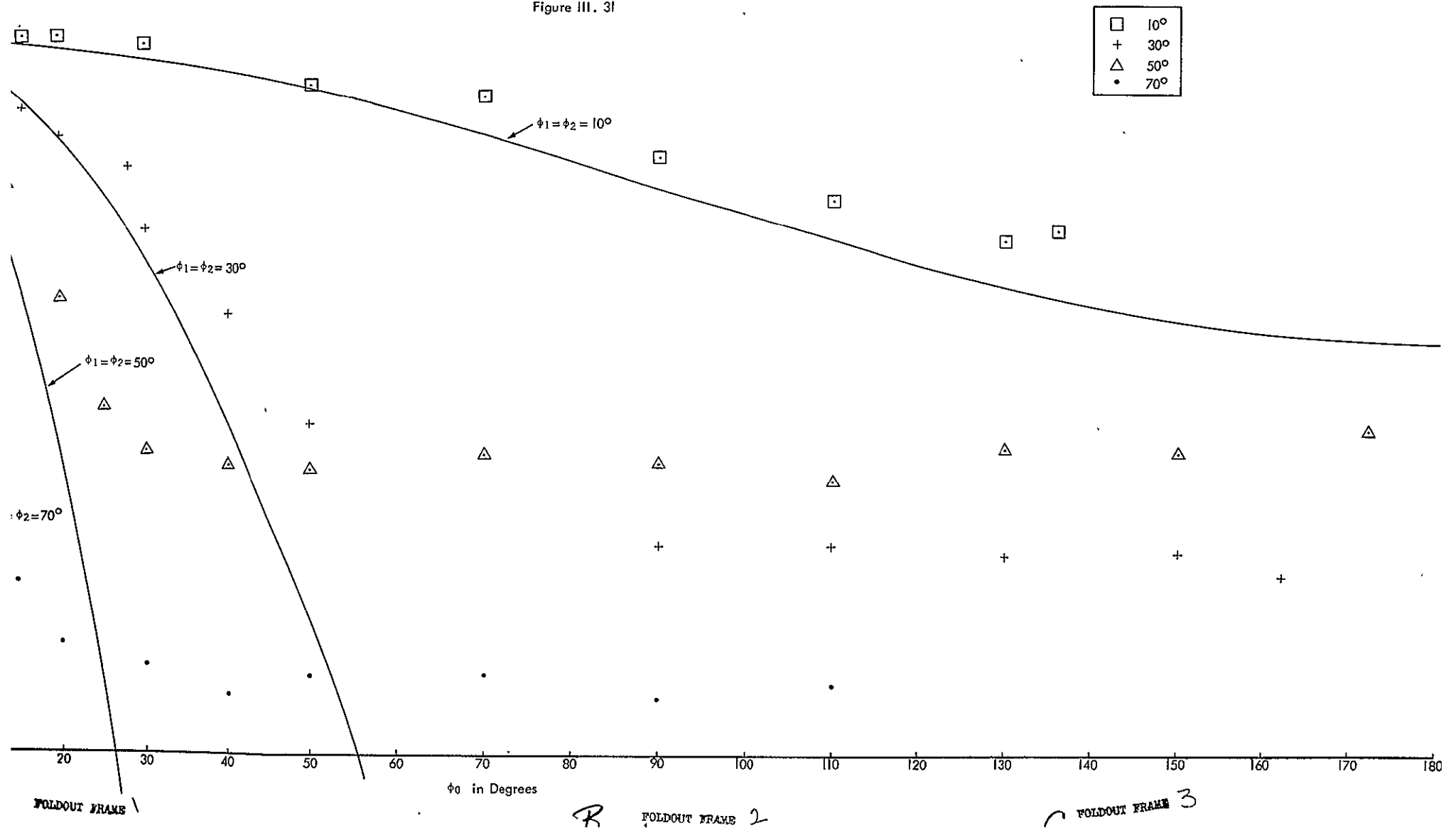
THEORETICAL AND EXPERIMENTAL AVERAGE DIFFERENTIAL SCATTERING CROSS SECTION
 FOR THE STEEL SURFACE VERSUS AZIMUTHAL ANGLE ϕ_0 WITH $\phi_1 = \phi_2 = 10^\circ, 30^\circ, 50^\circ, 70^\circ$, GAUSSIAN AUTOCORRELATION FUNCTION

Figure III. 31



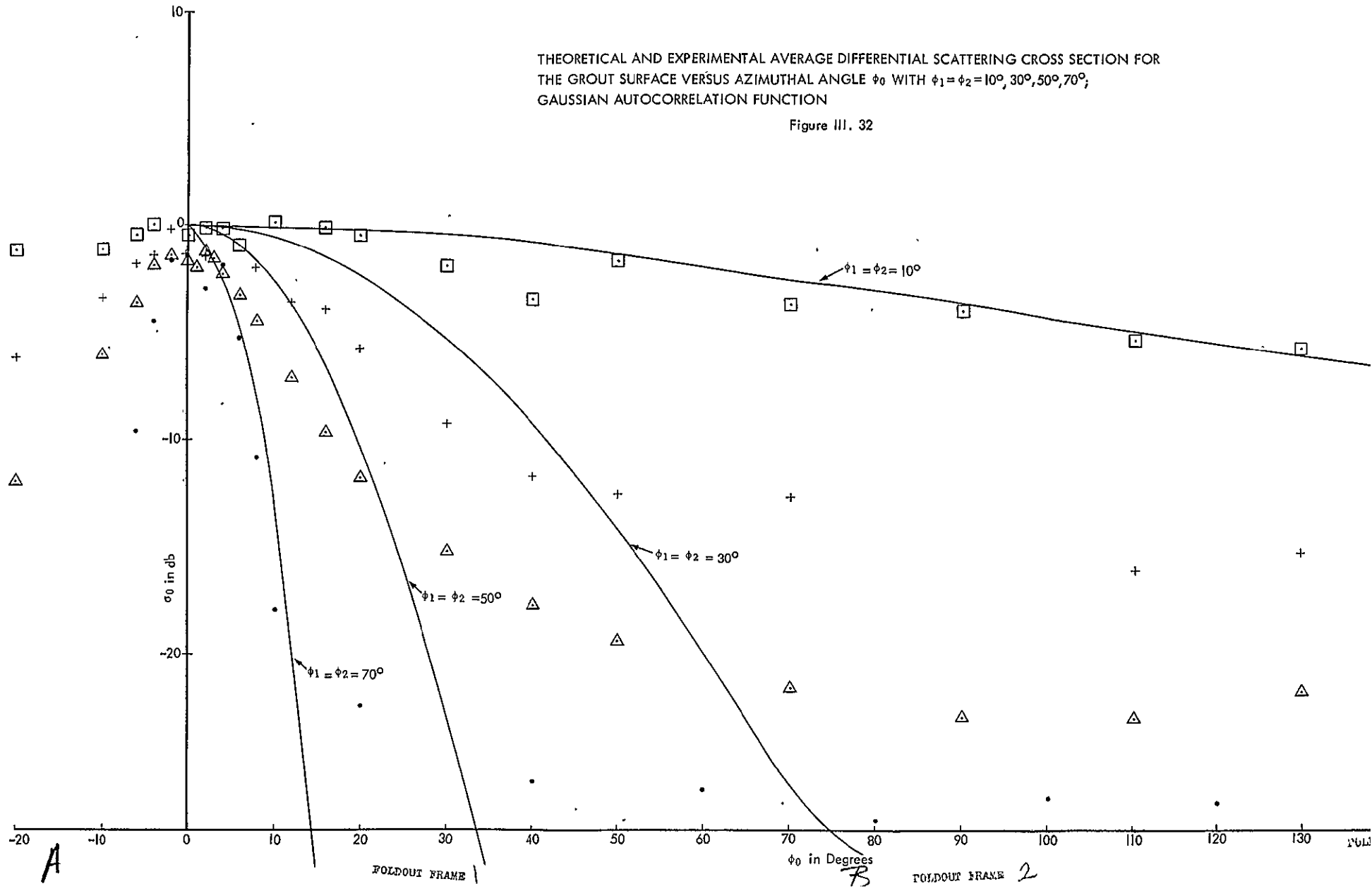
THEORETICAL AND EXPERIMENTAL AVERAGE DIFFERENTIAL SCATTERING CROSS SECTION
FOR THE STEEL SURFACE VERSUS AZIMUTHAL ANGLE ϕ_0 WITH $\phi_1 = \phi_2 = 10^\circ, 30^\circ, 50^\circ, 70^\circ$; GAUSSIAN AUTOCORRELATION FUNCTION

Figure III. 3!



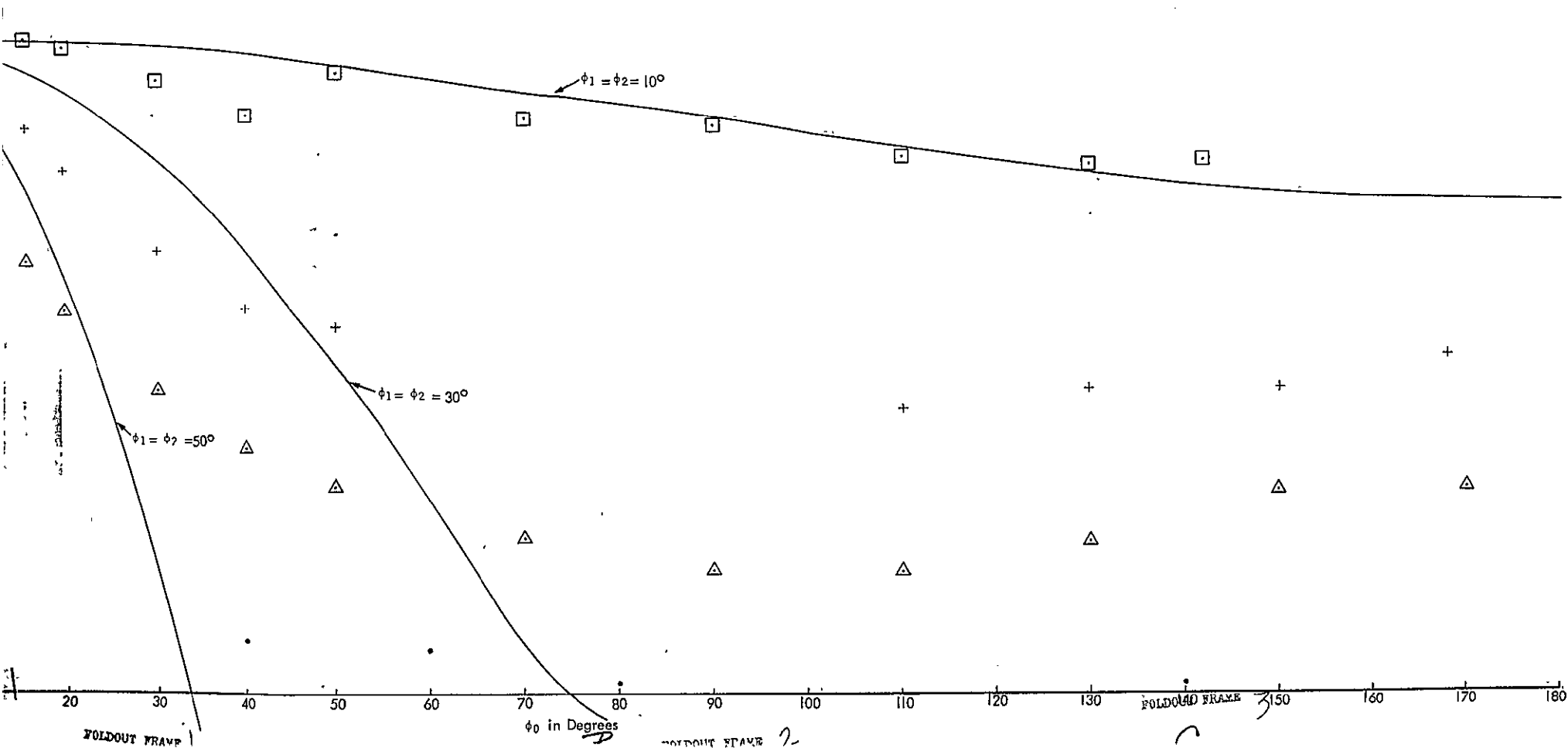
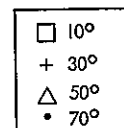
THEORETICAL AND EXPERIMENTAL AVERAGE DIFFERENTIAL SCATTERING CROSS SECTION FOR THE GROUT SURFACE VERSUS AZIMUTHAL ANGLE ϕ_0 WITH $\phi_1 = \phi_2 = 10^\circ, 30^\circ, 50^\circ, 70^\circ$, GAUSSIAN AUTOCORRELATION FUNCTION

Figure III. 32



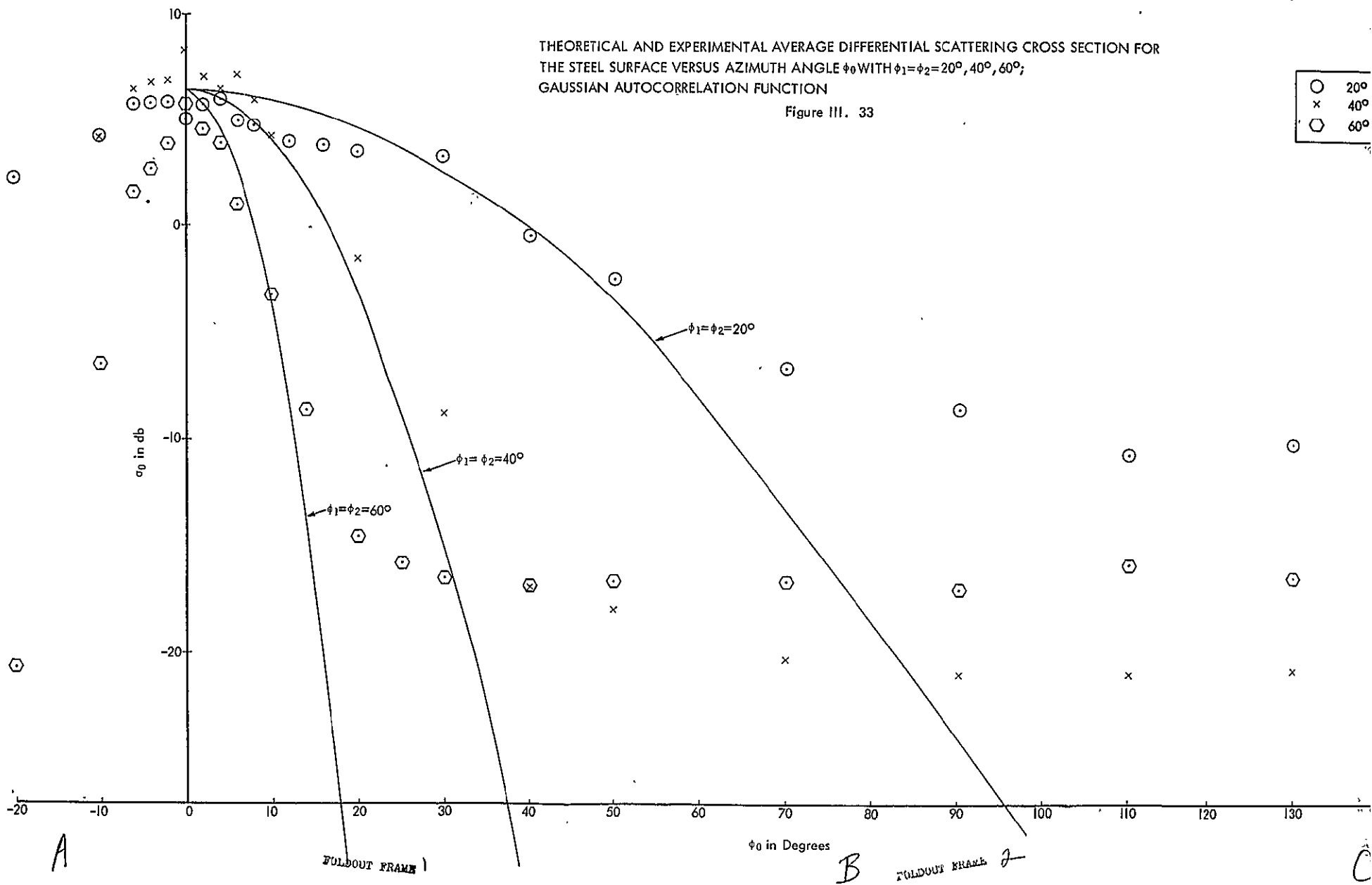
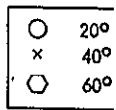
THEORETICAL AND EXPERIMENTAL AVERAGE DIFFERENTIAL SCATTERING CROSS SECTION FOR THE GROUT SURFACE VERSUS AZIMUTHAL ANGLE ϕ_0 WITH $\phi_1 = \phi_2 = 10^\circ, 30^\circ, 50^\circ, 70^\circ$; GAUSSIAN AUTOCORRELATION FUNCTION

Figure III. 32



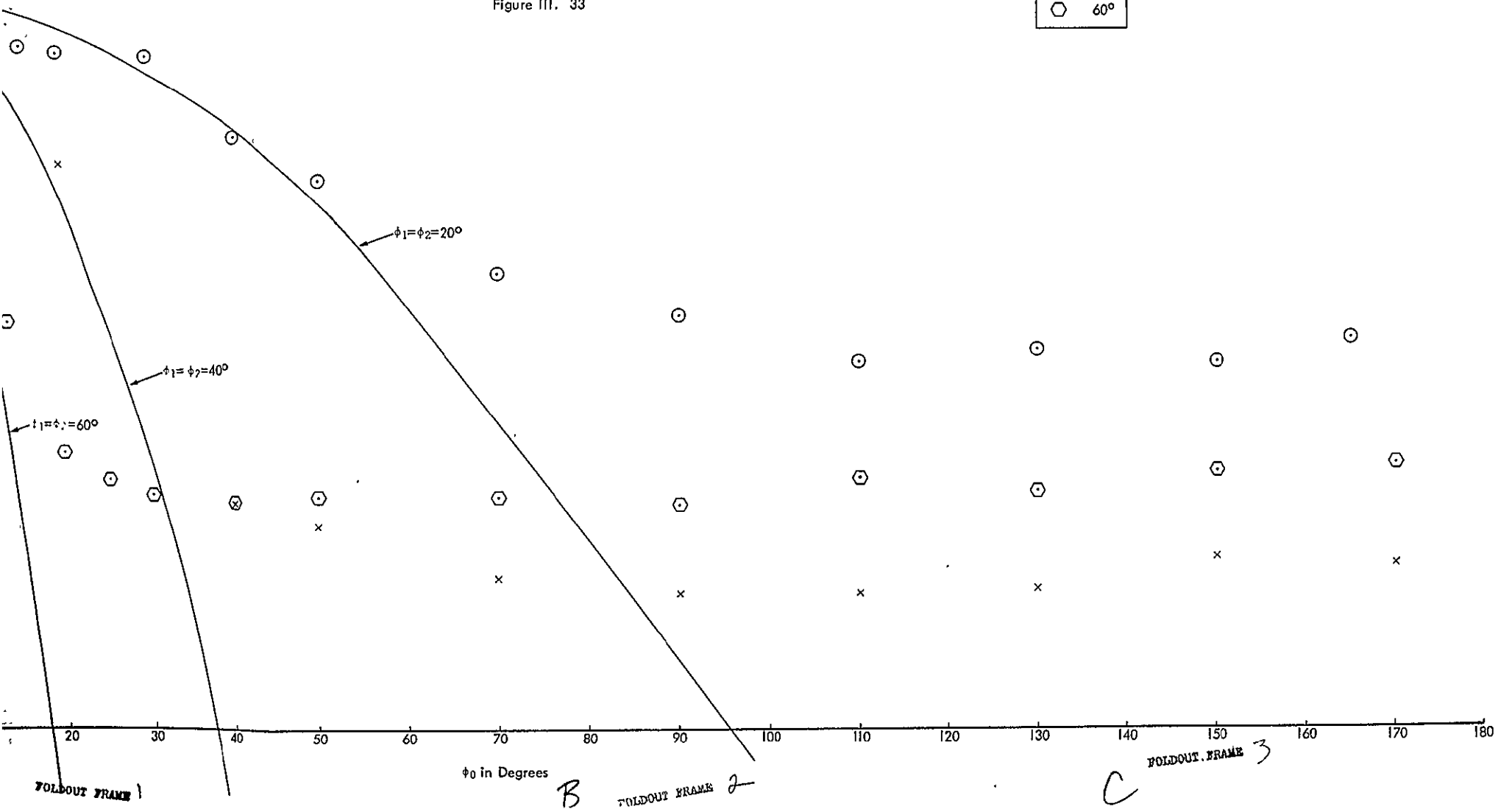
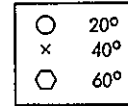
THEORETICAL AND EXPERIMENTAL AVERAGE DIFFERENTIAL SCATTERING CROSS SECTION FOR THE STEEL SURFACE VERSUS AZIMUTH ANGLE ϕ_0 WITH $\phi_1 = \phi_2 = 20^\circ, 40^\circ, 60^\circ$; GAUSSIAN AUTOCORRELATION FUNCTION

Figure III. 33



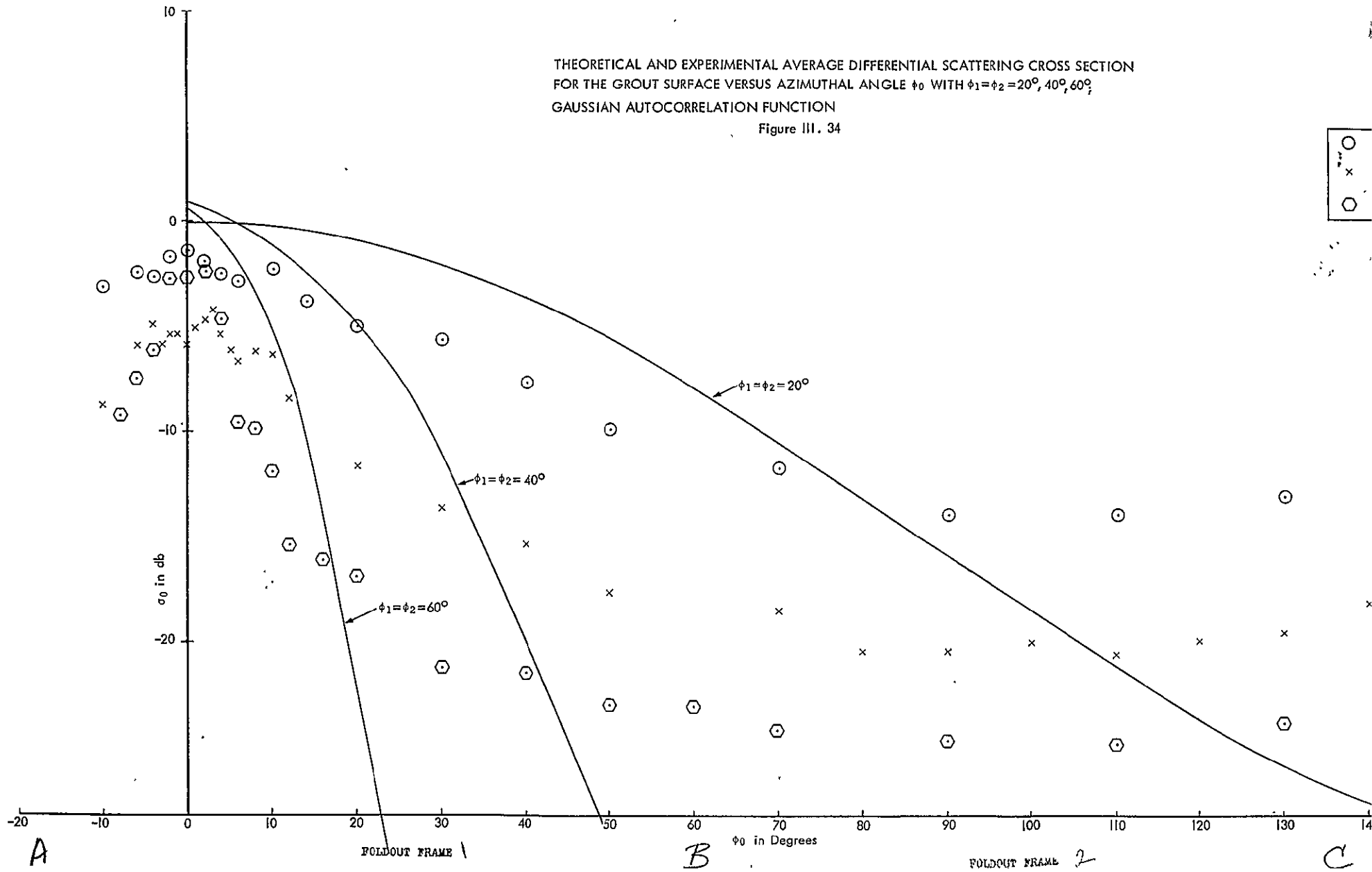
THEORETICAL AND EXPERIMENTAL AVERAGE DIFFERENTIAL SCATTERING CROSS SECTION FOR THE STEEL SURFACE VERSUS AZIMUTH ANGLE ϕ_0 WITH $\phi_1 = \phi_2 = 20^\circ, 40^\circ, 60^\circ$; GAUSSIAN AUTOCORRELATION FUNCTION

Figure III. 33



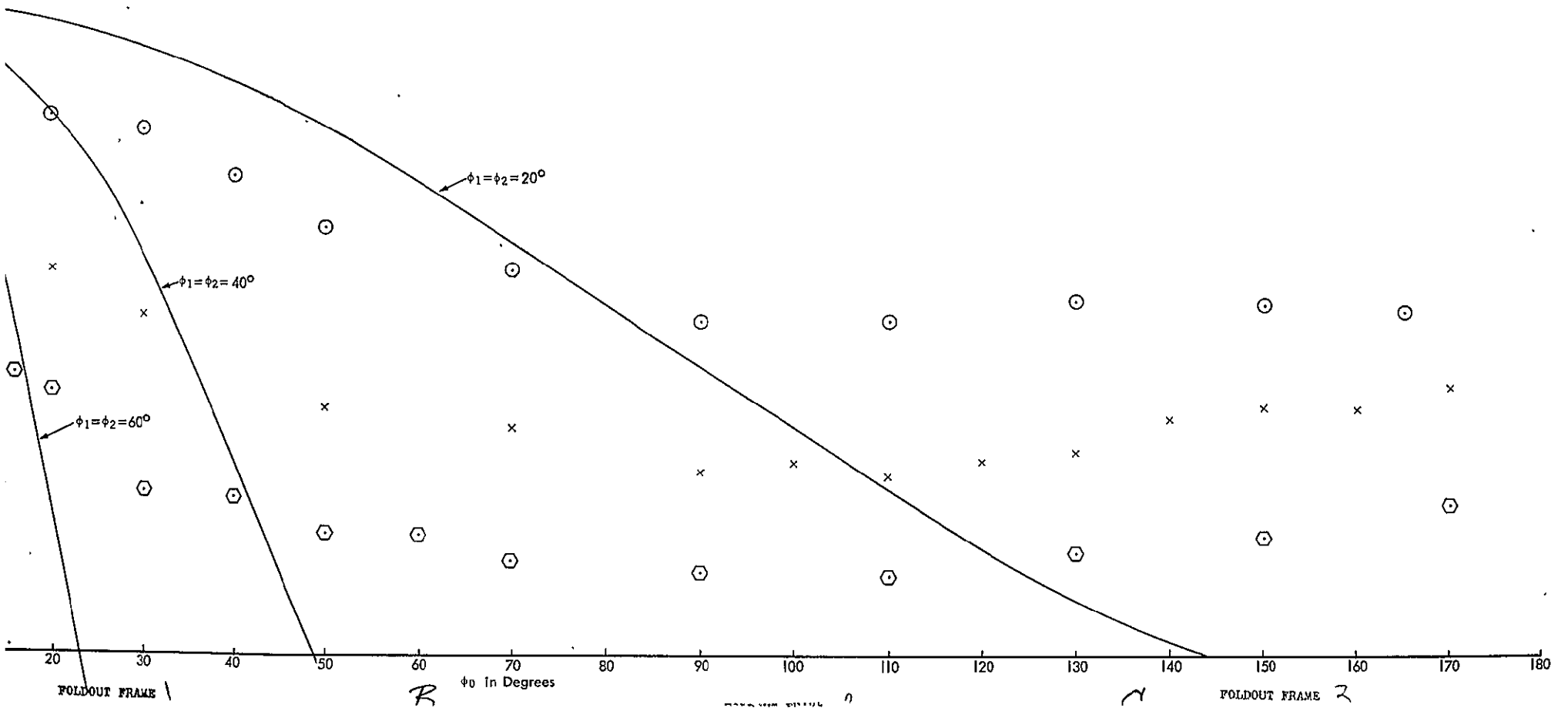
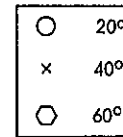
THEORETICAL AND EXPERIMENTAL AVERAGE DIFFERENTIAL SCATTERING CROSS SECTION
FOR THE GROUT SURFACE VERSUS AZIMUTHAL ANGLE ϕ_0 WITH $\phi_1 = \phi_2 = 20^\circ, 40^\circ, 60^\circ$,
GAUSSIAN AUTOCORRELATION FUNCTION

Figure III. 34



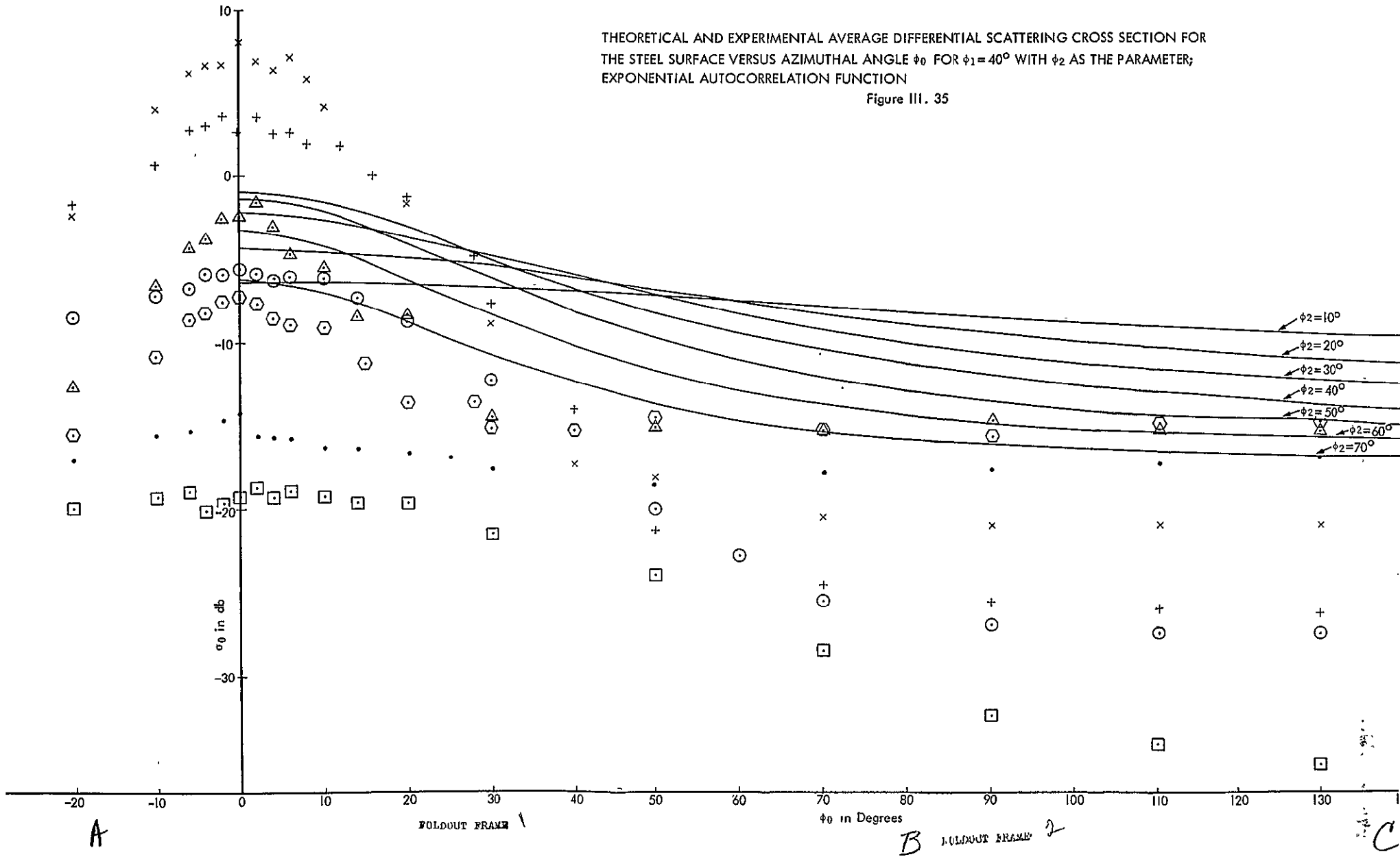
THEORETICAL AND EXPERIMENTAL AVERAGE DIFFERENTIAL SCATTERING CROSS SECTION
 FOR THE GROUT SURFACE VERSUS AZIMUTHAL ANGLE ϕ_0 WITH $\phi_1 = \phi_2 = 20^\circ, 40^\circ, 60^\circ$;
 GAUSSIAN AUTOCORRELATION FUNCTION

Figure III. 34



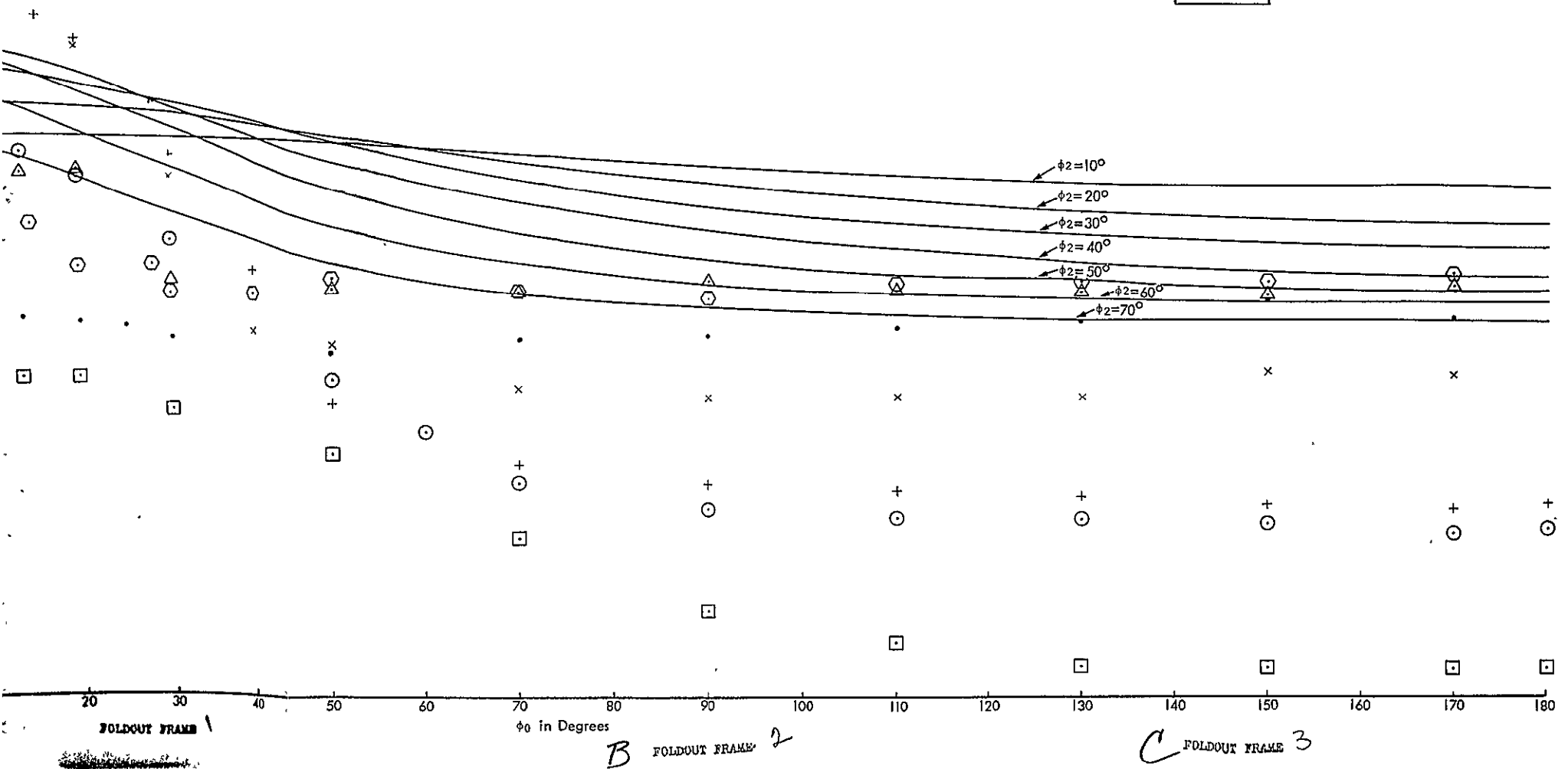
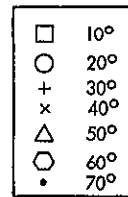
THEORETICAL AND EXPERIMENTAL AVERAGE DIFFERENTIAL SCATTERING CROSS SECTION FOR THE STEEL SURFACE VERSUS AZIMUTHAL ANGLE ϕ_0 FOR $\phi_1 = 40^\circ$ WITH ϕ_2 AS THE PARAMETER; EXPONENTIAL AUTOCORRELATION FUNCTION

Figure III. 35



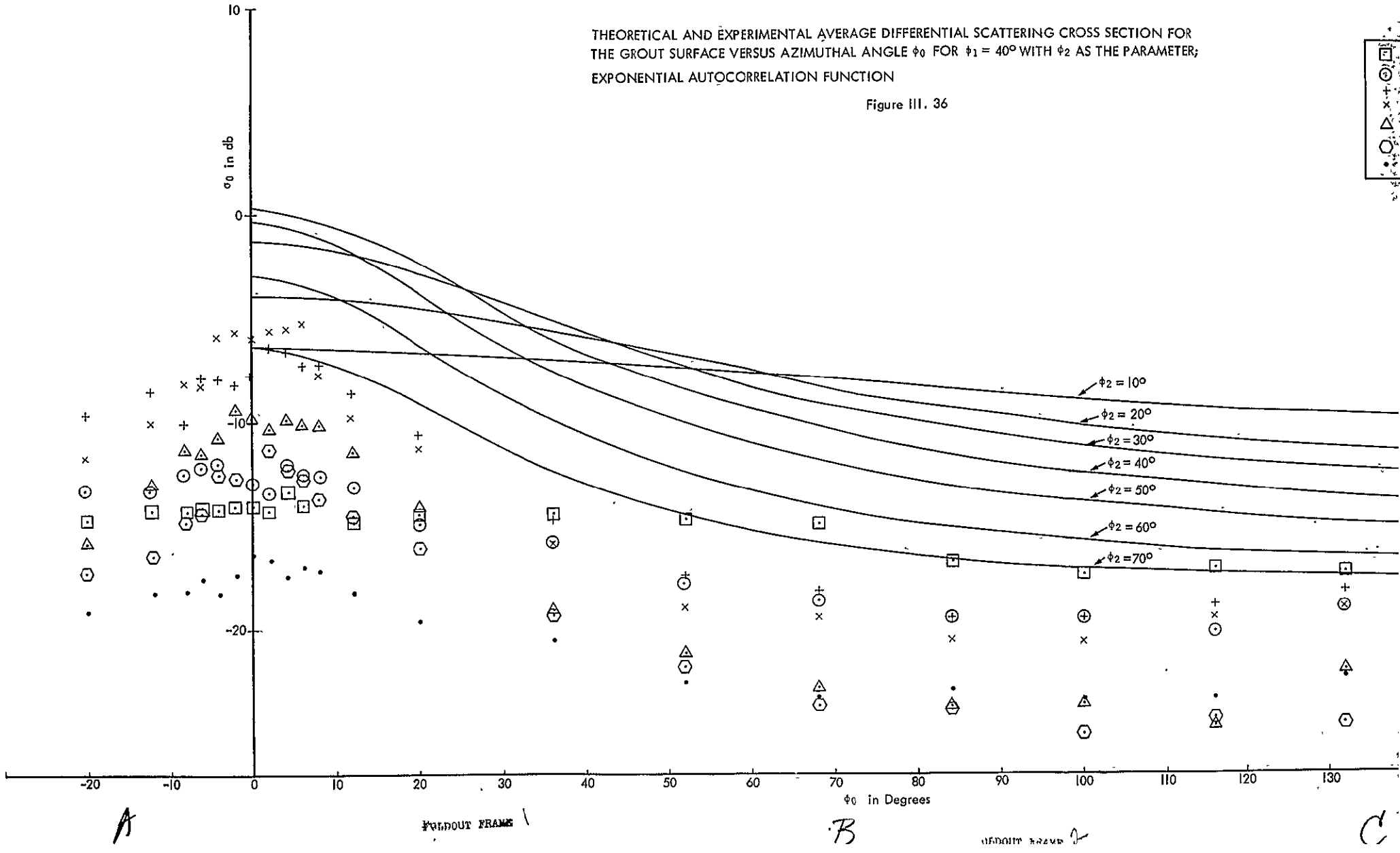
THEORETICAL AND EXPERIMENTAL AVERAGE DIFFERENTIAL SCATTERING CROSS SECTION FOR THE STEEL SURFACE VERSUS AZIMUTHAL ANGLE ϕ_0 FOR $\phi_1 = 40^\circ$ WITH ϕ_2 AS THE PARAMETER; EXPONENTIAL AUTOCORRELATION FUNCTION

Figure III. 35



THEORETICAL AND EXPERIMENTAL AVERAGE DIFFERENTIAL SCATTERING CROSS SECTION FOR THE GROUT SURFACE VERSUS AZIMUTHAL ANGLE ϕ_0 FOR $\phi_1 = 40^\circ$ WITH ϕ_2 AS THE PARAMETER; EXPONENTIAL AUTOCORRELATION FUNCTION

Figure III. 36

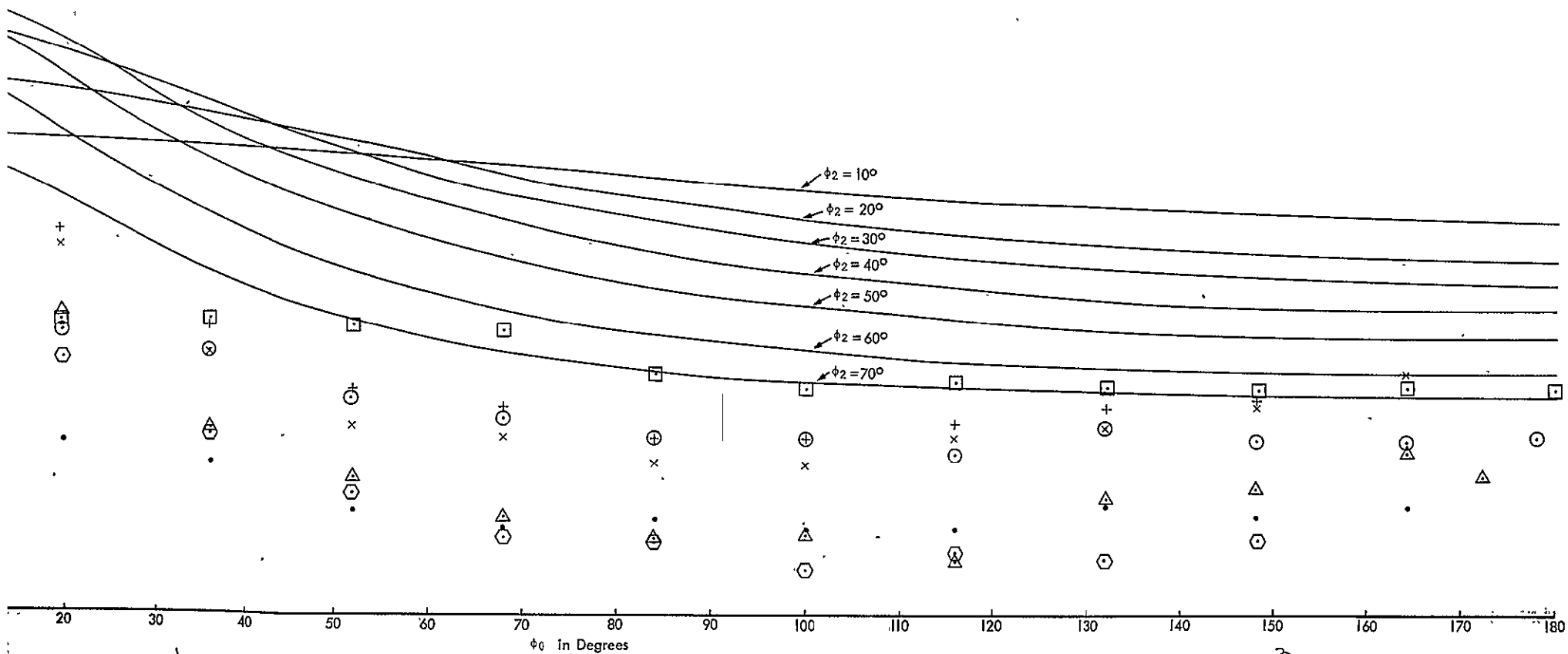
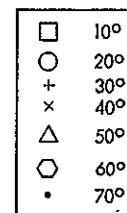


Legend for experimental data points:

- Circle with a dot inside
- Circle with a cross inside
- Circle with a plus sign inside
- Triangle with a dot inside
- Triangle with a cross inside
- Triangle with a plus sign inside
- Square with a dot inside
- Square with a cross inside
- Square with a plus sign inside

THEORETICAL AND EXPERIMENTAL AVERAGE DIFFERENTIAL SCATTERING CROSS SECTION FOR THE GROUT SURFACE VERSUS AZIMUTHAL ANGLE ϕ_0 FOR $\phi_1 = 40^\circ$ WITH ϕ_2 AS THE PARAMETER, EXPONENTIAL AUTOCORRELATION FUNCTION

Figure III. 36



PULLOUT FRAME 1

B

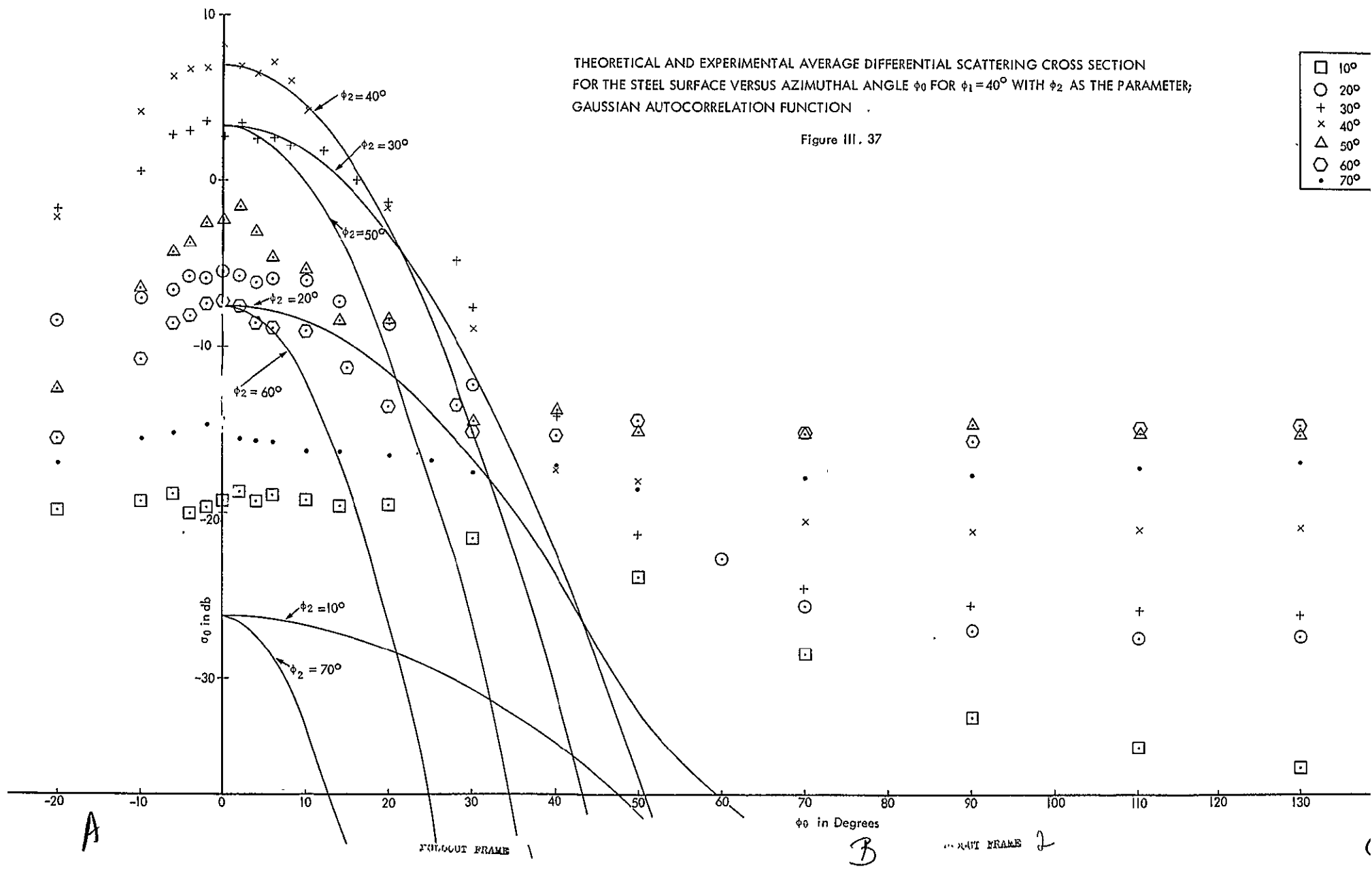
PULLOUT FRAME 2

PULLOUT FRAME 3

THEORETICAL AND EXPERIMENTAL AVERAGE DIFFERENTIAL SCATTERING CROSS SECTION FOR THE STEEL SURFACE VERSUS AZIMUTHAL ANGLE ϕ_0 FOR $\phi_1 = 40^\circ$ WITH ϕ_2 AS THE PARAMETER; GAUSSIAN AUTOCORRELATION FUNCTION .

Figure III. 37

- 10°
- 20°
- + 30°
- x 40°
- △ 50°
- ⊕ 60°
- 70°



THEORETICAL AND EXPERIMENTAL AVERAGE DIFFERENTIAL SCATTERING CROSS SECTION FOR THE STEEL SURFACE VERSUS AZIMUTHAL ANGLE ϕ_0 FOR $\phi_1 = 40^\circ$ WITH ϕ_2 AS THE PARAMETER; GAUSSIAN AUTOCORRELATION FUNCTION

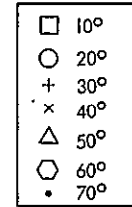
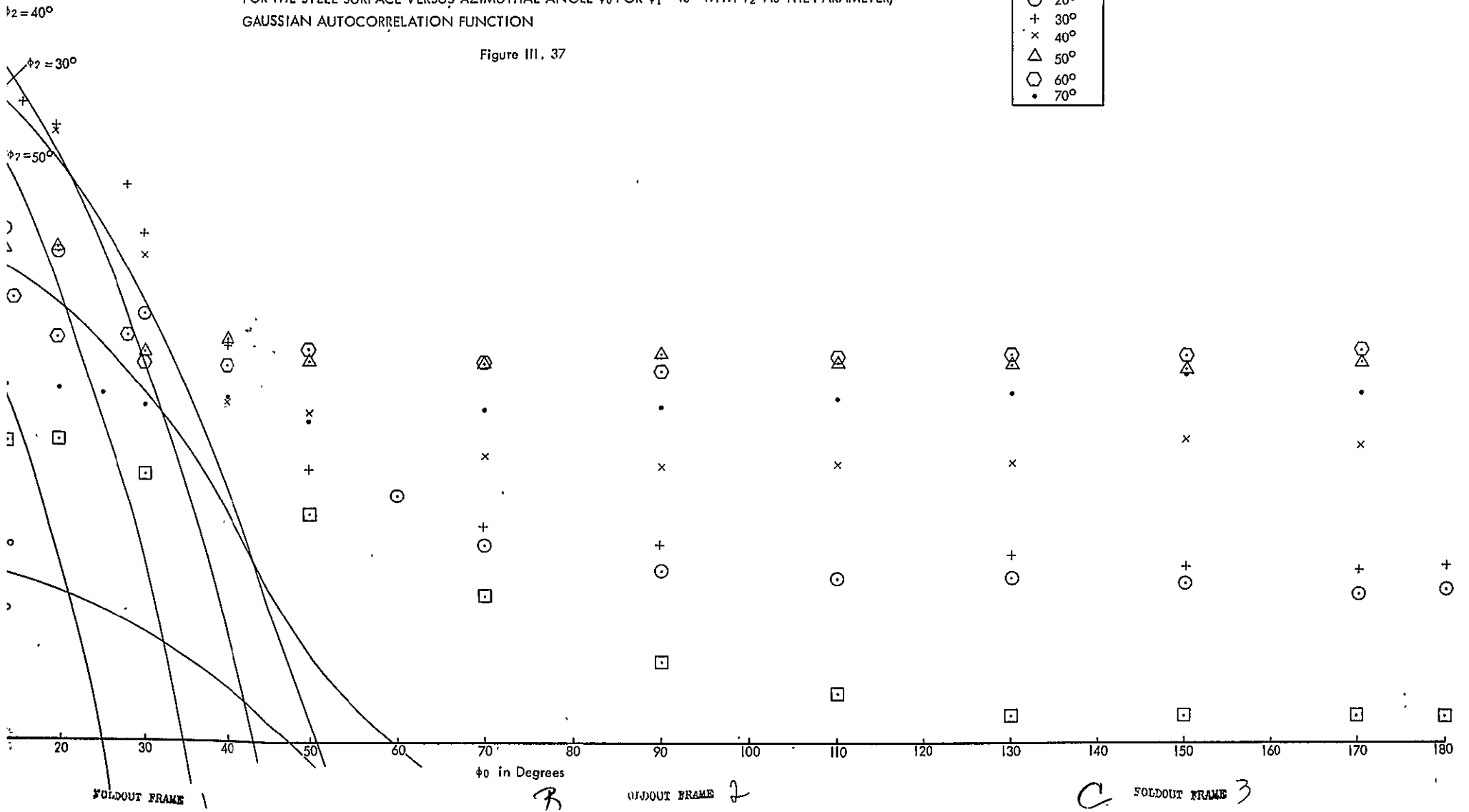
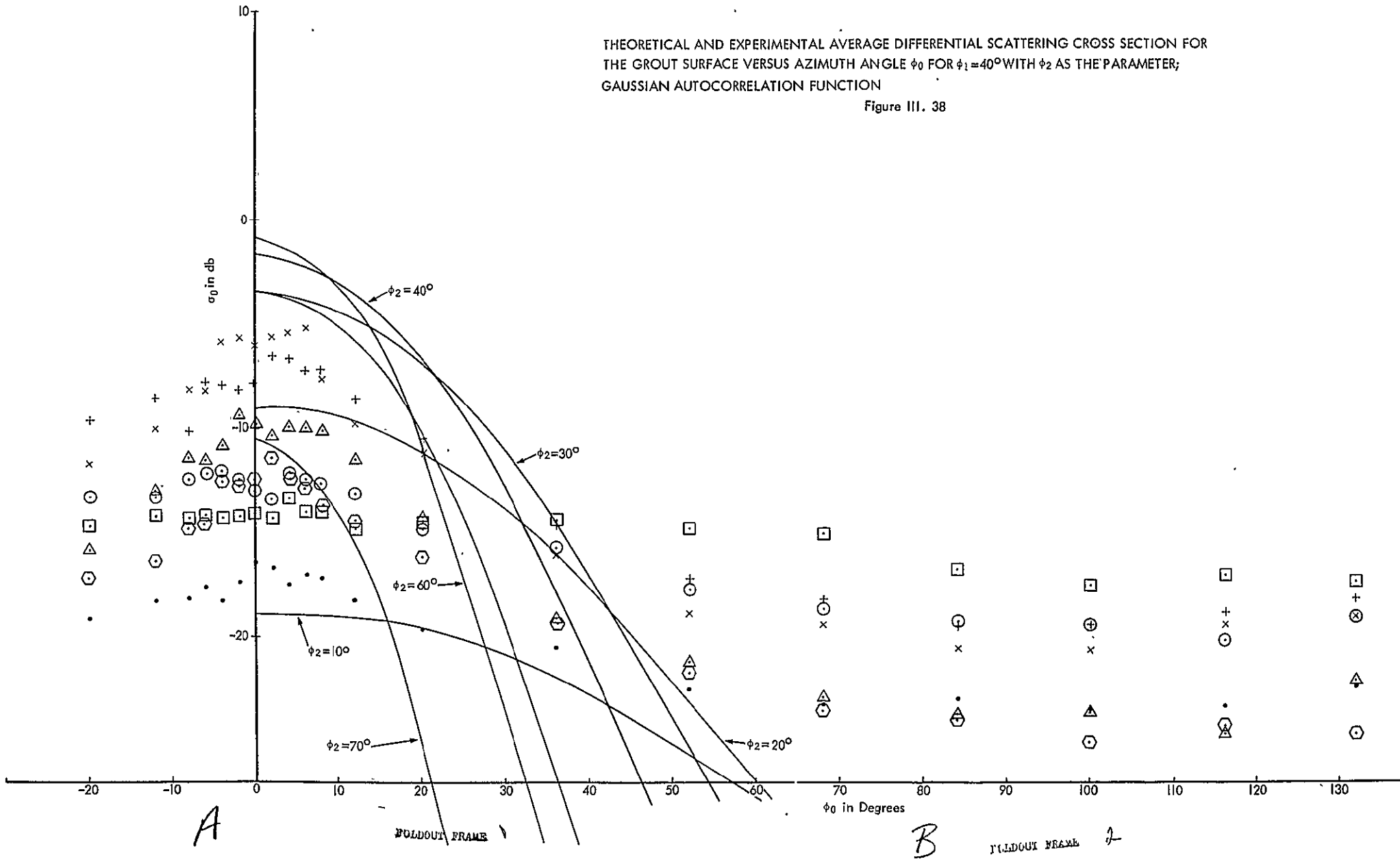


Figure III. 37



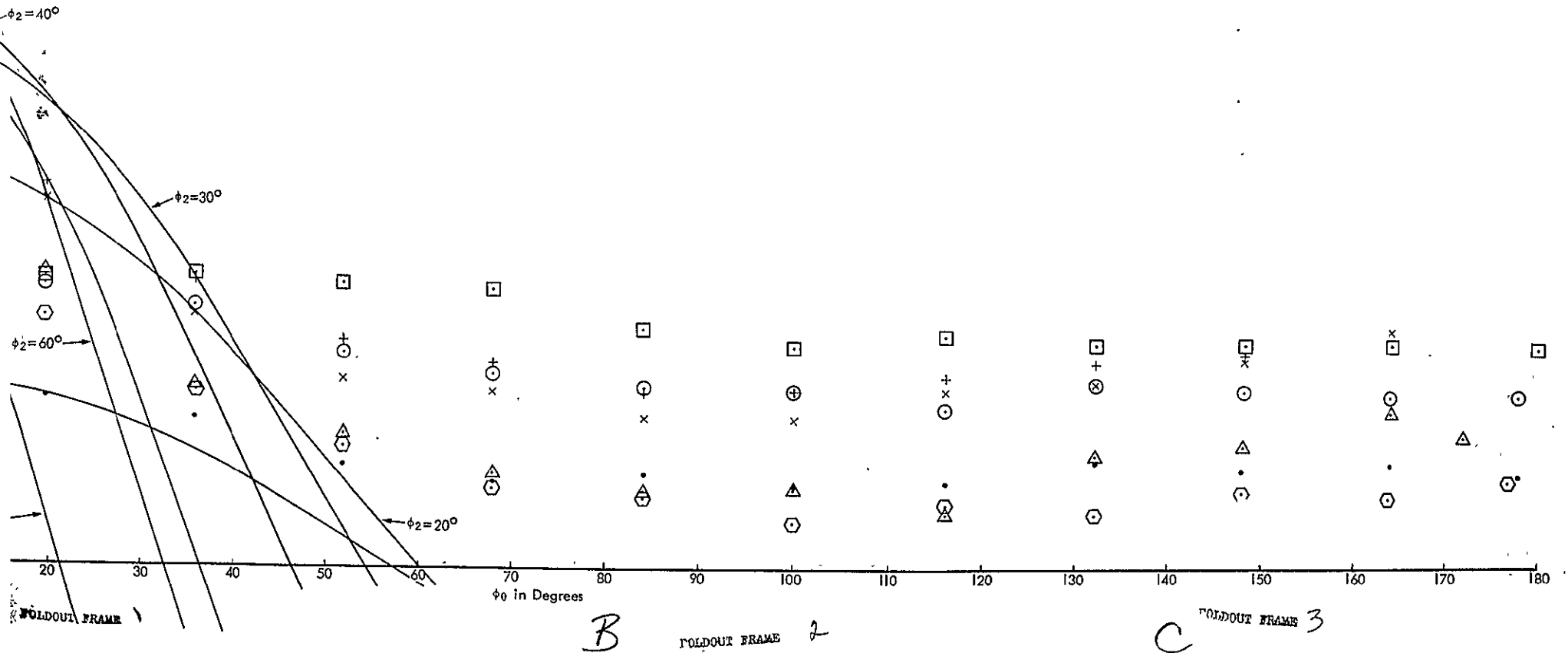
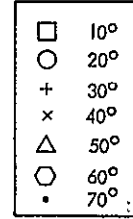
THEORETICAL AND EXPERIMENTAL AVERAGE DIFFERENTIAL SCATTERING CROSS SECTION FOR THE GROUT SURFACE VERSUS AZIMUTH ANGLE ϕ_0 FOR $\phi_1=40^\circ$ WITH ϕ_2 AS THE PARAMETER; GAUSSIAN AUTOCORRELATION FUNCTION

Figure III. 38



THEORETICAL AND EXPERIMENTAL AVERAGE DIFFERENTIAL SCATTERING CROSS SECTION FOR THE GROUT SURFACE VERSUS AZIMUTH ANGLE ϕ_0 FOR $\phi_1 = 40^\circ$ WITH ϕ_2 AS THE PARAMETER; GAUSSIAN AUTOCORRELATION FUNCTION

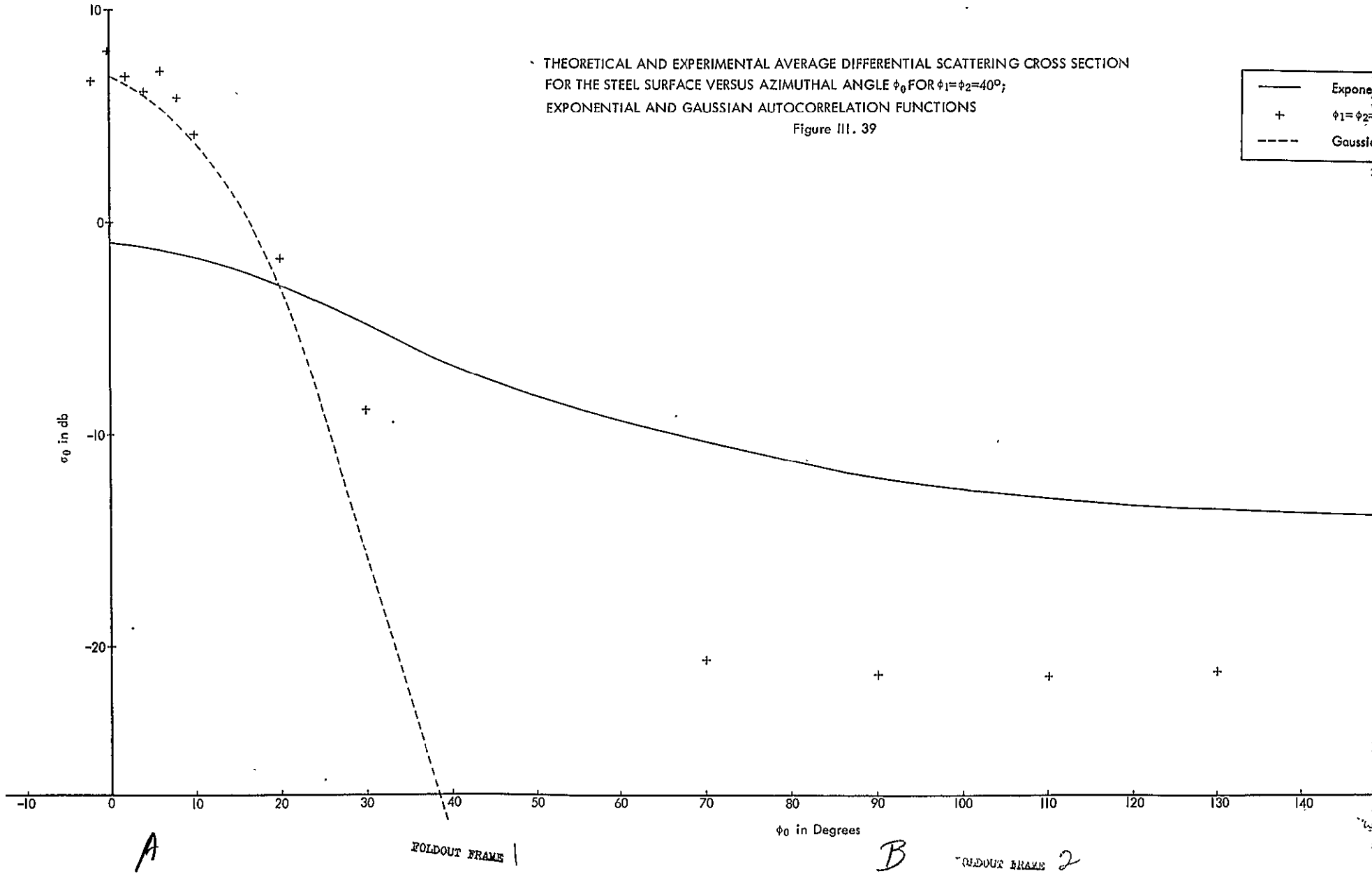
Figure III. 38



THEORETICAL AND EXPERIMENTAL AVERAGE DIFFERENTIAL SCATTERING CROSS SECTION
 FOR THE STEEL SURFACE VERSUS AZIMUTHAL ANGLE ϕ_0 FOR $\phi_1 = \phi_2 = 40^\circ$;
 EXPONENTIAL AND GAUSSIAN AUTOCORRELATION FUNCTIONS

Figure III. 39

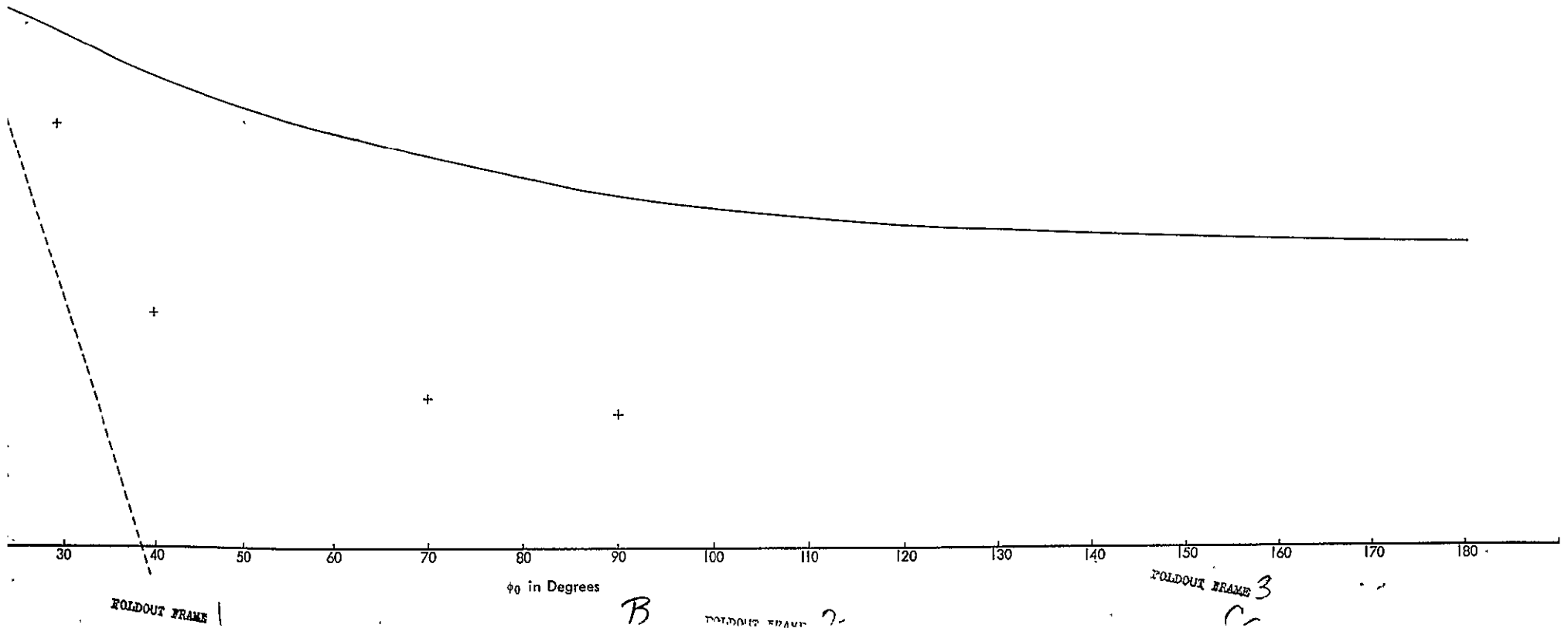
—	Expon.
+	$\phi_1 = \phi_2 =$
- - -	Gaussic



THEORETICAL AND EXPERIMENTAL AVERAGE DIFFERENTIAL SCATTERING CROSS SECTION
 FOR THE STEEL SURFACE VERSUS AZIMUTHAL ANGLE ϕ_0 FOR $\phi_1 = \phi_2 = 40^\circ$;
 EXPONENTIAL AND GAUSSIAN AUTOCORRELATION FUNCTIONS

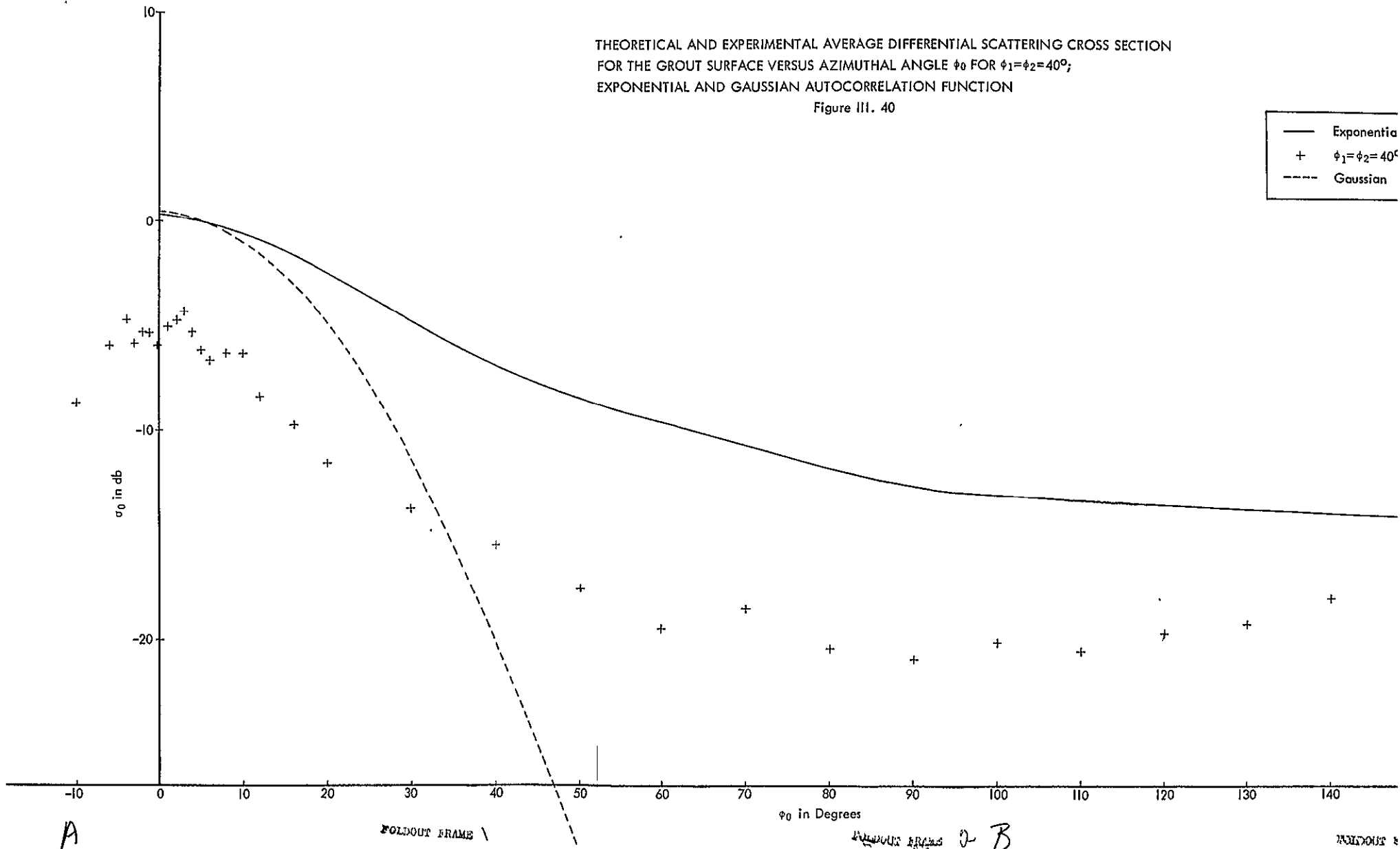
Figure III. 39

—	Exponential
+	$\phi_1 = \phi_2 = 40^\circ$ Experimental
- - -	Gaussian



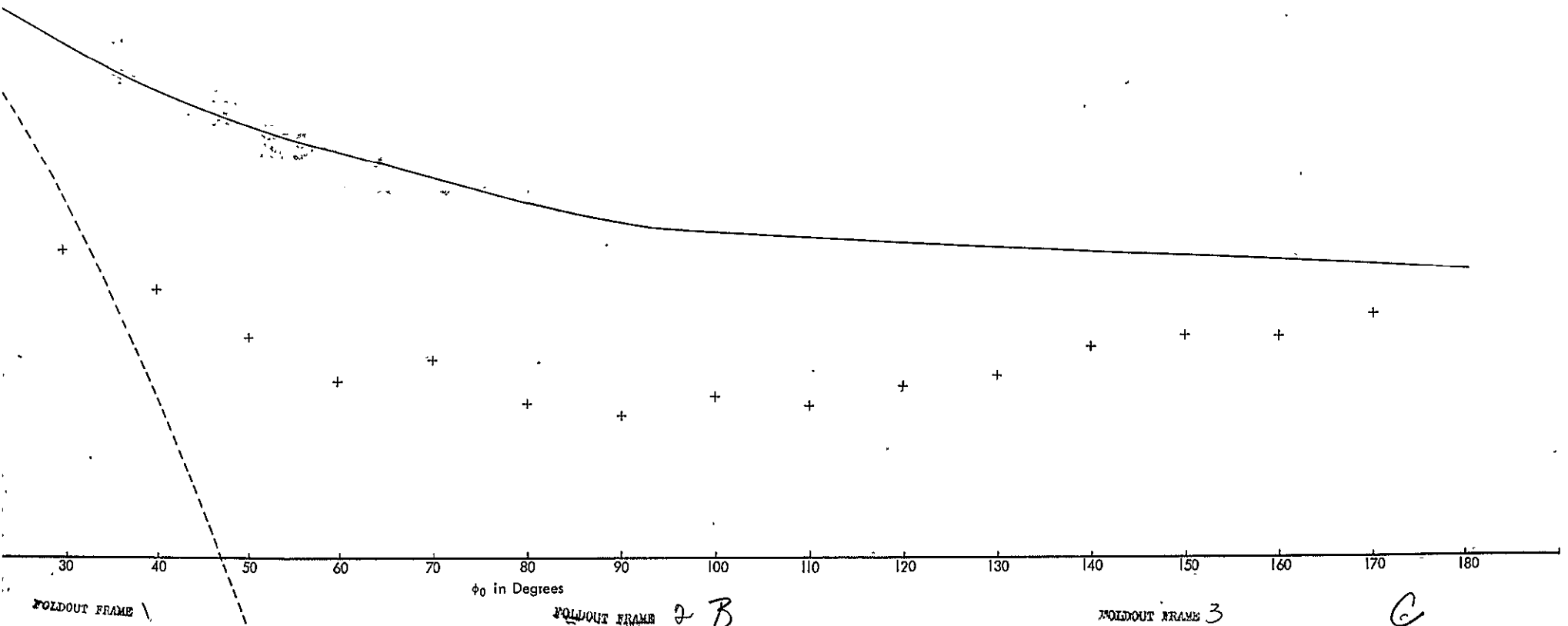
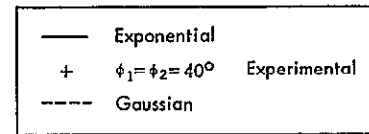
THEORETICAL AND EXPERIMENTAL AVERAGE DIFFERENTIAL SCATTERING CROSS SECTION
 FOR THE GROUT SURFACE VERSUS AZIMUTHAL ANGLE ϕ_0 FOR $\phi_1 = \phi_2 = 40^\circ$;
 EXPONENTIAL AND GAUSSIAN AUTOCORRELATION FUNCTION

Figure III. 40



THEORETICAL AND EXPERIMENTAL AVERAGE DIFFERENTIAL SCATTERING CROSS SECTION
 FOR THE GROUT SURFACE VERSUS AZIMUTHAL ANGLE ϕ_0 FOR $\phi_1=\phi_2=40^\circ$;
 EXPONENTIAL AND GAUSSIAN AUTOCORRELATION FUNCTION

Figure III. 40



FOLDOUT FRAME 1

FOLDOUT FRAME 2 B

FOLDOUT FRAME 3

C

CHAPTER IV

APPLICATION OF THE ACOUSTIC RESULTS
TO ELECTROMAGNETIC SCATTERING

Many of the radiation phenomena associated with different physical phenomena possess a high degree of similarity. A phenomenon such as diffraction is common to fields as diverse as acoustics and quantum mechanics. Advantage can be and has been taken of such similarities if they are sufficiently alike to permit analogue study. It is not even necessary for this to be true to benefit, for if theories for two (or more) physical processes have a common foundation then a verification of the theory for one process implies general applicability. The principal reason for performing model experiments whether for the verification of theories or for making analogue studies is economy of effort.

Acoustic model experiments have long been used to study a variety of electromagnetic problems. Jordan [1941] ; in an early application, made model studies of the properties of antenna arrays and Maestri [1961] has modeled antenna radiation patterns. Meyer [1958] made use of the technique to study microwave surface reflection losses and Edison [1963] has used it to investigate scattering in turbulent media. Recently, Ayiku and Moore [1965] have performed model experiments on knife edge diffraction in which both single and double edges were used. Probably the greatest amount of activity has been in the area of simulation of radar backscatter, the reason for this being the difficulty and expense incurred in performing full scale measurements [Moore, 1962]. Much of this work has been and is being done at the University of New Mexico where a number of simulation studies have been carried out. These studies include simulations of radar backscattering from several types of terrain including cities [Warner et al., 1962] [Edison, 1961], a simulation of the lunar radar echo [Hayre, 1962] and the modeling of the radar cross section measurement of geometric shapes [Koepsel and Ahmed, 1962]. A complete description of the modeling techniques used for radar backscatter as well as other electromagnetic problems is contained in the dissertation of Edison [1961].

A major difficulty in making acoustical analogue studies of some electromagnetic problems has been that the limits of applicability were not clearly defined. The reason for this is that the extent to which the scalar acoustic wave simulates the vector electromagnetic wave had not been fully described. In some problems the vector nature of the electromagnetic wave is not important and can be neglected, a case in point being scattering in a turbulent medium [Edison, 1961, 1963]. However, in other problems this is not possible. Consider the reflection of a plane electromagnetic wave of arbitrary polarization from a plane surface. The reflection is a vector phenomenon as the two polarization components are reflected unequally [Stratton, 1941]. A simulation can be made of the reflection of the separate components but it is not possible to model directly the generally oriented vector reflection.

The problem of the applicability of the analogue scalar measurements does not arise when the model experiments are being performed for the purpose of verifying electromagnetic theories that are based on assumptions identical to those of the analogous acoustic theory. This application of acoustic model experimentation is especially important for the study of the re-radiation of electromagnetic waves from rough surfaces as all electromagnetic theories have bases that allow the development of the simpler acoustic form.

The applicability of the results of model experiments of acoustic wave re-radiation from homogeneous, rough surfaces to the analogous electromagnetic problem is determined through the use of theory based on the Kirchhoff approximation. Of course, this determination is accurate only for situations for which this approximation applies. The limits of applicability are determined by comparing the expressions for the acoustic re-radiation field with the expressions for the analogous electromagnetic re-radiation field and determining under what conditions the vector re-radiation differs enough from the scalar to destroy the similarity. The acoustic expressions used in the comparison are those developed in Chapter II; the electromagnetic expressions are developed below.

The derivation of the expressions describing the re-radiation of a plane electromagnetic wave from a rough, homogeneous surface proceeds similarly to that for the acoustic case, the principal difference being the complexity caused by the vector re-radiation at the rough surface. A

form of the vector Helmholtz integral is used with values of the electric and magnetic fields tangent to the surface being determined through the use of the Kirchhoff approximation. This problem has been treated in this way before and the presentation here is similar to that of Kovalev and Pozdnyak [1961], the difference here being the inclusion of a two dimensional rough surface.

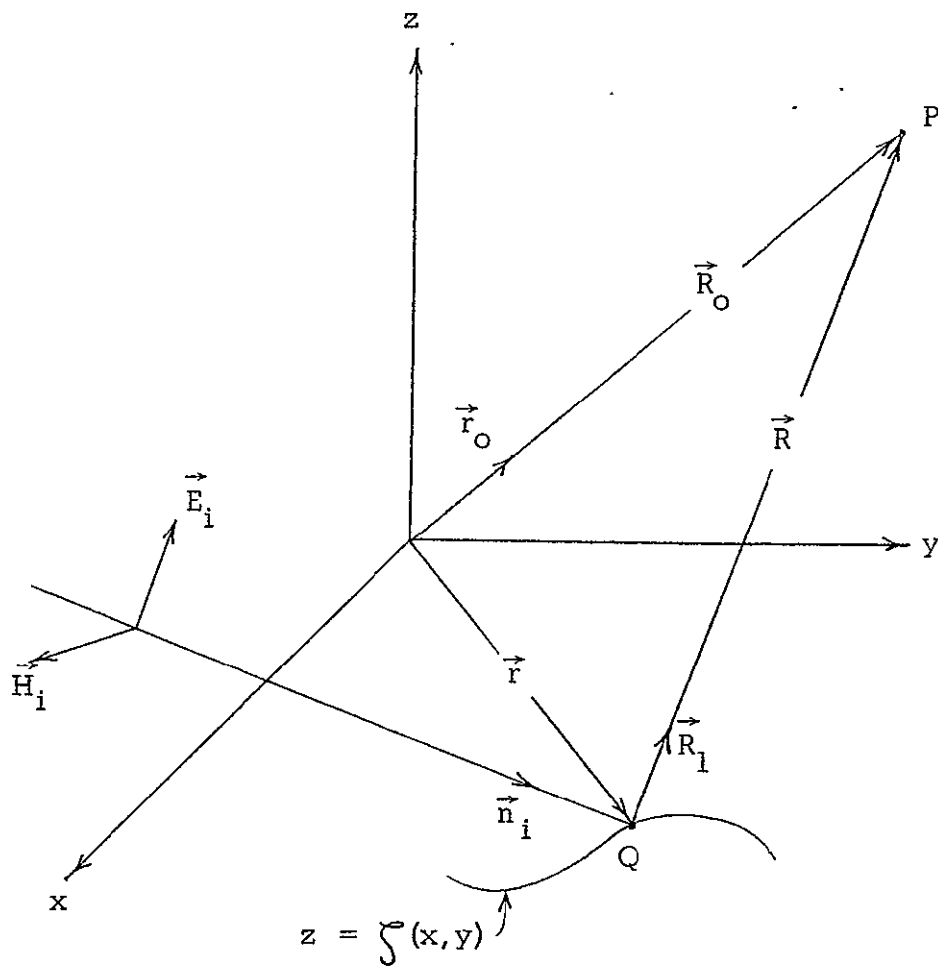
The re-radiated electric field, $\vec{E}(P)$, at the far field observation point P (see figure IV.1) is given by the form of the Helmholtz integral

$$\vec{E}(P) = \frac{i\omega\mu_0 E}{4\pi R_0} e^{-ikR_0} \iint_S \left\{ \vec{n} \times \vec{H} - \vec{r}_0 (\vec{n} \times \vec{H} \cdot \vec{r}_0) + \frac{1}{\sqrt{\mu_1/\epsilon_1}} \left[(\vec{E} \times \vec{n}) \times \vec{r}_0 \right] \right\} e^{i\vec{k}_0 \cdot \vec{r}} dS$$

IV.1

where \vec{r}_0 is the unit vector in the R_0 direction, μ_1 and ϵ_1 are the permeability and permittivity of the medium, respectively, S is an aperture of the size discussed in Section II. B and \vec{n} is the unit normal to the surface. This form is derived in Appendix V; a derivation apparently appears in the Russian literature [Frandin, 1957] but this was not available. For the purpose at hand, the factor of \vec{r}_0 in the second term of the integrand is neglected as components of the fields aligned in this direction of propagation carry no power in this direction.

The Kirchhoff approximation is used to determine the values of $\vec{n} \times \vec{E}$ and $\vec{n} \times \vec{H}$ at each point of the rough surface $z = \zeta(x, y)$. This is done by resolving the incident plane wave into local polarization components parallel and normal to a local plane of incidence and treating the reflection of the two components separately. The incident electric and magnetic fields are given by



The Defining Geometry

Figure IV. 1

$$\vec{E}_i = \vec{\alpha} E e^{-i\vec{k}_i \cdot \vec{r}} \quad \text{IV. 2a}$$

$$\vec{H}_i = \frac{\vec{n}_i \times \vec{\alpha} e^{-i\vec{k}_i \cdot \vec{r}}}{\sqrt{\mu_1/\epsilon_1}} \quad \text{IV. 2b}$$

where $\vec{\alpha}$ is the polarization vector and \vec{n}_i is the unit vector in the direction of propagation; $\vec{k}_i = \vec{n}_i k$. The resolution of \vec{E}_i and \vec{H}_i into local polarization components is facilitated by the establishment at each point of the surface a local coordinate system based on the plane of incidence formed by \vec{n}_i and \vec{n} . The unit vectors of this system are (see figure IV. 2)

$$\begin{aligned} \vec{z} &= \frac{\vec{n}_i \times \vec{n}}{\sin \theta} \\ \vec{p} &= \vec{n} \times \vec{z} \end{aligned} \quad \text{IV. 3}$$

where θ is the local angle of incidence and a function of (x, y) through \vec{n} , as described in Section II. B. Resolving the incident field into local polarization components using the local coordinate system gives

$$\vec{E}_i^{\perp} = (\vec{\alpha} \cdot \vec{z}) \vec{z} E e^{-i\vec{k}_i \cdot \vec{r}} \quad \text{IV. 4a}$$

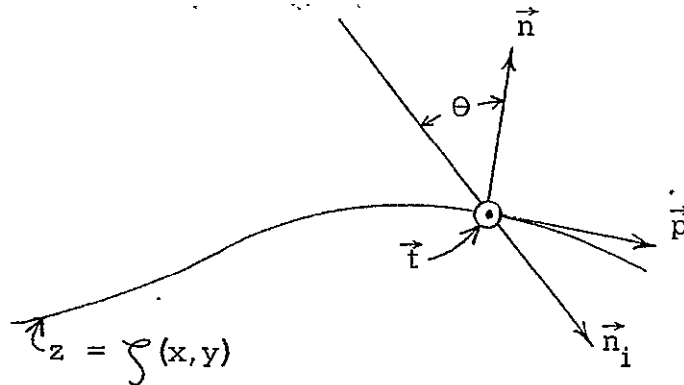
$$\vec{H}_i^{\perp} = \frac{(\vec{\alpha} \cdot \vec{z}) \vec{n}_i \times \vec{z}}{\sqrt{\mu_1/\epsilon_1}} E e^{-i\vec{k}_i \cdot \vec{r}} \quad \text{IV. 4b}$$

for the normally polarized components and

$$\vec{E}_i^{\parallel} = [(\vec{\alpha} \cdot \vec{n}) \vec{n} + (\vec{\alpha} \cdot \vec{p}) \vec{p}] E e^{-i\vec{k}_i \cdot \vec{r}} \quad \text{IV. 4c}$$

$$\vec{H}_i^{\parallel} = [(\vec{\alpha} \cdot \vec{n})(\vec{n}_i \times \vec{n}) + (\vec{\alpha} \cdot \vec{p})(\vec{n}_i \times \vec{p})] \frac{E e^{-i\vec{k}_i \cdot \vec{r}}}{\sqrt{\mu_1/\epsilon_1}} \quad \text{IV. 4d}$$

for the parallel polarized components.



The Local Coordinate System

Figure IV. 2

With the resolution into polarization components, the tangential fields, $\vec{n} \times \vec{H}$ and $\vec{n} \times \vec{E}$, are determined following Stratton [1941]. Beginning with the normally polarized component, the expression for the total tangential electric field for this component at the surface is

$$\vec{n} \times \vec{E}_\perp = \vec{n} \times \vec{E}_\perp^i (1 + \Gamma_\perp) \quad \text{IV. 5a}$$

where the reflection coefficient Γ_\perp is

$$\Gamma_\perp = \frac{\mu_0 k_2 \cos \theta - \mu_2 \sqrt{k^2 - k_2^2 \sin^2 \theta}}{\mu_0 k_2 \cos \theta + \mu_2 \sqrt{k^2 - k_2^2 \sin^2 \theta}}$$

and the subscripts 2 denote the parameters for the homogeneous medium upon which (\vec{E}_i, \vec{H}_i) is incident. The total tangential magnetic field for the normally polarized component is given by the following calculation

$$\begin{aligned} \vec{n} \times \vec{H}_\perp &= \vec{n} \times \vec{H}_\perp^i + \vec{n} \times \vec{H}_\perp^r = \frac{\vec{n} \times (\vec{n}_i \times \vec{E}_\perp^i)}{\sqrt{\mu_1/\epsilon_1}} + \frac{\vec{n} \times (\vec{n}_r \times \vec{E}_\perp^i)}{\sqrt{\mu_1/\epsilon_1}} \\ &= \frac{\vec{n} \times (\vec{n}_i \times \vec{E}_\perp^i)}{\sqrt{\mu_1/\epsilon_1}} + \frac{\vec{n} \times (\vec{n}_r \times \Gamma_\perp \vec{E}_\perp^i)}{\sqrt{\mu_1/\epsilon_1}} \end{aligned}$$

$$\vec{n} \times \vec{H}_\perp = -\frac{\vec{n} \cdot \vec{n}_i \vec{E}_\perp^i}{\sqrt{\mu_1/\epsilon_1}} + \frac{\vec{n} \cdot \vec{n}_i \vec{E}_\perp^i \Omega_\perp}{\sqrt{\mu_1/\epsilon_1}} = -\frac{\vec{n} \cdot \vec{n}_i \vec{E}_\perp^i (1 - \Omega_\perp)}{\sqrt{\mu_1/\epsilon_1}} \quad \text{IV. 5b}$$

where $(\vec{E}_\perp^r, \vec{H}_\perp^r)$ is the reflected field, \vec{n}_r is the reflected wave vector and

$$\vec{n}_i \cdot \vec{n} = -\vec{n} \cdot \vec{n}_r$$

The parallel polarized components are treated similarly. The expression for the total tangential magnetic field is for this polarization component

$$\vec{n} \times \vec{H}_\parallel = \vec{n} \times \vec{H}_\parallel^i (1 + \Omega_\parallel) \quad \text{IV. 5c}$$

where

$$\Omega_\parallel = \frac{\mu_2 k^2 \cos \theta - \mu_0 k_2 \sqrt{k^2 - k_2^2} \sin \theta}{\mu_2 k^2 \cos \theta + \mu_0 k_2 \sqrt{k^2 - k_2^2} \sin \theta}$$

The total tangential electric field for this component is given by

$$\begin{aligned} \vec{n} \times \vec{E}_\parallel &= \vec{n} \times \vec{E}_\parallel^i + \vec{n} \times \vec{E}_\parallel^r = \vec{n} \times (\vec{H}_\parallel^i \times \vec{n}_i) \sqrt{\mu_1/\epsilon_1} + \vec{n} \times (\vec{H}_\parallel^r \times \vec{n}_r) \sqrt{\mu_1/\epsilon_1} \\ &= \vec{n} \times (\vec{H}_\parallel^i \times \vec{n}_i) \sqrt{\mu_1/\epsilon_1} + \vec{n} \times (\vec{H}_\parallel^i \Omega_\parallel \times \vec{n}_r) \sqrt{\mu_1/\epsilon_1} \\ &= \vec{n} \cdot \vec{n}_i \vec{H}_\parallel^i \sqrt{\mu_1/\epsilon_1} - \vec{n} \cdot \vec{n}_i \Omega_\parallel \vec{H}_\parallel^i \sqrt{\mu_1/\epsilon_1} \\ &= \vec{n} \cdot \vec{n}_i \sqrt{\mu_1/\epsilon_1} \vec{H}_\parallel^i (1 - \Omega_\parallel) \end{aligned}$$

IV. 5d

The total tangential electric field is given by the sum of the tangential fields of the two polarization components, or

$$\vec{n} \times \vec{E} = \vec{n} \times \vec{E}_{\perp} + \vec{n} \times \vec{E}_{\parallel} \quad \text{IV. 6a}$$

and similarly the total magnetic field is

$$\vec{n} \times \vec{H} = \vec{n} \times \vec{H}_{\perp} + \vec{n} \times \vec{H}_{\parallel} \quad \text{IV. 6b}$$

where the right hand sides are given by eq. (IV. 5).

The solution for the electric field at the observation point P is obtained by substituting eq. (IV. 5) into eq. (IV. 6) and substituting this result into eq. (IV. 1). The expression which results from these substitutions is quite lengthy for the general case and is not given. Instead, expressions are developed for special cases under several conditions of approximation for comparison with the analogous acoustical expression. These cases are those of normal and parallel polarization relative to the plane of incidence defined by the mean normal, \vec{k} , and \vec{n}_i . The acoustical quantity with which comparison is made is the pressure and the expression used is obtained from eq. (II. 9) by neglecting second order partial derivatives of the surface and writing the reflection coefficient in closed form. This is

$$\phi(P) = - \frac{\phi^+ e^{-ikR_0}}{4\pi R_0} \int_S \left\{ i \vec{n} \cdot \vec{k}_i (1 - \Gamma) + i (\vec{k}_0 \cdot \vec{n}) (1 + \Gamma) e^{i \vec{k}_0 \cdot \vec{r}} \right\} dS$$

IV. 7

It is recalled that eq. (II. 9) was obtained under the condition of a plane wave incident upon a rough aperture of homogeneous material.

The acoustic quantity used in the comparison is chosen to be the pressure for reasons of convenience. The particle velocity can, of course, be used; however, by judiciously choosing the analogous electromagnetic quantity, this calculation can be spared. Edison [1961] has shown that for the case of parallel polarization the tangential component of the incident electric field and the normal component of the incident particle velocity

both vary as $\cos\theta$ and, therefore, are necessarily analogues. The analogy is complete for this case because the incident magnetic field and the incident pressure do not vary with θ (except in the phase factor which is common to all quantities). For normal polarization the situation is reversed and the pressure is analogous to the electric field. Therefore, for the case of parallel polarization the expression for the re-radiated pressure field is compared with that for the re-radiated magnetic field (to be developed subsequently) and for normal polarization with the electric field.

The incident field for polarization normal to the y - z plane is

$$\vec{E}_i = \lambda E e^{-i\vec{k}_i \cdot \vec{r}}$$

$$\vec{H}_i = \frac{\vec{n}_i \times \lambda E e^{-i\vec{k}_i \cdot \vec{r}}}{\sqrt{\mu_1/\epsilon_1}}$$

where $\vec{n}_i = \vec{j} \cos\theta_{1y} + \vec{k} \cos\theta_{1z}$. For \vec{n}_i in the y - z plane the unit vectors are, at a point (x, y) on the surface

$$\vec{e} = \frac{\vec{n}_i \times \vec{n}}{\sin\theta} \frac{\vec{n}_i \times \vec{n}}{\sqrt{1 - (\vec{n}_i \cdot \vec{n})^2}}$$

$$= \frac{\vec{n}_i \times \vec{n}}{\sqrt{1 - \frac{(-Zx \cos\theta_{1x} - Zy \cos\theta_{1y} + \cos\theta_{1z})^2}{1 + Zx^2 + Zy^2}}}$$

$$= \frac{\lambda(\cos\theta_{1y} + Zy \cos\theta_{1z}) - \vec{j} Zx \cos\theta_{1z} + \vec{k} Zx \cos\theta_{1y}}{\sqrt{1 + Zx^2 + Zy^2 - (-Zx \cos\theta_{1x} - Zy \cos\theta_{1y} + \cos\theta_{1z})^2}} \quad \text{IV.8a}$$

$$\vec{p} = \vec{n} \times \vec{e} = \left\{ \hat{x} \left[-Z_y Z_x \cos \theta_{1y} + Z_x \cos \theta_{1z} \right] \right. \\ \left. + \hat{y} \left[Z_x^2 \cos \theta_{1y} + \cos \theta_{1y} + Z_y \cos \theta_{1z} \right] \right. \\ \left. + \hat{z} \left[Z_y (\cos \theta_{1y} + Z_y \cos \theta_{1z}) + Z_x^2 \cos \theta_{1z} \right] \right\}$$

$$\sqrt{(1+Z_x^2+Z_y^2) \left[1+Z_x^2+Z_y^2 - (-Z_x \cos \theta_{1x} - Z_y \cos \theta_{1y} + \cos \theta_{1z})^2 \right]}$$

IV. 8b

and

$$\vec{n} = \frac{-\hat{x} Z_x - \hat{y} Z_y + \hat{z}}{\sqrt{1+Z_x^2+Z_y^2}}$$

IV. 8c

as before. These expressions are clearly complicated; to obtain a simple first order approximation, Z_x and Z_y are set equal to zero (smooth surface). Then

$$\vec{r} = \hat{i} \quad \vec{p} = \hat{j} \quad \vec{n} = \hat{k}$$

as expected and, therefore, from eq. 's (IV. 4)

$$\vec{E}_{\perp}^{\dot{i}} = \hat{x} E e^{-i\vec{k}_1 \cdot \vec{r}}$$

$$\vec{H}_{\perp}^{\dot{i}} = \frac{\vec{n} \times \hat{x} E e^{-i\vec{k}_1 \cdot \vec{r}}}{\sqrt{\mu_1 / \epsilon_1}}$$

$$\vec{E}_{\parallel}^{\dot{i}} = \vec{H}_{\parallel}^{\dot{i}} = 0$$

From eq. 's (IV. 5) and (IV. 6)

$$\begin{aligned}\vec{n} \times \vec{E} &= \vec{n} \times \vec{E}_\perp = \vec{n} \times \vec{E}_\perp (1 + \Omega_\perp) \\ &= \vec{n} \times \lambda E (1 + \Omega_\perp) e^{-i\vec{k}_1 \cdot \vec{r}}\end{aligned}$$

IV. 9a

and

$$\vec{n} \times \vec{H} = \vec{n} \times \vec{H}_\perp = -\frac{\vec{n} \cdot \vec{n}_0 (1 - \Omega_\perp) \lambda E e^{-i\vec{k}_1 \cdot \vec{r}}}{\sqrt{\mu_1/\epsilon_1}}$$

IV. 9b

Substituting eq. 's (IV. 9) into eq. (IV. 1) and neglecting the factor of \vec{r}_0 gives for the electric field at P

$$\begin{aligned}\vec{E}(P) &= \frac{i\omega\mu_1 e^{-ikR_0}}{4\pi R_0} \iint_S \left\{ \frac{-\vec{n} \cdot \vec{n}_0 (1 - \Omega_\perp) \lambda E}{\sqrt{\mu_1/\epsilon_1}} \right. \\ &\quad \left. + \frac{(\vec{\lambda} \times \vec{n}) \times \vec{r}_0 E (1 + \Omega_\perp)}{\sqrt{\mu_1/\epsilon_1}} \right\} e^{i(\vec{k}_0 - \vec{k}_1) \cdot \vec{r}} dS\end{aligned}$$

$$= \frac{-i E e^{-ikR_0}}{4\pi R_0} \iint_S \left\{ \vec{n} \cdot \vec{k}_1 (1 - \Omega_\perp) \lambda \right.$$

$$\left. + (\vec{n} \cdot \vec{k}_0) \lambda (1 + \Omega_\perp) - (\vec{\lambda} \cdot \vec{k}_0) \vec{n} (1 + \Omega_\perp) \right\} e^{i\vec{k} \cdot \vec{r}} dS$$

IV. 10

where, as before, $\vec{K} = \vec{k}_0 - \vec{k}_1$ and $\vec{k}_1 = \vec{n}_1 k$, $\vec{k}_0 = \vec{r}_0 k$. Comparison of this expression with the analogous acoustic expression given by eq. (IV.7) shows that when the observation point P lies in the plane of incidence the integrals are identical since $\vec{I} \cdot \vec{k}_0 = 0$. For this case, the electromagnetic re-radiation is essentially scalar; there is no depolarization of the incident wave and it is necessary to give only the single reflection coefficient Γ_{\perp} . Out of the plane of incidence, there is a change of polarization which is a vector effect that cannot be simulated by scalar means. However, it remains to investigate the possibility of simulating the amplitude of the vector field. To do this it is necessary to examine only those components of $\vec{E}(P)$ normal to \vec{r}_0 , the direction of propagation. These components vary as the sine of the angle between \vec{r}_0 and $\vec{E}(P)$. For the first two terms of the integrand of eq. (IV.10), there is a difference in the variation of $\sin\theta_{ox}$ from the similar terms in eq. (IV.7). For the last term in the integrand of eq. (IV.10) for which there is no comparable acoustical term, the power producing components vary as the sines of their respective angles with \vec{r}_0 times $\vec{I} \cdot \vec{k}_0$, which causes the disappearance of this term in the plane of incidence. Therefore, the exactness of the simulation of the re-radiated field becomes less as the vector \vec{r}_0 moves away from the plane of incidence whether polarization is considered or not. The degree to which this occurs is determined by the variation of $\sin\theta_{ox}$ and $\vec{I} \cdot \vec{k}_0 = \cos\theta_{ox}$.

The expression for the electric field given by eq. (IV.10) was developed under the approximation that the fields were re-radiated as if the surface were smooth. The effect of the surface roughness on the vector re-radiation is brought out through consideration of the simpler case of re-radiation in the plane of incidence ($\cos\theta_{1x} = \cos\theta_{ox} = 0$). This is done under the less severe restriction that $Z_x, Z_y \ll 1$. The unit vectors are approximately from eq. (IV.8)

$$\vec{n} = \vec{k} \quad \text{IV.11a}$$

$$\vec{e} = \frac{\hat{x}(\cos\theta_{1y} + Z_y \cos\theta_{1z}) - \hat{y} Z_x \cos\theta_{1z} + \hat{z} Z_x \cos\theta_{1y}}{\sqrt{1 + Z_x^2 + Z_y^2 - (-Z_y \cos\theta_{1y} + \cos\theta_{1z})^2}} \quad \text{IV.11b}$$

$$\vec{p} = \left\{ \hat{x} \left[-Z_y Z_x \cos \theta_{1y} + Z_x \cos \theta_{1z} \right] \right. \\ \left. + \hat{y} \left[Z_x^2 \cos \theta_{1y} + \cos \theta_{1y} + Z_y \cos \theta_{1z} \right] \right. \\ \left. + \hat{z} \left[Z_y (\cos \theta_{1y} + Z_y \cos \theta_{1z}) + Z_x^2 \cos \theta_{1z} \right] \right. \\ \left. \right\} \\ \frac{1}{\sqrt{1 + Z_x^2 + Z_y^2 - (-Z_y \cos \theta_{1y} + \cos \theta_{1z})^2}}$$

IV.11c

The resolution of the normally polarized field into local polarization components gives, from eq. (IV. 4)

$$\vec{E}_{\perp}^i = (\cos \theta_{1y} + Z_y \cos \theta_{1z}) E e^{-i\vec{k}_1 \cdot \vec{r}} \\ \frac{\hat{x} (\cos \theta_{1y} + Z_y \cos \theta_{1z}) - \hat{y} Z_x \cos \theta_{1z} + \hat{z} Z_x \cos \theta_{1y}}{\left[1 + Z_x^2 + Z_y^2 - (-Z_y \cos \theta_{1y} + \cos \theta_{1z})^2 \right]} \\ \vec{H}_{\perp}^i = \frac{(-Z_x Z_y \cos \theta_{1y} + Z_x \cos \theta_{1z}) E e^{-i\vec{k}_1 \cdot \vec{r}}}{\sqrt{\mu_1/\epsilon_1} \left[1 + Z_x^2 + Z_y^2 - (-Z_y \cos \theta_{1y} + \cos \theta_{1z})^2 \right]} \\ \hat{x} (Z_x \cos^2 \theta_{1y} + Z_x \cos^2 \theta_{1z}) + \hat{y} \left[\cos \theta_{1z} (\cos \theta_{1y} + Z_y \cos \theta_{1z}) \right] \\ + \hat{z} \left[-\cos \theta_{1y} (\cos \theta_{1y} + Z_y \cos \theta_{1z}) \right] \\ \vec{E}_{\parallel}^i = \frac{(-Z_x Z_y \cos \theta_{1y} + Z_x \cos \theta_{1z}) E e^{-i\vec{k}_1 \cdot \vec{r}}}{\left[1 + Z_x^2 + Z_y^2 - (-Z_y \cos \theta_{1y} + \cos \theta_{1z})^2 \right]} \\ \hat{x} (Z_x \cos \theta_{1z} - Z_y Z_x \cos \theta_{1y}) + \hat{y} (Z_x^2 \cos \theta_{1y} + \cos \theta_{1y} + Z_y \cos \theta_{1z}) \\ + \hat{z} \left[Z_y (\cos \theta_{1y} + Z_y \cos \theta_{1z}) + Z_x^2 \cos \theta_{1z} \right]$$

$$\begin{aligned} \vec{H}_{\parallel}^i &= \frac{(-Z_x Z_y \cos \theta_{1y} + Z_x \cos \theta_{1z}) E e^{-i\vec{k}_1 \cdot \vec{r}}}{\sqrt{\mu_1/\epsilon_1} \left[1 + Z_x^2 + Z_y^2 - (-Z_y \cos \theta_{1y} + \cos \theta_{1z})^2 \right]} \\ &\quad \hat{x} \left\{ \cos \theta_{1y} \left[Z_y (\cos \theta_{1y} + Z_y \cos \theta_{1z}) + Z_x^2 \cos \theta_{1z} \right. \right. \\ &\quad \quad \left. \left. - \cos \theta_{1z} \left[Z_x^2 \cos \theta_{1y} + \cos \theta_{1y} + Z_y \cos \theta_{1z} \right] \right\} \\ &\quad + \hat{y} \left[\cos \theta_{1z} (-Z_y Z_x \cos \theta_{1y} + Z_x \cos \theta_{1z}) \right] \\ &\quad + \hat{z} \left[-\cos \theta_{1y} (-Z_y Z_x \cos \theta_{1y} + Z_x \cos \theta_{1z}) \right] \end{aligned}$$

Substituting into eq. 's (IV. 6) and (IV. 5) gives

$$\begin{aligned} \vec{n} \times \vec{E} &= \vec{n} \times \vec{E}_{\perp} + \vec{n} \times \vec{E}_{\parallel} \\ &= \frac{(\cos \theta_{1y} + Z_y \cos \theta_{1z}) E e^{-i\vec{k}_1 \cdot \vec{r}} (1 + \Omega_{\perp})}{\left[1 + Z_x^2 + Z_y^2 - (-Z_y \cos \theta_{1y} + \cos \theta_{1z})^2 \right]} \\ &\quad + \frac{\hat{x} Z_x \cos \theta_{1z} + \hat{y} Z_y \cos \theta_{1y} \cos \theta_{1z} + (\cos \theta_{1z}) (Z_x Z_y \cos \theta_{1y} + Z_x \cos \theta_{1z}) (1 - \Omega_{\parallel}) E e^{-i\vec{k}_1 \cdot \vec{r}}}{\left[1 + Z_x^2 + Z_y^2 - (-Z_y \cos \theta_{1y} + \cos \theta_{1z})^2 \right]} \\ &\quad \hat{x} \left\{ \cos \theta_{1y} \left[Z_y (\cos \theta_{1y} + Z_y \cos \theta_{1z}) + Z_x^2 \cos \theta_{1z} \right. \right. \\ &\quad \quad \left. \left. - \cos \theta_{1z} \left[Z_x^2 \cos \theta_{1y} + \cos \theta_{1y} + Z_y \cos \theta_{1z} \right] \right\} \\ &\quad + \hat{y} \left[\cos \theta_{1z} (-Z_x Z_y \cos \theta_{1y} + Z_x \cos \theta_{1z}) \right] \\ &\quad + \hat{z} \left[-\cos \theta_{1y} (-Z_x Z_y \cos \theta_{1y} + Z_x \cos \theta_{1z}) \right] \end{aligned}$$

$$\begin{aligned}
\vec{n} \times \vec{H} &= \vec{n} \times \vec{H}_{\parallel} + \vec{n} \times \vec{H}_{\perp} \\
&= \frac{(-Z_x Z_y \cos \theta_{1y} + Z_x \cos \theta_{1z}) E e^{-i\vec{k}_1 \cdot \vec{r}} (1 + \Gamma_{\parallel})}{\sqrt{\mu_1} \epsilon_1 \left[1 + Z_x^2 + Z_y^2 - (-Z_y \cos \theta_{1y} + \cos \theta_{1z})^2 \right]} \\
&\quad \vec{x} \left[-\cos \theta_{1z} (-Z_y Z_x \cos \theta_{1y} + Z_x \cos \theta_{1z}) \right] + \vec{y} \left\{ \cos \theta_{1y} \right. \\
&\quad \left. [Z_y (\cos \theta_{1y} + Z_y \cos \theta_{1z}) + Z_x^2 \cos \theta_{1z}] - \cos \theta_{1z} [Z_x^2 \cos \theta_{1y} \right. \\
&\quad \left. + \cos \theta_{1y} + Z_y \cos \theta_{1z}] \right\} \\
&\quad + \frac{(-\cos \theta_{1z}) (\cos \theta_{1y} + Z_y \cos \theta_{1z}) (1 - \Gamma_{\perp}) E e^{-i\vec{k}_1 \cdot \vec{r}}}{\sqrt{\mu_1} \epsilon_1 \left[1 + Z_x^2 + Z_y^2 - (-Z_y \cos \theta_{1y} + \cos \theta_{1z})^2 \right]} \\
&\quad \vec{x} (\cos \theta_{1y} + Z_y \cos \theta_{1z}) - \vec{y} (Z_x \cos \theta_{1z}) + \vec{z} (Z_x \cos \theta_{1y})
\end{aligned}$$

Substituting into eq. (IV.1) and neglecting the factor of \vec{r}_0 as before gives the result

$$\begin{aligned}
\vec{E}(\rho) &= \frac{ik e^{-ikR_0}}{4\pi R_0} \iint_S \left\{ \vec{x} \left\{ -\cos \theta_{1z} (\cos \theta_{1y} + Z_y \cos \theta_{1z})^2 (1 - \Gamma_{\perp}) \right. \right. \\
&\quad \left. \left. - \cos \theta_{1z} (-Z_x Z_y \cos \theta_{1y} + Z_x \cos \theta_{1z})^2 (1 + \Gamma_{\parallel}) - \cos \theta_{1z} \cos \theta_{1y} \cos \theta_{0y} \right. \right. \\
&\quad \left. \left. (-Z_x Z_y \cos \theta_{1y} + Z_x \cos \theta_{1z})^2 (1 - \Gamma_{\parallel}) - \cos^2 \theta_{1z} \cos \theta_{0z} (-Z_x Z_y \cos \theta_{1y} \right. \right. \\
&\quad \left. \left. + Z_x \cos \theta_{1z})^2 (1 - \Gamma_{\parallel}) - \cos \theta_{0z} (\cos \theta_{1y} + Z_y \cos \theta_{1z})^2 (1 + \Gamma_{\perp}) \right\} \right. \\
&\quad \left. + \vec{y} \left\{ (\cos \theta_{1z})^2 (\cos \theta_{1y} + Z_y \cos \theta_{1z}) Z_x (1 - \Gamma_{\perp}) + (-Z_x Z_y \cos \theta_{1y} \right. \right. \\
&\quad \left. \left. + Z_x \cos \theta_{1z}) (\cos \theta_{1y} + Z_y \cos \theta_{1z}) Z_y^2 \cos \theta_{1y} (1 + \Gamma_{\parallel}) \right. \right. \\
&\quad \left. \left. + (-Z_x Z_y \cos \theta_{1y} + Z_x \cos \theta_{1z}) Z_x^2 \cos \theta_{1y} \cos \theta_{1z} (1 + \Gamma_{\parallel}) \right. \right. \\
&\quad \left. \left. - (-Z_x Z_y \cos \theta_{1y} + Z_x \cos \theta_{1z}) (Z_x^2 \cos \theta_{1y} + \cos \theta_{1y} + Z_y \cos \theta_{1z}) \right. \right. \\
&\quad \left. \left. \cos \theta_{1z} (1 + \Gamma_{\parallel}) + \cos \theta_{1z} \cos \theta_{0z} (-Z_x Z_y \cos \theta_{1y} + Z_x \cos \theta_{1z}) \right. \right. \\
&\quad \left. \left. (\cos \theta_{1y} + Z_y \cos \theta_{1z}) Z_y \cos \theta_{1y} (1 - \Gamma_{\parallel}) \right. \right.
\end{aligned}$$

$$\begin{aligned}
& + \omega s^2 \theta_{12} \omega s \theta_{0z} \omega s \theta_{1y} (-Z_x Z_y \omega s \theta_{1y} + Z_x \omega s \theta_{1z}) Z_x^2 (1 - \Gamma_{//}) \\
& - \omega s^2 \theta_{12} \omega s \theta_{0z} (-Z_x Z_y \omega s \theta_{1y} + Z_x \omega s \theta_{1z}) (Z_x^2 \omega s \theta_{1y} \\
& + \omega s \theta_{1y} + Z_y \omega s \theta_{1z}) (1 - \Gamma_{//}) + (\omega s \theta_{1y} + Z_y \omega s \theta_{1z}) \\
& (\cos \theta_{0z} \omega s \theta_{1z}) Z_x (1 + \Gamma_{\perp}) \Big\} \\
& + \vec{k} \Big\{ (-\omega s \theta_{1z}) (\omega s \theta_{1y} + Z_y \omega s \theta_{1z}) Z_x \omega s \theta_{1y} (1 - \Gamma_{\perp}) \\
& + (\omega s \theta_{1y} + Z_y \omega s \theta_{1z}) (-\omega s \theta_{0y} \omega s \theta_{1z}) Z_x (1 + \Gamma_{\perp}) \\
& - \omega s \theta_{1z} \omega s \theta_{0y} \omega s \theta_{1y} (-Z_x Z_y \omega s \theta_{1z} + Z_x \omega s \theta_{1z}) \\
& (\omega s \theta_{1y} + Z_y \omega s \theta_{1z}) Z_y (1 - \Gamma_{//}) \\
& - \omega s \theta_{1z} \omega s \theta_{0y} \omega s \theta_{1y} (-Z_x Z_y \omega s \theta_{1y} + Z_x \omega s \theta_{1z}) \\
& (Z_x^2 \omega s \theta_{1z}) (1 - \Gamma_{//}) + \omega s \theta_{1z} \omega s \theta_{0y} \omega s \theta_{1z} (-Z_x Z_y \omega s \theta_{1y} \\
& + Z_x \omega s \theta_{1z}) + (Z_x^2 \omega s \theta_{1y} + \omega s \theta_{1y} + Z_y \omega s \theta_{1z}) (1 - \Gamma_{//}) \Big\}
\end{aligned}$$

$$E e^{i \vec{k} \cdot \vec{r}}$$

$$\frac{E e^{i \vec{k} \cdot \vec{r}}}{\left[1 + Z_x^2 + Z_y^2 - (-Z_y \omega s \theta_{1y} + \omega s \theta_{1z})^2 \right]}$$

IV.12

The comparison of this result, eq. (IV.12), with eq. (IV.10) indicates the severity of the approximation made in developing this latter equation, thereby illustrating the effects of the vector re-radiation. One of these is the depolarization of the incident radiation by the rough surface; this is seen by the presence of the non-zero factors of \vec{j} and \vec{k} , which are the cross polarized components relative to the polarization vector \vec{i} of the incident wave. However, the depolarization components all have Z_x or

Z_y or both as factors which indicates their smallness relative to the polarized component which has terms that do not depend upon the slope of the surface. These slope independent terms also depend only upon

Γ_{\perp} and not upon Γ_{\parallel} , as expected. For backscatter at normal incidence ($\cos\theta_{1z} = -1$, $\cos\theta_{0z} = 1$, $\cos\theta_{1y} = \cos\theta_{0y} = 0$) eq. (IV.12) reduces (considerably) to

$$\vec{E}(p) = \frac{i k e^{-i k R_0}}{4\pi R_0} 2E \iint_S \left\{ \frac{\Gamma_{\parallel} z_x^2 - \Gamma_{\perp} z_y^2}{z_x^2 + z_y^2} + \frac{z_x z_y (\Gamma_{\parallel} + \Gamma_{\perp})}{z_x^2 + z_y^2} \right\} e^{i \vec{k} \cdot \vec{r}} dS$$

IV.13

At normal incidence, the reflection coefficients have the same magnitude but differ in sign, and their slopes with respect to angle of incidence are zero [Stratton, 1941]; therefore, the cross polarized component disappears. The same result is obtained for the case of perfect conductivity of the rough surface for which $\Gamma_{\parallel} = 1$, $\Gamma_{\perp} = -1$.

The field re-radiated from a perfect conductor is obtained more generally by using the boundary conditions

$$\begin{aligned} \vec{n} \times \vec{E} &= 0 \\ \vec{n} \times \vec{H} &= 2\vec{n} \times \vec{H}_i \end{aligned} \quad \text{IV.14}$$

which are obtained from eq. 's (IV.5) using $\Gamma_{\parallel} = 1$, $\Gamma_{\perp} = -1$. For the case of normal polarization, substitution of eq. (IV.14) into eq. (IV.1) gives

$$\vec{E}(p) = \frac{i e^{-i k R_0}}{4\pi R_0} 2E \iint_S \left\{ (\vec{n} \cdot \vec{x}) \vec{k}_1 - (\vec{n} \cdot \vec{k}_1) \vec{x} \right\} e^{i \vec{k} \cdot \vec{r}} dS \quad \text{IV.15}$$

which has a depolarization component in the plane of incidence in that the factor of \vec{k}_1 is not zero; however under the approximation $\vec{n} = \vec{k}$ this result readily reduces to eq. (IV.13) for the case of perfect conductivity.

Comparison of the acoustic results given by eq. (IV. 7) with eq. (IV.13) shows that a simulation is possible for the case of back-scattering at normal incidence from an imperfectly conducting surface under the approximation $\vec{n} = \vec{k}$. Under the same approximation, it is seen that the re-radiation from a perfectly conducting surface can be simulated but as before only in the plane of incidence because of depolarization effects. In considering the possibility of simulation out of the plane of incidence for the case of a perfect conductor, the same conclusion is reached as earlier. However in this case, the quantity which has no comparable acoustic term, $(\vec{n} \cdot \vec{i}) \vec{k}_1$, vanishes only upon approximation and not as $\cos\theta_{ox}$.

The incident field for the case of polarization parallel to the y-z plane is

$$\vec{E}_i = \vec{\lambda} \times \vec{n}_i E e^{-i\vec{k}_i \cdot \vec{r}}$$

$$\vec{H}_i = \frac{\vec{\lambda} E e^{-i\vec{k}_i \cdot \vec{r}}}{\sqrt{\mu_1/\epsilon_1}}$$

where \vec{n}_i is the same as earlier as are \vec{n} , \vec{t} , and \vec{p} , the unit vectors of the local coordinate system. The re-radiated magnetic field which contributes to the power flow in the direction of \vec{r}_o is determined from

$$\vec{H}(P) = \frac{\vec{r}_o \times \vec{E}(P)}{\sqrt{\mu_1/\epsilon_1}}$$

Substituting eq. (IV.1) into this expression gives the result

$$\vec{H}(P) = \frac{ike^{-ikR_0}}{4\pi R_0} \iint_S \left\{ \vec{r}_o \times (\vec{n} \times \vec{H}) \right.$$

$$\left. + \frac{1}{\sqrt{\mu_1/\epsilon_1}} \left[\vec{E} \times \vec{n} - \vec{r}_o \cdot (\vec{E} \times \vec{n}) \vec{r}_o \right] \right\} e^{i\vec{k} \cdot \vec{r}} dS$$

The factor of \vec{r}_0 in eq. (IV.14) is neglected here as it was in eq. (IV.1). Making the same severe approximation

$$\vec{r} = \vec{r} \quad \vec{p} = \vec{j} \quad \vec{n} = \vec{k}$$

that led to eq. 's (IV.9) results in

$$\vec{E}_{\parallel}^{\dot{j}} = \vec{\lambda} \times \vec{n}_{\lambda} E e^{-i\vec{k}_1 \cdot \vec{r}}$$

$$\vec{H}_{\parallel}^{\dot{j}} = \frac{\vec{\lambda} E e^{-i\vec{k}_1 \cdot \vec{r}}}{\sqrt{\mu_1/\epsilon_1}}$$

$$\vec{E}_{\perp}^{\dot{j}} = \vec{H}_{\perp}^{\dot{j}} = 0$$

Using these in eq. 's (IV.6) and (IV.5) gives the tangential electric and magnetic fields at the surface; these are

$$\vec{n} \times \vec{E} = \vec{n} \cdot \vec{n}_{\lambda} \vec{\lambda} E (1 - \Gamma_{\parallel}) e^{-i\vec{k}_1 \cdot \vec{r}} \quad \text{IV.17a}$$

$$\vec{n} \times \vec{H} = \frac{\vec{n} \times \vec{\lambda} E (1 + \Gamma_{\parallel}) e^{-i\vec{k}_1 \cdot \vec{r}}}{\sqrt{\mu_1/\epsilon_1}} \quad \text{IV.17b}$$

Substitution of eq. 's (IV.17) into eq. (IV.16) gives, again neglecting the factor of \vec{r}_0

$$\vec{H}(\rho) = \frac{i k e^{-i k R_0}}{4 \pi R_0} \int_S \left\{ \vec{r}_0 \times (\vec{n} \times \vec{\lambda}) (1 + \Gamma_{\parallel}) \frac{E}{\sqrt{\mu_1/\epsilon_1}} \right. \\ \left. - (\vec{n} \cdot \vec{n}_{\lambda}) \vec{\lambda} E (1 - \Gamma_{\parallel}) \right\} e^{i(\vec{k}_0 - \vec{k}_1) \cdot \vec{r}} dS$$

$$\vec{H}(P) = \frac{-i k e^{-i k R_0} E}{4 \pi R_0 \sqrt{\mu_1 / \epsilon_1}} \iint_S \left\{ \left[(\vec{k}_0 \cdot \vec{n}) \vec{\lambda} - (\vec{k}_0 \cdot \vec{\lambda}) \vec{n} \right] (1 + \Gamma_{\parallel}) + (\vec{k}_1 \cdot \vec{n}) \vec{\lambda} (1 - \Gamma_{\parallel}) \right\} e^{i \vec{k} \cdot \vec{r}} dS$$

IV. 18

Comparison of eq. (IV. 18) with eq. (IV. 7) leads to the same conclusion that was made in connection with the comparison of this equation and eq. (IV. 10); i. e., the similarity exists exactly only in the plane of incidence where no depolarization is present and the electromagnetic re-radiation process appears to be scalar. The degree of approximation in simulation out of the plane of incidence is the same in both cases.

The approximation made in obtaining the tangential electric and magnetic fields at the surface is just as severe in this case of parallel polarization as it was earlier. The calculation of the re-radiation in the plane of incidence made earlier is not done for this case; however, the conclusion made with respect to simulation of normal incidence backscattering is still valid since at normal incidence there is no difference in polarization. It remains to determine the magnetic field re-radiated from a perfect conductor for the case of parallel polarization. Using

$$\vec{n} \times \vec{E} = 0$$

$$\vec{n} \times \vec{H} = 2 (\vec{n} \times \vec{H}_i)$$

in eq. (IV. 16) gives

$$\begin{aligned} \vec{H}(P) &= \frac{i k e^{-i k R_0} 2 E}{4 \pi R_0 \sqrt{\mu_1 / \epsilon_1}} \iint_S \left\{ \vec{r}_0 \times (\vec{n} \times \vec{\lambda}) \right\} e^{i \vec{k} \cdot \vec{r}} dS \\ &= \frac{i e^{-i k R_0} 2 E}{4 \pi R_0 \sqrt{\mu_1 / \epsilon_1}} \iint_S \left\{ (\vec{k}_0 \cdot \vec{\lambda}) \vec{n} - (\vec{k}_0 \cdot \vec{n}) \vec{\lambda} \right\} e^{i \vec{k} \cdot \vec{r}} dS \end{aligned}$$

IV. 19

which differs in form with the corresponding result for normal polarization given by eq. (IV.15). A result of these differences is that there is no depolarization of the parallel polarized incident wave in the plane of incidence ($\vec{r}_0 \cdot \vec{i}_0 = 0$) while, it is recalled, there is for the case of normal polarization (however, under the approximation $\vec{n} = \vec{k}$ the depolarization disappears). These differences in form appear again and must be taken into consideration in the simulation of the re-radiation of electromagnetic waves from perfectly conducting surfaces. Comparison of eq.'s (IV.15) and IV.19) with eq. (IV.17) shows that simulation of a parallel polarized wave requires a perfectly rigid surface ($\Gamma = 1$) while an inelastic or pressure release surface ($\Gamma = -1$) is required for the normally polarized case.

The use of the Kirchhoff approximation has enabled a determination to be made of the conditions and the degree of approximation under which an acoustic simulation can be made of the re-radiation of electromagnetic waves from rough, homogeneous surfaces. Comparison of the analogous acoustic and electromagnetic expressions derived under this approximation shows in what way similarity exists and the manner in which the vector nature of the electromagnetic re-radiation creates the difference existing between these two phenomena. For the case of a perfectly conducting surface on which both local polarization components are re-radiated equally and for the case in which one of the local polarization components was ignored (smooth surface approximation) it was found that in the plane of incidence the electromagnetic re-radiation is essentially scalar (the minor exception to be noted is in connection with eq. (IV.15)), and an acoustic simulation is possible. Out of the plane of incidence for these two cases a change in polarization and a difference in form from the acoustic occur, but it is still possible to make an approximate simulation. From the general investigation of re-radiation in the plane of incidence from an arbitrary (yet isotropic) homogeneous surface, it was found that the vector re-radiation process creates dependencies on both reflection coefficients, Γ_{\perp} and Γ_{\parallel} , which shows that even in the plane of incidence, the re-radiation is in general a vector process. However, the dependence of the polarized component on the reflection coefficient of its orthogonal component is only through the slope dependent terms which are also the only terms contributing to depolarization. For backscatter

at normal incidence for the general case, there is no dependence upon slope terms under the approximation $\vec{n} = \vec{k}$ with the result that the vector nature of the re-radiation disappears and an acoustic simulation is possible.

CHAPTER V

SUMMARY AND CONCLUSIONS

A theory has been developed for the scattering of plane waves from rough surfaces of the type for which the method of physical optics is applicable. The theory was developed for surfaces which are generated by stationary, ergodic random processes and which have a Gaussian distribution of surface heights. The surfaces are allowed to be imperfectly reflecting but are restricted to be homogeneous with no variation, random or otherwise, of the material parameters. The far-zone power density re-radiated omnidirectionally from the rough surface was calculated from the far zone pressure field and the separation made between reflected and scattered power densities. The average differential scattering cross section, σ_{\circ} , was calculated from the scattered power density under the condition that the surface was sufficiently rough to neglect the reflected power. σ_{\circ} was then determined for the cases of Gaussian and exponential dependence of the autocorrelation function, and the results of these calculations were seen to have strong differences in variation which demonstrates the heavy dependence of σ_{\circ} on the functional form of the autocorrelation coefficient. The expressions for σ_{\circ} are composed of a sum of terms all but one of which, the quasi-specular term, have their origin in the first partial derivative of the surface under the approximation made. These slope-derived terms depend upon the rate of variation of the reflection coefficient with angle of incidence, whereas the quasi-specular term depends upon the reflection coefficient alone. In and near the specular direction, the quasi-specular term was seen to dominate; in other directions, the scattering depends more on the slope-derived terms and consequently on the rate of variation of the reflection coefficient with angle of incidence.

The theoretical values of σ_{\circ} have been compared with the results of experiments that were specially designed to allow a determination of the usefulness of the Kirchhoff method. To make the comparison more valid, the measured statistical parameters of the surface were used in the calculation of the theoretical results. The comparison was made using results for σ_{\circ} which were calculated for Gaussian and exponential

autocorrelation functions which bracketed the true autocorrelation coefficient. The evidence obtained by proceeding in this indirect manner is sufficiently strong to justify making the conclusion that the theory is a valid one.

In making the comparison of theory with experiment, the closeness of the agreement between the results for the exponential autocorrelation function and the experimental data at backscatter is to be noted. If the experimental observations had been restricted to backscatter, it would be tempting to conclude that the surface is described by an exponential autocorrelation function. However, the poorness of the fit given by the use of this function in the specular direction shows that this is not the case as do the measurements performed on the rough surfaces. This illustrates the necessity of making omnidirectional measurements. It is important to note that to achieve this fit at backscatter it was not necessary to use "unreasonable" values for the parameters in the exponential function, i. e., the parameters used do describe the surface with some accuracy.

To determine the similarity of acoustic and electromagnetic re-radiation from surfaces, comparison was made between analogous expressions for the two cases. The electromagnetic expressions were obtained by an application of the Kirchhoff method which is a derivation similar to that used to arrive at the acoustic results. It was found that in some cases the vector nature of the electromagnetic re-radiation does not appear and for these cases an exact acoustic simulation is possible. In some other cases where vector effects such as depolarization and dependence upon both reflection coefficients, Γ_{\perp} and Γ_{\parallel} , are present, it is still possible to make an approximate simulation.

CHAPTER VI

RECOMMENDATIONS FOR FURTHER WORK

In making this study many unsolved rough surface scattering problems common to both acoustic and electromagnetics were found. The most important of these are the following:

First and foremost is the development of an approach that will yield solutions, even approximate ones, for scattering from surfaces of arbitrary roughness. At present, there is no way to treat surfaces with irregularities neither small nor large with respect to wavelength.

An experimental study of the frequency dependence of rough surface scattering is badly needed as there has been very little verification of the theoretical predictions in hand. A study like this is best accomplished acoustically because of the ease with which experimental parameters can be varied.

There is need for an experimental and theoretical investigation of the effect of a layer of different material beneath a rough surface. This is another case in which an experimental acoustical study would be especially applicable; the experimental results of this work provide a starting point for this study.

APPENDIX I

DEFINITION OF CONSTANTS

The coefficients used in obtaining eq. (II.14) are defined as follows:

$$a_1 = (k_{1z} + k_{oz}) + \Gamma(\alpha)(k_{oz} - k_{1z})$$

$$a_2 = [B_{1x}(k_{oz} - k_{1z}) + \Gamma(\alpha)(k_{1x} - k_{ox}) - (k_{1x} + k_{ox})]$$

$$a_3 = [B_{1y}(k_{oz} - k_{1z}) + \Gamma(\alpha)(k_{1y} - k_{oy}) - (k_{1y} + k_{oy})]$$

APPENDIX II

CALCULATION OF THE MEANS OF TERMS
CONTRIBUTING TO THE AVERAGE OF THE RE-RADIATED POWER

In obtaining the ensemble average of eq. (II.14), use is first made of the ergodicity assumption and, following this, the mean of the terms in the integrand is taken. This is done by making use of the Karhunen-Loève theorem [Karhunen, 1947] and the method of characteristic functions [Davenport and Root, 1958]. This calculation was first made by Hoffman [1955b] who was one of the first to make a definitive study of the statistical difficulties of the scattering problem.

The Karhunen-Loève theorem states that a random process $z = \int(x, y)$ which is continuous in the mean over a finite region D has a representation

$$z = \text{l. i. m.} \sum_{m,n} \lambda_{mn}^{-1/2} \phi_{mn}(x,y) Z_{mn} \quad \text{A II. 1}$$

where $\langle Z_{mn} Z_{pq} \rangle = \delta_{mp} \delta_{nq}$ and $\langle Z_{mn} \rangle = 0$ if and only if the λ_{mn} are the eigenvalues and the $\phi_{mn}(x, y)$ the orthonormal eigenfunctions of the integral equation —

$$\phi(x,y) = \lambda \iint_D R(x,y; x', y') \phi(x', y') dx' dy'$$

Here $R = r\sigma^2$ is the un-normalized autocorrelation function. It is noted that R is a function of both x, y , and x', y' and stationarity is not assumed at this point.

This theorem enables the functions of the integrand of eq. (II.14) to be written in terms of the ϕ_{mn} with the properties of the random process being given by the expansion coefficients, the Z_{mn} . As an example, consider

$$Z_x e^{ik_z z}$$

This is written as

$$z_x e^{i k_z z} = \sum_{m,n} \lambda_{mn}^{-1/2} \frac{\partial \phi_{mn}(x,y)}{\partial x} z_{mn} \exp \left[i k_z \sum_{m,n} \phi_{mn}(x,y) \lambda_{mn}^{-1/2} z_{mn} \right]$$

The average of this quantity is given by

$$\langle z_x e^{i k_z z} \rangle = \sum_{m,n} \lambda_{mn}^{-1/2} \frac{\partial \phi_{mn}(x,y)}{\partial x} \langle z_{mn} \exp \left[i k_z \sum_{m,n} \phi_{mn}(x,y) \lambda_{mn}^{-1/2} z_{mn} \right] \rangle$$

A II. 2

To carry the calculation further, the method of characteristic functions is introduced. The characteristic function $M[F(x,y)]$ of the function $F(x,y)$ with respect to the random variable Z_{mn} is defined to be

$$M[F(x,y)] = \langle \exp [iF(x,y)Z_{mn}] \rangle$$

Therefore, it follows that

$$\langle e^{i k_z z} \rangle = \prod_{m,n} M [k_z \lambda_{mn}^{-1/2} \phi_{mn}(x,y)]$$

and consequently

$$\langle z_{mn} e^{i k_z z} \rangle = -i \frac{d \left\{ \prod_{m,n} M [k_z \lambda_{mn}^{-1/2} \phi_{mn}(x,y)] \right\}}{d [k_z \lambda_{mn}^{-1/2} \phi_{mn}(x,y)]}$$

Assuming the random process $z = \int (x,y)$ is Gaussian with mean zero, the characteristic function of the function $k_z \lambda_{mn}^{-1/2} \phi_{mn}(x,y)$ is

$$M [k_z \lambda_{mn}^{-1/2} \phi_{mn}(x,y)] = \exp \left[- \frac{\phi_{mn}^2(x,y) k_z^2 \lambda_{mn}^{-1}}{2} \right]$$

In obtaining this, the relation

$$\langle z_{mn} - \langle z_{mn} \rangle \rangle^2 = 1$$

which is obtained from above, is used. Therefore

$$\begin{aligned} \langle e^{i k_z z} \rangle &= \prod_{m,n} \exp \left[- \frac{\phi_{mn}^2(x,y) k_z^2 \lambda_{mn}^{-1}}{2} \right] \\ &= \exp \left[- \sum_{m,n} \frac{k_z^2 \lambda_{mn}^{-1} \phi_{mn}^2(x,y)}{2} \right] \end{aligned}$$

The factor of the exponent

$$\sum_{m,n} \lambda_{mn}^{-1} \phi_{mn}^2(x,y)$$

is seen to be

$$\begin{aligned} \langle z - \langle z \rangle \rangle^2 &= \left\langle \sum_{m,n} \sum_{p,q} \lambda_{mn}^{-1/2} \lambda_{pq}^{-1/2} \phi_{mn}(x,y) \phi_{pq}(x,y) z_{mn} z_{pq} \right\rangle \\ &= \sum_{m,n} \sum_{p,q} \lambda_{mn}^{-1/2} \lambda_{pq}^{-1/2} \phi_{mn}(x,y) \phi_{pq}(x,y) \delta_{mp} \delta_{nq} \\ &= \sum_{m,n} \lambda_{mn}^{-1} \phi_{mn}^2(x,y) \end{aligned}$$

which is the variance $\sigma^2(x,y)$ (not a constant) of the process.

Therefore

$$\langle e^{i k_z z} \rangle = e^{-k_z^2 \sigma^2(x,y)/2}$$

and finally

$$\langle z_{mn} e^{i k_z z} \rangle = i k_z \lambda_{mn}^{-1/2} \phi_{mn}(x, y) e^{-k_z^2 \sigma^2(x, y)/2}$$

Substituting this result into eq. (A II. 2) gives

$$\langle z_x e^{i k_z z} \rangle = \sum_{m, n} \phi_{mn}(x, y) \frac{\partial \phi_{mn}(x, y)}{\partial x} \lambda_{mn}^{-1} e^{-k_z^2 \sigma^2(x, y)/2}$$

A factor of this is recognized to be the first partial derivative of the variance with respect to x ; i. e.

$$\sum_{m, n} \phi_{mn}(x, y) \frac{\partial \phi_{mn}(x, y)}{\partial x} \lambda_{mn}^{-1} = \frac{\partial [\sigma^2(x, y)]}{\partial x}$$

So finally

$$\langle z_x e^{i k_z z} \rangle = \frac{\partial [\sigma^2(x, y)]}{\partial x} e^{-k_z^2 \sigma^2(x, y)/2}$$

Which, for a stationary process, is zero because $\sigma^2(x, y)$ is a constant.

The evaluation of the means of the terms in the integrand of eq. (II. 14) is accomplished by following procedures similar to that used above; the calculations are lengthier, however, due to the additional complexity of the functions to be averaged. For a stationary, Gaussian process with variance σ^2 and normalized autocorrelation coefficient r , the results are, using α and β to represent x or y or both

$$\langle e^{i k_z (z - z')} \rangle = \exp [k_z^2 \sigma^2 (1 - r)]$$

$$\langle z_\beta e^{i k_z (z - z')} \rangle = -i k_z \sigma^2 \frac{\partial r}{\partial \beta} \exp [k_z^2 \sigma^2 (1 - r)]$$

$$\langle z_{\beta'} e^{i k_2 (z - z')} \rangle = i k_2 \sigma^2 \frac{\partial \Gamma}{\partial \beta'} \exp[-k_2^2 \sigma^2 (1 - r)]$$

$$\langle z_{\alpha} z_{\beta'} e^{i k_2 (z - z')} \rangle = \left[\sigma^2 \frac{\partial^2 \Gamma}{\partial \alpha \partial \beta'} + k_2^2 \sigma^4 \frac{\partial \Gamma}{\partial \alpha} \frac{\partial \Gamma}{\partial \beta'} \right] \exp[-k_2^2 \sigma^2 (1 - r)]$$

APPENDIX III

CALCULATION OF THE ORDER OF MAGNITUDE OF
THE PARTIALLY INTEGRATED TERMS OCCURRING IN THE
EXPRESSION FOR RE-RADIATED POWER

The partially integrated terms appearing in eq. (II. 21) are of two types; these are

$$\int_{-l}^l \int_{-l}^l \int_{x-l}^{x+l} \exp\left\{-\left[k_2^2 \sigma^2 (1-r) + i(k_x u + k_y v)\right]\right\} \Big|_{y-l}^{y+l} du dx dy \quad \text{A III. 1}$$

and

$$\int_{-l}^l \int_{-l}^l \int_{x-l}^{x+l} \frac{\partial r}{\partial v} \exp\left\{-\left[k_2^2 \sigma^2 (1-r) + i(k_x u + k_y v)\right]\right\} \Big|_{y-l}^{y+l} du dx dy \quad \text{A III. 2}$$

and there are similar terms in which the first integration is performed with respect to u .

The variations of the autocorrelation coefficient and its partial derivative in the integrands of the above integrals are given by

$$r(u, y+l); r(u, y-l); \frac{\partial r(u, v)}{\partial v} \Big|_{v=y+l}; \frac{\partial r(u, v)}{\partial v} \Big|_{v=y-l}$$

By the assumptions made earlier that the autocorrelation coefficient and its partial derivatives decay rapidly relative to the dimensions of the aperture, it is clear that these quantities are sensibly zero when the variation with respect to y is neglected. Making use of this in eq. (A III. 1) yields the result

$$\int_{-l}^l \int_{-l}^l \int_{x-l}^{x+l} \exp\left\{-\left[k_z^2 \sigma^2 + i(K_x u + K_y v)\right]\right\} \Big|_{y-l}^{y+l} du dx dy$$

$$= \frac{16 \sin^2 K_y l \sin^2 K_x l e^{-k_z^2 \sigma^2}}{i K_x^2 K_y}$$

A III. 3

and the integral A III. 2 is zero.

The result A III. 3 is, neglecting the constants involving the material parameters, within a factor of $1/K_y$ of equalling the specular power density given by eq. (II. 17). It is because of this factor of $1/K_y$ that A III. 3 goes to zero in directions for which $K_y = 0$ (one of which is the specular direction) and the specular power density does not. Therefore, the variation of A III. 3 is not the same as the specular power density due to the factor $1/K_y$ and also due to the constants involving the material parameters, but both vanish in the same way as the surface roughness increases. It is important to note that the result A III. 3 is similar to the "edge effect" terms found by Beckman 1963 .

Similar results are obtained for the terms in which the partial integrations are first performed with respect to u .

APPENDIX IV

CALCULATION OF THE APERTURE EFFECT

The aperture effect is evaluated by calculating the integral of eq. (III. 4)

$$\iint_S \frac{g_T(\Psi_T) g_r(\Psi_r)}{r_T^2 r_r^2} dA \quad \text{A IV. 1}$$

for the measured laboratory parameters as a function of the set of angles (ϕ_0, ϕ_1, ϕ_2) .

The normalized gain functions, $g_T(\Psi_T)$ and $g_r(\Psi_r)$, are given by the square of the normalized antenna voltage patterns shown in figure III.10. Because of the close fit to the experimental curves obtained with the theoretical pattern, the gain functions are, to a very good approximation

$$g_T(\Psi_T) = \left[\frac{2 J_1(k a \sin \Psi_T)}{k a \sin \Psi_T} \right]^2 \quad \text{A IV. 2a}$$

$$g_r(\Psi_r) = \left[\frac{2 J_1(k a \sin \Psi_r)}{k a \sin \Psi_r} \right]^2 \quad \text{A IV. 2b}$$

where $ka = 34$. Substitution of eq. 's (A IV. 2) into (A IV. 1) and use of the coordinate system of figure III.1 to define the integration gives the result

$$\int_{-\infty}^{\infty} \int_{-\infty}^{\infty} \left[\frac{2 J_1(k a \sin \Psi_T)}{k a \sin \Psi_T} \right]^2 \left[\frac{2 J_1(k a \sin \Psi_r)}{k a \sin \Psi_r} \right]^2 \frac{dx dy}{r_T^2 r_r^2}$$

The illuminated area S is usually defined, for reasons of convenience, on the half power points of the antenna beam and this gives a finite illuminated area. It is not necessary to do this here and the limits of integration are infinite. The quantities $\sin\Psi_T$, $\sin\Psi_r$, r_T and r_r are functions of (x,y) , the coordinates of the point on the mean plane.

These functions are

$$r_T^2 = (x_{T0} - x)^2 + (y_{T0} - y)^2 + z_{T0}^2$$

$$r_r^2 = (x_{r0} - x)^2 + (y_{r0} - y)^2 + z_{r0}^2$$

$$\sin^2\Psi_T = 1 - \cos^2\Psi_T$$

$$\sin^2\Psi_r = 1 - \cos^2\Psi_r$$

where

$$\cos^2\Psi_T = \frac{r_{T0}^2 + r_T^2 - r^2}{2r_{T0}r_T}$$

$$\cos^2\Psi_r = \frac{r_{r0}^2 + r_r^2 - r^2}{2r_{r0}r_r}$$

$$\text{and } r^2 = x^2 + y^2$$

The rectangular coordinates giving the locations of the transmitting and receiving antennas are converted from the spherical co-ordinates $(r_{T0}, r_{r0}, \phi_0, \phi_1, \phi_2)$ by the transformation

$X_{T0} = 0$ (principal ray of the transmitting antenna chosen to lie in the y - z plane)

$$y_{T0} = r_{T0} \cos\phi_1$$

$$z_{T0} = r_{T0} \sin\phi_1$$

$$x_{r_0} = r_{r_0} \sin\phi_2 \sin\phi_0$$

$$y_{r_0} = r_{r_0} \sin\phi_2 \cos\phi_0$$

$$z_{r_0} = r_{r_0} \cos\phi_2$$

The integral proved to be too complex to be done analytically and it was necessary to resort to a numerical technique of integration which was done by machine calculation. The technique is based on the method of Gaussian quadratures and is described in the book by Krylov [1962]. The results of the machine integration are too lengthy to be included here; however, a similar calculation has been performed by the workers at the Ohio State University and is available in report form [Barrick, 1964]. The results are not the same due to a difference in antenna patterns; however, the variation as a function of (ϕ_0, ϕ_1, ϕ_2) is similar and representative.

APPENDIX V

DERIVATION OF A VECTOR FORM
OF THE HELMHOLTZ INTEGRAL

Stratton [1941] has shown that the electric field $\vec{E}(P)$ at an observation point P (see figure IV.1) due to an electric field \vec{E} and a magnetic field \vec{H} distributed over an area S enclosed by a contour C is

$$\begin{aligned} \vec{E}(P) = & \frac{1}{i\omega \epsilon_1 4\pi} \oint_C \nabla \phi \vec{n} \cdot d\vec{l} \\ & - \frac{1}{4\pi} \iint_S \left[-i\omega \mu_1 (\vec{n} \times \vec{H}) \phi + (\vec{n} \times \vec{E}) \times \nabla \phi \right. \\ & \left. + (\vec{n} \cdot \vec{E}) \nabla \phi \right] dS \end{aligned}$$

A V. 1

where the time variation has been changed from $e^{-i\omega t}$ to $e^{i\omega t}$ The Green's function ϕ for this time variation is

$$\phi = \frac{e^{-ikR}}{R}$$

A V. 2

as before and

$$\nabla \phi = \frac{ike^{-ikR}}{R} \vec{R}_1$$

A V. 3

approximately for the far field case, $k \gg \frac{1}{R}$. In eq. (A V. 3) \vec{R}_1 is the unit vector in the \vec{R} direction. Stratton has further shown that a surface current

$$\vec{K} = -\vec{n} \times \vec{H}$$

A V. 4

and a surface charge

$$\eta = -\epsilon_1 \vec{n} \cdot \vec{E} \quad \text{A V. 5}$$

can be introduced and used; these two quantities are related through the continuity equation

$$-i\omega\eta = \nabla \cdot \vec{K} \quad \text{A V. 6}$$

Combining eq. 's (A V. 6) and (A V. 5) and then using eq. A V. 4 gives

$$\vec{n} \cdot \vec{E} = - \frac{\nabla \cdot (\vec{n} \times \vec{H})}{i\omega\epsilon_1}$$

Using this and eq. (A V. 3), the last integral on the right hand side of eq. (A V. 1) becomes

$$-\frac{1}{4\pi} \iint_S \vec{n} \cdot \vec{E} \nabla \phi \, dS = \frac{k \vec{R}_1}{4\pi\omega\epsilon_1} \iint_S \frac{e^{ikR}}{R} \nabla \cdot (\vec{n} \times \vec{H}) \, dS$$

A V. 7

Using the identity

$$\left[\nabla \cdot (\vec{n} \times \vec{H}) \right] \frac{e^{ikR}}{R} = \nabla \cdot \left[(\vec{n} \times \vec{H}) \frac{e^{-ikR}}{R} \right] - ik \frac{e^{-ikR}}{R}$$

in eq. (A V. 7) yields

$$-\frac{1}{4\pi} \iint_S \vec{n} \cdot \vec{E} \nabla \phi \, dS = \frac{k \vec{R}_1}{4\pi\omega\epsilon_1} \iint_S \nabla \cdot \left[\frac{(\vec{n} \times \vec{H}) e^{-ikR}}{R} \right] \, dS$$

$$-\frac{k \vec{R}_1}{4\pi\omega\epsilon_1} \iint_S \frac{ik}{R} e^{-ikR} \vec{n} \times \vec{H} \cdot \vec{R}_1 \, dS$$

Reducing the first integral on the right hand side using Gauss' Law in two dimensions, this becomes

$$-\frac{1}{4\pi} \iint_S \vec{n} \cdot \vec{E} \nabla \phi \, dS = \frac{k \vec{R}_1}{4\pi\omega\epsilon_1} \oint \frac{e^{-ikR}}{R} \vec{n} \times \vec{H} \cdot \vec{n}' \, dl$$

$$-\frac{k \vec{R}_1}{4\pi\omega\epsilon_1} \iint_S \frac{ik}{R} e^{-ikR} \vec{n} \times \vec{H} \cdot \vec{R}_1 \, dS$$

where \vec{n}' is the normal unit vector pointing outward from C .

Since

$$\vec{n} \times \vec{H} \cdot \vec{n}' = \vec{n}' \times \vec{n} \cdot \vec{H}$$

and since

$$\vec{n}' \times \vec{n} = -\vec{d}l$$

the result is finally

$$-\frac{1}{4\pi} \iint_S \vec{n} \cdot \vec{E} \nabla \phi \, dS = \frac{-k \vec{R}_1}{4\pi\omega\epsilon_1} \oint \frac{e^{-ikR}}{R} \vec{H} \cdot \vec{d}l$$

$$\frac{-k \vec{R}_1}{4\pi\omega\epsilon_1} \iint_S \frac{ike^{-ikR}}{R} \vec{n} \times \vec{H} \cdot \vec{R}_1 \, dS$$

A V. 8

Substituting eq. 's (A V. 8), (A V. 2) and (A V. 3) into eq. (A V. 1) gives

$$\begin{aligned} \vec{E}(\rho) = & \frac{1}{4\pi} \iint_S \left\{ i\omega\mu_1 (\vec{n} \times \vec{H}) \frac{e^{-ikR}}{R} \right. \\ & + (\vec{E} \times \vec{n}) \times \vec{R}_1 \frac{(ik e^{-ikR})}{R} \\ & \left. - \frac{k\vec{R}_1}{\omega\epsilon_1} \left(\frac{ik e^{-ikR}}{R} \right) \vec{n} \times \vec{H} \cdot \vec{R}_1 \right\} dS \end{aligned}$$

A V. 9

Making S an aperture of the size discussed in Section II. B and manipulating, eq. (A V. 9) becomes

$$\begin{aligned} \vec{E}(\rho) = & \frac{i\omega\mu e^{-ikR_0}}{4\pi R_0} \iint_S \left\{ \vec{n} \times \vec{H} - \vec{n}_0 (\vec{n} \times \vec{H} \cdot \vec{n}_0) \right. \\ & \left. + \frac{(\vec{E} \times \vec{n}) \times \vec{n}_0}{\sqrt{\mu_1/\epsilon_1}} \right\} e^{i\vec{k}_0 \cdot \vec{r}} dS \end{aligned}$$

A V. 10

BIBLIOGRAPHY

- Aksenov, V. I., "On the Scattering of Electromagnetic Waves from Sinusoidal and Trochoidal Surfaces of Finite Conductivity," Radio Engineering and Electronic Physics, vol. 3, p. 459, 1958.
- Aksenov, V. I., "Experimental Investigation of the Scattering of Electromagnetic Waves by Periodically Rough Surfaces," Radio Engineering and Electronic Physics, vol. 5, pp. 782-795, 1960.
- Aksenov, V. I., "Application of the Kirchhoff Approximation to the Problem of the Scattering from Periodically Rough Surfaces of Finite Conductivity," Radio Engineering and Electronic Physics, vol. 6, pp. 307-314, 1961.
- Alpert, Y. L., V. L. Ginzburg, and E. L. Feinberg, The Propagation of Radio Waves, Gostekhizdat, Moscow, 1953.
- Ament, W. S., "Toward a Theory of Reflection by a Rough Surface," Proc. IRE, vol. 41, pp. 142-146, 1953.
- Ament, W. S., "Application of a Weiner-Hopf Technique to Certain Diffraction Problems," Naval Research Laboratory Report No. 4334, May 1964.
- Ament, W. S., "Forward and Backscattering by Certain Rough Surfaces," Trans. IRE AP-4, pp. 369-373, 1956.
- Ament, W. S., "Reciprocity and Scattering by Certain Rough Surfaces," Trans. IRE AP-8, pp. 167-174, 1960.
- Anatolsky, M. L., "The Reflection of Waves from a Rough Perfectly Reflecting Surface," Dokl. Akad. Nauk SSSR, vol. 62, p. 302, 1948.
- Andronov, A. and M. Leontowica, "Zur Theorie der Molekularen Lichtzerstreuung an Flüssigkeitsoberflächen," Z. Physik, vol. 38, p. 485, 1926.
- Archer-Thomson, H., N. Grooke, T. Gold, and F. Hoyle, "Preliminary Report on the Reflection of Nine Centimeter Radiation at the Surface of the Sea," ASE Report No. M-542, 1943.

- Artman, K. , "On the Theory of Anomalous Reflection of Periodic Structures, " Z. Physic, vol. 119, p. 529, 1942.
- Ayiku, M. N. B. and R. K. Moore, "Acoustic Simulation of Knife Edge Diffraction, " Spring Meeting International Scientific Radio Union, 1965.
- Bachynski, M. P. , "Microwave Propagation Over Rough Surfaces, " RCA Rev. , vol. 20, pp. 308-335, 1959.
- Barantsev, R. G. "Plane Wave Scattering by a Double Periodic Surface of Arbitrary Shape, " Soviet Physics-Acoustics, vol. 7, p. 123, Oct. 1961.
- Barrick, D. E. , "Normalization of Bistatic Radar Return, " The Ohio State University Antenna Laboratory Report No. 1388-13, 1964.
- Bass, F. G. , "Boundary Conditions for the Mean Electromagnetic Field on a Surface with Random Irregularities and Fluctuations of Impedance, " Izv. Vyssh. Zav. Radiofiz. , vol. 3, pp. 72-78, 1960.
- Bass, F. G. , "On the Theory of Combinational Scattering of Waves by a Rough Surface, " Izv. Vyssh. Zav. Radiofiz. , vol. 4, pp. 58-66, 1961.
- Bass, F. G. , and V. G. Bocharov, "On the Theory of Scattering of Electromagnetic Waves from a Statistically Uneven Surface, " Radiotekhn. i Elektr. , vol. 3, p. 251, 1958.
- Bass, F. G. and I. M. Fuks, "Allowance for Shadows in the Scattering of Waves by a Statistically Uneven Surface, " Institute of Radiophysics and Electronics, Academy of Sciences, UkrSSR, pp. 147-164, 1964.
- Bay, Z. , "Reflection of Microwaves from the Moon, " Acta Phys. Hungar. , vol. 1, pp. 1-22, 1946.
- Beckmann, P. , "Shadowing Functions for Random Rough Surfaces, " Univ. of Colorado Elec. Engr. Report No. 3, Sept. 1964.
- Beckmann, P. , "Scattering by Composite Rough Surface, " Univ. of Colorado, Elec. Engr. Report No. 4, Nov. 1964.

- Beckmann, P. , "The Depolarization of Electromagnetic Waves Scattered from Rough Surfaces, " Acta. Techn. CSAV, vol. 6, 1961.
- Beckmann, P. , and A. Spizzichino, The Scattering of Electromagnetic Waves from Rough Surfaces, The MacMillan Co. , New York, 1963.
- Bendat, J.S. , Principles and Applications of Random Noise Theory, John Wiley and Sons, Inc. , New York, 1958.
- Bennet, H. E. , "Specular Reflectance of Aluminized Ground Glass and the Height Distribution of Surface Irregularities, " J. Opt. Soc. Am. , vol. 53, no. 12, Dec. 1963.
- Biot, M. A. , "Reflection on a Rough Surface from an Acoustic Point Source, " J. Acoust. Soc. Am. , vol. 29, pp. 1193-1200, 1957a.
- Biot, M. A. , "Some New Aspects of the Reflection of Electromagnetic Waves on a Rough Surface, " J. Appl. Phys. , vol. 28, pp. 1455-1483, 1957b.
- Biot, M. A. , "On the Reflection of Electromagnetic Waves on a Rough Surface, " J. Appl. Phys. , vol. 29, p. 998, 1958.
- Blackman, R. B. and J. W. Tukey, The Measurement of Power Spectra, Dover Publications, Inc. , New York, 1958.
- Blake, L. V. , "Reflection of Radio Waves from a Rough Sea, " Proc. IRE, vol. 38, pp. 201-304, 1950.
- Blevis, B. C. and J. H. Chapman, "Characteristics of 488 Mc/s Radio Signal Reflected from the Moon, " J. Res. NBS, vol. 64, pp. 331-334, 1960.
- Bocharov, V. G. and F. G. Bass, "On the Scattering of Electromagnetic Waves by a Statistically Rough Surface, " Radiotekhn. i Elektr. , vol. 3, pp. 577-578, 1958.
- Bouix, M. , "Study of the Electromagnetic Field in the Vicinity of a Reflecting Surface, " Compt. Rend. Acad. Sci. , vol. 240, pp. 1763-1765, 1955.

- Branely, E. N., "The Diffraction of Waves by an Irregular Refracting Medium," Proc. Roy. Soc., vol. A225, p. 515, 1954.
- Braude, S. Ya., "The Fresnel Coefficients for a Rough Surface," Izv. Vyssh. Zav. Radiofiz., vol. 2, pp. 691-696, 1959.
- Braude, S. Ya, N. N. Komarov, and I. E. Ostrovsky, "On the Statistical Character of the Scattering of Centimetre Radio Waves by the Rough Surfaces of the Sea," Radiotekhn. i Elektr., vol. 3, pp. 172-179, 1958.
- Brekhovskikh, L. M., "Diffraction of Sound Waves by a Rough Surface," Dokl. Akad. Nauk. SSSR, vol. 79, p. 585, 1951a.
- Brekhovskikh, L. M., "Diffraction of Electromagnetic Waves by a 'Rough Surface'," Dokl. Akad. Nauk SSSR, vol. 81, p. 1023, 1951b.
- Brekhovskikh, L. M., "The Diffraction of Waves by a Rough Surface," Part I and Part II, Zh. Eksper. i Teor. Fiz., vol. 23, pp. 275-304, 1952.
- Briggs, B. H., "Roughness of the Moon as a Radar Reflector," Nature, vol. 187, p. 490, 1960.
- Brown, W. E., "A Lunar and Planetary Echo Theory," J. Geophys. Res., vol. 65, p. 3087, 1960.
- Browne, I. C. and J. V. Evans, "The Moon as a Scatterer of Radio Waves," Radio Astronomy, University Press, Cambridge, pp. 408-409, 1957.
- Browne, I. C., J. V. Evans, J. K. Hargreaves, and W. A. S. Murray, "Radio Echoes from the Moon," Proc. Phys. Soc. London, vol. 69, pp. 901-920, 1956.
- Bullington, K., "Reflection Coefficients of Irregular Terrain," Proc. IRE, vol. 42, pp. 1258-1262, 1954.
- Bullington, K., "Radio Propagation at Frequencies above 30 Mc/s," Proc. IRE, vol. 35, p. 1122, 1947.

- Bullington, K. , "Radio Propagation Variations at UHF and VHF, " Proc. IRE, vol. 38, p. 27, 1950.
- Burke, J. E. and V. Twersky, "On Scattering of Waves by the Grating of Elliptical Cylinders, " Sylvania Electronic Defense Laboratories Report EDL-E44, 1960.
- Burrows, C. R. and S. S. Atwood, Radio Wave Propagation, Academic Press, New York, 1949.
- Bussey, H. E. , "Suppressing Microwaves by Zonal Screens, " Tele-Tech. vol. 10. p. 45, 1951.
- Campbell, J. P. , "Backscattering Characteristics of Land and Sea at X-Band, " Proc. of National Conf. on Aero Elect., May 1958.
- Campbell, J. P. , "Backscattering Characteristics of Land and Sea at X-Band, " Trans. of the 1959 Symposium on Radar Return, Univ. of New Mexico, NOTS TP 23338, May 1959.
- Carlson, J. F. and A. E. Heins, "The Reflection of an Electromagnetic Plane Wave by an Infinite Set of Plates, " Quart. Appl. Math. , vol. 4, pp. 313-329, 1946 and vol. 5, pp. 82-88, 1947.
- Chu, C. M. and S. W. Churchill, "Multiple Scattering by Randomly Distributed Obstacles--Method of Solution, " Trans. IRE, vol. AP-4, p. 142, 1956.
- Clarke, R. H. , "Theoretical Characteristics of Radiation Reflected Obliquely from a Rough Conducting Surface, " Proc. IEE, vol. 110, p. 91, 1963a.
- Clarke, R. H. , "Measurements on Radiation Reflected Obliquely from a Rough Surface, " Proc. IEE, vol. 110, p. 1921, 1963b.
- Clapp, R. E. , "A Theoretical and Experimental Study of Ground Return, " MIT Rad. Lab. Report No. 6024, April, 1946.
- Cockroft, A. L. , H. Davies, and R. A. Smith, "A Quantitative Study of Sea Returns at Centimeter Wavelengths for Moderately Small Angles of Elevation, " Proc. Phys. Soc. , vol. 58, p. 717, 1946.

- Constant, F. W., Theoretical Physics, Addison-Wesley Publishing Co., Cambridge, Mass., 1954.
- Cosgriff, R. F., W. H. Peake, and R. C. Taylor, "Terrain Scattering Properties for Sensor System Design, Terrain Handbook II," Engr. Exp. Sta., Ohio State Univ., May, 1960.
- Cowan, E. W., "X-Band Sea Return Measurements," MIT Research Laboratory Report No. 870, 1946.
- Cox, C. and W. Munk, "Measurement of the Roughness of the Sea Surface from Photographs of the Sun's Glitter," J. Opt. Soc. Am., vol. 44, pp. 838-850, 1959.
- Cox, C. and W. Munk, "Statistics of the Sea Surface Derived from Sun Glitter," J. Marine Res., vol. 13, pp. 198-227, 1954b.
- Crawford, A. B., D. C. Hoggs, and W. H. Kummer, "Studies in Tropospheric Propagation Beyond the Horizon," Bell Syst. Tech. Jour., vol. 38, pp. 1067-1178, 1959.
- Crawford, A. B. and W. C. Jakes, "Selective Fadings of Microwaves," Bell Syst. Tech. Jour., vol. 31, p. 68, 1952.
- Daniels, F. B., "A Theory of Radar Reflection from the Moon and Planets," J. Geophys. Res., vol. 66, p. 1787, 1961.
- Daniels, F. B., "Radar Reflections from a Rough Moon Described by a Composite Correlation Function," J. Geophys. Res., vol. 68, p. 6251, 1963.
- Daniels, F. B., "Radar Determination of the Root Mean Square Slope of the Lunar Surface," J. Geophys. Res., vol. 68, p. 449, 1963.
- Daniels, F. B., "Radar Determination of the Lunar Slopes: Correction for the Diffuse Component," J. Geophys. Res., vol. 68, p. 2864, 1963.
- Davenport, W. B. and W. L. Root, An Introduction to the Theory of Random Signals and Noise, McGraw-Hill Book Co., Inc., 1958.
- Davies, H., "The Reflection of Electromagnetic Waves from a Rough Surface," Proc. IEE, Part III, vol. 101, pp. 209-214, 1954.

- Davies, H. , "The Reflection of Electromagnetic Waves from a Rough Surface, " Proc. IEE, Part III, vol. 102, p. 148, 1955.
- Davies, H. and G. G. MacFarlane, "Radar Echoes from the Sea Surface of One Centimeter Wavelength, " Proc. Phys. Soc. , vol. 58, p. 717, 1946.
- De, A. C. "Reflection of Microwaves from Earth's Surface, " Indian J. of Meteorol. Geophys. vol. II, pp. 45-49, 1960.
- Deryugin, L. N. , "The Reflection of a Laterally Polarized Plane Wave from a Surface of Rectangular Corrugations, " Radiotekhn. , vol. 15, no. 2, pp. 15-26, 1960a.
- Deryugin, L. N. , "The Reflection of a Longitudinally Polarized Plane Wave from a Surface of Rectangular Corrugations, " Radiotekhn. , vol. 15, no. 5, pp. 9-16, 1960b.
- DeWitt, J. H. and E. K. Stodola, "Detection of Radio Signals Reflected by the Moon, " Proc. IRE, vol. 37, pp. 229-242, 1949.
- Dye, J. E. , "Ground and Sea Return Signal Characteristics of Microwave Pulse Altimeters, " Trans. of Symposium on Radar Return, Univ. of New Mexico, NOTS TP 23338, 1959.
- Eckart, C. , "The Scattering of Sound from the Sea Surface, " J. Acoust. Soc. Am. , vol. 25, pp. 566-570, 1953.
- Edison, A. R. , "An Acoustic Simulator for Modeling Backscatter of Electromagnetic Waves, " Univ. of New Mexico Engr. Exp. Sta. Tech. Report. No. EE-62, 1961.
- Edison, A. R. , D. Bliss, and G. Policky, "Acoustic Wave Propagation in a Random Medium, " Fall Meeting International Scientific Radio Union, 1963.
- Edison, A. R. , R. K. Moore, and B. D. Warner, "Radar Terrain Return Measured at Near-Vertical Incidence, " Trans. IRE, vol. AP-8, pp. 246-254, 1960.

- Ergin, K. , "Energy Ratio of the Seismic Waves Reflected and Refracted at a Rock-Water Boundary, " Bull. Seism. Soc. Amer., vol. 42, pp. 349-372, 1952.
- Evans, J. V. , "The Scattering of Radio Waves by the Moon, " Proc. Phys. Soc. London, vol. 70, pp. 1105-1112, 1957.
- Evans, J. V. , "Radar Methods of Studying Distant Planetary Surfaces, " Proc. of the Conf. on Physics of the Solar System and Re-Entry Dynamics, pp. 237-259, 1962, in Va. Poly. Inst. , Blacksburg.
- Evans, J. V. , S. Evans, and J. H. Thompson, "The Rapid Fading of the Moon Echoes at 100 Mc/s, " Paris Symp. on Radio Astronomy, Stanford Univ. Press, 1959.
- Evans, J. V. and G. H. Pettengill, "The Scattering Behavior of the Moon at Wavelengths of 3.6, 68, and 784 Centimeters, " J. Geophys. Res., vol. 68, p. 423, 1963.
- Ewing, W. M. , W. S. Jardetsky and F. Press, Elastic Waves in Layered Media, McGraw-Hill Book Company, Inc. , New York, 1957. .
- Feinberg, Ye. L. , "The Propagation of Radio Waves along the Surface of the Earth, " Izd. Akad. Nauk SSSR, Moscow, 1961.
- Feinstein, J. , "Some Stochastic Problems in Wave Propagation, Part I, " Trans. IRE, vol. AP-2, pp. 23-30, 1954.
- Felsen, L. B. , "The Scattering of Electromagnetic Waves by a Corrugated Sheet, " Can. J. Phys., vol. 37, p. 1565, 1959.
- Fishback, W. T. and P. J. Rubenstein, "Further Measurements of 3 and 10 Centimeter Reflection Coefficients of Sea Water at Small Grazing Angles, " MIT Research Laboratory Report No. 568, May, 1964.
- Frandin, A. Z. , "Antenny Suerkhuysoikh Chastot, " Izd. Sovetskoe Radio, 1957.
- Fricker, F. J. , R. P. Ingalls, W. C. Mason, and M. L. Stone, "UHF Moon Reflections, " Spring Meeting International Scientific Radio Union, 1958.

- Fung, A. K., "Theory of Radar Scatter from Rough Surfaces, Bistatic and Monostatic, with Application to Lunar Radar Return," J. Geophys. Res., vol. 69, no. 6, pp. 1063-1073, Mar. 1964.
- Fung, A. K., and R. K. Moore, "Effects of Structure Size on Moon and Earth Radar Returns at Various Angles," J. Geophys. Res., vol. 69, no. 6, pp. 1075-1087, Mar. 1964.
- Fung, A. K., R. K. Moore, and B. E. Parkins, "Notes on Backscattering and Depolarization by Gently Undulating Surfaces," J. Geophys. Res., pp. 1559-1562, Mar. 1965.
- Goldstein, H., "The Frequency Dependence of Radar Echoes from the Surface of the Sea," Phys. Rev., vol. 69, p. 695, 1946a.
- Goldstein, H., "Frequency Dependence of the Properties of Sea Echo," Phys. Rev., vol. 70, pp. 838-846, 1946b.
- Gourt, C. W., "Determination of Reflection Coefficient of the Sea," Proc. IEE, Part B, vol. 102, pp. 827-830, 1955.
- Grant, C. R. and B. S. Yapplee, "Backscattering from Water and Land at Centimeter and Millimeter Wavelengths," Proc. IRE, vol. 45, pp. 976-982, 1957.
- Grasyuk, D. S., "Scattering of Sound Waves by the Uneven Surface of an Elastic Body," Soviet Physics-Acoustics, vol. 6, pp. 26-29, 1960.
- Gulin, E. P., "Amplitude and Phase Fluctuations of a Sound Wave Reflected from a Statistically Uneven Surface," Soviet Physics-Acoustics, vol. 8, pp. 335-339, 1963.
- Gulin, E. P., "Amplitude and Phase Fluctuations of a Sound Wave Reflected from a Sinusoidal Surface," Soviet Physics-Acoustics, vol. 8, pp. 223-227, 1963.
- Gulin, E. P., "The Correlation of Amplitude and Phase Fluctuations in Sound Waves Reflected from a Statistically Rough Surface," Soviet Physics-Acoustics, vol. 8, pp. 335-339, 1963.

- Gulin, E. P., and K. I. Malyshev, "Statistical Characteristics of Sound Signals Reflected from the Undulating Sea Surface," Soviet Physics-Acoustics, vol. 8, pp. 228-234, 1963.
- Hagfors, T., "Some Properties of Radio Waves Reflected from the Moon and Their Relation to the Lunar Surface," J. Geophys. Res., vol. 66, no. 3, p. 777, Mar. 1961.
- Hagfors, T., "Backscatter from an Undulating Surface with Applications to Radar Returns from the Moon," J. Geophys. Res., vol. 69, pp. 3779-3784, 1964.
- Hargreaves, J. K., "Radio Observations of the Lunar Surface," Proc. Phys. Soc., vol. 73, pp. 536-537, 1959.
- Hayre, H. S., "Radar Scattering Cross-Section Applied to Moon Return," Proc. IRE, vol. 49, p. 1433, 1961.
- Hayre, H. S., "Lunar Backscatter Theories," Ph.D. Thesis, University of New Mexico, 1962.
- Hayre, H. S., and R. K. Moore, "Theoretical Scattering Coefficient for Near Vertical Incidence from Contour Maps," J. Res. NBS D. Radio Propagation, vol. 65-D, pp. 427-432, 1961.
- Heaps, H. S., "Reflection of Plane Waves of Sound from a Sinusoidal Surface," J. Appl. Phys., vol. 28, pp. 815-818, 1957.
- Heaps, H. S., "Nonspecular Reflection of Sound from a Sinusoidal Surface," J. Acoust. Soc. Am., vol. 27, pp. 698-705, 1955.
- Hewish, A., "The Diffraction of Radio Waves in Passing Through a Phase-Changing Ionosphere," Proc. Roy. Soc., vol. A 209, p. 81, 1951.
- Hey, J. S. and V. A. Hughes, Paris Symp. on Radio Astronomy, Stanford Univ. Press, 1959.
- Hey, J. S., J. J. Parsons, and F. Jackson, "Reflection of Centimeter Electromagnetic Waves over Ground and Diffraction Effects with Wire Netting Screens," Proc. Phys. Soc., vol. 59, p. 847, 1947.

- Hiatt, R. E., T. B. A. Senior, and W. H. Weston, "A Study of Surface Roughness and its Effect on the Backscattering Cross Section of Spheres," Proc. IRE, vol. 48, pp. 2008-2016, 1960.
- Hoffman, W. C., "Backscatter from Perfectly Conducting Doubly-trochoidal and Doubly-sinusoidal Surfaces," Trans. IRE, vol. AP-3, p. 96, 1955a.
- Hoffman, W. C., "Scattering of Electromagnetic Waves from a Rough Surface," Quart. Appl. Math., vol. 13, p. 291, 1955b.
- Hughes, V. A., "Roughness of the Moon as a Radar Reflector," Nature, vol. 186, no. 4728, pp. 873-874, 1960.
- Hughes, V. A., "Radio Wave Scattering from the Lunar Surface," Proc. Phys. Soc., vol. 78, pp. 988-997, 1961.
- Hughes, V. A., "Discussion of Paper by Daniels 'A Theory of Radar Reflections from the Moon and Planets,'" J. Geophys. Res., vol. 67; pp. 892-894, 1962.
- Ingalls, R. P., L. E. Bird, and J. W. B. Day, "Band Pass Measure of a Lunar Reflection," Proc. IRE, vol. 49, pp. 631-632, 1961.
- Isakovich, M. A., "The Scattering of Waves from a Statistically Rough Surface," Zhurn. Eksp. Teor. Fiz., vol. 23, pp. 305-314, 1952.
- Jacobson, A. D., "Luneberg-Kline Analysis of Scattering from a Sinusoidal Dielectric Interface," IRE Trans. Ant. and Prop., vol. AP-10, pp. 715-721, 1962.
- Jones, J. L., C. B. Leslie, and L. E. Barton, "Acoustic Characteristics of Underwater Bottoms," J. Acoust. Soc. Am., vol. 36, pp. 154-163, 1964.
- Jordan, E. C., "Acoustic Models of Radio Antennas," The Ohio State University Engr. Exp. Sta. Bull. #108, 1941.
- Kalinin, A. I., "Approximate Methods for Calculating the Field Strength of Very Short Waves with Respect to the Effect of the Terrain Relief," Radiotekhn., vol. 12, no. 4, pp. 13-23, 1957.

- Karhunen, K., "Über lineare Methoden in der Wahrscheinlichkeitsrechnung," Ann. Acad. Scient. Fennicae (A), vol. 37, pp. 1-79, 1947.
- Katsenelenbaum, B. A., "On the Problem of Normal Incidence of a Plane Electromagnetic Wave onto a Periodic Boundary Between Two Dielectrics," Radiotekhn. i. Elektr., vol. 5, pp. 1929-1932, 1960.
- Katz, I. and L. M. Spetner, "Polarization and Depression Angle Dependence of Radar Terrain Return," J. Res. NBS, vol. 64-D, pp. 483-486, 1960.
- Katzin, M., "Backscattering from the Sea Surface," IRE Convention Record, Part I, pp. 72-77, 1955.
- Katzin, M., "Recent Developments in the Theory of Sea Clutter," IRE Convention Record, Part I, p. 19, 1956.
- Katzin, M., "On the Mechanism of Sea Clutter," Proc. IRE, vol. 45, pp. 44-54, 1957.
- Kay, I. and R. A. Silverman, "Multiple Scattering by a Random Stack of Dielectric Slabs," Nuovo Cimento, vol. 9, pp. 626-645, 1958.
- Kaydonovsky, N. L. and A. E. Salomonovich, "Determining the Characteristics of the Surface of the Moon from the Observations by Radio-telescopes with High Resolving Power," Izv. Vyssh. Zav. Radiofiz., vol. 4, pp. 40-43, 1961.
- Kerr, D. E., Propagation of Short Radio Waves, McGraw-Hill Book Company, Inc., New York, 1951.
- Kerr, F. J., "Radio Echoes from Sun, Moon and Planets," Encycl. of Phys., vol. 52, pp. 449-464, 1959.
- Kerr, F. J., C. A. Shain, and C. S. Higgins, "Moon Echoes and Penetration in the Ionosphere," Nature, vol. 163, pp. 310-313, 1949.

- Kerr, F. J. and C. A. Shain, "Moon Echoes and Transmissions Through the Ionosphere," Proc. IRE, vol. 39, pp. 230-242, 1951.
- Kiely, D. G., "Measurements of the Reflection Coefficient of Water at $\lambda = 8.7$ mm," Proc. Phys. Soc., vol. 63, pp. 46-49, 1950.
- Kobrin, N. M., "Radio Echoes from the Moon in the X and S Band," Radiotekhn. i Elektr., vol. 4, pp. 892-894, 1959.
- Koepsel, W. W. and N. Ahmed, "Radar Cross Section of a Geometric Shape Using Acoustic Simulation," University of New Mexico Engr. Exp. Sta. Tech. Report EE-80, 1962.
- Kovalev, A. A., and S. I. Posdnyak, "The Scattering of Electromagnetic Waves by Statistically Rough Surfaces with Finite Conductivity," Radiotekhn., vol. 16, pp. 31-36, 1961.
- Krylov, V. I., Approximate Calculation of Integrals, The MacMillan Company, New York, 1962.
- Kur'yanov, B. F., "The Scattering of Sound at a Rough Surface with Two Types of Irregularities," Soviet Physics-Acoustics, vol. 8, pp. 252-257, 1963.
- LaCasce, E. O. and P. Tamarkin, "Underwater Sound Reflection from a Corrugated Surface," J. Appl. Phys. vol. 27, pp. 138-148, 1956.
- Lapin, A. D., "The Scattering of a Plane Wave at a Serrated Surface," Soviet Physics-Acoustics, vol. 9, pp. 37-38, 1963.
- Lapin, A. D., "Sound Scattering at a Rough Solid Surface," Soviet Physics-Acoustics, vol. 10, no. 1, p. 58, July 1964.
- Lapin, A. D., "Note on the Scattering of a Plane Wave on a Periodically Uneven Surface," Soviet Physics-Acoustics, vol. 8, pp. 347-349, 1963.
- Leadabrand, R. L. et. al., "Radio Scattering from the Surface of the Moon," Proc. IRE, vol. 48, pp. 932-933, 1960.

- Leadabrand, R. L. et. al. , "Evidence that the Moon is a Rough Scatterer at Radio Frequencies, " J. Geophys. Res. , vol. 65, pp. 3071-3078, 1960.
- Leporskii, A. N. , "Experimental Study of the Diffraction of Acoustic Waves at Periodic Structures, " Akust. Zhurn. , vol. 1, no. 1, pp. 48-57, 1955.
- Leporskii, A. N. , "Study of the Scattering of the Sound Waves at Uneven Surfaces, " (Dissertation) Acoustics Inst. Acad. Sci. USSR, 1955.
- Leporskii, A. N. , "On the Scattering of Sound Waves at Sinusoidal and Sawtooth Surfaces, " Akust. Zhurn. , vol. 2, pp. 177-181, 1956.
- Lieberman, L. N. , "Analysis of Rough Surfaces by Backscattering, " J. Acoust. Soc. Am. , vol. 35, p. 932, 1963.
- Lynn, V. L. , M. D. Sohigian, and E. A. Crocker, "Radar Observations of the Moon at a Wavelength of 8.6 millimeters, " J. Geophys. Res. , vol. 69, no. 4, 1964.
- Lysanov, Iu. P. , "On the Problem of the Scattering of Electromagnetic Waves at Uneven Surfaces, " Dokl. Akad. Nauk SSSR, vol. 87, pp. 719-722, 1952.
- Lysanov, Iu. P. , "On the Theory of the Scattering of Waves at Uneven and Inhomogeneous Surfaces, " (Dissertation) Acoustics Inst. Acad. Sci. USSR, 1955.
- Lysanov, Iu. P. , "On the Field of a Point Radiator in a Laminar-Inhomogeneous Medium Bounded by an Uneven Surface, " Soviet Physics-Acoustics, vol. 7, no. 3, pp. 255-257, 1962.
- Lysanov, Iu. P. "One Approximate Solution of the Problem of the Scattering of Sound Waves at an Uneven Surface, " Akust. Zhurn. , vol. 2, no. 2, pp. 182-'87, 1956. [see Soviet Physics-Acoustics, p. 190, 1956].
- Lysanov, Iu. P. , "Theory of the Scattering of Waves at Periodically Uneven Surfaces, " Soviet Physics-Acoustics, vol. 4, no. 1, pp. 1-7, Jan.-Mar. 1958.

- Macdonald, F. D., "The Correlation of Radar Sea Clutter on Vertical and Horizontal Polarization with Wave Height and Slope," IRE Convention Record, Part 4, pp. 29-32, 1956.
- Mackenzie, K. V., "Bottom Reverberation for 530 and 1030 cps Sound in Deep Water," J. Acoust. Soc. Am., vol. 33, pp. 1498-1504, 1961.
- MacLusky, G. S. R. and H. Davies, IRE Report No. T1933, 1945.
- Maestri, A., "Hydroacoustic Simulation of Antenna Radiation Characteristics," Melpar, Inc., Falls Church, Va., Tech. Report. No. TP-1-26, 1961.
- Magnus, W., "On the Scattering Effect of a Rough Plane Surface," Research Report EM-40, Inst. Math. Sc., New York University, 1952.
- Manton, R. G., The Reflection of Radio Waves from Rough Surfaces, Ph.D. thesis, London University, 1958.
- Marsh, H. W., "Exact Solution of Wave Scattering by Irregular Surfaces," J. Acoust. Soc. Am., vol. 33, no. 3, pp. 330-333, Mar. 1961.
- Marsh, H. W., "Sound Reflection and Scattering from the Sea Surface," J. Acoust. Soc. Am., vol. 35, pp. 240-244, 1963.
- Marsh, H. W., "Nonspecular Scattering of Underwater Sound by the Sea Surface," Underwater Acoustics, pp. 193-197, 1962.
- Marsh, H. W., M. Schulkin, and S. G. Kneale, "Scattering of Underwater Sound by the Sea Surface," J. Acoust. Soc. Am., vol. 33, no. 3, pp. 334-340, Mar. 1961.
- McGavin, R. E. and L. J. Maloney, "Study at 1.046 Mc/s of the Reflection Coefficient of Irregular Terrain at Grazing Angles," J. Res. NBS, vol. 63D, pp. 235-248, 1959.
- McKinney, C. M. and C. D. Anderson, "Measurements of Backscattering of Sound from the Ocean Bottom," J. Acoust. Soc. Am., vol. 36 pp. 158-163, 1964.

McPetre, J. S., "The Reflection Coefficient of the Earth's Surface for Radio Waves," J. IEEE, vol. 82, p. 214, 1938.

Meecham, W. C., "Variation Method for the Calculation of the Distribution of Energy Reflected from a Periodic Surface," J. Appl. Phys., vol. 27, pp. 361-367, 1956a.

Meecham, W. C.; "A Method for the Calculation of the Distribution of Energy Reflected from a Periodic Surface," Trans. IRE, vol. AP-4, p. 581, 1956b.

Meecham, W. C., "Fourier Transform Method for the Treatment of the Problem of the Reflection of Radiation from Irregular Surfaces," J. Acoust. Soc. Am., vol. 28, p. 370, 1956c.

Mellen, R. H., "Doppler Shift of Sonar Backscatter from the Sea Surface," J. Acoust. Soc. Am., vol. 36, pp. 1395-1396, 1964.

Men', A. V., S. Ya. Brande, and V. I. Gorbach, "Experimental Investigation of the Phase Fluctuations of Centimetre Radio Waves over the Surface of the Sea," Izv. Vyssh. Zav. Radiofiz., vol. 2, pp. 848-857, 1959.

Meyer, E., "Experiments on CM Waves with Acoustic Techniques Made in Gottingen," J. Acoust. Soc. Am., vol. 30, pp. 624-632, 1958.

Middleton, D., An Introduction to Statistical Communication Theory, McGraw-Hill Book Company, Inc., New York, 1960.

Miles, J. W., "On Nonspecular Reflection at a Rough Surface," J. Acoust. Soc. Am., vol. 26, pp. 191-199, 1954.

Millman, G. H. and F. L. Rose, "Radar Reflections from the Moon at 425 Mc/s," J. Res. NBS, vol. 67D, p. 107, 1963.

Millington, G., "The Reflection Coefficient of a Linearly Graded Layer," Marconi Rev., vol. 12, p. 140, 1949.

Mitzner, K. M., "Theory of the Scattering of Electromagnetic Waves by Irregular Interfaces," Antenna Laboratory, Calif. Inst. Tech., Tech. Report No. 30, Jan. 1964.

- Mofensen, J. , "Radar Echoes from the Moon, " Electronics, vol. 19, pp. 92-98, 1946.
- Moore, R. K. , "Acoustic Simulation of Radar Return, " Microwaves, vol. 1, pp. 20-25, 1962.
- Moore, R. K. , "Resolution of Vertical Incidence Radar Return into Random and Specular Components, " Univ. of New Mexico, Albuquerque, Engr. Exp. Sta. Tech. Report E.E. 6, July 1957.
- Moore, R. K. and C. S. Williams, "Radar Terrain Return at Near Vertical Incidence, " Proc. IRE, vol. 45, pp. 228-238, 1957.
- Morse, P. M. , Vibration and Sound, McGraw-Hill Book Company, Inc. New York, 1948.
- Morse, P. M. and H. Feshbach, Methods of Theoretical Physics, McGraw-Hill Book Company, Inc. , 1953.
- Muhleman, D. O. , "Radar Scattering from Venus and the Moon, " Astronomical J., Feb. 1964.
- Nolle, A. W. , W. A. Hoyer, J. F. Mifsud, W. R. Runyan, and M. B. Ward, "Acoustical Properties of Water-Filled Sands, " J. Acoust. Soc. Am., vol. 35, pp. 1394-1408, 1963.
- The Ohio State University, "Theoretical and Experimental Analysis of the Electromagnetic Scattering and Radiative Properties of Terrain, with Emphasis on Lunar-Like Surfaces, " Antenna Laboratory Report No. 1388-12, 1963.
- Ornstein, L. S. and H. Van der Burg, "Reflectivity of Corrugated Surfaces, " Physica, vol. 4, p. 1181, 1937.
- Oxehufwud, A. , "Tests Conducted over Highly Reflective Terrain at 4,000, 6,000, and 11,000 Mc. , " Trans. Amer. IEE, vol. I, no. 78, pp. 265-270, 1959.
- Parker, J. G. , "Reflection of Plane Sound Waves from an Irregular Surface, " J. Acoust. Soc. Am., vol. 28, pp. 672-680, 1956.

- Parker, J. G., "Reflection of Plane Sound Waves from a Sinusoidal Surface," J. Acoust. Soc. Am., vol. 29, pp. 377-380, 1957.
- Patterson, R. B., "Backscatter of Sound from a Rough Boundary," J. Acoust. Soc. Am., vol. 35, no. 12, p. 2010, Dec. 1963.
- Pettengill, G. H., "Measurement of Lunar Reflectivity Using the Millstone Radar," Proc. IRE, vol. 48, pp. 933-934, 1960.
- Pierson, W. J. Jr., "The Directional Spectrum of a Wind Generated Sea as Determined from Data Obtained by the Stereo Wave Observation Project," Meteorological Papers, vol. 2, no. 6, New York Univ., 1960.
- Price, R., P. E. Green, J. J. Goblick, R. H. Kingston, L. T. Kraft, G. H. Pettengill, R. Silver, and W. B. Smith, "Radar Echoes from Venus," Science, vol. 129, pp. 751-753, Mar. 1959.
- Proud, J., "Reflection of Sound from a Surface of Saw-tooth," J. Appl. Phys., vol. 28, p. 1298, 1957.
- Proud, J. M., R. T. Beyer, and P. Tamarkin, "Reflection of Sound from Randomly Rough Surfaces," J. Appl. Phys., vol. 31, pp. 543-553, 1960.
- Rayleigh, Lord, The Theory of Sound, 3rd ed. MacMillan, London, 1896.
- Rea, D. G., N. Hetherington, and R. Mifflin, "The Analysis of Radar Echoes from the Moon," J. Geophys. Res., vol. 69, no. 24, pp. 5217-5223, Dec. 1964.
- Redheffer, R., "The Dependence of Reflection on the Incidence Angle," Trans. IRE, vol. MIT-7, pp. 423-429, 1959.
- Reitz, "Development of Airborne and Laboratory Equipment," Contract NORD 16165, Goodyear Aircraft Corp., Sept. 1958.
- Rice, S. O., "Reflection of Electromagnetic Wave from Slightly Rough Surfaces," Comm. Pure Appl. Math., vol. 4, pp. 351-378, 1951.

- Richter, R., J. Bessis, and P. Catella, "Application au Radar du Phénomène de Réflexion des Ondes Électromagnétiques par le Sol," L'Onde Electrique, vol. 40, pp. 392-410, 1960.
- Saxton, J. A. and J. A. Lane, "Electrical Properties of Sea Water. Reflection and Attenuation Characteristics at VHF," Wirel. Eng., vol. 29, pp. 269-275, 1952.
- Schooley, A. H., "A Simple Optical Method for Measuring the Statistical Distribution of Water Surface Slopes," J. Opt. Soc. Am., vol. 44, pp. 37-40, 1954.
- Schooley, A. H., "Radar Reflections from Sea Waves," Tele-Tech. 14, pp. 70-71, 1955.
- Schooley, A. H., "Some Limiting Cases of Radar Sea Clutter Noise," Proc. IRE, vol. 44, p. 1043, 1956.
- Schouten, J. P. and A. T. de Hoop, "Sur la Reflexion d'une Onde Électromagnétique Plane par une Surface Rugueuse Parfaitement Conductrice," Ann. Télécomm., vol. 12, pp. 211-214, 1957.
- Schulkin, M. and R. Shaffer, "Backscattering of Sound from the Sea Surface," J. Acoust. Soc. Am., vol. 36, No. 9, p. 1699, Sept. 1964.
- Semenov, A. A., D. K. Kvavadze, L. G. Nazarov, and I. I. Zvyagintseva, "Investigation of the Reflecting Properties of Some Systems with a Periodic Structure," Vyest. Mosk. Univers. Ser. Matem., Astron., Fiz., No. 1, pp. 107-114, 1958.
- Senior, T. B. A., "The Scattering of Electromagnetic Waves by a Corrugated Sheet," Canada J. Phys., vol. 37, pp. 787-797, 1959; also correction Canada J. Phys. vol. 37, p. 1572, 1959.
- Senior, T. B. A., "Radar Reflection Characteristics of the Moon," Paris Symposium on Radioastronomy, Stanford Univ. Press, 1959.
- Senior, T. B. A. and K. M. Siegel, "A Theory of Radar Scattering by the Moon," J. Res. NBS, vol. 64D, pp. 217-229, 1960.

- Sherwood, E. M. , "S Band Measurements of Reflection Coefficients for Various Types of Earth, " Sperry Gyroscope Co. Report No. 5220-129, Oct. 1943.
- Sherwood, E. M. , "Reflection Coefficients of Irregular Terrain at 10 cm, " Proc. IRE, vol. 43, pp. 877-878, 1955.
- Shulman, L. A. , "The Reflection of Electromagnetic Waves from a Semi-Infinite Periodic Layer Structure, " Uch. Zap. Tadzh. Univ. , vol. 10, pp. 103-109, 1957.
- Sofaer, E. , "Phase-coherent Backscatter of Radio Waves at the Surface of the Sea, " Proc. IEE, Part B, no. 105, pp. 383-394, 1958.
- Spetner, L. M. , "A Statistical Model for Radar Terrain Return, " Trans. IRE, vol. AP-8, pp. 242-246, 1960.
- Spizzichino, M. A. , "La Reflexion des Ondes Électromagnétiques par Une Surface Irregulière, " Research Report No. 549T, Centre National d'Etudes des Télècommunications, 4.11.1959, 1959.
- Straiton, A. , "Reflection of Centimeter Water Waves from Ground and Water, " Trans. IRE, vol. AP-4, Aug. 1955.
- Straiton, A. W. , J. P. Gerhardt, A. H. LaGrone, and C. W. Tolbert, "Reflection of Centimeter and Millimeter Radio Waves from the Surface of a Small Lake, " Elec. Engr. Res. Lab. Univ. of Texas, Report No. 63, May 1952.
- Straiton, A. W. and C. W. Tolbert, "Moon Reflection Studies with Bistatic Radar at 3000 Mc/s, " Comm. and Electr. , vol. 50, pp. 436-460, 1960.
- Stratton, J. A. , Electromagnetic Theory, McGraw-Hill Book Company, Inc. , New York, 1941.
- Tai, C. T. , "Reflection and Refraction of a Plane Electromagnetic Wave at a Periodical Surface, " Harvard Tech. Report No. 28, Cruft Lab. , Jan. 1948.
- Taylor, R. C. , "Terrain Return Measurements at X, Ku, and Ka Band, " IRE Convention Record Part I, vol. 7, 1959.

- Taylor, R. C. , "The Terrain Scattering Problem, " Radar Reflectivity Measurements Symposium, Space Surveillance and Instrumentation Branch, Rome Air Development Center Research and Tech. Division, Air Force Systems Command, Griffiss Air Force Base, New York, Tech. Report RADC-TDR-64-24, April 1964.
- Tonakanov, O. S. , "Sound Fluctuations in Double Reflection from an Undulating Water Surface, " Soviet Physics-Acoustics, vol. 10, no. 2, p. 211, Oct. 1964.
- Trexler, J. H. , "Lunar Radio Echoes, " Proc. IRE, vol. 46, pp. 286-292, 1958.
- Twersky, V. , "On the Non-specular Reflection of Plane Waves of Sound, " J. Acoust. Soc. Am., vol. 22, pp. 539-546, 1950.
- Twersky, V. , "On the Non-specular Reflection of Sound from Planes with Absorbent Bosses, " J. Acoust. Soc. Am., vol. 23, pp. 336-338, 1951a.
- Twersky, V. , "On the Nonspecular Reflection of Electromagnetic Waves, " J. Appl. Phys., vol. 22, pp. 825-835, 1951b.
- Twersky, V. , "Reflection Coefficients for Certain Rough Surfaces, " J. Appl. Phys., vol. 24, pp. 569-660, 1953.
- Twersky, V. , "Certain Transmission and Reflection Theorems, " J. Appl. Phys., vol. 25, pp. 859-862, 1954.
- Twersky, V. , "Scattering Theorems for Bounded Periodic Structures, " J. Appl. Phys., vol. 27, pp. 1118-1122, 1956.
- Twersky, V. , "On the Scattering and Reflection of Electromagnetic Waves by Rough Surfaces, " Trans. IRE, vol. AP-5, pp. 81-90, 1957a.
- Twersky, V. , "On the Scattering and Reflection of Sound by Rough Surfaces, " J. Acoust. Soc. Am., vol. 29, pp. 209-225, 1957b.
- Twersky, V. , "Calcul des Coefficients de Réflexion et des Sections Droites Différentielles de Diffraction pour les Surfaces Irrégulières, " Ann. Télécomm. vol. 12, pp. 214-216, 1957c.

- Twersky, V., "Scattering by Quasi-periodic and Quasi-random Distributions," Trans. IRE, vol. AP-7, pp. 307-319, 1959.
- Twersky, V., "Signals, Scatterers, and Statistics," Trans. IRE, AP-11, pp. 608-680, 1963.
- Urick, R. J., "The Backscattering of Sound from a Harbor Bottom," J. Acoust. Soc. Am., vol. 26, pp. 231-235, 1954.
- Urick, R. J., "The Processes of Sound Scattering at the Ocean Surface and Bottom," J. Marine Research, vol. 15, pp. 134-148, 1957.
- Urick, R. J. and R. M. Hoover, "Backscattering of Sound from the Sea Surface: its Measurement, Causes, and Application to the Prediction of Reverberation Levels," J. Acoust. Soc. Am., vol. 28, p. 1038, 1956.
- Urusovskii, I. A., "Sound Scattering by a Sinusoidally Uneven Surface Characterized by Normal Acoustical Conductivity," Soviet Physics-Acoustics, vol. 5, pp. 362-369, 1960.
- Urusovskii, I. A., "Diffraction of Sound on a Periodically Uneven and Inhomogeneous Surface," Soviet Physics-Doklady, vol. 5, pp. 345-348, 1960.
- Urusovskii, I. A., "Diffraction by a Periodic Surface," Soviet Physics-Acoustics, p. 287, Jan. 1965.
- Victor, W. K., R. Stevens, and S. W. Golomb, "Radar Exploration of Venus," Goldstone Observatory Report for March-May 1961. Jet Propulsion Laboratory, Calif. Inst. Tech., Pasadena, Calif. Tech. Report No. 32-132, Aug. 1961.
- Warner, B. D., R. K. Moore, and A. R. Edison, "Acoustic Simulation of Radar Altimeter Signals from Cities," University of New Mexico Engr. Exp. Sta. Tech. Report EE-77, 1962.
- Wilf, H. S., Mathematics for the Physical Sciences, John Wiley and Sons, New York, 1962.
- Wiltse, I. C., S. P. Schlesinger, and C. M. Johnson, "Backscattering Characteristics of the Sea in the Region from 10 to 50 kMc," Proc. IRE, vol. 45, pp. 220-228, pp. 244-246, 1957.

Winter, D. F., "A Theory of Radar Reflection from a Rough Moon,"
J. Res. NBS, vol. 66D, p. 215, 1962.

Yapplee, B. S., R. H. Bruton, K. J. Craig, and N. G. Roman, "Radar
Echoes from the Moon at the Wavelength of 10 cm," Proc. IRE,
vol. 46, pp. 293-297, 1958.

Yapplee, B. S., N. G. Roman, K. J. Craig, and T. F. Scanlan, "A
Lunar Radar Study at 10 cm Wavelength," Paris Symposium on
Radio Astronomy, Stanford Univ. Press, 1959.